

**APPLICATION OF NOVEL STABLE ISOTOPE METHODS
TO RECONSTRUCT PALEOENVIRONMENTS:
COMPOUND-SPECIFIC HYDROGEN ISOTOPES
AND PORE-WATER OXYGEN ISOTOPES**

A dissertation submitted to the

SWISS FEDERAL INSTITUTE OF TECHNOLOGY ZÜRICH

for the degree of

DOCTOR OF NATURAL SCIENCES

presented by

HILARY A. PAUL

Master of Science, University of California, Santa Cruz, CA, USA

born October 23, 1970

citizen of The United States of America

Accepted on the recommendation of

Prof. Dr. J.A. McKenzie

examiner

Dr. S.M. Bernasconi

1. co-examiner

Prof. Dr. K.C. Emeis

2. co-examiner

ZÜRICH, 2002

TABLE OF CONTENTS

Abstract	i
Zusammenfassung	iii
Acknowledgements	v
CHAPTER 1	
Introduction	1
CHAPTER 2 - ANALYTICAL TECHNIQUES AND METHODS	
Determining the Hydrogen Isotopic Composition of Organic Material	11
Organic Compounds: Selection and Analysis	21
References	25
CHAPTER 3	
Fractionation of Stable Hydrogen Isotopes of C ₃₇ alkenones from Laboratory-Cultured Coccolithophorid <i>Emiliana huxleyi</i>	27
CHAPTER 4 - CASE STUDIES IN THE MEDITERRANEAN SEA	
Background: Modern Mediterranean Oceanography and Sapropels	33
Hydrogen Isotopes in Biomarkers Track Mediterranean Paleohydrologic Change during Sapropel Deposition	53
Oxygen Isotopic Composition of the Mediterranean Sea Since the Last Glacial Maximum: Constraints from Pore-Water Analyses	61
References	77
CHAPTER 5	
Tropical Sea Surface Temperature and Salinity Change in the Cariaco Basin at the Last Glacial Maximum: Quantification from Pore-Water $\delta^{18}\text{O}$	85
CHAPTER 6	
Proxy Assessment and Future Work	105
APPENDIX I	
Geochemical Data	109
APPENDIX II	
Notes on Advection-Diffusion Modeling	119
APPENDIX III	
Advection-Diffusion Model Sensitivity Studies	123
APPENDIX IV	
Large and Rapid Climate Variability During the Messinian Salinity Crisis: Evidence from Deuterium Concentrations of Individual Biomarkers	131
CURRICULUM VITAE	141

ABSTRACT

The focus of this thesis is to further the development and application of two new paleoenvironmental proxies. These proxies are based on the fractionation of light stable isotopes in natural systems and include the δD of individual organic compounds and the $\delta^{18}O$ of interstitial-waters in deep-sea sediments. These geochemical signals are used in combination with marine carbonate $\delta^{18}O$ records to more precisely describe past periods of environmental change, including the reconstruction of sea-surface temperature and paleohydrologic conditions.

A new approach to determining the glacial-interglacial change in the $\delta^{18}O$ value of seawater ($\delta^{18}O_{sw}$) has recently been developed based on measurements of the isotopic composition of deep-sea pore waters in conjunction with a diffusion-advection model. Here this method is taken one step further and we examine pore-fluid isotopic data from sites where deep and surface waters are well mixed at the Last Glacial Maximum (LGM). Hence, in addition to the global ice volume signal, these sites record some glacial-interglacial hydrologic change with which we can examine variations in paleosalinity. Using this approach, we are also able to estimate changes in marine surface temperature by coupling the reconstructions of $\delta^{18}O_{sw}$ with measurements of $\delta^{18}O$ from planktonic foraminiferal calcite. This technique is applied to samples from ODP Leg 165, Site 1002 in the Cariaco Basin to reconstruct glacial-interglacial sea surface temperature and salinity changes. Results indicate that tropical sea surface temperatures were $\sim 3\text{-}4^\circ\text{C}$ cooler, and seawater ~ 2 psu more saline during the LGM than at present, supporting the theory that the tropics are an important factor in the global climate system and play a dynamic role in initiating climate change.

The hydrogen and oxygen isotopic ratios of seawater change as a function of evaporation and with the addition of meteoric waters. They are therefore complementary tracers for the examination of regional water balance and as indicators of freshwater input. Yet, hydrogen is more susceptible to fractionation, and hence, more sensitive to environmental perturbation than oxygen. We have developed two new techniques for measuring the hydrogen isotopic composition of sedimentary organic matter to exploit this proxy for paleoenvironmental research. Both experimental methods, one for analyzing bulk organic matter and the second for measuring individual organic compounds, are described and calibrated in this thesis. In addition, a laboratory calibration was carried out to determine the fractionation factor between C_{37} alkenones and water by growing batch cultures of the coccolithophorid *Emiliana huxleyi* in seawater with a controlled isotopic composition. Results of this study indicate a constant fractionation between the source water and $C_{37:2}$ alkenones of $\sim -232\text{‰}$.

To evaluate the change in freshwater balance and potential circulation variations that occurred in the Mediterranean Sea during Sapropel Event 1 (S1), a period of increased organic matter deposition thought to coincide with warm and wet climatic conditions ~9-6 thousand years ago, and at the LGM (~20 ka), we apply both of the new proxy methods described above. An overview of modern Mediterranean oceanography and paleoceanography is provided, focusing on the past ~25,000 years to include the LGM and S1. Samples obtained during two trans-Mediterranean cruises in 1998 and 1999, including detailed water-column δD and $\delta^{18}O$ isotopic profiles and several geochemical analyses conducted on sediments from short cores, are presented and used to illustrate the paleoenvironmental changes that occurred in conjunction with the deposition of the youngest sapropel layer in the eastern Mediterranean.

Sedimentary interstitial-water samples obtained from ODP Leg 161, Site 976 in the western Mediterranean Sea are used to model the past $\delta^{18}O_{sw}$ and hence, derive the sea surface salinity and temperature that existed at both the LGM and S1. Results suggest ~9°C of regional cooling at the LGM and only a 0.2‰ enrichment in $\delta^{18}O$ due to salinity increase. This estimate of salinity change is much smaller than previous studies have proposed and demonstrates that records of foraminiferal calcite $\delta^{18}O$ from the last glacial period include a strong temperature component in the Mediterranean. Alternatively, the model indicates a decrease of 1.1‰ in the $\delta^{18}O_{sw}$ value at S1 relative to present, likely caused by freshwater input and reduced surface water salinity. These results reveal that isotopically light water was circulating down to deepwater depths and support the continued existence of an “anti-estuarine” thermohaline circulation pattern during the deposition of the sapropel. Compound-specific δD of *n*-alkane and alkenone biomarkers in sediments from the eastern basin of the Mediterranean Sea are used to quantify the magnitude of marine surface water hydrologic change at S1. The molecular proxies reveal that the hydrogen isotopic composition of Mediterranean surface water was about 35‰ lighter at S1 than at present. In conjunction with the ~1.1‰ decrease in seawater $\delta^{18}O$, these isotopic values attest to the significant increase in freshwater input, yet indicate that evaporative conditions still must have existed during sapropel formation in the eastern Mediterranean Sea.

ZUSAMMENFASSUNG

Der zentrale Punkt dieser Arbeit ist die Weiterentwicklung und Anwendung zweier neuer Paläoumwelt-Proxies. Die theoretische Grundlage dieser Arbeit ist die Fraktionierung leichter, stabiler Isotope in natürlichen Systemen, im Spezifischen δD charakteristischer organischer Komponenten sowie $\delta^{18}O$ von Porenwässern aus Tiefsee- Sedimenten. Diese geochemischen Signale werden mit $\delta^{18}O$ Aufzeichnungen mariner Karbonate kombiniert, um zeitliche Umweltveränderungen präziser zu beschreiben, z. B. die Rekonstruktion von marinen Oberflächentemperaturen und paläohydrologischen Bedingungen.

Ein neu entwickelter Ansatz, um glazial-interglaziale Veränderungen in den $\delta^{18}O$ Werten des Meerwassers ($\delta^{18}O_{sw}$) zu bestimmen, basiert auf der Bestimmung der Isotopenzusammensetzung von Porenwässern mariner Tiefsee-Sedimente in Verbindung mit einem Diffusion-Advektions Modell für chemischen Transport. In dieser Arbeit, wird diese Methode erweitert, indem die Isotopenzusammensetzung der Porenwässer in Sedimentprobenkernen untersucht wird, in denen Tiefen- und Oberflächenwasser während des Letzten Glazialen Maximums (LGM) gut durchmischt waren. Diese Kerne haben daher, zusätzlich zu dem Signal aus der Veränderung des global Eisvolumens, während der glazial-interglazial Wechsel hydrologische Veränderungen erfahren, die durch die Veränderungen in der Paläosalinität quantifiziert werden können. Basierend auf diesem Ansatz können wir zusätzlich Veränderungen in der marinen Oberflächentemperatur abschätzen, indem wir die Rekonstruktionen von $\delta^{18}O_{sw}$ mit Messungen von $\delta^{18}O$ aus dem Kalk planktischer Foraminiferen koppeln. Diese Methode wird auf Proben von ODP Leg 165, Kern 1002 im Cariaco Becken angewandt, um glazial-interglaziale Veränderungen von Oberflächenwasser- Temperaturen und Salinität zu rekonstruieren. Unsere Ergebnisse weisen darauf hin, dass während des Glazials die tropische Oberflächenwassertemperatur $\sim 3-4^{\circ}C$ kälter, und dass das Meerwasser ~ 2 psu salziger war als heute. Dies unterstützt die Theorie, dass die Tropen ein bedeutender Faktor im globalen Klimasystem waren und eine dynamische Rolle bei der Einleitung des Klimawandels gespielt haben.

Wasserstoff- und Sauerstoffisotopenverhältnisse des Meereswassers sind das Resultat von Evaporation und dem Zufluss meteorischer Wässern. Daher sind diese Isotopenverhältnisse sich ergänzende Indikatoren zur Untersuchung von regionalen Wasserbilanzen und Frischwassereinträgen. Wasserstoff ist allerdings anfälliger gegenüber Fraktionierung und reagiert daher sensitiver auf Störungen in den Umweltbedingungen als Sauerstoff. Wir haben zwei neue Messtechniken entwickelt, die es uns ermöglichen die Wasserstoffisotopen-Zusammensetzung organischen Materials in Sedimenten als Proxi in Untersuchungen der Paläoumweltbedingungen zu benutzen. Die erste Methode, erlaubt die Gesamtmasse an organischem Material zu analysieren, die zweite ermöglicht die Messung einzelner organischer Komponenten. Beide

experimentelle Methoden sind in dieser Arbeit beschrieben und kalibriert. Zusätzlich wurde ein Laborversuch durchgeführt, um den Fraktionierungsfaktor zwischen C_{37} Alkenonen und Wasser beim Wachstum der Coccolithophoride *Emiliana huxleyi* in Meereswasser-Kulturen mit kontrollierter Isotopenzusammensetzung zu kalibrieren. Die Ergebnisse dieser Studie zeigen eine konstante Fraktionierung zwischen dem Ursprungswasser und den $C_{37:2}$ Alkenonen von $\sim -232\%$.

Die beiden beschriebenen neuen Proxies wurden zu einer Untersuchung möglicher Veränderungen der Frischwasserbilanz und potentiellen Zirkulationsveränderungen in zwei geologischen Zeitintervallen angewandt, zum einen das Sapropel 1 (S1), das im Zeitraum von ~ 9 bis 6 tausend Jahren vor heute abgelagert wurde, zum anderen während des LGM (~ 20 ka). Das S1 ist ein Zeitintervall mit einer erhöhten Ablagerung organischen Materials, welche mit warmen und feuchten Bedingungen zusammentrifft. Als erstes wird eine Übersicht über die Ozeanographie und Paläoozeanographie erstellt, die sich auf die letzten 25'000 Jahre konzentriert, um das LGM und den S1 zu beschreiben. Die untersuchten Proben wurden während zweier Trans-Mittelmeer-Fahrten in 1998 und 1999 genommen. Sie umfassen detaillierte Wassersäulen Profile von δD und $\delta^{18}O$ Isotopen, und mehrere geochemische Analysen von Sedimenten aus kurzen Probenkernen. Anhand dieser Daten werden die Umweltveränderungen beschrieben, die im Zusammenhang mit der Ablagerung des jüngsten Sapropels im östlichen Mittelmeer stehen.

Porenwasserprofile aus Sedimenten von ODP Leg 161, Kern 976 im westlichen Mittelmeer werden benutzt, um die $\delta^{18}O_{sw}$ zu modellieren und darauf basierend die Salinität des Oberflächenwassers und die -Temperatur für das LGM und das S1 zu berechnen. Die Ergebnisse deuten auf eine regionale Abkühlung von $\sim 9^\circ C$ während des LGM hin und eine nur geringe Anreicherung von 0.2% im $\delta^{18}O$ durch einen Salinitätsanstieg. Die Salinitätsveränderung ist viel kleiner als vorangegangene Studien es vorgeschlagen haben und demonstriert, dass die $\delta^{18}O$ Daten aus dem Kalzit planktischer Foraminiferen für das Glazial im Mittelmeer eine starke Temperaturkomponente beinhalten. Alternativ deutet der durch das Modell berechnete Abfall von 1.1% im $\delta^{18}O_{sw}$ Wert relativ zu heute während des S1 auf einen erhöhten Frischwassereintrag und eine verringerte Oberflächenwassersalinität hin. Diese Ergebnisse zeigen, dass isotopisch leichtes Wasser durch die Zirkulation in Tiefenwasserbereiche gelangte und unterstützen die Existenz eines "anti-estuarinen" thermohalinen Zirkulationsmusters zu dieser Zeit. Komponentenspezifisches δD von *n*-Alkanen und Alkenonen in sedimentären Biomarkern des östlichen Mittelmeerbeckens wurden zur Quantifizierung der Veränderung des marinen hydrologischen Oberflächenwassers während des S1 benutzt. Die molekularen Proxies zeigen, dass die Wasserstoffisotopen-Zusammensetzung des mediterranen Oberflächenwassers während des S1 $\sim 35\%$ leichter war als heute. Im Zusammenhang mit dem Abfall von $\sim 1.1\%$ im Oberflächenwasser $\delta^{18}O$ bestätigen diese Isotopenwerte einen signifikanten Anstieg des Frischwassereintrages, unter noch immer evaporativen Bedingungen, während der Bildung des Sapropel 1 im östlichen Mittelmeer.

ACKNOWLEDGEMENTS

Well who would have thought that coming to Zürich for one year of employment could so quickly amount to 5 years and a dissertation (and a new Swiss husband!)? I certainly would never have guessed... Now that I have had such a long stay, there are many people that I need to thank for making it so enjoyable and such a success. First and foremost, I have to thank Dr. Judy McKenzie for providing me with the opportunity to come to Zürich in the first place. I must also thank Dr. Bob Garrison who initially put me in contact with Judy and for telling me that Zürich would be an intellectually stimulating and fun place to live. I also want to thank Judy's first PhD student, Dr. Dave Hollander, for inviting me to spend a great weekend with him at his home in Chicago (I will never forget seeing Yo-Yo Ma live in the park) and giving me the chance to meet Judy and convincing me that Europe would be a great next step. Judy's enthusiasm for all aspects of the geosciences and enjoyment of life have been an inspiration since Day One.

It has been a great pleasure to work with Dr. Stefano Bernasconi over the past 5 years. His endless encouragement and excitement with each new result (how many times did I hear "call Nature!"), interest and expertise in isotope geology, and overall positive attitude for life have been a great motivation. One of the biggest lessons I have learned from Stefano's "just do it" philosophy, is that one should never be afraid of experimenting or of making mistakes – very few things in life are truly beyond repair – and that by trying something new and (unfortunately) making mistakes are the best ways to learn.

I want to thank all the people that helped me in the lab and with measuring/collecting samples during my time here: Nils Andersen for all the help with the GEO and organic geochemistry lessons; Robert Hofmann for the speedy repair of many parts and Franz Goenner for finding numerous blown fuses; Bill for changing all the filaments; Moktar for all the help with the off-line preparation of water samples for δD measurements; Adi for help with the coulometer and multi-sensor track and other random limno-lab work; and of course Flavio and Moritz for nice trips on the lake collecting sediment and water samples. I am indebted to Dr. V. Lykousis and the members of the MATER cruise for allowing me to take sediment and water samples and for providing shipboard data. Additionally, I am grateful to Dr. Kay Emeis for supplying Mediterranean samples and agreeing to be a co-examiner.

And what would life be like without all the other students / members of the D-ERDW? Thanks to everyone for all the fun over the years!! I have to extend special thanks to all the fellow students in the stable isotope lab and to my original office mates: Maureen for all the chats about home and sharing Salt & Vinegar chips, Giulio for letting Dani use his desk in the summer of '97 (although I wasn't happy at the time, it turned out to be a good thing!), and Andreas for the

many phone calls and “chuchi chäschtli” in my first year. I must thank Mario as my first flat mate in Zürich for “easing” me into life here and for making life entertaining, to say the least. I have to thank everyone who was patient enough to speak German with me in the beginning (especially Dani for even reverting to high-German for me!) and big thanks to Daniela for translating the abstract. Last but certainly not least, thanks to D.W. for all the companionship and adventures - may life never be lacking in these!

Ich möchte mich Familie Schmid-Keller, Leuggern herzlich für die vielen Köstlichkeiten, den Fisch und die gemütlichen Abende im Restaurant Schmid bedanken und für alle Liebe, Unterstützung und besonders die Aufnahme als Teil der Familie. And, of course, I have to thank my own mom and dad for all the care and support over the years, no matter how far away I may have been; especially Dad for instilling in me my love of nature and the great outdoors and Mom for her endless encouragement and always giving me the independence to follow my own path and pursue my own interests.

INTRODUCTION

1. RECONSTRUCTING THE HISTORY OF GLOBAL CLIMATE

The main task of climate researchers today is predicting what the future climate might be as we are increasingly faced with the threat (reality) of global warming. Perhaps, more importantly is the task of identifying the causes responsible for the observed climate change and deciphering which effects are a consequence of anthropogenic factors, such as increased greenhouse gas concentrations and environmental pollution, and which result from natural climate dynamics. Paleoclimatologists play an invaluable role in this work as they attempt to procure information from the available geological archives to improve our understanding of Earth's inherent climate variability by investigating climate events in the past. Records, produced on an array of temporal scales, from ocean and lake sediments, coral reefs, tree rings, and polar ice, encode information on natural variations of the climate system and on linkages between the ocean, atmosphere, and cryosphere.

Paleoclimatologists depend on geochemical proxies derived from the above mentioned archives to reconstruct the conditions of periods in the past with extreme or vastly different climate and to identify potential causes and mechanisms of climatic variation. Two of the most fundamental parameters needed to study climate dynamics and the evolution of the climate system are marine sea-surface temperature (SST) and the hydrologic cycle. Accurate reconstruction of these elements is essential for use in climate models, which are then used as a basis for testing hypotheses concerning the causes of climatic change. Only after the forcing factors have been properly identified and fully understood, will it be possible to forecast future climate evolution. Unfortunately, the understanding and interpretation of proxy data are not always straight forward and often entail careful analysis and many assumptions.

1.1. CARBONATE $\delta^{18}\text{O}$: THE (IM)PERFECT PROXY?

Despite the multitude of geochemical proxies that have been utilized to investigate the Earth's climatic history, carbonate $\delta^{18}\text{O}$ data have served as the most widely applied and accepted means of reconstructing global and regional climate, over a variety of geologic time scales, since the 1970s [Broecker and van-Donk, 1970; Shackleton and Opdyke, 1973]. For instance, the fundamental evolution of Earth's climate over the Cenozoic era has been defined based on the stable oxygen isotopic composition of deep-sea carbonate microfossils (summary in Zachos *et al.* [2001]). This record (Figure 1) depicts episodes of global warming and cooling and

ice-sheet growth and decay, and indicates that global climate changes can occur as both gradual trends and as extreme climate transients. As displayed by the marine oxygen isotope data, the “climatic mean” has changed dramatically over the past 65 million years, with the $\delta^{18}\text{O}$ values in essence providing constraints on the evolution of seawater temperature and continental ice volume. Studies of similar such records covering a range of spatial and temporal scales have shown that profound shifts in climate also occur cyclically on submillennial and longer (glacial-interglacial) time scales, clearly illustrated in Figure 1 by the SPECMAP record of Pleistocene glaciations based on a compilation of planktonic foraminiferal $\delta^{18}\text{O}$ data [Imbrie *et al.*, 1989].

As alluded to previously, the ideal proxy should vary quantitatively and should respond only to variations in the parameter of interest. Unfortunately, this is rarely the case and most geochemical proxies are influenced by multiple factors. For instance, the critical problem with converting foraminiferal $\delta^{18}\text{O}$ variations into a specific record of paleoceanic and/or paleoenvironmental change is that the oxygen isotopic composition of calcareous microfossils reflects a combination of both the $\delta^{18}\text{O}$ of seawater and a thermodynamic fractionation that is a function of the calcification temperature (and in some instances, biological vital effects) [Epstein *et al.*, 1953; Shackleton, 1974]. The $\delta^{18}\text{O}$ value of seawater is, in turn, dependent on the volume of continental ice, the $\delta^{18}\text{O}$ of this continental ice, and the local hydrologic (evaporation-precipitation) balance. Additionally, complications arise due to the fact that change in temperature and change in the $\delta^{18}\text{O}$ of seawater do not occur uniformly around the globe. Clearly, deciphering which portion of the total $\delta^{18}\text{O}$ change derives from which fractionation effect is a large obstacle in interpreting these records, in addition to distinguishing local and/or regional signals from global variability.

2. APPROACH AND GOALS

To circumvent these problems and to avoid mistaken interpretations, it is important to develop parallel, independent proxy records that can provide constraints and confirmations to one another. Alternative proxies can also supply complimentary information to existing geochemical data, improving the understanding of regional-scale processes or helping to distinguish paleoenvironmental from paleobiologic variability. With multiple proxies, it is possible to synthesize different lines of evidence, forming a more complete picture of past climate changes, and to scrutinize theories concerning the causes of climate change.

The focus of this thesis is to further the development and application of two new, innovative paleoenvironmental proxies, namely interstitial-water $\delta^{18}\text{O}$ from deep-sea sediments and compound specific δD from sedimentary organic matter. These proxies are used in combination with marine carbonate $\delta^{18}\text{O}$ records to more precisely describe past periods of environmental change, including the reconstruction of sea-surface temperature and paleohydrologic conditions.

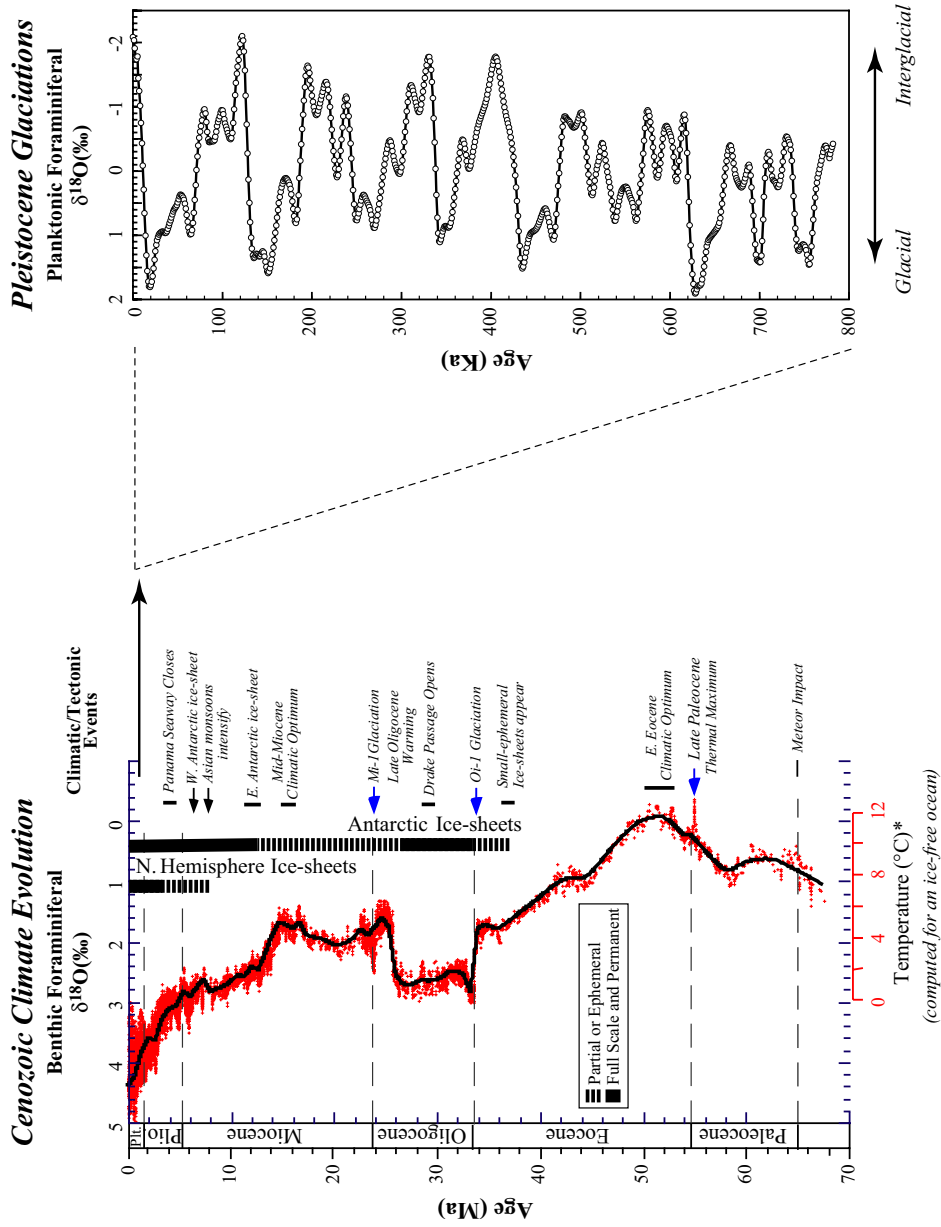


Figure 1.

Examples of climatic reconstructions based on the oxygen isotopic composition of foraminiferal calcite on different geologic time scales: the record of Cenozoic climate evolution as depicted by the $\delta^{18}\text{O}$ of benthic foraminifera over the past 70 million years (modified from Zachos *et al.* [2001]) and the record of Pleistocene glaciations based on planktonic foraminiferal $\delta^{18}\text{O}$ over the past 800 thousand years [Imbrie *et al.*, 1989]. More positive isotopic values indicate colder, glacial periods while less positive isotopic values indicate warmer, ice-free periods.

2.1. SEDIMENTARY PORE-FLUID OXYGEN ISOTOPIC COMPOSITION

In the past, researchers have attempted to isolate the glacial-interglacial change in the $\delta^{18}\text{O}$ value of seawater ($\delta^{18}\text{O}_{\text{sw}}$) from the total amount of isotopic change recorded in the carbonate shells of marine foraminifera ($\delta^{18}\text{O}_{\text{carb}}$) by subtracting out the portion due to temperature based on SST reconstructions from foraminiferal transfer functions, alkenone unsaturation ratios, Mg/Ca ratios, and other geochemical proxies (e.g., *Duplessy et al.* [1993]; *Rostek et al.* [1993]; *Cortijo et al.* [1999]; *Emeis et al.* [2000]; *Lea et al.* [2002]). Yet, many of these temperature proxies are subject to biological factors that are likely to vary between glacial and interglacial periods, such as seasonal growth patterns and habitat water depth (i.e., alkenones and transfer functions), and/or are ruled by geochemical processes that are not completely understood (i.e., Mg/Ca ratios and alkenones). A new approach to solving this problem was developed by *Schrag and DePaolo* [1993] who used measurements of the isotopic composition of deep-sea pore waters in conjunction with a diffusion-advection model of fluid transport to reconstruct the record of seawater $\delta^{18}\text{O}$ at the sediment-water interface; thus, eliminating the influence of temperature and obtaining a pure $\delta^{18}\text{O}_{\text{sw}}$ signal. Subsequent studies by *Schrag* and others [1996; 2002] have focused on quantifying the global average change in the $\delta^{18}\text{O}$ of seawater due to growth of continental ice sheets at the Last Glacial Maximum (LGM), which, based on a compilation of deep sites in the Atlantic Ocean, has been constrained to be $1.0 \pm 0.1\%$. Here, we go one step further and examine pore-fluid isotopic data from sites where deep and surface waters are well mixed at the LGM and hence, in addition to the global ice volume signal, experience some glacial-interglacial hydrologic change with which we can examine variations in paleosalinity. Using this approach, we are also able to estimate changes in marine surface temperatures by coupling the reconstructions of $\delta^{18}\text{O}_{\text{sw}}$ with measurements of $\delta^{18}\text{O}_{\text{carb}}$ from planktonic foraminifera.

The main difficulty with using sedimentary interstitial-water data to reconstruct changes in glacial-interglacial $\delta^{18}\text{O}_{\text{sw}}$ is that at any given site, changes in $\delta^{18}\text{O}_{\text{sw}}$ are due to both variations in global ice volume and local changes in seawater $\delta^{18}\text{O}$. These signals are not directly separable and, therefore, we must use the estimate of average global $\delta^{18}\text{O}$ change due to ice volume growth at the LGM as derived by *Schrag et al.* [1996; 2002] to determine the magnitude of local hydrologic variations. Locally, changes in $\delta^{18}\text{O}_{\text{sw}}$ can result from alterations in circulation patterns and the evaporation-precipitation balance. Circulation switches are mainly a problem for sites that are located in regions where fluctuations in the source of deepwater can occur. For instance, in the deep equatorial Atlantic there was a change from a North Atlantic Deep Water (NADW) source (as at present) to an Antarctic Bottom Water (AABW) source during the last glaciation [*Schrag et al.*, 1996; *Burns and Maslin*, 1999]. This shift is recorded in the pore-water $\delta^{18}\text{O}$ values because each deepwater source has a unique $\delta^{18}\text{O}$ signature (presently, NADW is enriched in ^{18}O relative to AABW). The sites investigated here are both bathed in waters origi-

nating from the surface-to-intermediate Atlantic. We assume that the source has been the same for the past ~20,000 years and, thus, interpret excess $\delta^{18}\text{O}_{\text{sw}}$ changes to result from variability in the local salinity.

2.2. COMPOUND-SPECIFIC HYDROGEN ISOTOPES OF SEDIMENTARY BIOMARKERS

The hydrogen and oxygen isotopic ratios of water change as a function of evaporation, enriching the water in heavy isotopic species (H_2^{18}O and ^1HDO), and with the addition of meteoric waters (including precipitation and continental runoff), which are depleted in the heavy isotopes with respect to seawater [Dansgaard, 1964]. Thus, the D/H and the $^{18}\text{O}/^{16}\text{O}$ ratios of water are complimentary tracers for the examination of regional water balance and as indicators of freshwater input. Additionally, due to the larger mass difference between its isotopes, hydrogen is more susceptible to fractionation, and hence, more sensitive to environmental perturbation than oxygen. In paleoclimatology, scientists have attempted to use the stable isotopes of hydrogen as a tool for climate reconstructions via kerogen from organic matter in lake sediments [Krishnamurthy *et al.*, 1995] and via fluid inclusions in speleothems [Harmon *et al.*, 1979]; for examining paleo-atmospheric circulation changes using groundwater [Sonntag *et al.*, 1978; Rozanski, 1985]; for examining paleo-humidity changes using cellulose in tree rings [Yapp and Epstein, 1977] and with ice cores [Jouzel *et al.*, 1982]; and for constraining temperature and atmospheric circulation changes from ice-core records (in conjunction with $\delta^{18}\text{O}$ values) [Johnson *et al.*, 1989; Anklin and Members, 1993]. Yet, complex sample preparation and analytical difficulties, in addition to the lack of calibration/validation for many of the above methods, have left hydrogen isotopes relatively unexploited in paleoclimate work, despite the fact that the isotopic composition of precipitation (including both δD and $\delta^{18}\text{O}$) is well established for correlating with local mean annual temperature and/or amount of precipitation [Dansgaard, 1964; Gat, 1996].

Due to recent advances in analytical techniques for measuring hydrogen isotopes [Prosser and Scrimgeour, 1995], the potential for utilizing the stable hydrogen isotopic composition from geologic media, such as organic material stored in deep-sea sediments, for paleo-hydrologic reconstructions, is substantial. Thus, one of the aims of this thesis was to examine the correlation between the hydrogen isotopic signature of modern marine surface waters and sedimentary organic matter as a first step in assessing the use of the stable isotopic ratios of hydrogen extracted from sediment cores as a new proxy for paleoclimate and paleoceanographic research. With this goal in mind, we have developed two new techniques for measuring the hydrogen isotopic composition of sedimentary organic matter to exploit this proxy for studies of paleoenvironment. Both experimental methods, one for analyzing the δD of bulk organic matter and the second for measuring the δD of individual organic compounds, are described and calibrated in this thesis.

Compound-specific analysis of organic material, in contrast to the more traditional method of bulk organic analysis, allows for the measurement of individual molecular components. Biomarkers, “molecular fossils” which are derived from once living organisms, can provide information on the organic matter in the source sediment including environmental conditions during deposition and burial, and degree of biodegradation and diagenesis. For paleoenvironmental applications, a biomarker must be chosen that spans the entire record of interest and that is present in abundances high enough to be measurable. Certain biomarkers are attributable to specific sources as some compounds are produced by only a restricted range of organisms growing in particular environmental conditions. Obviously, this can be very beneficial for studies trying to reconstruct environmental conditions in the geologic past. Here we focus on the examination of the D/H ratios in the lipid fraction of the organic matter as they have been shown to accurately record the D/H ratio of the surrounding environmental waters in freshwater aquatic plants [Sternberg, 1988]. Some of the important biomarkers targeted in this thesis for isotopic analysis are: *n*-alkanes, (C₁₇-C₃₃) produced by aquatic organisms and terrestrial plants; alkenones, (C₃₇-C₃₉) produced by prymnesiophyte algae; and steranes, produced by higher plants and phytoplankton [Volkman, 1986] (see sample molecular structures in Figure 2). Most hydrogen in lipidic biomarkers is bound to carbon and is nonexchangeable and therefore not easily prone to degradation [Schimmelmann *et al.*, 1999]. By focusing on singular molecular components that derive from specific groups of organisms, the compound-specific analysis of δD in a time series allows us to trace changes in source-water isotopic composition more precisely than would be possible using bulk sedimentary material.

3. THESIS OVERVIEW

The experimental methods are described in Chapter 2 focusing on the development of analytical techniques for measuring hydrogen isotopes extracted from sedimentary organic matter. Part I compares the original off-line method with the two recently developed, on-line methods, one devised to measure the δD of bulk organic material and the other for compound-specific δD analyses. Both of the new techniques use continuous flow systems, the first with an elemental analyzer (EA) connected to a mass spectrometer for sample pyrolysis, and the second with a gas chromatograph (GC) for separation of organic compounds prior to pyrolysis and admittance to the mass spectrometer. For comparison, measurements of *n*-alkane standards are presented for all methods. Part II describes the procedures used to extract the organic material from sediments, sterol derivatization experiments, and provides background information about the compounds chosen for the isotopic analyses and paleoenvironmental reconstructions.

Chapter 3 describes the results of a modern calibration between cell-water δD and compound-specific δD from biomarkers, carried out specifically for examining marine systems. In this study we determined the fractionation factor between C₃₇ alkenones and seawater by grow-

ing batch cultures of the coccolithophorid *Emiliana huxleyi* in a controlled laboratory environment in water of known isotopic composition. Results of this study indicate a constant fractionation of ~ -232 to -242‰ for both $C_{37:2}$ and $C_{37:3}$ alkenones [Andersen *et al.*, 2002]. We then apply this fractionation factor in Chapter 4, Part II, using the δD of biomolecules from these marine algae to track paleohydrologic change in the surface ocean of the Mediterranean Sea over the past $\sim 10,000$ years.

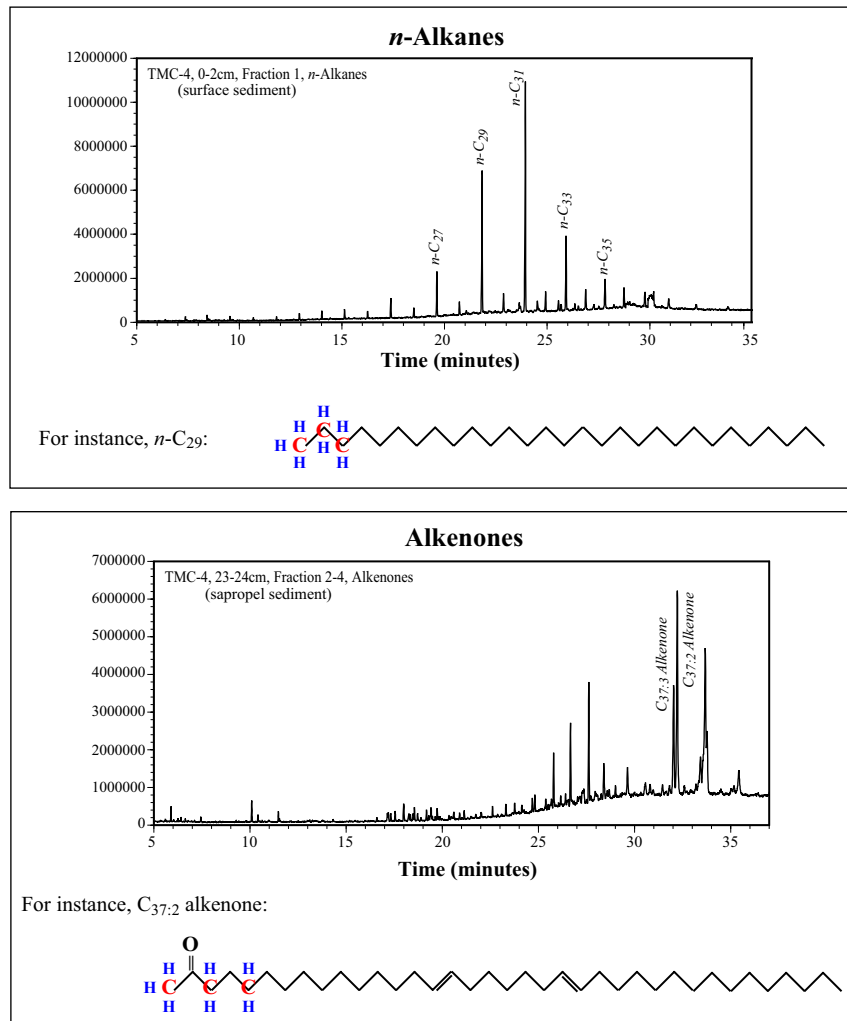


Figure 2. Examples of two organic compound classes, *n*-alkanes and alkenones, including schematic representations of molecular structures and total ion chromatograms from GC analyses. Individual compounds are labeled for illustration.

Chapter 4 is devoted to examination of the Mediterranean Sea. In Part I, overviews of modern Mediterranean circulation patterns and chemistry and Mediterranean paleoceanography are provided, focusing on the past $\sim 25,000$ years to include the LGM (~ 20 ka) and Sapropel Event 1 (S1), a period of increased organic matter deposition thought to coincide with warm and

wet climatic conditions ~9-6 thousand years ago. Data obtained during the MATER (Mass Transfer and Ecosystem Response) trans-Mediterranean cruise in June-July of 1999, including detailed water-column δD and $\delta^{18}O$ isotopic profiles and several geochemical analyses conducted on sediment short cores, are presented and used to illustrate the environmental changes that occurred in conjunction with the deposition of the youngest sapropel layer in the eastern Mediterranean. To evaluate the change in freshwater balance and potential circulation variations in the Mediterranean Sea during the deposition of S1 and at the LGM, we apply both of the new proxy methods described above. In Part II, compound-specific δD of *n*-alkane and alkenone biomarkers in sediments from the eastern basin of the Mediterranean Sea, also collected during the MATER cruise, are used to quantify the magnitude of marine surface water hydrologic change at S1. The molecular proxies reveal that the hydrogen isotopic composition of Mediterranean surface water was approximately 35‰ lighter at S1 than at present. In conjunction with the ~1.1‰ decrease in seawater $\delta^{18}O$ (see Part III), these isotopic values attest to the significant increase in freshwater input, yet still evaporative conditions and increased seasonality, that existed during sapropel formation in the eastern Mediterranean Sea. Part III presents the investigation of sedimentary interstitial-water $\delta^{18}O$ using samples obtained from ODP Leg 161, Site 976 in the western Mediterranean Sea to model the past oxygen isotopic composition of seawater to determine the sea surface salinity and temperature that existed at both the LGM and S1. Results suggest ~9°C of regional cooling and only a 0.2‰ enrichment in $\delta^{18}O$ due to salinity increase during the last glaciation. Alternatively, the model indicates a decrease of 1.1‰ in the $\delta^{18}O_{sw}$ value relative to present at S1 caused by freshwater input and reduced surface-water salinity. These results reveal that isotopically light water was circulating down to deep water depths and support the existence of an “anti-estuarine” thermohaline circulation pattern at this time.

A reconstruction of glacial-interglacial sea surface temperature and salinity changes from the Cariaco Basin based on the modeling of pore-water $\delta^{18}O$ is presented in Chapter 5. Samples for this study were obtained from ODP Leg 165, Site 1002 in the Cariaco Basin. The results indicate that tropical SST was approximately 3-4°C cooler, and seawater around 2-3 psu more saline, during the LGM than at present, and indicate that the sea surface temperature of the equatorial ocean is not as stable as previously thought. These findings support the theory that the tropics are an important factor and play a dynamic role in the global climate system.

An assessment of the two new proxies is provided in Chapter 6, including the respective pros and cons of each method in comparison to the traditional use of carbonate $\delta^{18}O$ for paleoenvironmental reconstructions. In addition, a few thoughts and suggestions about future research directions are discussed. The appendices include relevant measured data along with some references for the modeling work (derivations of the model formulas and a summary of sensitivity tests carried out) and an additional published study using compound-specific δD for paleoenvironmental reconstruction during the Messinian period.

4. REFERENCES

- Andersen, N., C. Klaas, H.A. Paul, and S.M. Bernasconi, Fractionation of stable hydrogen isotopes of C₃₇ alkenones from laboratory-cultured coccolithophorid *Emiliana huxleyi*, submitted to *Organic Geochemistry*, 2002.
- Anklin, M., and G.I.-C.P.G. Members, Climate instability during the last interglacial period recorded in the GRIP ice core, *Nature*, 364, 203-207, 1993.
- Broecker, W.S., and J. van-Donk, Insolation changes, ice volumes, and the O¹⁸ record in deep-sea cores, *Real Geophysical Space Physics*, 8, 169-198, 1970.
- Burns, S.J., and M.A. Maslin, Composition and circulation of bottom water in the western Atlantic Ocean during the last glacial, based on pore-water analyses from the Amazon Fan, *Geology*, 27, 1011-1014, 1999.
- Cortijo, E., S. Lehman, L. Keigwin, M. Chapman, D. Paillard, and L. Labeyrie, Changes in meridional temperature and salinity gradients in the North Atlantic Ocean (30°-72° N) during the last interglacial period, *Paleoceanography*, 14, 23-33, 1999.
- Dansgaard, W., Stable isotopes in precipitation, *Tellus*, 16, 436-467, 1964.
- Duplessy, J.C., E. Bard, L. Labeyrie, J. Duprat, and J. Moyes, Oxygen isotope records and salinity changes in the northeastern Atlantic ocean during the last 18,000 years, *Paleoceanography*, 8, 341-350, 1993.
- Emeis, K.-C., U. Struck, H.-M. Schulz, R. Rosenberg, S. Bernasconi, H. Erlenkeuser, T. Sakamoto, and F. Martinez-Ruiz, Temperature and salinity variations of Mediterranean Sea surface waters over the last 16,000 years from records of planktonic stable oxygen isotopes and alkenone unsaturation ratios, *Palaeogeography, Palaeoclimatology, Palaeoecology*, 158, 259-280, 2000.
- Epstein, S., R. Buchsbaum, H.A. Lowenstam, and H.C. Urey, Revised carbonate-water isotopic temperature scale, *Geological Society of America Bulletin*, 64, 1315-1325, 1953.
- Gat, J.R., Oxygen and hydrogen isotopes in the hydrologic cycle, *Annual Reviews in Earth and Planetary Sciences*, 24, 225-262, 1996.
- Harmon, R.S., H.P. Schwarcz, and J.R. O'Neil, D/H ratios in speleothem fluid inclusions: A guide to variations in the isotopic composition of meteoric precipitation?, *Earth and Planetary Science Letters*, 42, 254-266, 1979.
- Imbrie, J., A. McIntyre, and A. Mix, Oceanic response to orbital forcing in the late Quaternary: Observational and experimental strategies, in *Climate and Geo-Sciences*, edited by A. Berger, S. Schneider, and J.C. Duplessy, pp. 121-164, Kluwer Academic, Dordrecht, 1989.
- Johnson, S.J., W. Dansgaard, and J.W.C. White, *Tellus*, B41, 452-468, 1989.
- Jouzel, J., L. Merlivat, and C. Lorius, Deuterium excess in an East Antarctic ice core suggests higher relative humidity at the ocean surface during the last glacial maximum, *Nature*, 299, 688-691, 1982.
- Krishnamurthy, R.V., K.A. Syrup, M. Baskaran, and A. Long, Late glacial climate record of midwestern United States from the hydrogen isotope ratio of lake organic matter, *Science*, 269, 1565-1567, 1995.
- Lea, D.W., P.A. Martin, D.K. Pak, and H.J. Spero, Reconstructing a 350 ky history of sea level using planktonic Mg/Ca and oxygen isotope ratios from a Cocos Ridge core, *Quaternary Science Reviews*, 21, 283-293, 2002.
- Prosser, S.L., and C.M. Scrimgeour, High-precision determination of ²H/¹H in H₂ and H₂O by continuous-flow isotope ratio mass spectrometry, *Analytical Chemistry*, 67, 1992-1997, 1995.
- Rostek, F., G. Ruhland, F.C. Bassinot, P.J. Müller, L.D. Labeyrie, Y. Lancelot, and E. Bard, Reconstructing sea surface temperature and salinity using δ¹⁸O and alkenone records, *Nature*, 364, 319-321, 1993.

- Rozanski, K., Deuterium and oxygen-18 in European groundwaters: Links to atmospheric circulation in the past, *Chemical Geology*, 52, 349-363, 1985.
- Schimmelmann, A., M.D. Lewan, and R.P. Wintsch, D/H isotope ratios of kerogen, bitumen, oil and water in hydrous pyrolysis of source rocks containing kerogen types I, II, IIS, and III, *Geochimica et Cosmochimica Acta*, 63, 3751-3766, 1999.
- Schrag, D.P., J.F. Adkins, K. McIntyre, J.L. Alexander, D.A. Hodell, C.D. Charles, and J.F. McManus, The oxygen isotopic composition of seawater during the Last Glacial Maximum, *Quaternary Science Reviews*, 21, 331-342, 2002.
- Schrag, D.P., and D.J. DePaolo, Determination of $\delta^{18}\text{O}$ of seawater in the deep ocean during the Last Glacial Maximum, *Paleoceanography*, 8, 1, 1993.
- Schrag, D.P., G. Hampt, and D.W. Murray, Pore fluid constraints on the temperature and oxygen isotope composition of the glacial ocean, *Science*, 272, 1930-1932, 1996.
- Shackleton, N.J., Attainment of isotopic equilibrium between ocean water and the benthonic foraminifera genus *Uvigerina*: Isotopic changes in the ocean during the last glacial, *Centre National de la Recherche Scientifique Colloquium International*, 219, 203-209, 1974.
- Shackleton, N.J., and N.D. Opdyke, Oxygen isotope and paleomagnetic stratigraphy of equatorial Pacific core V28-238: Oxygen isotope temperatures and ice volumes on a 10^5 and 10^6 year scale, *Quaternary Research*, 3, 39-55, 1973.
- Sonntag, C., E. Klitzsch, P. Löhnert, K.O. Münnich, C. Junghans, U. Thorweihe, K. Weistroffer, and F.M. Swailem, Paleoclimate information from deuterium and oxygen-18 in C-14 dated north Saharan groundwaters: Groundwater information in the past, in *Isotope Hydrology*, pp. 569-581, International Atomic Energy Agency (IAEA), Vienna, 1978.
- Sternberg, L., D/H ratios of environmental water recorded by D/H ratios of plant lipids, *Nature*, 333, 59-61, 1988.
- Volkman, J.K., A review of sterol markers for marine and terrigenous organic matter, *Organic Geochemistry*, 9 (2), 83-99, 1986.
- Yapp, C.J., and S. Epstein, Climatic implications of D/H ratios of meteoric waters over North America (9500-22,000 B.P.) as inferred from ancient wood cellulose C-H hydrogen, *Earth and Planetary Science Letters*, 34, 333-348, 1977.
- Zachos, J., M. Pagani, L. Sloan, E. Thomas, and K. Billups, Trends, rhythms, and aberrations in global climate 65 Ma to Present, *Science*, 292, 686-693, 2001.

ANALYTICAL TECHNIQUES AND METHODS

PART I**DETERMINING THE HYDROGEN ISOTOPIC COMPOSITION OF ORGANIC MATERIAL****1. INTRODUCTION**

In earth sciences, the hydrogen isotopic composition of both natural waters and organic compounds has many applications as a natural tracer in hydrologic cycle modeling, environmental and climate change reconstruction, biogeochemical and petroleum research, and in physiological studies observing biological process pathways. Yet, rapid and accurate analytical techniques for the measurement of the D/H ratio of hydrogen have been slower to develop than for other light stable isotopes due to complications such as the low natural abundance of deuterium (0.0148%), the extreme sensitivity of hydrogen isotopes to fractionation, and the use of helium as a carrier gas. Described here are two recently developed, on-line continuous-flow techniques for the rapid analysis of the stable isotopes of hydrogen in organic materials. The first method is appropriate for measuring bulk organic samples and utilizes standard isotope laboratory instruments, a CNS elemental analyzer coupled to a classical isotope ratio mass spectrometer (Micro-mass Optima). The second method couples gas chromatography with mass spectrometry and is specialized for measuring the isotopic composition of individual organic molecules (compound-specific). Both methods are much faster, less labor intensive, and require smaller sample quantities than the traditional, off-line reduction method of converting organic matter to hydrogen gas.

Continuous-flow isotope ratio mass spectrometry (CF-IRMS) techniques have simplified the measurement and increased the utility of light stable isotopes (i.e., O, N, C, S, and H) in geological and biochemical studies. Compared to more traditional dual-inlet (DI) IRMS, which allows for very high-precision analyses, CF methods do not require conversion to gas prior to analysis, thus eliminating the often timely preparative separation of samples. CF analyses also require smaller initial sample size and allow for higher analytical throughput than classical methods. The ability to interface a gas chromatograph (GC) to a CF system is also of great benefit, allowing for compound-specific analysis of complex, organic mixtures.

Continuous-flow systems require an inert carrier gas, most commonly pure He gas, to sweep the analytes through the system to the mass spectrometer. The analysis of hydrogen isotopes requires the simultaneous detection of H₂ ($m/z = 2$; where m/z is atomic mass/charge) and HD ($m/z = 3$) to calculate the D/H ratio of a sample. However, with continuous flow systems, difficulty arises due to a potential interference of He with the detection of the HD⁺ ion as a substan-

tial $^4\text{He}^+$ beam (10^4 - 10^5 times larger than the HD^+ beam) is created in the source of the mass spectrometer. It has been supposed that conventional IRMS instruments do not have sufficient abundance sensitivity to resolve the HD^+ beam from the $^4\text{He}^+$ tail, thus causing saturation of the m/z 3 detector. For this reason, most investigators have employed a specially developed, high-dispersion mass spectrometer to ensure that there is no interference at m/z 3 from m/z 2 or m/z 4 [Prosser and Scrimgeour, 1995; Begley and Scrimgeour, 1997; Kelly *et al.*, 1998]. Here we describe a method for high-precision determination of D/H ratios in bulk organic materials employing a conventional mass spectrometer, initially designed for DI-IRMS analyses of H_2 using an extra, shorter spur for collecting the $^1\text{H}^1\text{H}^+$ m/z 2 ion beam (i.e., without the specialized, high-dispersion design). We demonstrate that it is possible to carry out these analyses using a traditional elemental analyzer - IRMS setup, both of which are quite standard stable-isotope laboratory equipment. Figure 1 shows schematic illustrations of the two analytical systems: in (A) the CF-IRMS system for measuring bulk organic matter is displayed, using a classic IRMS collector set-up, and in (B), the isotope-ratio-monitoring, gas chromatography-mass spectrometry (IRM-GC-MS) system for measuring compound-specific isotopic composition, using a mass spectrometer with high mass dispersion.

2. DESCRIPTION AND COMPARISON OF ANALYTICAL TECHNIQUES

The following section contains detailed descriptions, including analytical set-up and instrumentation, of the three methods used to determine the hydrogen isotopic composition of organic material. The traditional off-line method was used to measure standards in order to calibrate the isotopic values of the two new analytical techniques.

2.1. "TRADITIONAL" OFF-LINE SAMPLE REDUCTION METHOD

The off-line sample preparation method was used until the recent development of the on-line, continuous flow system. This technique is based on the methods developed by Friedman [1953] and Stump and Frazer [1973] and entails two steps in which, first, the hydrogen from an organic sample must be converted to gas and isolated, and second, the H_2 gas must be analyzed on a mass spectrometer (using a DI-IRMS system). Preparation is as follows: Sample (enough to produce 2 μl of water - approximately 5 mg dry/decarbonated sample) and copper oxide (approximately 2 g of precombusted CuO) are added to precombusted quartz reaction vessels and covered with quartz wool. Tubes are attached to a vacuum line and heated slightly with a heat gun to drive off any excess water and then left to evacuate for about 3 hours (oil samples are left for only 1 hour). After evacuation, tubes are sealed off with a flame and then heated for 4 hours at 850°C to initiate the reaction between organic matter and CuO . After cooling, samples are placed in a cracking device and attached to a vacuum line along with 2 pyrex tubes, one of which contains 40 mg of zinc (pre-heated with heat gun to drive off impurities). After evacuating any

present atmospheric gases, the sample tube is cracked and the gaseous reaction products, H_2O and CO_2 , are frozen into the pyrex tube containing the zinc using liquid N_2 . After this first transfer is complete, the CO_2 is then passed to the second pyrex tube using a methanol/dry ice mixture to retain the water in the first tube and liquid N_2 to collect the CO_2 . Both tubes are then sealed off with a flame. The zinc is used to reduce the collected H_2O by baking at 500°C for half an hour to produce H_2 gas ($\text{H}_2\text{O} + \text{Zn} \rightarrow \text{ZnO} + \text{H}_2$). The resultant pure H_2 is then analyzed on a Micromass Optima IRMS.

Clearly, this procedure is time intensive, requires relatively large sample quantities (i.e., ~ 5 mg of *pure* organic material), and, due to the preparative separation on a vacuum line, is particularly susceptible to isotopic fractionations and contaminations. Thus, the introduction of CF-IRMS methods, using on-line sample preparation, has been a welcome advance for isotope geochemists.

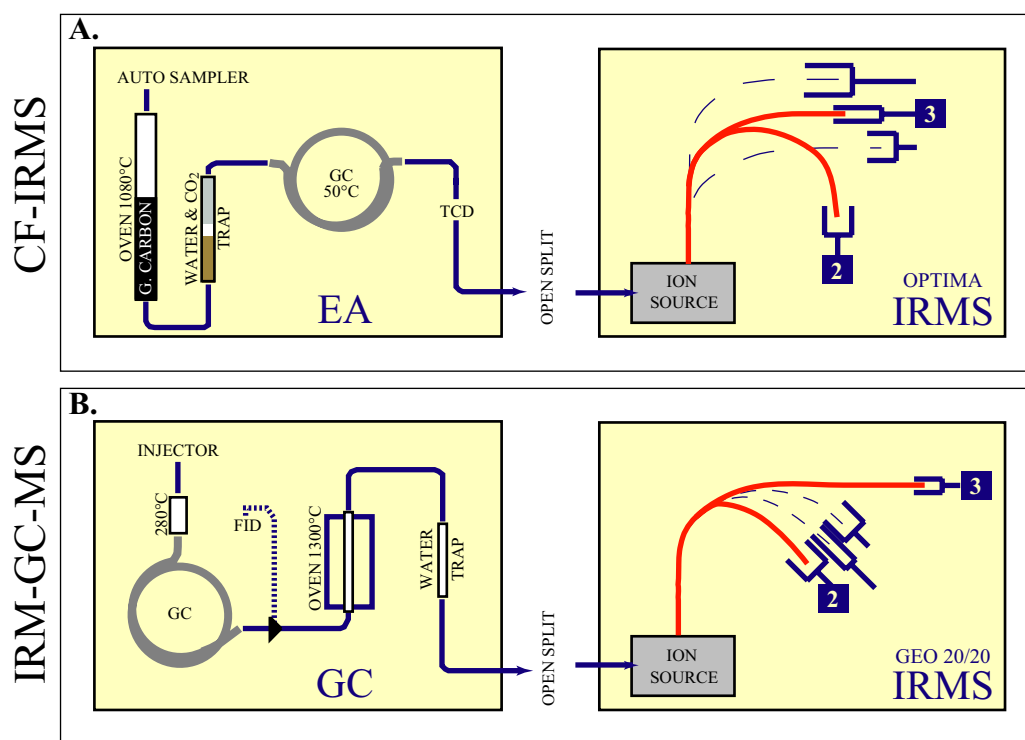


Figure 1. Schematic illustrations of on-line, continuous-flow mass spectrometry systems. (A.) CF-IRMS system with elemental analyzer connected to a Micromass Optima isotope ratio mass spectrometer with conventional collector set up (modified from Anderson [2000]). (B.) IRM-GC-MS system with gas chromatograph connected to a Europa Geo 20/20 high-dispersion isotope ratio mass spectrometer, specifically designed for increased precision analysis of D/H ratios.

2.2. CF-IRMS δD ANALYSIS OF BULK ORGANIC MATTER

This continuous-flow technique for measuring bulk organic material employs a Carlo Erba, CNS-2500 elemental analyzer (EA) interfaced via an open split to a Micromass Optima IRMS (Figure 1a). Solid and oil samples (approximately 200-300 μg , equivalent to $\sim 30 \mu\text{g}$ hydrogen) are wrapped in tin capsules and are dropped via autosampler into a pyrolysis oven at 1080°C . A modified quartz reaction column (i.e., 460 mm long tube (20 mm o.d., 18 mm i.d.) attached to a 120 mm long capillary (6 mm o.d., 2 mm i.d.) [Farquhar *et al.*, 1997]) is filled with quartz wool and 7-10 cm of glassy carbon to the zone of maximum temperature in the oven (modified from Werner *et al.* [1996]). Glassy carbon (Sigradur G, 3150-4000 μm grit) is used to provide a source of elemental-C necessary to carry out the Schütze-Unterzaucher reaction ($\text{H}_2\text{O} + \text{C} \rightarrow \text{CO} + \text{H}_2$) during water pyrolysis. The main reaction products, H_2 and CO , are then carried by a stream of helium gas (grade 6.0; flow rate of 80 ml/min) through a chemical trap containing magnesium perchlorate and Carbsorb for removal of any present water vapor and CO_2 , respectively. The pyrolysis gases are then passed through a GC column (Molecular Sieve 5Å; 1 m x 4 mm i.d.) heated to 50°C to separate H_2 from the other constituents. A thermal conductivity detector (TCD) is used to detect the reaction products as they flow out of the GC and enter the mass spectrometer where the ratio m/z 2 to m/z 3 is determined. The ion source pressure was $2\text{--}3.5 \times 10^{-6}$ mbar under typical continuous-flow conditions with average 250 μg samples giving a major beam intensity of around 5 nA. The two ion beams H_2 , m/z 2, and HD , m/z 3, are measured simultaneously and the peak areas integrated over time (Figure 2). Figure 3 illustrates the sufficient physical separation between the m/z 4 (derived from He^+) and m/z 3 (from HD^+) beams generated in the ion source of the Optima mass spectrometer.

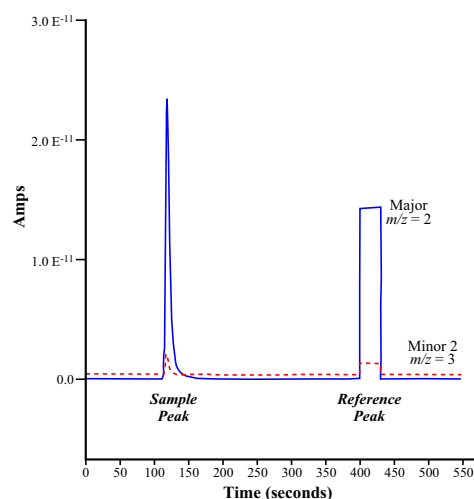
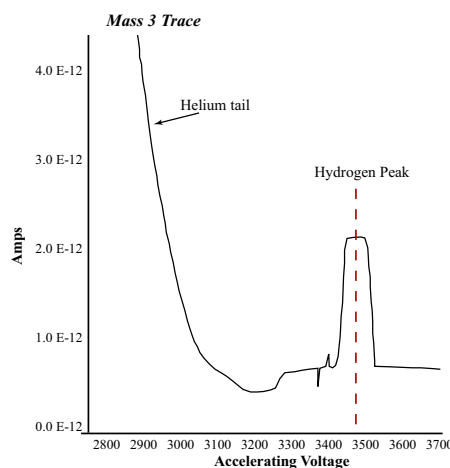


Figure 2. Sample analysis on the CF-IRMS system showing traces of the m/z 2 (H_2) and m/z 3 (HD) beams through time. Sample peak is followed by the reference peak.

Figure 3. Scan of accelerating voltage vs. m/z 3 peak intensity to show the sufficient separation between the helium tail and the hydrogen peak in the source of the Optima mass spectrometer.



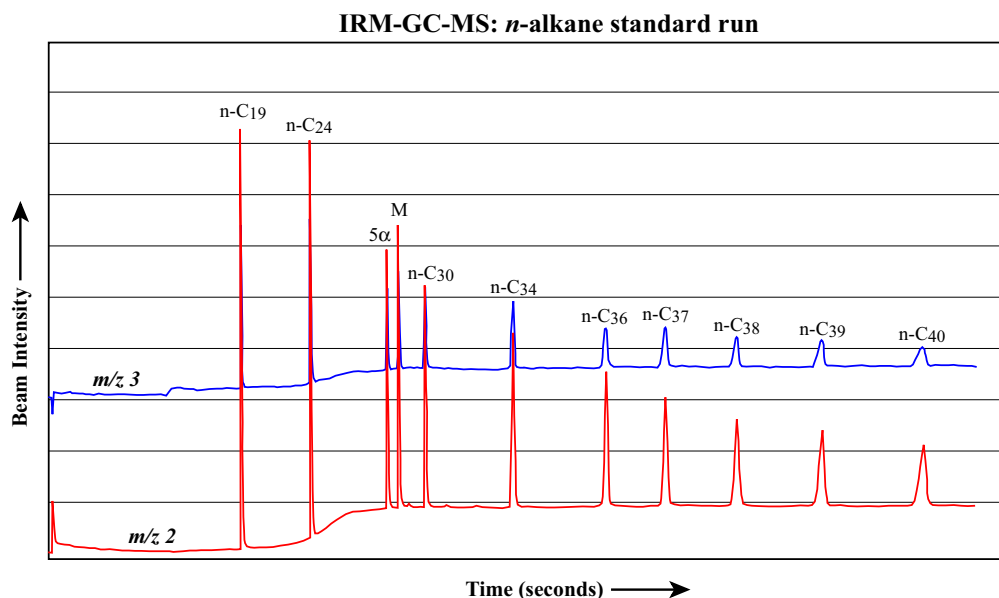
2.3. IRM-GC-MS COMPOUND-SPECIFIC δD ANALYSIS

The δD values of individual organic compounds were obtained by isotope-ratio monitoring gas chromatography-pyrolysis-mass spectrometry using a high-dispersion mass spectrometer [Scrimgeour *et al.*, 1999] (Figure 1b). Extracted organic matter dissolved in solvent (>200 ng/ μ l of each compound) is injected (1-3 μ l) at 280°C in splitless mode. Compounds are separated using a Hewlett-Packard 6890 Series gas chromatograph fitted with a high-capacity, mega-bore GC column (50 m, 0.53 mm i.d., 1 μ m film) using He as the carrier gas. The GC oven is temperature programmed, beginning at 50°C and increasing at 30°/min to 150°C then 8°/min to 230°C and finally at 6°/min to a maximum temperature of 320°C where it is held constant until all compounds have eluted (for 10-30 minutes). The column effluent then flows through an alumina tube heated to 1300°C where pyrolysis of compounds occurs converting organic compounds into H₂, CO, elemental C, and possibly small amounts of CH₄. A mega-bore molesieve (5Å) is used to separate any methane, and water is trapped by a nafion tube. Hydrogen gas is introduced via open split into a Geo 20-20 (PDZ Europa) isotope ratio mass spectrometer, specifically designed to produce a large physical separation between the ²H¹H⁺ and ⁴He⁺ beams [Prosser and Scrimgeour, 1995] for measuring D/H ratios in continuous flow mode. The D/H ratios of individual compounds are calculated by integrating the mass-2 and mass-3 signals (Figure 4).

3. RESULTS AND DISCUSSION

3.1. H₃⁺ FORMATION AND CORRECTION

Measurement of the ²H/¹H ratio is additionally complicated by the formation of H₃⁺ ions in the ion source, the intensity of which depends on the frequency of H-H collisions. The mass spectrometer cannot distinguish between the H₃⁺ ions and the HD⁺ ions, thus both are detected by the m/z 3 collector, resulting in an overestimation of the mass ²H/¹H ratio. Correction for this is possible as a linear relationship exists between the measured D/H ratio and the pressure of H₂

**Figure 4.**

Scan of beam intensity (m/z 2 and 3) vs. time from an IRM-GC-MS run on the Europa Geo 20/20. Individual peaks represent specific organic compounds, here a mixture of *n*-alkanes (including n -C₁₉ to n -C₄₀) from the house standard. Note increase in background between n -C₁₉ and 5α due to changing column bleed (caused by increasing GC temperature). Also note the large reduction and slight broadening of peak height with time and increasing molecular weight (compounds are approximately the same concentration in the mixture).

in the ion source (see discussions by *Prosser and Scrimgeour* [1995] and *Sessions et al.* [1999]). The H_3^+ correction is especially important in chromatographic analyses where peak intensities are difficult to standardize and sometimes vary over a large range depending on sample quantity and composition. Here, unique H_3^+ corrections were derived for each day of analyses by examining the peak intensity vs. D/H ratio for varying sample sizes of the standard materials.

3.2. STANDARDIZATION

Reference materials with calibrated hydrogen isotopic compositions were acquired from the National Bureau of Standards (NBS, United States) and from the International Atomic Energy Agency (IAEA, Vienna, Austria). Here NBS 22 ($\delta D = -118.5 \pm 2.8\%$) and PEF 1 polyethylene foil from IAEA ($\delta D = -100.3 \pm 2.0\%$) were used. Organic samples, 99.5% pure *n*-alkanes of varying molecular weights, were obtained from Fluka Chemie (Switzerland). Pressed tin cups (4 x 3.2 mm) and modified reaction tubes were purchased from Elemental Microanalysis Ltd. (Devon, UK).

All δD values presented here are reported in permil notation relative to the VSMOW standard: $\delta D\%_{\text{VSMOW}} = \left(\left(\frac{[{}^2\text{H}]_{\text{sample}}/[{}^1\text{H}]_{\text{sample}}}{[{}^2\text{H}]_{\text{standard}}/[{}^1\text{H}]_{\text{standard}}} \right) - 1 \right) \times 1000$. The two new on-line methods were calibrated to the international δD scale by first analyzing Vienna

Standard Mean Ocean Water (VSMOW = 0.0‰) and Vienna Standard Light Arctic Precipitation (VSLAP = -428‰) water standards and NBS 22 and PEF organic standards with the traditional off-line approach and then measuring the organic standards with the CF-IRMS method (i.e., both using the Optima mass spectrometer). After completing the calibration of bulk organic materials using the CF-IRMS technique, a series of several *n*-alkanes was measured using the same method and then used to create an in-house standard for calibration between the CF-IRMS and IRM-GC-MS systems. In the next section, a comparison of standard measurements and results is provided.

3.3. CF-IRMS CALIBRATION

The results of the isotope analyses of the organic samples and standards using the CF-IRMS method are shown in Table 1. Using the continuous-flow technique, the precision of analyses within a run are between ~1.5 and 3.5‰, and the reproducibility of measurements between runs ranges from 0.5 to 3.5‰. The precision of analyses using this instrumental set up is comparable to results of *Kelly et al.* [1998] who report a precision of 1.1 to 3.3‰ for measurements of organic materials using an elemental analyzer with a high-dispersion mass spectrometer; these results strongly support our conclusion that a conventional mass spectrometer is sufficient for such analyses. To ascertain the accuracy of the determined δD values derived by this technique, two international standards, NBS 22 oil and IAEA-PEF foil, were analyzed. The measured values agree well with the published standard values (Table 2), though it would be beneficial to include other standards with less similar δD values to resolve the range of accuracy of the method. Analyses of water samples, including SMOW and SLAP standards, produced inconsistent results with this technique and thus were not used for calibrating the continuous-flow measurements. We recommend that samples and standards of like material are used for calibration of D/H ratios.

To evaluate the accuracy and reproducibility of the CF-IRMS analytical technique for measuring the hydrogen isotopic composition of organic materials, a subset of the *n*-alkane samples acquired was also analyzed using the traditional, off-line method for chemical conversion of organic matter to hydrogen gas. The results of this comparison are shown in Table 2. The excellent agreement (better than $\pm 0.70\%$) between the D/H ratios derived from these two, completely different analytical techniques again supports the utility of conventional mass spectrometers for these measurements.

The hydrogen isotopic ratio abundance of natural organic substances may vary widely, thus it is important to ensure that each individual analysis is not influenced or contaminated by previous samples. Table 3 displays the results of sequential measurements and shows that memory effects for this technique are insignificant when compared to the analytical precision. The test samples ranged in isotopic composition from -76.23 to -291.95‰, thus differing by approx-

imately 215‰. Throughout the entire run listed in Table 3, there is only one sample showing a hint of a memory effect. Sample number 53 is slightly depleted (-83.67‰) with respect to the other *n*-C₃₄ samples measured (average -76.23‰), though as the δ D value of the previous sample was approximately -217‰, this influence is clearly not very significant.

Table 1.

Results of on-line CF-IRMS measurements of organic compounds including a list of the measured δ D values, mean value and standard deviation, and number of samples analyzed (*n*). Lines within each sample separate analyses made on different days. Measured $\delta^{13}\text{C}$ data are also given for reference.

Organic Material	Measured δ D	Mean \pm s.d.	<i>n</i>	Measured $\delta^{13}\text{C}$	\pm s.d.
NBS-22	-----	-118.40 \pm 3.26	35		
		-117.90 \pm 1.75	19		
		-118.53 \pm 2.96	40		
PEF foil	-----	-101.09 \pm 2.82	6		
		-98.89 \pm 3.69	15		
		-100.22 \pm 3.12	7		
n-C₁₉	-142.51, -139.72, -140.01, -141.70, -137.47, -139.41	-140.14 \pm 1.78	6	-32.63	0.03
	-139.56, -146.98, -139.49, -140.14, -138.65, -143.90, -143.13	-141.69 \pm 3.05	7		
	-136.61, -135.67, -138.98, -139.79, -134.59, -134.31, -136.81, -140.97	-137.22 \pm 2.45	8		
n-C₂₄	-83.76, -90.16, -89.24, -85.60, -83.48, -82.51, -86.24, -85.26	-85.78 \pm 2.72	8	-33.50	0.07
	-82.56, -90.48, -90.83, -86.82, -88.10	-87.76 \pm 3.35	5		
	-89.01, -83.56, -86.67, -86.60, -80.52, -84.22, -89.88	-85.78 \pm 3.26	7		
n-C₃₀	-217.28, -213.18, -216.64, -212.76, -219.90, -212.50	-215.38 \pm 3.02	6	-29.41	0.02
	-217.47, -215.36, -214.46, -218.22, -215.00, -221.06, -218.30	-217.12 \pm 2.34	7		
n-C₃₄	-78.71, -78.02, -76.89, -74.29, -76.67, -72.83	-76.23 \pm 2.25	6	-31.82	0.05
n-C₃₆	-250.62, -249.50, -242.51, -251.82, -251.10, -251.62	-249.53 \pm 3.54	6	-28.84	0.03
	-251.52, -252.81, -251.24, -253.02, -259.05	-253.53 \pm 3.18	5		
	-247.41, -247.23, -254.34, -250.89, -250.41	-250.06 \pm 2.92	5		
n-C₃₇	-93.61, -92.80, -93.06, -98.64, -91.44, -94.98	-94.09 \pm 2.51	6	-29.29	0.02
n-C₃₈	-104.68, -100.75, -106.23, -108.48, -102.40, -103.73	-104.38 \pm 2.75	6	-31.17	0.05
	-112.18, -103.3, -107.44, -107.24, -109.37	-107.91 \pm 3.25	5		
n-C₃₉	-100.92, -99.59, -96.84, -94.10, -95.46	-97.38 \pm 2.84	5	-29.87	0.08
n-C₄₀	-190.58, -189.79, -189.72, -188.66, -190.84, -186.65, -189.78	-189.43 \pm 1.41	7	-29.66	0.03
	-186.95, -184.09, -182.22, -186.62, -186.09, -190.46	-186.07 \pm 2.80	6		
5α-cholestane	-289.16, -289.81, -292.57, -294.78, -292.71, -288.66, -295.99	-291.95 \pm 2.84	7	-26.30	0.05

Table 2.

Summary of results comparing the average of measurements from the on-line CF-IRMS technique vs. the traditional off-line DI-IRMS method.

Sample	$\delta D\%$ CF	Std Dev	$\delta D\%$ off-line	Std Dev	Published value
PEF foil	-100.07	3.41	-99.57	---	-100.3 \pm 2.0
NBS 22	-118.28	2.65	---	---	-118.5 \pm 2.3
n-C ₁₉	-139.54	3.10	-140.92	0.13	
n-C ₂₄	-86.28	3.03	-85.40	---	
n-C ₃₀	-216.32	2.71	-215.61	1.95	
n-C ₃₆	-250.94	3.53	-249.56	4.12	

3.4. IRM-GC-MS CALIBRATION

Calibrating the IRM-GC-MS method is a bit more difficult. The continuous elution of compounds from the GC complicates the isotopic calibration of this technique with the organic-material standards used for the other methods. In addition, the variable temperature program used for the gas chromatography causes changes in column bleed, and hence, in background conditions (Figure 4), further complicating the calculation of peak area and height and the peak integration. For these reasons, standards and analytes should (ideally) be introduced into the mass spectrometer at conditions and retention times that are as similar as possible. Yet, the introduction of standards should not interfere with the measurement of the analytes of interest. To satisfy these criteria, we created a standard of 11 homologous *n*-alkanes (*n*-C₁₉ to *n*-C₄₀ at \sim 300 ng/ μ l concentration; Figure 4) to be used as the in-house laboratory standard. The hydrogen isotopic composition of these compounds were determined independently using the traditional off-line method and the CF-IRMS technique (Tables 1 and 2).

Each D/H ratio reported here represents the average of 4-8 measurements of compounds injected at varying volumes. Multiple injections are necessary to make the H₃⁺ corrections and to monitor instrument performance. Repeat measurements of the *n*-alkane standard using the IRM-GC-MS method shows the reproducibility of analyses to be typically better than 1-3‰ for short-chain compounds (<*n*-C₃₆) and \sim 5-6‰ for compounds of higher molecular weight. The precision of analyses using this instrumental set up is comparable to results of *Sessions et al.* [1999] who report precisions of \sim 5‰ for compound-specific measurements of organic materials (up to *n*-C₃₃). The large range in δD values of the individual *n*-alkanes included in the standard mixture, and the accuracy with which we can measure these values, suggests that memory effects with this system are also very small and/or insignificant.

Table 3.
Test for memory effect using the CF-IRMS method.

Sample Name	Sample Number	Measured $\delta D\%$	Mean $\delta D\%$	Standard Deviation
NBS 22	12	-119.34		
NBS 22	13	-123.07		
NBS 22	15	-116.19		
NBS 22	16	-114.08		
NBS 22	17	-120.61		
NBS 22	18	-116.16		
NBS 22	19	-121.42		
NBS 22	20	-118.5	-118.67	3.04
n-C ₁₉	21	-136.61		
n-C ₁₉	22	-135.67		
n-C ₁₉	23	-138.98		
n-C ₁₉	24	-139.79		
n-C ₁₉	25	-134.59		
n-C ₁₉	26	-134.31		
n-C ₁₉	27	-136.81		
n-C ₁₉	28	-140.97	-137.22	2.45
n-C ₂₄	29	-89.01		
n-C ₂₄	30	-83.56		
n-C ₂₄	31	-86.67		
n-C ₂₄	32	-86.60		
n-C ₂₄	33	-80.52		
n-C ₂₄	35	-84.22		
n-C ₂₄	36	-89.88	-85.78	3.26
5 α -cholestane	37	-289.16		
5 α -cholestane	38	-289.81		
5 α -cholestane	39	-292.57		
5 α -cholestane	40	-294.78		
5 α -cholestane	41	-292.71		
5 α -cholestane	42	-288.66		
5 α -cholestane	43	-295.99	-291.95	2.84
n-C ₃₀	45	-217.47		
n-C ₃₀	46	-215.36		
n-C ₃₀	47	-214.46		
n-C ₃₀	49	-218.22		
n-C ₃₀	50	-215.00		
n-C ₃₀	51	-221.06		
n-C ₃₀	52	-218.30	-217.12	2.34
n-C ₃₄	53	-83.67		
n-C ₃₄	54	-78.71		
n-C ₃₄	56	-78.02		
n-C ₃₄	57	-76.89		
n-C ₃₄	58	-74.29		
n-C ₃₄	59	-76.67		
n-C ₃₄	60	-72.83	-76.23	2.25

PART II

ORGANIC COMPOUNDS: SELECTION AND ANALYSIS

1. BIOMARKERS

Organisms are sensitive to geochemical and hydrographic changes in the environment in which they grow and record this information in their organic material that is then deposited in the sediments after they die. Investigations of organic matter extracted from sediment cores can be used to reconstruct the conditions of previous periods and thus, help us to understand environmental and climatic variations that occurred in the past. Biomarkers are complex organic compounds composed of carbon, hydrogen, and other elements that are found in rocks, sediment, and petroleum. Their basic molecular structures remain essentially intact through the processes of sedimentation and early burial causing only minor changes in structure from that of their parent organic molecules in living organisms. The advantage of using compound-specific isotopes for paleoenvironmental research is that individual organic compounds allow for the investigation of a distinct biological source restricting the number of parameters that influence the isotopic signal. The following section provides a brief summary of some of the more important biomarkers that have been targeted for paleoenvironmental research and the extraction techniques used to isolate the individual compounds.

1.1. N-ALKANES

Stable molecules of carbon and hydrogen that contain only single bonds (saturated hydrocarbons) are called alkanes. When the carbon atoms have a linear arrangement, these compounds are called normal (or *n*-) alkanes. These compounds are likely the degradation products of biologically produced alcohols, carboxylic acids, or other *n*-alkanes, which are used in marine organisms for buoyancy and in terrestrial plants for building protective tissues and biosynthesis of waxes. Alkanes occur in virtually all geologic samples containing organic matter, thus, they are less useful as biomarkers because of their multiple, non-specific origins. Bimodal *n*-alkane distributions and those skewed toward the range *n*-C₂₃ to *n*-C₃₀ are usually associated with terrestrial higher plant waxes. Certain algae also contain higher molecular weight *n*-alkanes and this parameter should be used with caution as an environmental indicator [*Peters and Moldowan, 1993; Chikaraishi and Naraoka, 2001*].

1.2. ALKENONES

Alkenones (unsaturated methyl and ethyl ketones) are only biosynthesized by a specific group of haptophyte algae and are produced most notably by *Emiliana huxleyi* and *Gephyrocapsa spp.* [*Marlowe et al., 1984; Marlowe et al., 1990*] in the upper 50 m of open marine envi-

ronments. Recent studies suggest that these lipids are used for cellular metabolic storage [Epstein *et al.*, 2001]. These compounds have been widely used in paleoceanography for assessing past sea surface temperature changes, since the degree of ketone unsaturation is dependent on growth temperature [Brassell *et al.*, 1986; Prahl and Wakeham, 1987], and reconstructing paleo-pCO₂ [Jasper and Hayes, 1990] in the oceans. Here we focus on the unsaturated C₃₇ alkenones (C_{37:2} or Heptatriaconta-15E,22E-dien-2-one; and C_{37:3} or Heptatriaconta-8E,15E,22E-trien-2-one) as they are the most abundant in our sedimentary samples.

1.3. STERANES

Steranes are biomarkers created by the conversion of sterols due to dehydration and reduction that occurs during diagenesis. The precursor steroid/sterol compounds generally have one or more oxygen atoms and double bonds that are converted into more stable, often saturated, hydrocarbons that are preserved in sedimentary samples. Sterols are found in most higher plants and algae acting to increase the rigidity and strength of membranes, but they are rare or absent in procaryotic organisms [Volkman, 1986]. Specific sterane biomarkers are known commonly as cholestane (C₂₇), ergostane (C₂₈), and sitostane (C₂₉). Dinosterane is a 4-methylsterane (cholestane with three additional methyl groups, e.g., 4 α ,23,24-trimethylcholestane) and is specifically derived from dinoflagellates in marine and non-marine environments [Goodwin *et al.*, 1988].

1.4. FATTY ACIDS

Fatty acids are compounds composed of a long hydrocarbon chain attached to a carboxylic acid group (COOH). The chain is typically linear and may contain 4-30 carbon atoms and usually has an even number of carbons. They occur as both saturated and with varying degrees of unsaturation (i.e., monounsaturated and polyunsaturated). Short-chain fatty acids represent microbial origin, while long-chain fatty acids indicate plant-derived material [Duan *et al.*, 1997]. Some of the common fatty acids are: palmitic acid (hexadecanoic acid; 16 carbons), stearic acid (octadecanoic acid; 18 carbons), oleic acid (9-octadecenoic acid; 18 carbons), and linoleic acid (9,12-octadecenoic acid; 18 carbons). The fatty acids 20:5 n-3 and 22:6 n-3 are biomarkers specific to phytoplankton.

2. EXTRACTION TECHNIQUE

All sediments are freeze dried and thoroughly homogenized with an agate mortar and pestle prior to extraction. Depending on the %TOC content of the sediment, enough sediment is weighed out to extract approximately 0.5 to 1 g of organic carbon. Bulk organic material is extracted with 25 ml of solvent per 5 g of sediment by ultrasonic agitation (UP 200S sonic disrupter probe; 200W; amplitude 0.5; pulse 0.5) for 3 minutes each, using 2x-distilled solvents in order of decreasing polarity; here we use methanol (CH₃OH), methanol:dichloromethane (DCM)

mixture (1:1 v/v), and dichloromethane (CH_2Cl_2). Samples are centrifuged (Hettich EBA22) at 3600 rpm for 6 minutes to separate the extract from the sediment and then the three extracts are combined. Marine samples are desalted by adding 50 ml of 2x-distilled water, shaking well, and then letting the liquid settle (often overnight). After the liquid has separated into two phases (one a DCM-rich phase, including the dissolved organics; the other a water/methanol-rich phase containing the dissolved salts), the water phase is siphoned off and any remaining water is absorbed with water-free Na_2SO_4 . Lacustrine samples are treated with activated copper trimmings (oxidized in 30% HCl, then rinsed in deionized water and methanol) to remove any sulfur present in the extract. Finally, the sample is concentrated on a rotary evaporator, transferred to a sample vial, and then dried under a pure N_2 stream.

Bulk organic extracts are further fractionated into compound classes via column chromatography. This step is necessary to decrease the potential co-elution of compounds from the GC so that we can ensure the analysis of single molecular species for isotope ratio measurements. A glass column (~8.5 cm long and 1.1 cm inner diameter) is filled with a ~1 cm long quartz-wool plug and 3.5 g of silica gel (Merck 60; grain size 0.063-0.2 mm; pre-heated at 500°C to drive off contaminants). The prepared column is rinsed multiple times with methanol, DCM, and finally n-hexane prior to use and should have a solvent flow speed of ~3.2 ml/min. Using a method modified from *Prahl et al.* [1989] and solvents in order of increasing polarity, the fractions collected were:

Fraction 1	(15ml n-Hexane)	Hydrocarbons (<i>n</i> -alkanes / Hopanes)
Fraction 2	(15ml n-Hexane + 15ml Toluene)	
Fraction 3	(10ml n-Hexane + 10ml Toluene)	
Fraction 4	(9.5ml n-Hexane + 500 μ l Ethylacetate)	Alkenones
Fraction 5	(10.6ml n-Hexane + 1.8ml Ethylacetate)	Sterols / Alcohols
Fraction 6	(10ml n-Hexane + 2.5ml Ethylacetate)	Sterols / Alcohols
Fraction 7	(10ml n-Hexane + 10ml Ethylacetate)	

Both the bulk extracts and individual organic fractions of each sediment sample were analyzed via gas chromatography-mass spectrometry (GC-MS) on an Hewlett Packard 6890 Series GC coupled to a HP 5973 Mass Selective Detector to identify organic compounds of interest. 1 μ l aliquots of the extracts were injected in split mode (1:20 to 1:5) at 250°C and analyzed using a HP-5MS column (cross-linked 5% PH ME Siloxane; 30 m x 0.25 mm x 0.25 μ m film thickness) (or with an HP-1 column, Methyl Siloxane; 50 m x 320 μ m x 0.17 μ m nominal, from March 7 to August 23, 2000) with helium as the carrier gas and a temperature program as follows: starting at 50°C then heating 30°/min to 150°C, with 8°/min to 230°C, with 6°/min to 320°C and then constant for 10 minutes (total time 38 minutes). Compounds were identified

based on mass spectra and gas chromatographic retention times. A list of characteristic ions for some of the different compound classes is given below for reference:

compound class	<i>m/z</i>
<i>n</i> -alkanes	57, 71, 85
Triterpanes (Hopanoids)	191, 369
Squalene (C ₃₀ H ₆₂)	183, 422
Botryococcane (C ₃₄ H ₇₀)	183, 238, 239, 294, 295
C ₃₇ Alkenones	528-530
Steranes (diasteranes)	261; 217 (218)
5 α (β) steranes	149 (151)
14 α (β) steranes	217 (218)
4-methyl steranes (e.g., dinosteranes)	231 (98, 414)
17 α (β) steranes	257 (259)
Gammacerane (C ₃₀ H ₅₂)	191, 412

PART III

REFERENCES

- Begley, I.S., and C.M. Scrimgeour, High precision $\delta^2\text{H}$ and $\delta^{18}\text{O}$ measurement for water and volatile organic compounds by continuous-flow pyrolysis isotope ratio mass spectrometry, *Analytical Chemistry*, *69*, 1530-1535, 1997.
- Brassell, S.C., G. Eglinton, I.T. Marlowe, U. Pflaumann, and M. Sarnthein, Molecular stratigraphy: A new tool for climatic assessment, *Nature*, *320*, 129-133, 1986.
- Chikaraishi, Y., and H. Naraoka, Hydrogen and carbon isotopic compositions of individual long-chain *n*-alkanes in a lake system with relevance to their sources, in *20th International Meeting on Organic Geochemistry*, pp. 121-122, Nancy, France, 2001.
- Duan, Y., Q.B. Wen, G.D. Zheng, B.J. Luo, and L.H. Ma, Isotopic composition and probable origin of individual fatty acids in modern sediments from Ruergai Marsh and Nansha Sea, China, *Organic Geochemistry*, *27*, 583-589, 1997.
- Epstein, B.L., S. D'Hondt, and P.E. Hargraves, The possible metabolic role of C_{37} alkenones in *Emiliana huxleyi*, *Organic Geochemistry*, *32*, 867-875, 2001.
- Farquhar, G.D., B.K. Henry, and J.M. Styles, A rapid on-line technique for determination of oxygen isotope composition of nitrogen-containing organic matter and water, *Rapid Communications in Mass Spectrometry*, *11*, 1554-1560, 1997.
- Friedman, I., Deuterium content of natural waters and other substances, *Geochimica et Cosmochimica Acta*, *4*, 89-103, 1953.
- Goodwin, N.S., A.L. Mann, and R.L. Patience, Structure and significance of C_{30} 4-methyl steranes in lacustrine shales and oils, *Organic Geochemistry*, *12*, 495-506, 1988.
- Jasper, J.P., and J.M. Hayes, A carbon isotope record of CO_2 levels during the late Quaternary, *Nature*, *347*, 462-464, 1990.
- Kelly, S.D., I.G. Parker, M. Sharman, and M.J. Dennis, On-line quantitative determination of $^2\text{H}/^1\text{H}$ isotope ratios in organic and water samples using an elemental analyser coupled to an isotope ratio mass spectrometer, *Journal of Mass Spectrometry*, *33*, 735-738, 1998.
- Marlowe, I.T., S.C. Brassell, G. Eglinton, and J.C. Green, Long chain unsaturated ketones and esters in living algae and marine sediments, *Organic Geochemistry*, *6*, 135-141, 1984.
- Marlowe, I.T., S.C. Brassell, G. Eglinton, and J.C. Green, Long-chain alkenones and alkyl alkenoates and the fossil coccolith record of marine sediments, *Chemical Geology*, *88*, 349-375, 1990.
- Peters, K.E., and J.M. Moldowan, *The Biomarker Guide: Interpreting molecular fossils in petroleum and ancient sediments*, Prentice Hall, New Jersey, 1993.
- Prahl, F.G., L.A. Muehlhausen, and M. Lyle, An organic geochemical assessment of oceanographic conditions at Manop site C over the past 26,000 years, *Paleoceanography*, *4*, 410-510, 1989.
- Prahl, F.G., and S.G. Wakeham, Calibration of unsaturation patterns in long-chain ketone compositions for paleotemperature assessment, *Nature*, *330*, 367-369, 1987.
- Prosser, S.L., and C.M. Scrimgeour, High-precision determination of $^2\text{H}/^1\text{H}$ in H_2 and H_2O by continuous-flow isotope ratio mass spectrometry, *Analytical Chemistry*, *67*, 1992-1997, 1995.
- Scrimgeour, C.M., I.S. Begley, and M.L. Thomason, Measurements of deuterium incorporation into fatty acids by gas chromatography/isotope ratio mass spectrometry, *Rapid Communications in Mass Spectrometry*, *13*, 271-274, 1999.
- Sessions, A.L., T.W. Burgoyne, A. Schimmelmann, and J.M. Hayes, Fractionation of hydrogen isotopes in lipid biosynthesis, *Organic Geochemistry*, *30*, 1193-1200, 1999.

- Stump, R.K., and J.W. Frazer, Simultaneous determination of carbon, hydrogen, and nitrogen in organic compounds, *Nuclear Science Abstracts*, 28, 746-751, 1973.
- Volkman, J.K., A review of sterol markers for marine and terrigenous organic matter, *Organic Geochemistry*, 9 (2), 83-99, 1986.
- Werner, R.A., B.E. Kornexl, A. Rossmann, and H.-L. Schmidt, On-line Determination of $d^{18}O$ values of Organic Substances, *Analytica Chimica Acta*, 319, 159-164, 1996.

**FRACTIONATION OF STABLE HYDROGEN ISOTOPES OF
C₃₇ ALKENONES FROM LABORATORY-CULTURED
COCCOLITHOPHORID *EMILIANA HUXLEYI***

N. Andersen, C. Klaas, H.A. Paul, and S.M. Bernasconi
to be submitted to: *Organic Geochemistry*, 2002.

ABSTRACT

We have determined the hydrogen stable isotopic fractionation factor (ϵ) that exists between water and C₃₇ alkenones biosynthesized by the coccolithophorid *Emiliana huxleyi*. By growing cultures in seawater of known isotopic composition and under controlled laboratory conditions, a constant fractionation of ~ -232 to -242‰ for both C_{37:2} and C_{37:3} alkenones was found. No systematic change in ϵ was caused by variations in the algal growth rate. Our results indicate that it is not necessary to consider the algal growth rate for environmental reconstructions using compound-specific hydrogen isotopes of alkenones, an interesting result that can probably also be extrapolated to other biomarkers.

1. INTRODUCTION

The analysis of compound-specific hydrogen isotopes is a recently developed technique with many potential applications in the Earth sciences. To date, only a few studies have made use of this tool for making environmental reconstructions [Sessions *et al.*, 1999; Paul *et al.*, 2000; Xie *et al.*, 2000; Andersen *et al.*, 2001; Sauer *et al.*, 2001]. In initial work by Sessions *et al.* [1999], the hydrogen isotopic composition of a variety of organic compounds from cultured organisms were analyzed to evaluate the fractionation between cellular water and individual lipid molecules. This study included the examination of such compounds as hydrocarbons, sterols, and fatty acids (up to *n*-C₃₃). A later study by Sauer *et al.* [2001] showed that the hydrogen isotopic composition of algal sterols provides a viable means of reconstructing the past D/H of environmental waters, based on a core-top calibration of lipid biomarkers extracted from modern aquatic sediments. Compound-specific δD values of the *n*-alkane *n*-C₂₃ from a peat profile covering approximately the last 200 years have also been demonstrated to correlate with historical climate records by Xie *et al.* [2000]. In addition, samples from earlier periods in the geological record have been analyzed by Andersen *et al.* [2000; 2001] indicating that primary δD compositions can be found in samples at least as old as Miocene and Eocene age. In fact, samples were found to

track climatically driven hydrographic changes that occurred during the Messinian salinity crisis in response to extreme evaporation using compound-specific δD measurements [Andersen *et al.*, 2001].

All of these studies have made use of recent advancements in mass spectrometry that have greatly improved the ability and accuracy with which we are able to measure the D/H ratio in organic samples [Prosser and Scrimgeour, 1995; Scrimgeour *et al.*, 1999]. Research completed until now has focused on the shorter-chain organic compounds of lower molecular weight because of the greater ease with which these components are analyzed. Due to the nature of flow through the GC column, heavier, longer-chain hydrocarbon species need more time to elute and have somewhat broader (and lower intensity) peaks than the lighter compounds (as demonstrated in Chapter 2, Part 1, Figure 4), hence, they are more difficult to measure.

Alkenones (unsaturated methyl and ethyl ketones) are only biosynthesized by a specific group of haptophyte algae and are produced most notably by *Emiliana huxleyi* and *Gephyrocapsa spp.* [Marlowe *et al.*, 1984; Marlowe *et al.*, 1990] in the upper 50 m of open marine environments. Recent studies suggest that these lipids are used for cellular metabolic storage [Epstein *et al.*, 2001]. These compounds have been widely used in paleoceanography for assessing past sea surface temperature changes [Brassell *et al.*, 1986; Prahl and Wakeham, 1987] and reconstructing paleo- pCO_2 [Jasper and Hayes, 1990] in the oceans. The fact that these molecular fossils are already well known to researchers in the field of paleoceanography and established as proxies for investigating the marine surface water environment make these organic compounds ideal for use in reconstructions of paleo-seawater δD .

In this study we have used compound-specific hydrogen isotope measurements to constrain the fractionation between source water and C_{37} alkenones with the goal of using this method for future paleoceanographic reconstructions. In addition, we want to assess the effect of algal growth rate (μ) on the isotopic composition of these compounds and determine if there is a need to consider μ when using this tool for environmental reconstructions.

2. METHODS

2.1. CULTURE EXPERIMENTS

To produce source waters with a wide range of isotopic compositions in which to grow the cultures, we mixed natural seawater (salinity ~ 35 psu) with varying amounts of pure D_2O . The final mixtures contained water ranging from $\sim 0\%$ to $\sim 400\%$ VSMOW. Batch cultures ($f/2$) of the coccolithophorid *Emiliana huxleyi* were isolated from a strain (*Iso3*) collected in the North Atlantic ($41^\circ 43.5N$; $9^\circ 06.5W$) from 40 m water depth at a temperature of $13.0^\circ C$. In the laboratory, the water temperature was kept constant at $18-19^\circ C$ and the cultures grew under continuous light with an intensity of $40-45 \mu E m^{-2} s^{-1}$. After growing in Erlenmeyer flasks for several days, the cultures were transferred to 1L bottles and afterwards to 2L bottles. Cultures from

each bottle were harvested by filtration when cell concentrations of $1.5\text{-}3.4 \times 10^5$ cells ml^{-1} were reached. The filters were stored frozen (-18°C) until the time of analysis.

2.2. EXTRACTION

The alkenones were extracted from freeze-dried filters (each $\sim 1\text{L}$ culture) by ultrasonification using a UP 200S sonic disruptor probe (200W, amplitude 0.5, pulse 0.5) and successively less polar mixtures of methanol (MeOH) and methylene chloride (DCM): 25 ml MeOH 100%, 25 ml MeOH-DCM 1:1, 25 ml DCM; each for three minutes. The resulting extracts were combined, desalted with 50 ml ultra-pure H_2O , dried over Na_2SO_4 , concentrated under a pure N_2 stream, and finally taken up in ~ 40 μl of a 1:1 MeOH/DCM mixture. The bulk organic matter extracted from the sediment sample was fractionated by column chromatography similar to the method of *Prahl et al.* [1989]. We modified the method by using silica gel that was pre-heated at 500°C for 1 hour and by using only half the amount of silica gel and organic solvents.

2.3. COMPOUND-SPECIFIC HYDROGEN ISOTOPE MEASUREMENTS

The δD values of individual organic compounds were obtained by isotope-ratio-monitoring gas chromatography-mass spectrometry using a high-dispersion Geo 20-20 (PDZ Europa) mass spectrometer. The organic compounds were separated on a high-capacity GC column (50 m, 0.53 mm i.d., 1 μm film) with helium as the carrier gas. H_2 gas was produced via pyrolysis at 1195°C (conversion efficiency of 99.8-99.9%; *Ian Begley, personal communication, 2000*) or later at 1300°C . A mega-bore molesieve (5\AA) was used to separate any methane, and water was trapped by a nafion tube. The *n*-alkanes *n*- C_{38} and *n*- C_{39} were used as internal standards for calibration and for determining the H_3^+ correction factor. By using standards with retention times similar to those of the sample compounds, the effect of changing column-bleed and variations in the baseline value can be compensated for. Each D/H ratio reported here represents the average of 5-8 measurements of compounds injected at varying volumes within the same day. Multiple injections are necessary to make the H_3^+ corrections and to monitor instrument performance. Standard errors of the means (SEM) depend mainly on peak intensity and vary between 1.4-9.1%. The hydrogen isotopic composition of the source-water samples was measured using the conventional off-line, reduction method with zinc as the reducing metal [*Friedman, 1953*].

3. RESULTS AND DISCUSSION

On the basis of laboratory cultures with *E. huxleyi*, we found a constant fractionation ϵ between water and $\text{C}_{37:2}$ alkenones of $\sim -232\text{‰}$ (Figure 1; Table 1). There is no significant difference between the fractionation factors found for the two dominant alkenone species: $\epsilon_{\text{C}_{37:2}} = -232 \pm 13.7\text{‰}$ and $\epsilon_{\text{C}_{37:3}} = -242 \pm 12.1\text{‰}$. The low degree of scatter in this relationship (as shown in Figure 1) suggests that the source water is indeed the main factor controlling the isotopic com-

position of the alkenones. In addition, there appears to be no effect on ϵ caused by the algal growth rate (e.g., $\epsilon_{C_{37:2}}$ vs. μ ; $r^2 = 0.09$) and, consequently, it will not be necessary to consider this factor for using hydrogen isotopes of alkenones in environmental reconstructions.

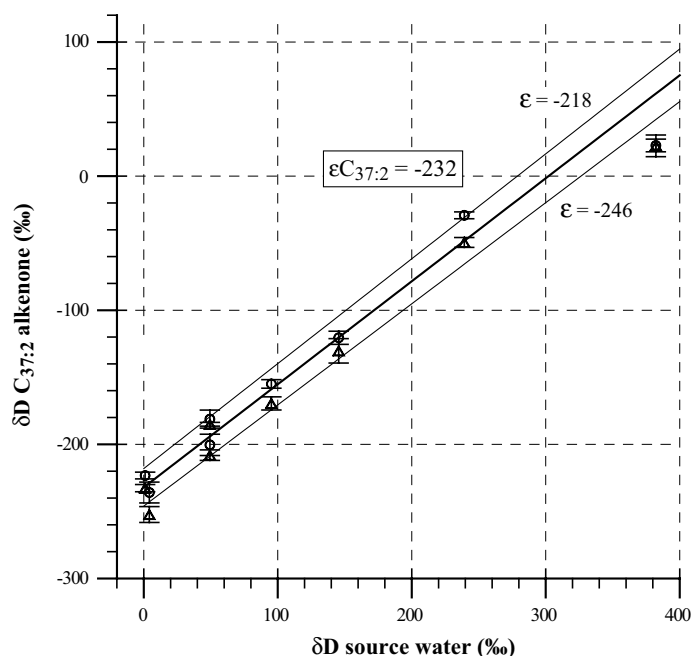


Figure 1.

Fractionation of the stable hydrogen isotopes between water and $C_{37:2}$ alkenones (circles) and $C_{37:3}$ alkenones (triangles) from laboratory-cultures of the coccolithophorid *Emiliana huxleyi*. The error bars on the alkenone δD values are the standard errors of the means. The mean fractionation of the $C_{37:2}$ alkenones is shown by a bold line.

The biosynthetic pathway used to produce alkenones is still unknown. The hydrogen isotopic fractionation of alkenones is very similar to the fractionations described in the literature for sterols, which are known to be produced in the cytosol by the MVA pathway during biosynthesis [Sessions *et al.*, 1999; Sauer *et al.*, 2001]. Our results may indicate a MVA pathway during alkenone biosynthesis. The recently described DOXP pathway is less likely, because this would probably imply a much greater ϵ [Sessions *et al.*, 1999].

4. CONCLUSIONS

On the basis of laboratory cultures with *E. huxleyi*, we have determined that a constant fractionation exists between the source water and the C_{37} alkenones biosynthesized by coccolithophorids. This fractionation factor, $\epsilon = -232\text{‰}$, is approximately the same for both the $C_{37:2}$ and $C_{37:3}$ alkenone compounds. There appears to be no significant effect due to the algal growth rate. Therefore, this fractionation factor can be directly applied to the hydrogen isotopic composition of compounds extracted from sedimentary organic matter for environmental reconstructions and the effect of μ must not be considered.

Table 1.
Data from the culture experiments with *E. huxleyi*.

Sample	$\delta D_{\text{water}}^a$	$\delta D_{\text{C37:2}}^a$	SEM ^b	n^c	$\delta D_{\text{C37:3}}^a$	SEM ^b	n^c	Growth rate	$\epsilon_{\text{C37:2}}^d$	$\epsilon_{\text{C37:3}}^d$
test (2L,0.5)	4.2	-236 ^e	7.7	8	-252.3 ^e	5.9	6	0.90	-239	-255
0 (0.9L)	1.0	-223	2.5	5	-232.6	2.7	5	1.18	-224	-233
50 (1L)	49.4	-181.2 ^e	6.7	5	-185 ^e	1.4	5	0.64	-220	-223
50 (2L,0.5)	49.4	-200.4	8.0	5	-208	3.9	6	0.83	-238	-245
100 (1L)	95.2	-154.9 ^e	3.6	4	-169.4 ^e	4.9	5	0.69	-228	-242
150 (1L)	145.4	-120.5 ^e	4.9	5	-130.3 ^e	9.1	5	0.87	-232	-241
250 (1L)	239.2	-29.2	2.6	5	-49.4	3.7	5	1.01	-217	-233
400 (1L)	382.2	+22.9	4.7	6	+22.6	8.1	6	1.08	-260	-260
Average:									-232	-242

^a in ‰ VSMOW (Vienna standard mean ocean water)

^b SEM = standard error of the mean

^c n = number of analyses

^d $\epsilon = 1000 [(\delta D_{\text{C37alkenone}} + 1000)/(\delta D_{\text{water}} + 1000) - 1]$

^e pyrolysis temperature = 1195°C; other samples at 1300°C

5. REFERENCES

- Andersen, N., S.M. Bernasconi, R.M. Carlson, and M. Schoell, Early diagenetic incorporation of strongly deuterium-depleted hydrogen in poly-unsaturated bio-molecules, in *AGU Fall Meeting*, AGU, San Francisco, 2000.
- Andersen, N., H.A. Paul, S.M. Bernasconi, J.A. McKenzie, A. Behrens, P. Schaeffer, and P. Albrecht, Large and rapid climate variability during the Messinian salinity crisis: Evidence from deuterium concentrations of individual biomarkers, *Geology*, 29, 799-802, 2001.

- Brassell, S.C., G. Eglinton, I.T. Marlowe, U. Pflaumann, and M. Sarnthein, Molecular stratigraphy: A new tool for climatic assessment, *Nature*, *320*, 129-133, 1986.
- Epstein, B.L., S. D'Hondt, and P.E. Hargraves, The possible metabolic role of C₃₇ alkenones in *Emiliana huxleyi*, *Organic Geochemistry*, *32*, 867-875, 2001.
- Friedman, I., Deuterium content of natural waters and other substances, *Geochimica et Cosmochimica Acta*, *4*, 89-103, 1953.
- Jasper, J.P., and J.M. Hayes, A carbon isotope record of CO₂ levels during the late Quaternary, *Nature*, *347*, 462-464, 1990.
- Little, M.G., R.R. Schneider, D. Kroon, B. Price, T. Bickert, and G. Wefer, Rapid paleoceanographic changes in the Benguela upwelling system for the last 160,000 years as indicated by abundances of planktonic foraminifera, *Palaeogeography, Palaeoclimatology, Palaeoecology*, *130*, 135-161, 1997.
- Marlowe, I.T., S.C. Brassell, G. Eglinton, and J.C. Green, Long chain unsaturated ketones and esters in living algae and marine sediments, *Organic Geochemistry*, *6*, 135-141, 1984.
- Marlowe, I.T., S.C. Brassell, G. Eglinton, and J.C. Green, Long-chain alkenones and alkyl alkenoates and the fossil coccolith record of marine sediments, *Chemical Geology*, *88*, 349-375, 1990.
- Müller, P.J., M. Cepek, G. Ruhland, and R.R. Schneider, Alkenone and coccolithophorid species changes in late Quaternary sediments from the Walvis Ridge: Implications for the alkenone paleotemperature method, *Palaeogeography, Palaeoclimatology, Palaeoecology*, *135*, 71-96, 1997.
- Östlund, H.G., H. Craig, W.S. Broecker, and D. Spenser, GEOSECS Atlantic, Pacific and Indian Ocean expeditions: Shore based data and graphics, in *Tech. Rep.*, Nat. Sci. Found., Washington D.C., 1987.
- Paul, H.A., N. Andersen, S.M. Bernasconi, C. Klaas, and J.A. McKenzie, Hydrogen isotopic composition of long-chain *n*-alkanes and alkenones as tracers of paleohydrologic change, in *AGU Fall Meeting*, AGU, San Francisco, 2000.
- Prahl, F.G., L.A. Muehlhausen, and M. Lyle, An organic geochemical assessment of oceanographic conditions at Manop site C over the past 26,000 years, *Paleoceanography*, *4*, 410-510, 1989.
- Prahl, F.G., and S.G. Wakeham, Calibration of unsaturation patterns in long-chain ketone compositions for paleotemperature assessment, *Nature*, *330*, 367-369, 1987.
- Prosser, S.L., and C.M. Scrimgeour, High-precision determination of ²H/¹H in H₂ and H₂O by continuous-flow isotope ratio mass spectrometry, *Analytical Chemistry*, *67*, 1992-1997, 1995.
- Sauer, P.E., T.I. Eglinton, J.M. Hayes, A. Schimmelmann, and A.L. Sessions, Compound-specific D/H ratios of lipid biomarkers from sediments as a proxy for environmental and climatic conditions, *Geochimica et Cosmochimica Acta*, *65*, 213-222, 2001.
- Scrimgeour, C.M., I.S. Begley, and M.L. Thomason, Measurements of deuterium incorporation into fatty acids by gas chromatography/isotope ratio mass spectrometry, *Rapid Communications in Mass Spectrometry*, *13*, 271-274, 1999.
- Sessions, A.L., T.W. Burgoyne, A. Schimmelmann, and J.M. Hayes, Fractionation of hydrogen isotopes in lipid biosynthesis, *Organic Geochemistry*, *30*, 1193-1200, 1999.
- Thierstein, H.R., K.R. Geitzenauer, and B. Molino, Global synchronicity of late Quaternary coccolith datum levels: validation by oxygen isotopes, *Geology*, *5*, 400-404, 1977.
- Xie, S., C.J. Nott, L.A. Avsejs, F. Volders, D. Maddy, F.M. Chambers, A. Gledhill, J.F. Carter, and R.P. Evershed, Palaeoclimate records in compound-specific δD values of a lipid biomarker in ombrotrophic peat, *Organic Geochemistry*, *31*, 1053-1057, 2000.

CASE STUDIES IN THE MEDITERRANEAN SEA

PART I**BACKGROUND: MODERN MEDITERRANEAN OCEANOGRAPHY AND SAPROPELS****1. INTRODUCTION**

The Mediterranean Sea is in many ways a unique marine environment among the contemporary global oceans. The nearly total enclosure of the basin by land, combined with the distinct regional climate and a negative hydrologic budget, induces specific physical, biological, and geochemical characteristics. In addition, the vast size of this semi-enclosed sea allows it to behave as a dynamic, marine system, though its restricted exchange with the rest of the world's oceans causes it to be particularly sensitive to local environmental and climatic fluctuations. Despite its oceanographic seclusion, the Mediterranean is the source of an important intermediate water mass to the Atlantic Ocean [*Zahn et al.*, 1987; *Bigg*, 1994] and has been shown to be a significant component in driving global thermohaline circulation.

The Mediterranean is also noted for the occurrence of unique sedimentary deposits called sapropels [*Kidd et al.*, 1978], which are black, highly organic-rich (greater than 2% and up to 30% total organic carbon) sediments first discovered in the eastern Mediterranean basin [*Kullenberg*, 1952]. Sapropel layers are noteworthy as the expected fate of most organic matter in the oceans is oxidation and decomposition rather than accumulation. The modern Mediterranean Sea is classified as a semi-oligotrophic to oligotrophic system with well oxygenated bottom waters, thus, special conditions must have prevailed in the past allowing for deposition of these unusual sediments. The formation of sapropels has been attributed to distinct changes in the hydrographic regime and biogeochemical cycling in the Mediterranean triggered by global and regional climatic variations.

The present-day hydrologic budget of the Mediterranean basin is dominated by evaporative water loss causing anomalously high salinity in the sea, though freshwater inputs via precipitation, rivers, and continental runoff are also important factors. Surface inflow from the Atlantic and subsurface outflow through the Strait of Gibraltar maintain the basin's marine connection. Variations in the glacial-interglacial oxygen isotopic composition of seawater are amplified compared to those observed in open-ocean samples (e.g., North Atlantic surface waters [*Thunell and Williams*, 1989]) due to the dominance of evaporation and limited freshwater exchange. Consequently, the Mediterranean Sea is an appropriate region for studying the effect of climatic and environmental influences on isotopic signals.

Many models of water circulation, salinity, and nutrient balance have been developed for the Mediterranean (e.g., *Béthoux* [1979]; *Béthoux* [1980]; *Béthoux* [1984]; *Bryden and Stommel* [1984]), including changes in the hydrologic budget related to sea level variations since the last glaciation [*Rohling and Bryden*, 1994; *Lane-Serff et al.*, 1997]. Yet only a few studies have examined the Mediterranean water balance coupled with the $\delta^{18}\text{O}$ isotope budget [*Gat et al.*, 1996; *Rohling and Bigg*, 1998; *Rohling*, 1999] and even fewer have considered the hydrogen isotope budget [*Gat et al.*, 1996]. Here we present a compilation of vertical water-column profiles of oxygen and hydrogen stable isotope measurements from two east-west transects in the Mediterranean Sea in attempt to link oceanographic processes with isotopic composition and to characterize the different water masses existing today. In addition, results of geochemical analyses on the sedimentary material of a short-core from the eastern basin are used to introduce sapropels and to describe the paleoceanographic setting and environmental conditions that existed during the most recent period of sapropel deposition approximately 9,000 years ago.

2. SAMPLING STATIONS AND METHODS

Water samples were obtained during two east-west transects of the Mediterranean sea. Hydrographic stations (Figure 1) include those from a cruise of the F.S. *Meteor* in January-February 1998 (collaboration with Dr. K.-C. Emeis, Institut für Ostseeforschung, Warnemünde, Germany) and a cruise of the R.V. *Aegaeo* in June 1999 (MTP II MATER project). Temperature and salinity (S) were measured in situ at the sampling stations using standard oceanographic techniques (CTD device). Waters for isotopic analysis were collected with a rosette of Niskin bottles from designated depths at each site, down to 400 m on the *Meteor* cruise and to 4000 m on the MATER cruise. Samples from the *Meteor*-40 cruise were poisoned with 2 ml/L of 36% HCl to prevent biologic activity following sample collection. In addition, two short sediment cores, each ~30 cm in length, were obtained during the MATER cruise using a multi-corer device, thus allowing for minimal disturbance of the surface sediments.

All water samples were analyzed for oxygen and hydrogen isotopic composition at the ETH Stable Isotope Laboratory. The stable oxygen isotopic composition of 2 ml sample aliquots was determined by equilibration with CO_2 using an automated Isoprep-18 device (equilibration for 6 hours at 25°C) coupled to a Micromass Optima isotope ratio mass spectrometer (IRMS). Analytical reproducibility based on repeat analysis of internal standards is $\pm 0.05\%$. Samples for hydrogen isotopic analyses were prepared off-line according to the zinc reduction method of *Friedman* [1953] (see Chapter 2, Part I for details). Analysis of VSMOW and VSLAP standards indicate an analytical reproducibility of around $\pm 1.0\%$. All isotope data are reported in the standard delta notation (δ) with respect to Vienna Standard Mean Ocean Water (VSMOW).

Sediment cores obtained in the eastern Mediterranean during the MATER cruise were opened and sampled at sea a few hours after collection. Approximately 2-cm slices were cut,

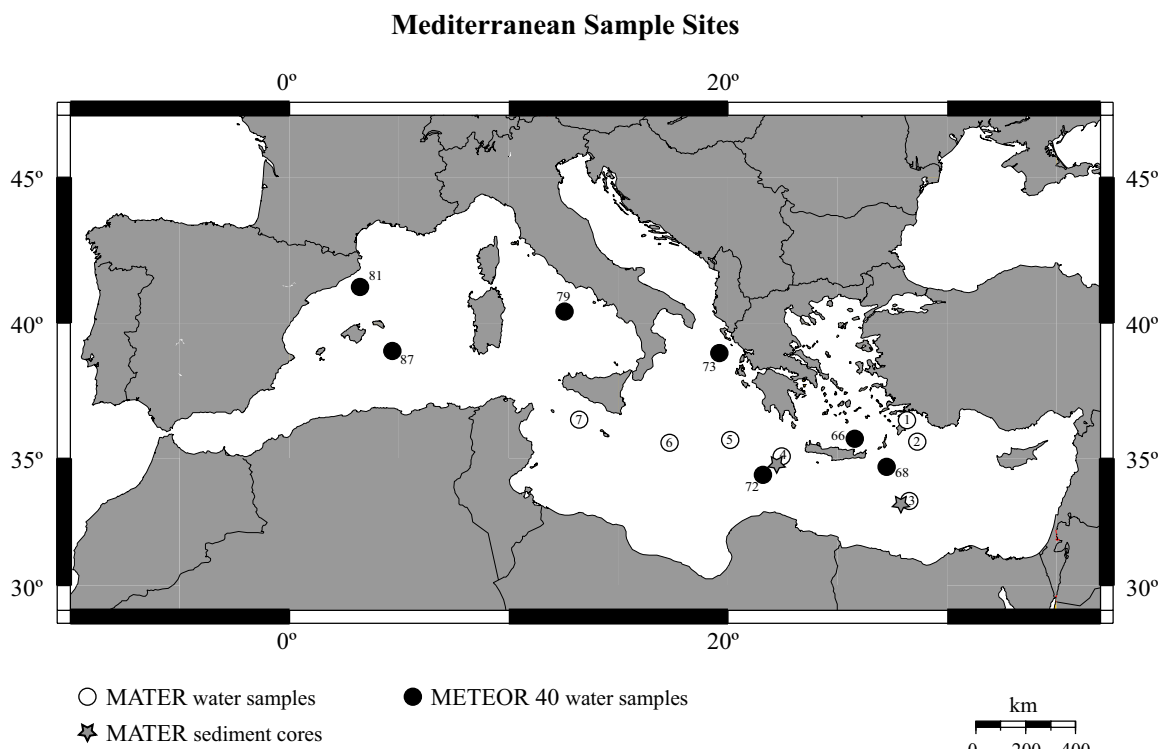


Figure 1.
Map of the Mediterranean Sea indicating the locations of the hydrologic sampling stations (circles) and core locations (stars) from the Meteor-40 (January-February, 1998) and the MATER (June, 1999) cruises.

wrapped in aluminum foil, and kept frozen until time of processing. Samples were first freeze dried and then thoroughly homogenized with a mortar and pestle prior to geochemical analysis. Of the two short cores obtained, cores TMC-3 and TMC-4, only TMC-4 was sampled continuously from the present back to the first sapropel layer providing a complete sedimentary profile. For this reason, TMC-4 was investigated in greater detail than TMC-3, though sediments from TMC-3 were useful in conducting tests for the development of the compound-specific hydrogen isotope technique. The stable carbon and oxygen isotope ratios were measured on the bulk carbonate in both cores by subsampling 200-300 μg for isotopic analysis. Samples were first roasted at 375°C under vacuum for 1 hour to render inert organic contaminants and then reacted with phosphoric acid in a common acid bath system at 90°C. Stable isotopes were measured on a Micromass Prism IRMS and isotopic data are reported in delta notation (δ) relative to the Peedee Belemnite (PDB) carbonate standard. Analytical precision as determined from replicate carbonate standards (Carrara Marble) was typically $\pm 0.06\text{‰}$ for $\delta^{13}\text{C}$ and $\pm 0.08\text{‰}$ for $\delta^{18}\text{O}$.

Percent carbonate ($\%\text{CaCO}_3$) and total organic carbon ($\%\text{TOC}$) content, as well as the bulk organic matter stable carbon and nitrogen isotopic compositions, were all measured on core TMC-4. The total carbon and total inorganic carbon (i.e., weight percent carbonate) content of samples were measured using a UIC Inc. Coulometrics, CM-5012 CO_2 Coulometer and a CM-

5200 Furnace at the ETH Limnogeology Laboratory. Approximately 5 mg and 12 mg of sediment were used for the analysis of percent total carbon and inorganic carbon, respectively. A molar weight conversion factor of 8.333 was used to convert the inorganic carbon content measured to percent carbonate. Percent organic carbon in the sediment samples was determined by subtracting the carbonate carbon from the total carbon. Analytical precision of these measurements was approximately 0.5%.

Stable carbon and nitrogen isotopic compositions of sedimentary bulk organic matter and C/N ratios were measured using a Carlo-Erba, CNS-2500 elemental analyzer (EA) coupled to a Micromass Optima IRMS in continuous flow mode at the ETH Stable Isotope Laboratory. Due to the very low organic matter content of the non-sapropel sediments, only a few samples were selected for isotopic analysis outside the sapropel layer. Samples were first decarbonated with 1.16 M HCl then dried in an oven at 45°C. Attempts were made to measure the $\delta^{15}\text{N}$ of non-treated sediment as it has been suggested that acid may degrade the organic nitrogen compounds [Lehmann, *personal communication*, 2001]. Yet, due to the low organic nitrogen content of the sediments, and hence large sample sizes necessary for the analyses, complete combustion of the samples was not achieved producing spurious results. Precision as determined from replicate analyses of our in-house standard (Atropina) was typically $\pm 0.20\%$ for both $\delta^{13}\text{C}$ and $\delta^{15}\text{N}$ values and better than 3% for elemental compositions. All measured data from samples collected during these two cruises are listed in Appendix I.

3. MODERN MEDITERRANEAN HYDROGRAPHY

In its present configuration, the Mediterranean is a marginal sea connected to the Atlantic Ocean via the Strait of Gibraltar, ~284 m deep [Bryden and Kinder, 1991], and is composed of two sub-basins separated by the Sicilian Sill, ~330 m deep [Wüst, 1961]. Circulation in the Mediterranean is driven basin-wide by thermohaline processes and is characterized by eastward surface flow and westward subsurface flow. Relatively “fresh” water from the Atlantic (<37 psu) enters through the Strait of Gibraltar and is driven east by the wind. As the water moves eastward, evaporation greatly exceeds precipitation and input from fresh water causing the surface water to become increasingly saline and dense. Intermediate water forms in the Levantine basin, the easternmost extent of the Mediterranean, sinking to depths of a few hundred meters. This Levantine Intermediate Water (LIW; ~39.1 psu) is the main component forming the Mediterranean Intermediate Water (MIW) that circulates westwards, ~150-600 m beneath the east-flowing surface water, through the Straits of Sicily and Gibraltar and is the predominant source of Mediterranean outflow into the Atlantic Ocean [Robinson *et al.*, 1992]. Eastern Mediterranean Deep Water (EMDW; ~38.7 psu) forms in winter, primarily in the southern Adriatic Sea due to cooling of surface waters and deep convection, though some deepwater may also form in the Aegean Sea (Aegean Deep Water, AGDW). In the western basin, deepwater forms in late winter in the north-

ern Tyrrhenian Sea region (WMDW; ~ 38.4 psu). Although the Mediterranean deepwater masses are of slightly lower salinity than the intermediate water, the deepwater is colder and more dense than MIW [Robinson *et al.*, 1992]. Estimates of the residence time of deepwater in the basin are on the order of 50-80 years [Béthoux *et al.*, 1990; Schlitzer *et al.*, 1991].

In oceanography, the stable isotopes of water have been used as tracers of water mass circulation and of the evaporation-precipitation balance [Craig and Gordon, 1965; Kroopnick, 1985]. The relationship between salinity and $\delta^{18}\text{O}$ in the oceans was first demonstrated by Craig and Gordon [1965] and is explained by the fact that evaporation preferentially removes the light isotopes of water leaving the remaining seawater more saline and enriched in the heavy isotopes. Alternatively, meteoric water is depleted in ^{18}O and ^2H , thus causing a decrease in the isotopic composition of marine waters from precipitation and freshwater inflow. Due to these processes, the isotopic composition and the salinity of a water body are acquired at the ocean's surface and are transferred to other water masses via down welling to intermediate and deeper levels and by mixing.

3.1. ISOTOPIC COMPOSITION OF MEDITERRANEAN SURFACE WATER

The geochemical characteristics of surface water samples (3-10 m water depth) reflect the overall circulation pattern in the Mediterranean, corresponding to the larger freshwater input in the west and the dominance of evaporation in the east (see Figures 2 through 5). Hydrologic samples show an increase in salinity across the west-to-east transect ranging from a minimum of 37.25 psu in the west to a maximum of 39.17 psu in the east. This pattern is similarly displayed by both isotopic species: $\delta^{18}\text{O}$ values increase from 1.11 to 1.57‰ and δD values from 3.22 to 16.44‰, from west to east. The parallel behavior of these parameters in this environment indicates their sensitivity to, and hence ability to record, hydrographic and climatic variability.

Relationships between the three geochemical parameters for surface waters between 0-20 m depth are shown in Figure 6. The $\delta^{18}\text{O}$ vs. salinity relationship is best defined by the linear regression: $\delta^{18}\text{O} = 0.27 * S - 9.08$. This equation is very similar to that defined by Pierre [1999] for surface waters spanning the entire Mediterranean Sea ($\delta^{18}\text{O} = 0.25 * S - 8.20$) and by Gat *et al.* [1996] for surface waters in the eastern basin ($\delta^{18}\text{O} = 0.28 * S - 9.02$). The slope of this equation is much lower than the value of 0.45 characterizing the $\delta^{18}\text{O}$:S relationship in the northeast Atlantic Ocean [Craig and Gordon, 1965] and demonstrates the strong impact of the Mediterranean climate and evaporation on surface waters in this region.

The δD vs. salinity relationship is defined by the linear regression: $\delta\text{D} = 5.29 * S - 194.62$. In contrast to the similarity of the $\delta^{18}\text{O}$:S relationship to other published results, the δD :S equation is quite different from that produced by Gat *et al.* [1996] ($\delta\text{D} = 0.84 * S - 24.51$). The relationship between δD and $\delta^{18}\text{O}$ in surface waters is probably best described by the linear regression as defined by samples taken during the Meteor-40 cruise: $\delta\text{D} = 13.40 * \delta^{18}\text{O} - 10.99$,

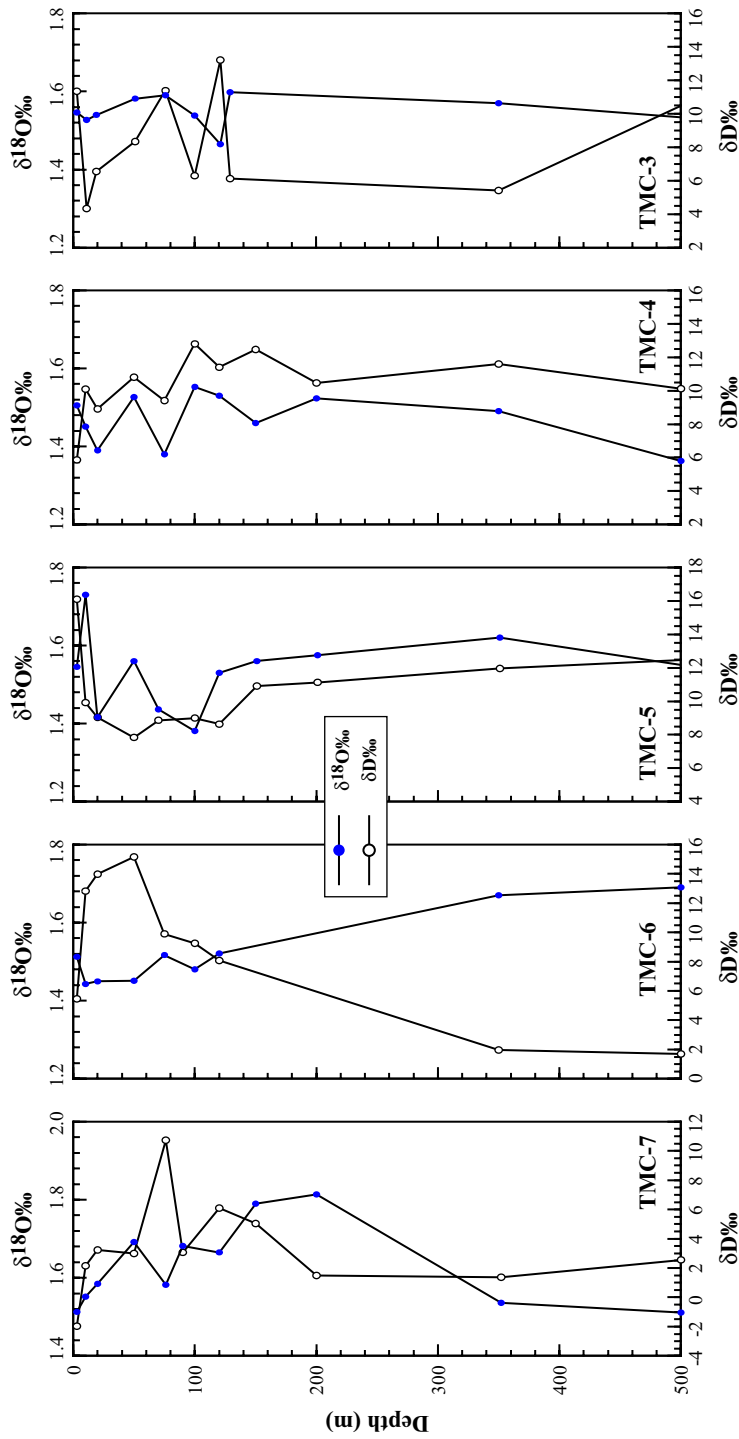


Figure 2. Vertical water-column profiles of salinity and $\delta^{18}O$ from hydrologic stations in the eastern Mediterranean Sea sampled in June, 1999 during the MATIER cruise (0-4000 m). Stations are arranged geographically to show the west-east transition in hydrographic conditions (note change in scale from west to east).

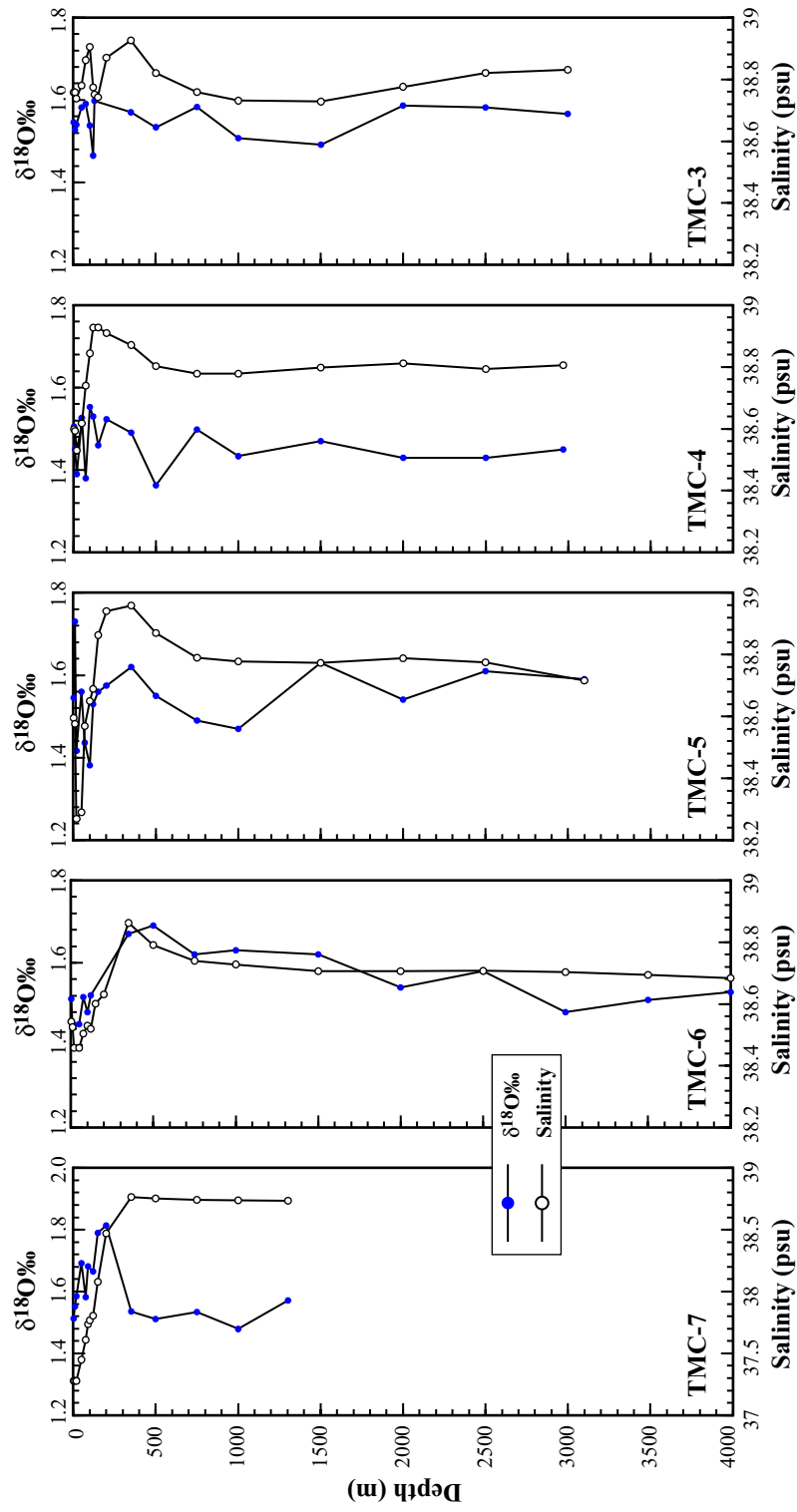


Figure 3. Vertical water-column profiles of $\delta^{18}\text{O}$ and δD from hydrologic stations in the eastern Mediterranean Sea sampled during the MATER cruise (0–4000 m).

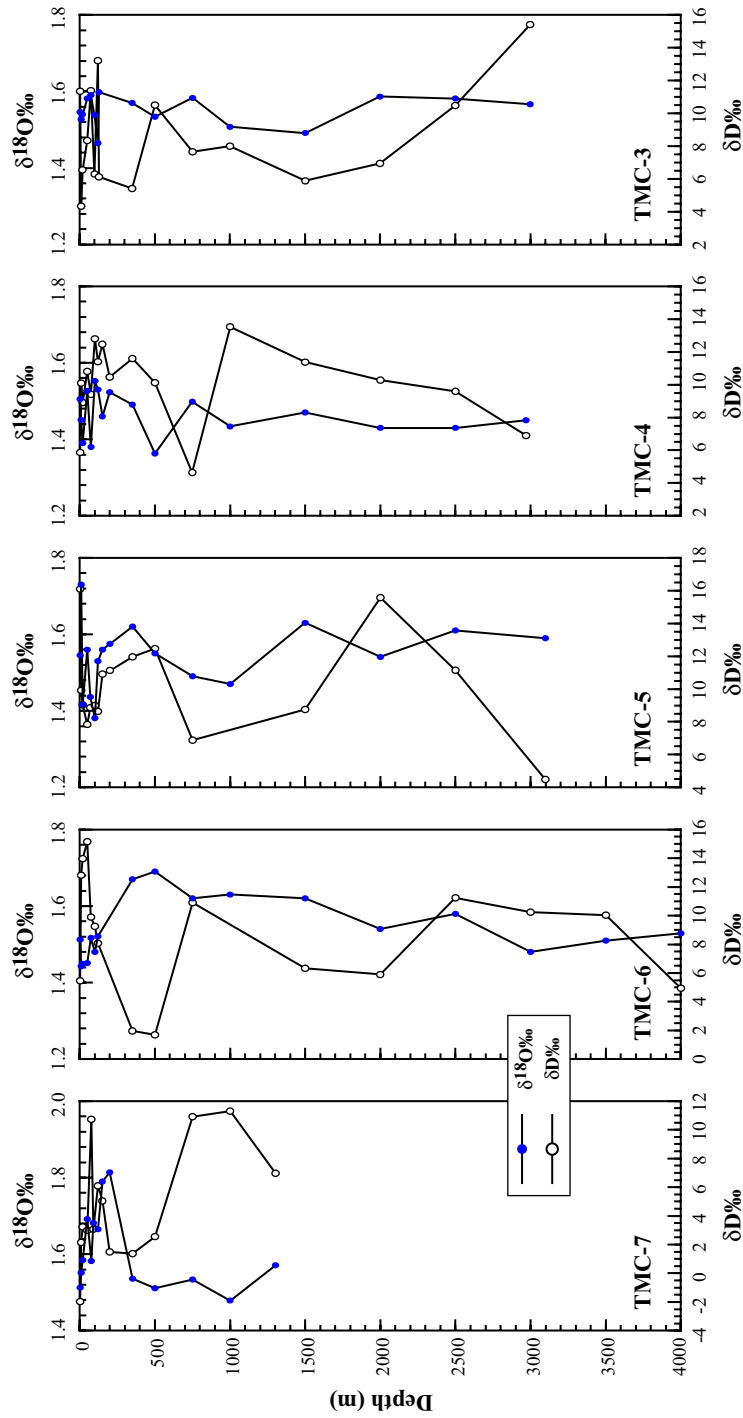


Figure 4. Upper water-column (0-500 m) profiles of $\delta^{18}\text{O}$ and δD from hydrologic stations in the eastern Mediterranean Sea sampled during the MATER cruise.

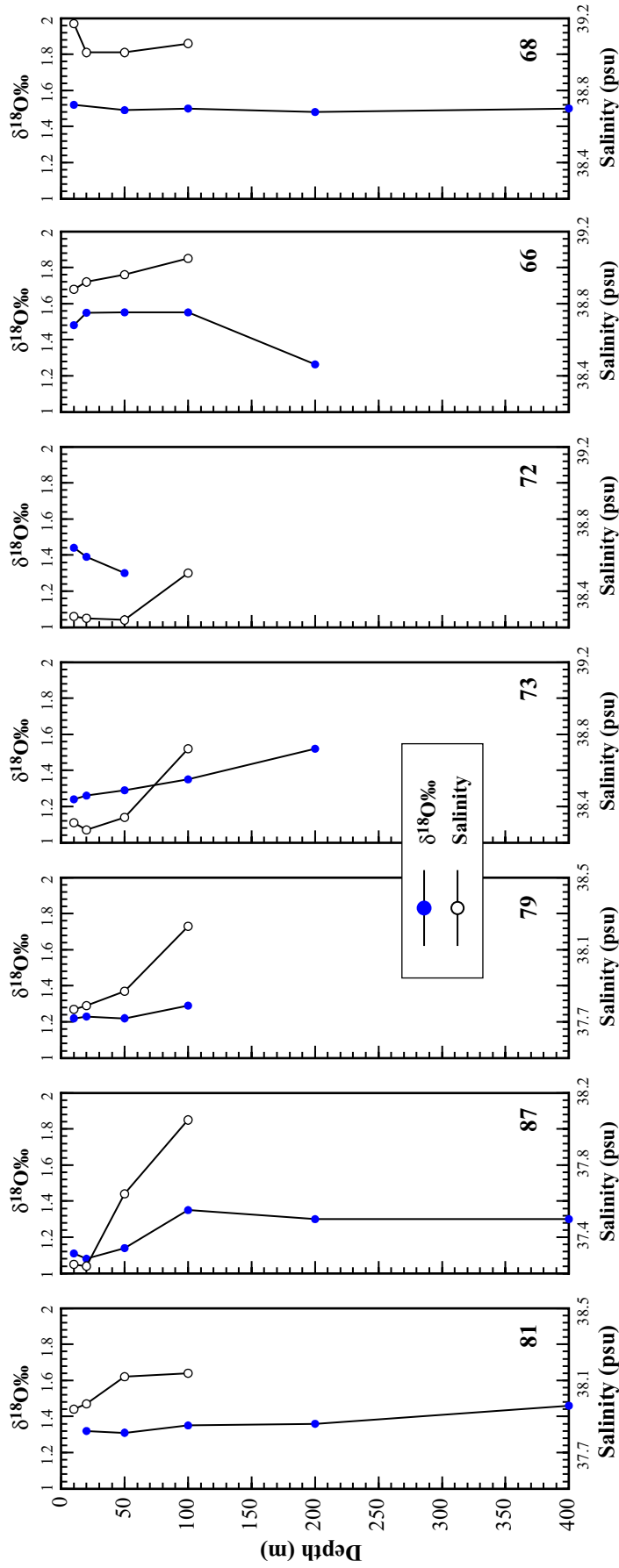


Figure 5. Vertical water-column profiles of $\delta^{18}\text{O}$ and salinity from hydrologic stations in the eastern and western Mediterranean Sea sampled in January-February, 1998 during the Meteor-40 cruise (0-400 m). Stations are arranged geographically to show the west-east transition in hydrographic conditions (note change in scale from west to east).

since the data from the MATER cruise show a very weak linear relationship and a significant amount of scatter (Figure 6c). In any case, the linear regression is also quite different to that defined by *Gat et al.* [1996], $\delta D = -0.286 * \delta^{18}O + 8.69$.

Comparison of our results with those of *Gat et al.* [1996], the only other isotopic survey published for the Mediterranean Sea in which hydrogen isotopes were measured, is puzzling. Isotopic results from the MATER cruise suggest fairly constant $\delta^{18}O$ values in the eastern basin (hovering around 1.5‰) co-existing with a large west-to-east trend in δD and salinity (Figure 6). Conversely, *Gat et al.* [1996] report almost constant δD values ($\sim 8‰$) across the eastern basin despite large variability in $\delta^{18}O$ values (ranging from ~ 1.3 to $2.2‰$), again irrespective of changes in salinity. From our set of measurements, the water samples taken near the Strait of Sicily produce especially odd $\delta^{18}O$ results (see Figure 6, circled points in the $\delta^{18}O$:Salinity plots) and hence, the final linear regressions have been determined without these points. *Gat et al.* [1996] explain the uniformity of surface water δD values in their data set by suggesting that concurrent evaporation and precipitation processes both influence the isotopic composition of seawater, yet, in winter when freshwater input is highest, changes in the two isotopic species are decoupled allowing for larger changes in $\delta^{18}O$ with respect to δD .

Our two data sets, composed of one survey conducted in winter (Meteor-40 cruise) and one in summer (MATER cruise), allow for the comparison of season-specific isotopic relationships. Surprisingly, the samples collected during the winter demonstrate much clearer relationships between the two isotopic species and with salinity, while the summer data set indicates much weaker relationships between the isotopes and salinity (Figure 6), hence, these results are just inverse to the findings of *Gat et al.* [1996]. This may indicate that the winter of 1998 was an unusually dry winter, with evaporation being more important than fresh water input. Alternatively, the data from the summer of 1999 clearly shows a decoupling between the water isotopes, indicating an abundance of fresh water input, based on the reasoning of *Gat et al.* [1996]. Yet, these surveys each provide only one temporal glimpse into the seasonality of the Mediterranean region; clearly longer time series are needed to produce an accurate characterization of the seasonal isotopic balance.

3.2. ISOTOPIC COMPOSITION OF MEDITERRANEAN WATER AT DEPTH

The increased salinity of the surface waters in the eastern basin is clearly displayed in the vertical water-column profiles of the Mediterranean Sea (Figures 2 and 5). This heightened salinity significantly weakens the water-column stability and causes the dense surface water to sink, mixing with the waters below. Evidence of this down welling is seen in the vertical profiles of the sites in the eastern basin (TMC-3 and TMC-4), where a pycnocline is visible between 100-150 m depth. This sharp salinity decrease marks the top of the MIW. The intermediate water mass can then be followed as it moves westwards in sites TMC-5 through TMC-7, though it becomes pro-

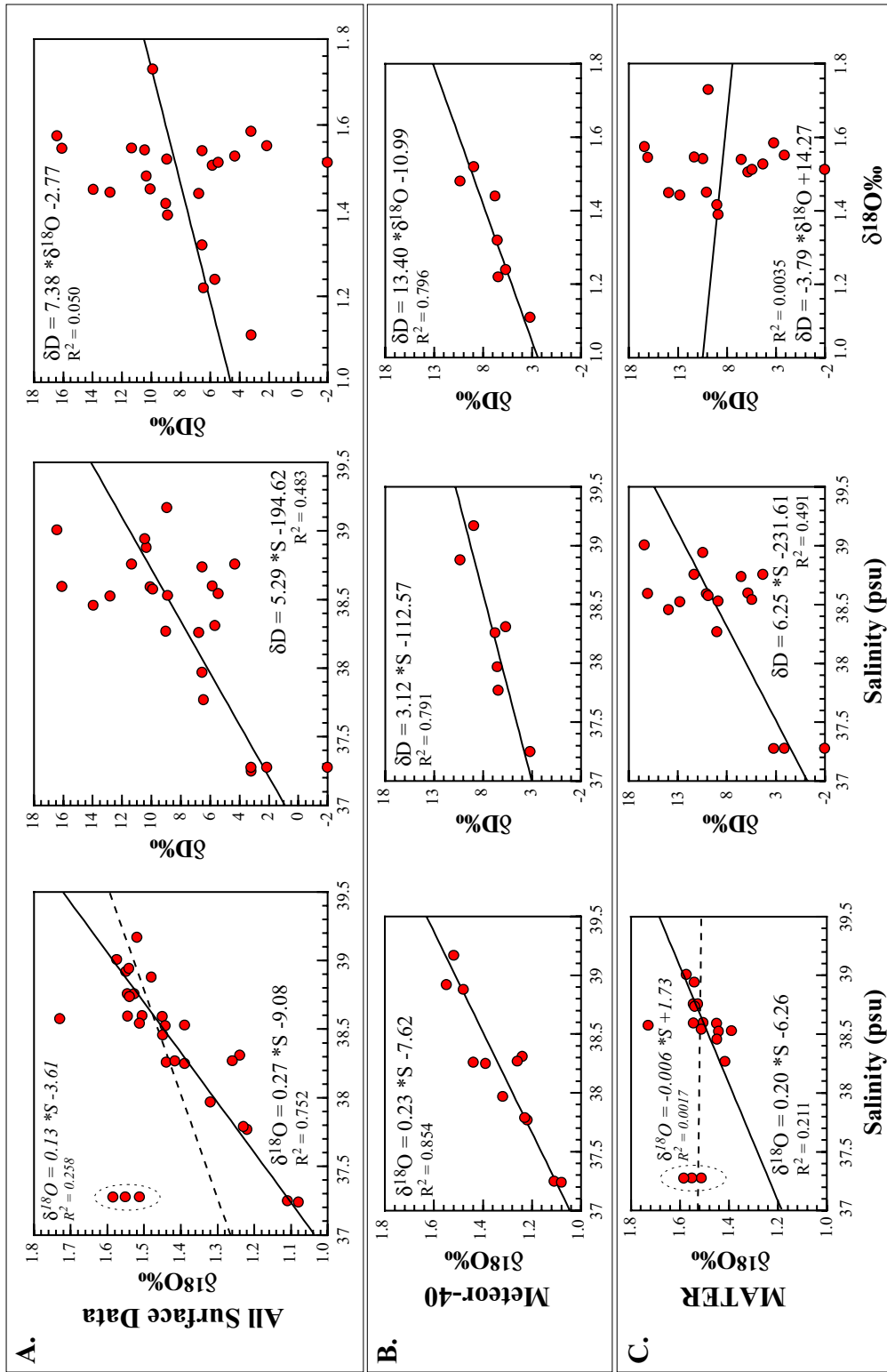


Figure 6. Relationships between geochemical parameters in the Mediterranean surface water (0-20 m water depth): $\delta^{18}\text{O}$ vs. salinity; δD vs. salinity; and $\delta^{18}\text{O}$ vs. δD . Data are displayed in three groups: (A.) all data plotted together; (B.) data from the Meteor-40 cruise (winter, 1998); and (C.) data from the MATER cruise (summer, 1999). In the plots of $\delta^{18}\text{O}$ vs. salinity, the dashed regression lines are based on a linear fit including the circled (outlier) points.

gressively deeper, reaching depths of ~400 m, and slightly less saline with distance from the source. The steepest vertical salinity gradients are seen between the surface and intermediate waters in the western Mediterranean (i.e., TMC-7 and Meteor station 87) and provide evidence that the saline intermediate water mass spreads over the Sicilian sill and into the western basin. Visible beneath the intermediate water at approximately 500 m is the slightly lower salinity, deepwater body. This water mass is characterized by very stable salinity profiles at depth and also shows a slight decrease in salinity from east to west ranging from ~38.9 to 38.4 psu.

Vertical profiles of the oxygen and hydrogen isotopic data are shown in Figures 2 through 5. The strong correlation between salinity and $\delta^{18}\text{O}$ is made evident in Figure 2, most notably in the surface waters of station TMC-3 and in the intermediate and deep waters at TMC-5 and 6. The close relationship between $\delta^{18}\text{O}$ and δD can similarly be seen in Figures 3 and 4, though it is sometimes a bit obscured due to the large range in δD values. For instance, close correlation between the isotopic species is visible at stations TMC-4 and 5 while little correlation is seen at station TMC-6. Contrary to salinity, the water isotopes less clearly display the transition between water masses, though comparably, the $\delta^{18}\text{O}$ values of seawater are relatively stable in the deep-water below 500 m and isotopic values become progressively depleted towards the west.

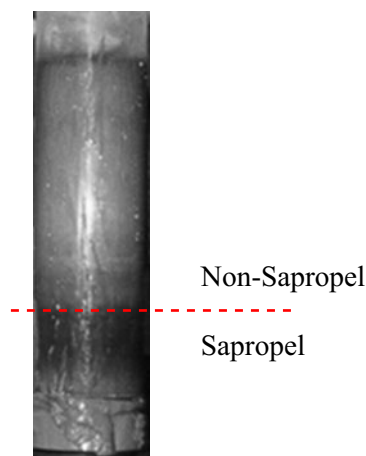
4. MEDITERRANEAN PALEOCEANOGRAPHY

Numerous studies have been conducted in attempt to constrain the distinguishing environmental conditions that accompanied the deposition of sapropel sediments. The two original models put forth to explain the occurrence of these organic carbon-rich sediments debated whether enhanced preservation (caused by stagnation and anoxia in bottom-waters) or increased productivity (causing associated increases in organic matter export to the sea floor) may have been responsible for the existence of these sediments. As ample evidence has accrued in support of both theories, scientists have recently begun to consider the likelihood that a combination of these mechanisms came into play; thus, increased productivity and decreased deep-water ventilation were contemporaneous. Yet, precise characterization of the climatological forcing that initiated sapropel accumulation is still lacking. Below, the results of geochemical analyses on sediment cores from the eastern Mediterranean are presented to provide a short review of what is known about the conditions existing in the basin during periods of sapropel deposition. In addition, a brief summary of the paleoceanographic setting in this region at the Last Glacial Maximum is given as background for Part III of this chapter.

4.1. SAPROPEL EVENT 1

Sapropels have been identified in sedimentary sequences throughout the entire eastern Mediterranean and, more recently, also in some parts of the western basin [Emeis *et al.*, 1991a; Comas *et al.*, 1996]. Sapropel deposits have been recovered in deep-sea cores dating from the

Figure 7.
 Photograph of core TMC-4 (approximately 30 cm long) taken on board before sampling. Note the darker color of the sapropel layer in contrast to the overlying non-sapropel sediments.



earliest Pliocene to the Holocene and are recognized in sediments from as far back as the Miocene. It is well established that these sediments correlate with minima in the cycle of precession, which occurs approximately every 21,000 years, and are thought to coincide with warm and wet climatic conditions [Rossignol-Strick *et al.*, 1982; Hilgen, 1991]. The youngest sapropel layer (S1) was deposited between 8300 and 6300 years B.P. based on ^{14}C dates by Jorissen *et al.* [1993]. Core TMC-4 (Figure 7) obtained during the MATER cruise was used to identify S1 and for geochemical investigations conducted to describe the paleoceanographic setting in the eastern Mediterranean basin. The site is located to the southwest of Crete (34.89°N; 22.53°W) at a water depth of ~2970 m. Clearly distinguishable in the photograph of the core is the transition with depth from the modern, light-colored sediments to the dark, sapropel layer at about 25 cm. Although no dating has been done on the core to determine the true age of the sapropel layer, using published estimates of ~9 ka, a sedimentation rate of around 2.5 – 3.0 cm/ky can be established.

Measurements of sedimentary TOC are used to formally define the sapropel layer, a designation that is not entirely coincident with that based on sediment color due to the “burn down-effect” caused by oxidation of the surface sediments with the return of oxygenated bottom-water conditions following sapropel deposition [Jung *et al.*, 1997]. In TMC-4, the sapropel is marked by an interval of high organic matter content (2.7-3.0% C_{org}) that sharply contrasts with the background sediments, typically containing less than 0.5% C_{org} (Figure 8). The percent carbonate in these sediments (% CaCO_3) ranges between 40-60% throughout the profile with the slightly lower quantities existing in the sapropel layer.

The record of $\delta^{18}\text{O}$ from bulk carbonate in core TMC-4 shows a decrease in oxygen isotopic composition beginning prior to the formation of S1 (similar to findings of Cita *et al.* [1977]; Vergnaud-Grazzini *et al.* [1977]; Thunell and Williams [1989]; Tang and Stott [1993]; etc. from planktonic foraminiferal $\delta^{18}\text{O}$ values) and indicates a decrease of more than 1.3‰ between the recent and sapropel sediments (Figure 8). This depletion in $\delta^{18}\text{O}$ values at S1 indi-

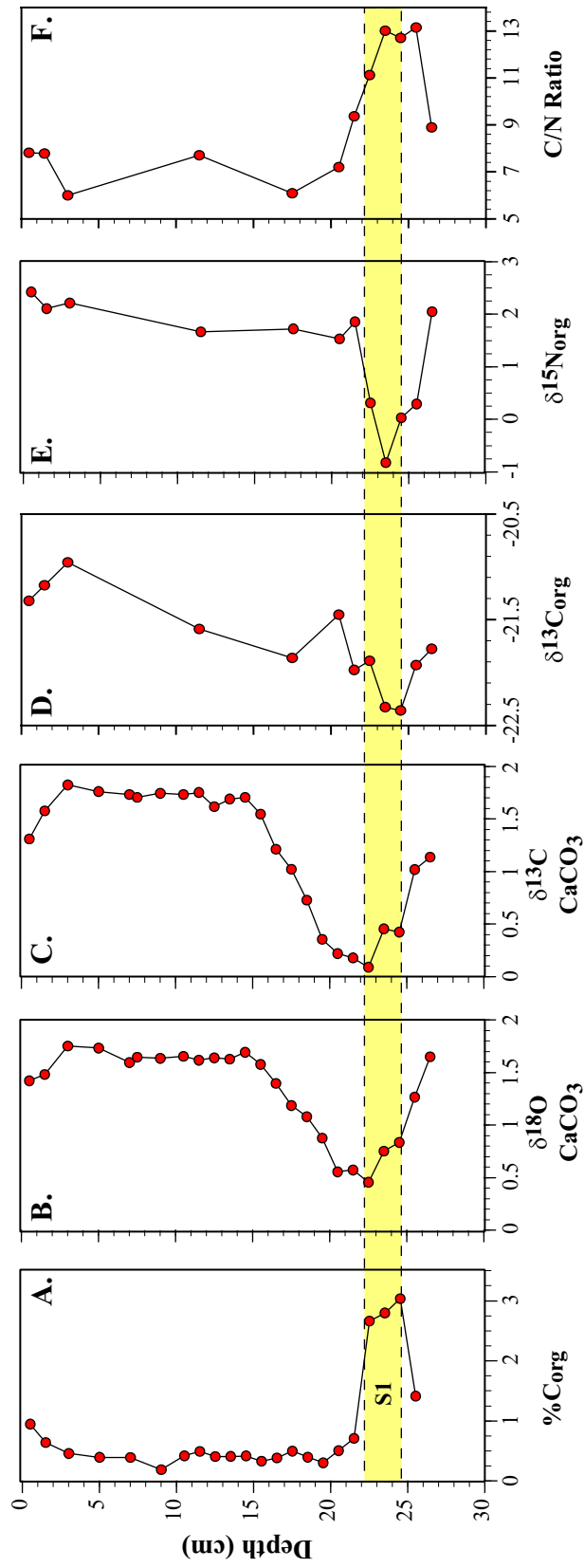


Figure 8. Results of geochemical analyses on core TMC-4: (A.) weight percent organic carbon, (B.) $\delta^{18}\text{O}$ and (C.) $\delta^{13}\text{C}$ of bulk carbonate, (D.) $\delta^{13}\text{C}$ and (E.) $\delta^{15}\text{N}$ of organic matter, and (F.) organic matter C/N ratios.

icates the presence of fresher, lower-salinity surface water than at present in the Mediterranean. Theories have, in turn, suggested that the existence of less saline water in the surface ocean allowed for stable stratification of the water column prohibiting the formation, and encouraging the stagnation, of deep water [Cita *et al.*, 1977; Vergnaud-Grazzini *et al.*, 1977], or even led to a reversal of the modern “anti-estuarine” circulation pattern [Calvert, 1983; Thunell *et al.*, 1984; Thunell and Williams, 1989]. The profile of $\delta^{13}\text{C}$ from bulk carbonate similarly shows a depletion in the sapropel layer with values decreasing by 1.75‰. The lighter carbon isotopic composition recorded in the carbonate has been interpreted to reflect a decrease in the $\delta^{13}\text{C}$ of ΣCO_2 due to the large fresh water contribution at S1 [Fontugne and Calvert, 1992], since fresh water contains more dissolved CO_2 than seawater with a $\delta^{13}\text{C}$ of approximately -5 to -10‰.

Examination of the bulk organic matter shows carbon and nitrogen isotopic compositions that are also systematically lighter in the sapropel layer (Figure 8). The carbon isotopes show a total decrease of -1.4‰ in $\delta^{13}\text{C}$ values, similar to the decrease seen in the bulk carbonate record, with values ranging from -20.96 to -22.36‰. These values can be used to address the question concerning the origin of organic matter that is found in the sapropel layer, i.e., marine vs. terrestrial. Considering the fact that C_3 plants have carbon isotopic values averaging around -27‰ and C_4 plants have values around -14‰ [Smith and Epstein, 1971; O’Leary, 1988], one could interpret the decrease in $\delta^{13}\text{C}$ values at S1 as reflecting increased input of terrestrial C_3 plant material from the surrounding land masses. Yet, modern plankton in the Mediterranean Sea has $\delta^{13}\text{C}$ values ranging from -24.5 (in the Alboran Sea) to -22‰ (in the eastern Mediterranean), both measured on plankton collected in winter [Fontugne, 1983], suggesting that the carbon isotopic composition of organic material in the sapropel layer is still characteristic of marine plankton [Fontugne and Calvert, 1992] (or even slightly heavier). Thus, the change in organic matter $\delta^{13}\text{C}$ is likely driven by the decrease in the $\delta^{13}\text{C}$ of ΣCO_2 due to freshwater flooding of the surface water at S1 with the signal perhaps slightly dampened by an increase in marine productivity (also see discussion in Part II). Nitrogen isotopes also support an increase in productivity and a higher marine organic flux during periods of sapropel formation [Calvert *et al.*, 1992]. The record shows a decrease in $\delta^{15}\text{N}$ values of 3.24‰ from the present to S1, with values ranging from 2.42 to -0.82‰. This pattern indicates enhanced nitrate availability at times of sapropel deposition (allowing for maximum isotopic fractionation and hence, preferential uptake of ^{14}N) and the importance of N-fixing primary producers in the photic zone [Calvert *et al.*, 1992].

The organic C/N ratio is also commonly applied as an indicator of the origin of organic matter since marine algae typically have values between 6-7 [Redfield *et al.*, 1963] and land plants typically have values greater than 20 [Hedges *et al.*, 1986]. Calculation of the elemental composition in the samples shows C/N ratios averaging 7.4 in the background sediments and 12.5 in the sapropel layer (Figure 8). The profile shows that there is a clear difference between the two lithologies and, at first glance, suggests that the sapropel layer contains a larger fraction

of terrestrial organic matter. Yet, the C/N ratios depicted here are still fairly low with respect to those common in terrestrial vegetation and the increase at S1 may just be a result of the higher productivity environment, which tends toward higher C/N ratios [Emeis *et al.*, 1991b] (causing preferential removal of nitrogenous organic material [Suess and Müller, 1980]), in contrast to the oligotrophic conditions present today.

An interesting observation made upon examination of the results shown in Figure 8 is that there is a clear offset in the timing of “maximum” sapropel conditions as depicted by the organic proxies and the carbonate records. The profiles based on organic material indicate an earlier and more abrupt transition to modern conditions than the isotopic records from bulk carbonate, which display more gradual changes in the isotopic composition of seawater. Perhaps this phenomena may also be explained by the “burn-down effect” whereby organic material present at the sediment surface became oxidized with the initial return of oxygenated bottom waters to the deep eastern basin [Jung *et al.*, 1997].

4.2. BIOLOGICAL MARKERS IN SAPROPEL SEDIMENTS

In particular, the organic matter contained in sapropel sediments provides a variety of information that may be useful for elucidating the environmental conditions existing at the time of their deposition. The quantification of molecular compounds may also be used to identify the sources of organic matter (i.e., marine vs. terrestrial and bacterial). Additionally, the concentration of these markers may prove useful in determining if higher rates of primary productivity or bottom-water anoxia actually existed during periods of sapropel deposition. A review of the main trends in the biological marker composition of sapropels in contrast to the background sediment is given by Bouloubassi *et al.* [1999], while ten Haven *et al.* [1987] focus specifically on the conditions at S1.

For this study, and for paleoceanographic applications in general, biomarkers must be chosen that span the entire record, thus existing both in sapropel and non-sapropel sediments, and with abundances high enough to be measurable. Here, we initially intended to focus on long-chain alkenones in sedimentary organic matter to track the paleoenvironmental conditions since S1, yet unfortunately found only very small traces of these compounds in the extracts from the organic-carbon lean sediments. Figure 9 clearly shows the high abundance of long-chain alkenones (C₃₇ – C₃₉) in the sapropel layer, indicating the enhanced input from marine prymnesiophyte algae [Volkman *et al.*, 1979]. Also evident in the sapropel samples is a high concentration of dinosterol, indicative of a major contribution from dinoflagellates [Robinson *et al.*, 1984; ten Haven *et al.*, 1987]. Due to the low abundances of these compounds in the more recent sediments, we decided to investigate *n*-alkanes, which are present throughout the sediment section, as an additional tracer of hydrologic change. The *n*-alkane distribution pattern in these samples shows a predominance of the odd carbon number, longer-chain homologs with *n*-C₂₅ to *n*-C₃₃

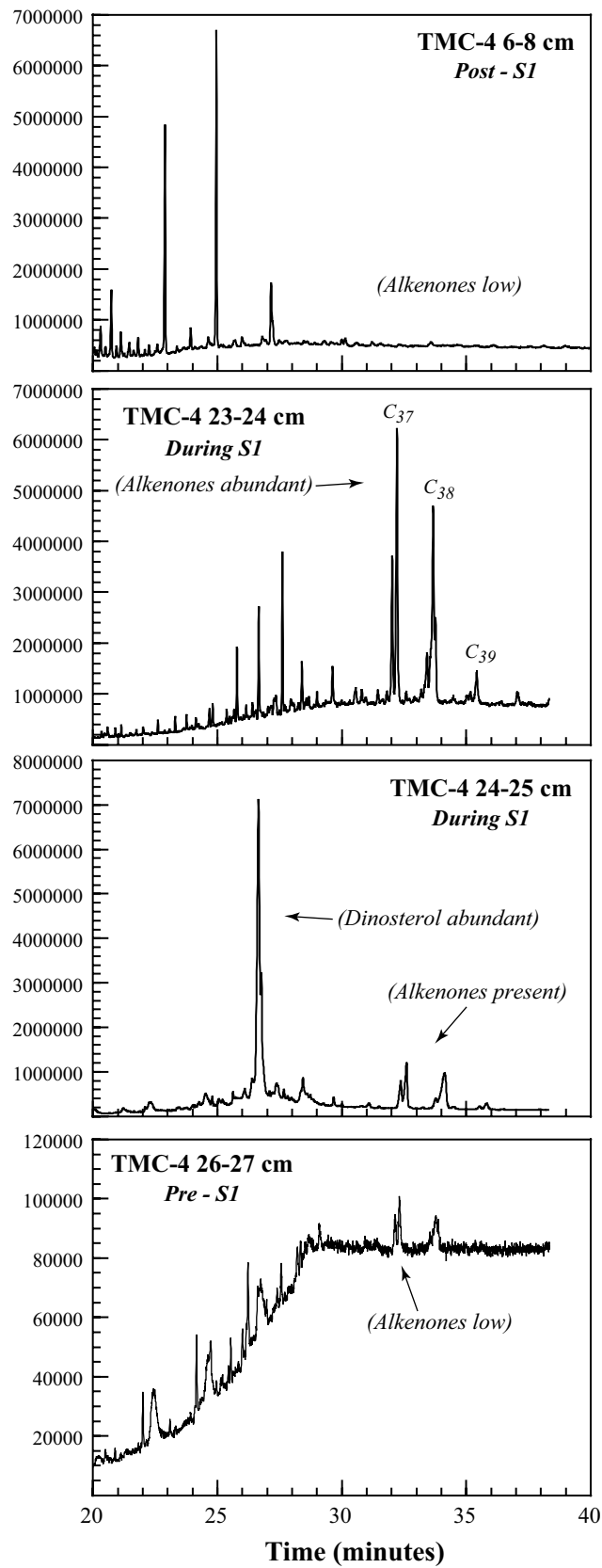


Figure 9. Total ion chromatograms of organic fractions containing the alkenone compounds from core TMC-4. Note the low abundance of compounds in the sediments above and below the sapropel layer.

dominating and only minor concentrations of the even homologs in this range. This pattern is typically interpreted as indicating an origin from higher land plants [Eglinton *et al.*, 1962] though this issue will be further addressed in Part II of this chapter. An excellent point made in the discussion of Bouloubassi *et al.* [1999] is that, relative to the profile of C_{org} content, the lipids assumed to be derived from a terrestrial source (i.e., longer-chain *n*-alkanes) represent a higher proportion of the organic carbon in the background sediments, whereas, in the sapropels, the “terrestrial” component is diluted by an increase in marine organic matter (i.e., abundance of clearly algal biomarkers, such as alkenones and dinosterol as illustrated in Figure 9). This implies that enhanced marine productivity is mainly responsible for the increase in organic carbon content found in sapropels. It also must be kept in mind that selective degradation of algal biomarkers typically biases *n*-alkane ratios towards terrestrial signatures [Meyers and Ishiwatari, 1993].

4.3. LAST GLACIAL MAXIMUM

The Mediterranean has been the focus of numerous reconstructions and studies attempting to characterize the global climatic state at the Last Glacial Maximum. The larger than average glacial-interglacial change in $\delta^{18}O$ recorded in the shells of planktonic foraminifera [Thunell and Williams, 1989], the potential impact of MIW outflow on the global thermohaline circulation, and the interest in understanding the climatological dynamics of the heavily populated European/Mediterranean region all make this marginal sea an intriguing target for paleoenvironmental research.

Due to the ~120 m fall in sea level during the last glacial period, the inflow of Atlantic seawater through the Strait of Gibraltar was reduced by as much as 50% [Bryden and Kinder, 1991]. Yet, the Mediterranean continued to supply the Atlantic Ocean with dense intermediate water [Thunell *et al.*, 1987; Zahn *et al.*, 1987]. Reconstructions show that the $\delta^{18}O$ of foraminiferal calcite was enriched by as much as 2.5 to 3.0‰ at the LGM compared to today [Thunell and Williams, 1989; Rohling and DeRijk, 1999], with the heavier values occurring in the eastern basin (see Figure 10). Comparison of the E-W gradients in $\delta^{18}O$ from the present and the LGM suggest that the Mediterranean basin acted as a slightly stronger concentration basin during the glacial period than today [Thunell and Williams, 1989], especially in the Levantine Basin [Rohling and DeRijk, 1999]. Despite this indication of excess evaporation and arid conditions, Rohling [1999] suggests that the relative humidity over the Mediterranean region has been more or less constant over the past 20,000 years. Studies of vegetation and water balance provide a more specific scenario, indicating that the basin was characterized by cold, wet winters and dry summers at the LGM due to increased seasonality [Prentice *et al.*, 1992]. Salinity reconstructions indicate enrichments of 0.5‰ in the west and 1.1‰ in the east (specified as change in $\delta^{18}O$ ‰) [Thunell and Williams, 1989]. Estimates of the degree of cooling in the basin range from 4-9°C (e.g., Thiede [1978]; Thunell [1979]; Bigg [1994]; Emeis *et al.* [2000]; Cacho *et al.* [2001]), with

the intensification of the Northern Hemisphere wind system suspected to play an important role in this temperature decrease [Rohling *et al.*, 1998; Cacho *et al.*, 1999].

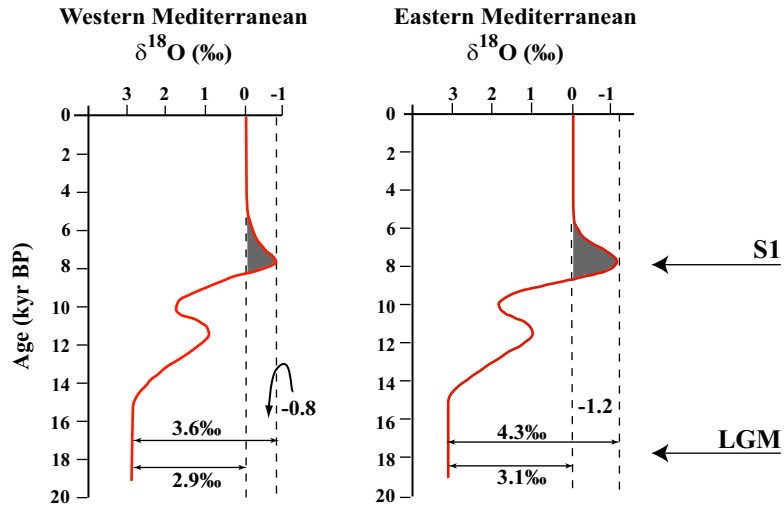


Figure 10.

Records of the oxygen isotopic composition of planktonic foraminifera [Thunell and Williams, 1989] showing the difference between changes in $\delta^{18}\text{O}$ in the western and eastern Mediterranean basins from the present back to the Last Glacial Maximum (LGM) including Sapropel Event 1 (S1). The total changes in the $\delta^{18}\text{O}$ values are displayed for ease of comparison.

PART II

HYDROGEN ISOTOPES IN BIOMARKERS TRACK MEDITERRANEAN PALEOHYDROLOGIC CHANGE DURING SAPROPEL DEPOSITION

H.A. Paul, S.M. Bernasconi, N. Andersen, C. Klaas, and J.A. McKenzie
to be submitted to: *Nature*, 2002.

ABSTRACT

Hypotheses explaining the origin of deep sea sapropels in the eastern Mediterranean Sea agree that deposition of these sediments coincides with intervals of increased seasonality and freshening of Mediterranean surface waters [Rossignol-Strick, 1985; Rohling and Hilgen, 1991; Kallel *et al.*, 1997b]. Here, we use the hydrogen isotopes of individual biomarkers in sediments from the eastern Mediterranean to quantify the magnitude of hydrologic change that occurred during Sapropel Event 1 (S1), a period of high organic matter deposition (3% C_{org}) thought to coincide with warm and wet climatic conditions approximately 9,000-6,000 years ago. Specifically, to reconstruct the δD of marine surface water in the past, we measured the D/H ratios of individual long-chain alkenones and *n*-alkanes. These molecular proxies reveal that the hydrogen isotopic composition of Mediterranean surface water during S1 was approximately 35‰ lighter than at present. In conjunction with the $\sim 1.2\%$ change in seawater $\delta^{18}O$ [Thunell and Williams, 1989], these isotopic values attest to the significant increase in freshwater input, yet still evaporative conditions, that existed during sapropel formation in the eastern Mediterranean Sea. In addition, the isotopic compositions of long-chain *n*-alkanes denote a marine origin for the biomarkers and indicate that hydrogen isotopes will be a vital tool for determining the sources of organic matter.

1. DISCUSSION

Sapropels are episodic, organic carbon-rich sedimentary layers in the Mediterranean Sea that are vestiges of past times when environmental conditions were vastly different than those prevailing today. The modern eastern Mediterranean is an oligotrophic system with a semi-arid climate and sediments that are organic carbon poor and oxidized. The hydrologic budget in the region is dominated by evaporation that exceeds the limited freshwater input from precipitation and continental runoff. The formation of sapropels has thus been attributed to distinct changes in the hydrographic regime and biogeochemical cycling in the sea resulting from global and regional climate variations. The observation that sapropels are associated with prominent negative $\delta^{18}O$ anomalies in planktonic foraminifera [Cita *et al.*, 1977; Williams *et al.*, 1978] has led to the conclusion that a significant increase in freshwater input to the sea occurred in the past and

initiated sapropel deposition. Yet, due to the ambiguity associated with trying to distinguish between the causes of fractionation in foraminiferal calcite, the full magnitude of hydrologic change has remained unquantified.

To evaluate the change in freshwater balance that occurred during deposition of S1, we focus on hydrogen isotopes in organic matter as they reflect the isotopic composition of ambient waters and are more sensitive to change in meteoric input than oxygen isotopes. Specifically, we determine the difference ($\Delta\delta D_{\text{MOD-SAP}}$) between present seawater, δD_{MOD} , and S1 seawater, δD_{SAP} , by measuring the D/H ratios of contemporary and fossil (S1) biomarkers preserved in sediments of the eastern Mediterranean Sea. The advantage of using compound-specific hydrogen isotopes for paleoceanographic research is that individual organic compounds are associated with particular biological sources, restricting the number of parameters that influence the isotopic signal. Here we focus on the examination of hydrogen isotopes from long-chain alkenones and *n*-alkanes as bulk lipids have been shown to accurately record the δD of surrounding environmental waters in freshwater aquatic plants [Sternberg, 1988].

Alkenones are biosynthesized by a specific group of haptophyte algae and are produced most notably by *Emiliania huxleyi* and *Gephyrocapsa spp.* [Marlowe *et al.*, 1984] in the upper 50 m of the water column. These compounds have been widely used in paleoceanography for assessing past sea surface temperature changes and reconstructing paleo- $p\text{CO}_2$ in the oceans. Here we focus on the C_{37} alkenones ($\text{C}_{37:2}$ and $\text{C}_{37:3}$) as they are the most abundant in our sedimentary samples. To reconstruct paleo-seawater δD , we use the fractionation factor determined by growing batch cultures of the coccolithophorid *Emiliania huxleyi* in seawater with a controlled isotopic composition ranging from 0 to 400‰. This calibration established that biosynthetic partitioning of D/H by living coccolithophorids yields $\text{C}_{37:2}$ alkenones that are on average 232‰ depleted relative to growth water and $\text{C}_{37:3}$ alkenones that are depleted by 242‰ (Footnote 1).

To validate the use of hydrogen isotopes from alkenones for paleoenvironmental applications, we wanted to test their ability to accurately portray the modern seawater hydrogen isotopic composition. To this end, we compared the δD of surface water samples from an east-west transect across the eastern Mediterranean Sea with the δD of organic compounds extracted from the surface sediments of a core (TMC-4) taken just southwest of Crete (Figure 1). Unfortunately, the surface sediments did not contain measurable abundances of alkenones. Thus, we examined the δD of long-chain *n*-alkanes (*n*- C_{27} , *n*- C_{29} , *n*- C_{31}) which are abundant throughout the core. Applying the previously derived fractionation of -158‰ for the total *n*-alkane fraction of organic matter [Estep and Hoering, 1980; Sessions *et al.*, 1999], close correlation exists between the modern surface water, average δD from hydrologic stations is 9.1‰, and the source water values estimated using these organic compounds, average δD is 9.4‰ (Figure 2a, Table 1).

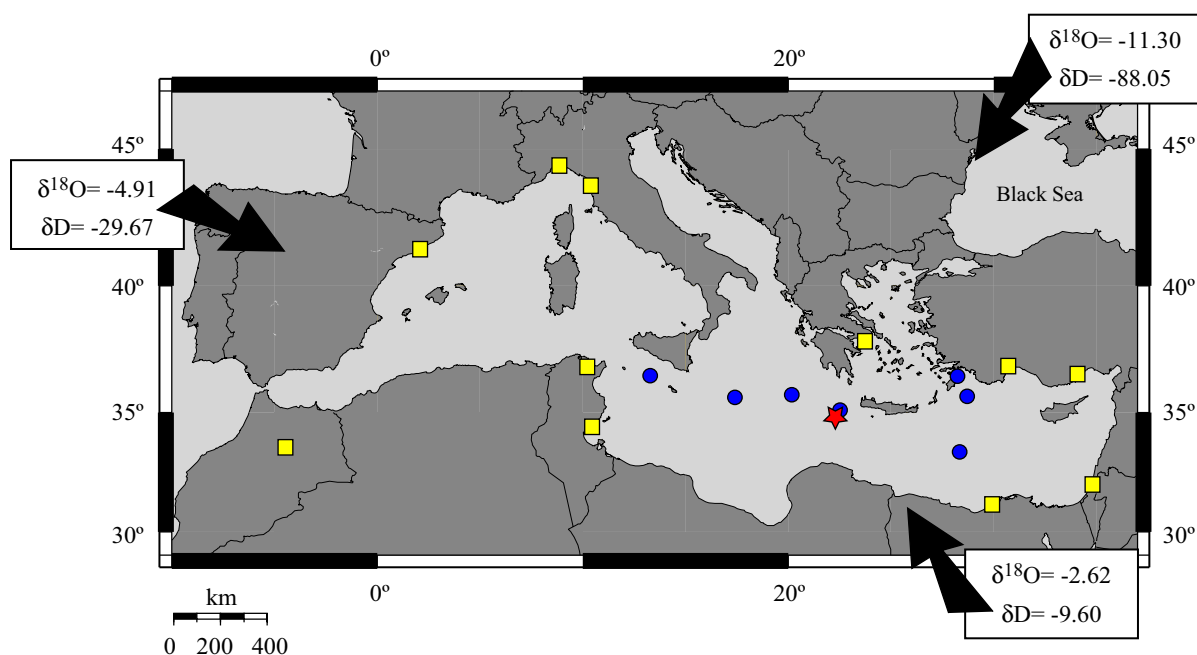


Figure 1.

Map of the Mediterranean Sea displaying locations of the surface water sampling stations (circles) and core TMC-4 (2970 m water depth; star) taken during the MATER cruise, June 1999; and precipitation stations [IAEA/WMO, 1998] (squares) used for comparison of modern meteoric water isotopic composition. Arrows denote the origin of the three main air masses converging over the Mediterranean region and the modern average isotopic composition from these moisture source regions [Rozanski *et al.*, 1993]: Atlantic/western Europe ($\delta^{18}\text{O} = -4.91\text{‰}$; $\delta\text{D} = -29.67\text{‰}$), north African ($\delta^{18}\text{O} = -2.62\text{‰}$; $\delta\text{D} = -9.60\text{‰}$), and Asian continental ($\delta^{18}\text{O} = -11.30\text{‰}$; $\delta\text{D} = -88.05\text{‰}$).

In general, *n*-alkanes with higher carbon numbers are assumed to originate from terrestrial, higher plants [Tissot and Welte, 1984]. The excellent agreement displayed here between the modern seawater and reconstructed source water δD using the biomarkers, however, contradicts this supposition and implies that the organic matter is dominantly derived from a marine algal source. For comparison, the isotopic compositions of modern Mediterranean precipitation at stations bordering the sea [IAEA/WMO, 1998] (Figure 1) are plotted in Figure 2a. Assuming that *n*-alkanes of terrestrial origin would indicate source values closer isotopically to meteoric water (annual average input to the Mediterranean: $\delta\text{D} = -37.96\text{‰}$; $\delta^{18}\text{O} = -6.12\text{‰}$ [Gat *et al.*, 1996]), it is clear from these measurements that the surface sediment *n*-alkanes resemble marine water more closely than precipitation values. Yet, considering studies of leaf water [Terwilliger and DeNiro, 1995] and plant cellulose [Epstein *et al.*, 1977] that suggest terrestrial organic matter may be enriched in deuterium relative to aquatic organic matter, it is possible that terrestrial input, despite the lighter δD source water composition, could appear similar in isotopic composition to marine surface water values. In attempt to verify the origin, we additionally measured the $\delta^{13}\text{C}$ of the *n*-alkanes (Table 1) and found the values to be within the range calculated for planktonic autotrophs, though we realize that the isotopic composition of terrestrial plants can also

have similar values [Hayes *et al.*, 1987; Prahl *et al.*, 1992]. These carbon isotopic values are almost identical to measurements on long-chain *n*-alkanes extracted from surface sediments of the Black Sea (-29.8 to -30.5‰), which Freeman *et al.* [1994] argue are representative of algal input in this setting. In addition, an isotopic study of long-chain *n*-alkanes from lacustrine sediments showed the *n*-C₂₉ and *n*-C₃₁ alkanes to originate mainly from phytoplankton [Chikaraishi and Naraoka, 2001]. Similarly, we conclude that the long-chain *n*-alkyl lipids present in these eastern Mediterranean sediments derive from aquatic organisms and are not wholly attributable to leaf waxes.

Table 1.

Compound-specific isotopic composition of biomarkers in sediment samples from core TMC-4, surface vs. sapropel layer.

sample	compound	measured δD	standard deviation	<i>n</i>	s.d. √ <i>n</i>	source δD†	ΔδD (MOD-SAP)	measured δ ¹³ C	standard deviation
0-2 cm (surface)	<i>n</i> -C ₂₇	-153.6	11.5	12	3.32	4.5		-29.94	0.7
	<i>n</i> -C ₂₉	-138.7	9.4	12	2.71	19.3		-31.53	0.3
	<i>n</i> -C ₃₁	-153.6	5.8	12	1.67	4.4		-30.98	0.1
						9.4			
						(average)			
23-24 cm (sapropel)	<i>n</i> -C ₂₇	-183.1	10.9	12	3.15	-25.1	29.54	-28.14	---
	<i>n</i> -C ₂₉	-168.5	6.9	12	1.99	-10.5	29.83	-30.54	0.2
	<i>n</i> -C ₃₁	-187.4	7.1	12	2.05	-29.4	33.79	-29.67	0.3
						-21.7	31.1		
						(average)	(average)		
	C _{37:2} alkenones	-260.8	16.8*	8	5.94	-28.8	37.9‡		
	C _{37:3} alkenones	-270.4	13.1*	8	4.63	-28.4	37.5‡		
						-28.6	37.7		
						(average)	(average)		

†Source water δD calculated using a fractionation factor of -158‰ for *n*-alkanes, -232‰ for C_{37:2} and -242‰ for C_{37:3} alkenones.

‡Calculation of ΔδD based on the modern average δD of surface waters in the eastern Mediterranean of 9.1‰.

*Our ability to measure the alkenone compounds is hindered by the closely eluting C_{37:2} and C_{37:3} peaks resulting in a lower obtainable analytical precision (*Footnote 2*).

To constrain the magnitude of the δD excursion at S1, we measured the δD of both alkenones and *n*-alkanes from within the sapropel layer. Reconstruction of the original seawater values indicates that Mediterranean Sea surface waters were approximately 35‰ lighter than at present and had an average δD of -22 to -28‰ (Table 1 and Figure 3). The close agreement between the reconstructed *n*-alkane and the alkenone source-water values (Figure 2a) further supports that the *n*-alkanes are indeed mainly of marine origin and that it is not mere coincidence that we are able to derive the modern seawater δD from the surface sediment *n*-alkanes. Obtain-

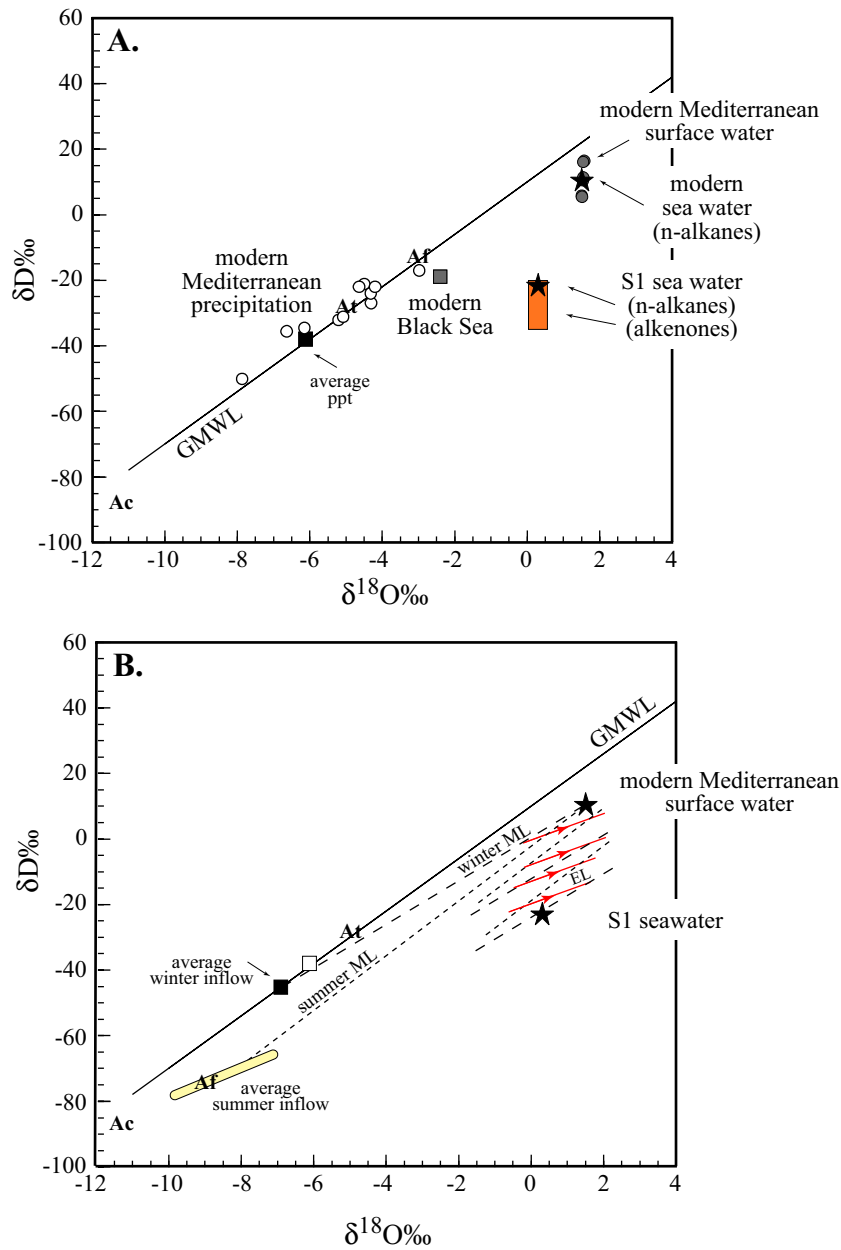


Figure 2.

Isotopic relationship of various hydrologic bodies and the reconstructed seawater values from individual organic compounds on a δD vs. $\delta^{18}O$ diagram. The three main moisture sources are denoted by At=Atlantic, Af=north Africa, and Ac=Asian continental. (A.) Modern vs. S1 comparison. Note the clear agreement between the modern eastern Mediterranean surface water (average isotopic composition from 3-10 m depth: $\delta D = 9.10$ ‰, $\delta^{18}O = 1.53$ ‰) and the source water value based on surface sediment *n*-alkanes; and the correspondingly large separation between the δD of modern Mediterranean precipitation (average: $\delta D = -38$ ‰, $\delta^{18}O = -6$ ‰ [Gat *et al.*, 1996]) and the surface sediment *n*-alkanes. Also note the excellent agreement between the reconstructed seawater δD values at S1 from the two independent biomarkers (*n*-alkanes and alkenones). Oxygen isotopic composition of surface water at S1 is set to a value of 0.30‰ based on a $\Delta\delta^{18}O_{MOD-SAP}$ of -1.2‰ [Thunell and Williams, 1989] in the eastern Mediterranean Sea. (B.) Evaporation line (EL) assumed equal to modern with a slope close to 4.0. Mixing lines (ML) connect the seawater and respective freshwater inflows. Here winter ML is due to input from Atlantic and Asian sources and the summer ML is due to the runoff from northern Africa (δD : -80 to -60‰ and $\delta^{18}O$: -10 to -7‰ [Edmunds and Wright, 1979; Thorweihe *et al.*, 1990]).

ing nearly equivalent results from the *n*-alkanes and marine water in two distinct cases would be highly unlikely if the organic matter were terrigenous, originating from vastly different source regions. Although studies aimed at constraining the fractionations induced by the processes of photosynthesis and evapotranspiration on individual lipid compounds in land plants are necessary to substantiate this, these initial results suggest that hydrogen isotopes can be a powerful tool for identifying the environmental origin of organic matter.

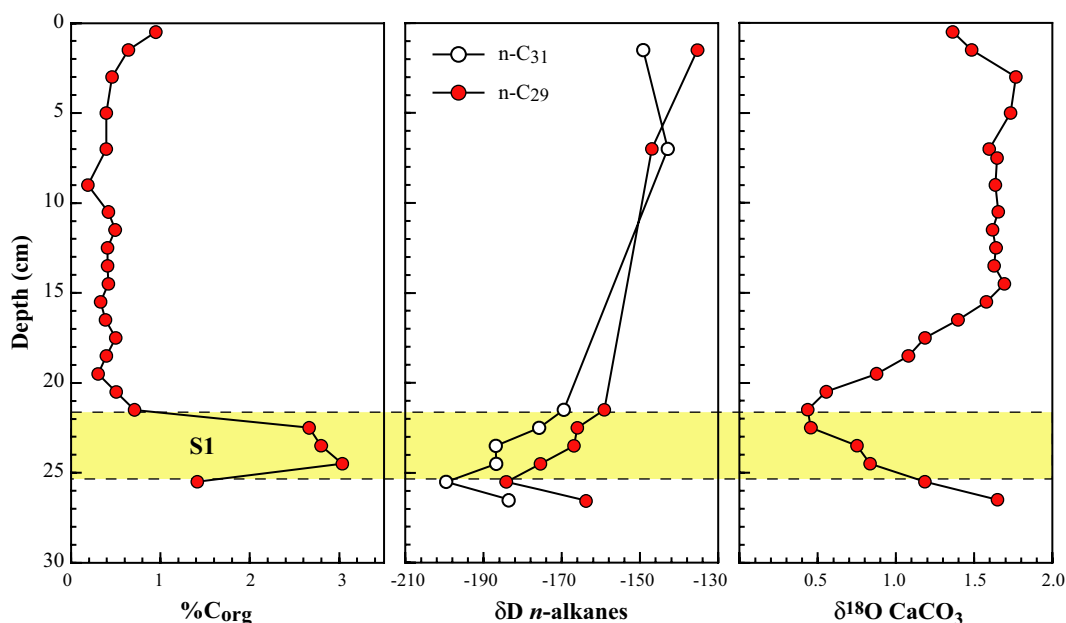


Figure 3. Geochemical analyses on core TMC-4 including percent organic carbon; the hydrogen isotopic composition of the C₂₉ and C₃₁ *n*-alkanes; and the oxygen isotopic composition of bulk carbonate. The sapropel layer is defined based on the period of high C_{org} values.

Based on measurements of kerogen from the Tyrrhenian Sea, *Krishnamurthy et al.* [2000] have suggested a change in Mediterranean Sea δD of -50% . This value is larger than expected based on measurements of $\Delta\delta^{18}O_{MOD-SAP}$ from calcareous microfossils which suggest a $\Delta\delta D_{MOD-SAP}$ of around -20% [Thunell and Williams, 1989; Bernasconi and Pika-Biolzi, 2000] based on the Global Meteoric Water Line (GMWL). Both our results and those of *Krishnamurthy et al.* [2000] provide clear evidence of extreme alteration in the regional hydrologic balance at S1 time. Comparison of the results from both studies suggests that geochemical proxies based on bulk organic material, such as kerogen, may be more subject to external parameters, for instance paleoproductivity (i.e., change in dominant type of organic matter deposited in sapropel layers [Bouloubassi et al., 1999]) and possibly post-depositional isotopic exchange [Schimmelmann et al., 1999]. Alternatively, compound-specific measurements provide less ambiguous reconstructions of paleo- δD because the biological sources are limited and may be more reliable since most

hydrogen in lipidic biomarkers is bound to carbon and is non-exchangeable [Schimmelmann *et al.*, 1999; Andersen *et al.*, 2001].

The period of S1 deposition, also referred to as the Holocene Climate Optimum, was dominated by intensification and northward displacement of the summer monsoons over northern Africa [Rossignol-Strick *et al.*, 1982; Kutzbach John and Street Perrott, 1985]. Hence, changes in the relative importance of the three air masses delivering precipitation to this region (Figure 1) occurred, likely including a major alteration in atmospheric circulation [McKenzie, 1993]. A shift in the source of north African precipitation allowed increased amounts of monsoonal rainfall, derived from the south [Edmunds and Wright, 1979], to migrate further north permitting an abundance of isotopically depleted meteoric waters to be transported into the Mediterranean region. North African aquifers recharged during the Holocene humid period, with average groundwater values of $\delta D \sim -70$ and $\delta^{18}O \sim -8\%$ [Edmunds and Wright, 1979; Thorweihe *et al.*, 1990] (Figure 2b), provide evidence of incoming precipitation with much lighter isotopic compositions than today. As this period is thought to have been slightly warmer than at present [Rossignol-Strick, 1985; Thorweihe *et al.*, 1990], these extremely depleted freshwater values have been interpreted as indicating an increase in the amount and intensity of precipitation. The intense tropical summer rainfall, likely to accompany a monsoon period, would have released enormous amounts of isotopically light water over a large area [Dansgaard, 1964].

Seasonal cycles of freshwater input and evaporation contribute to the isotope balance and dictate the final isotopic composition of marine surface waters. The groundwater produced from the strongly negative monsoon rains shows evaporative enrichment with respect to the GMWL (Figure 2b) and suggests that runoff coming from the north African coast in summer would produce a much steeper mixing line than the meteoric input from the northern Mediterranean region (assumed to be similar or just slightly lighter with respect to today [Bar-Matthews *et al.*, 2000]) delivered mainly during winter. Also, clear from these results is the continued importance of evaporation in the hydrologic balance of the basin. The $\delta^{18}O:\delta D$ relationship of marine surface water during the deposition of S1 is even more removed from the GMWL (Figure 2b) than today, thus attesting to the negative water budget. Clearly evaporation remained a dominant hydrologic factor even in this period of increased meteoric influx pointing towards increased seasonality. The combined effect of these processes produces a zig-zag pattern of enrichment and depletion [Gat *et al.*, 1996] (Figure 2b) depicting the path of seawater isotopic variation between S1 and the present.

2. CONCLUSIONS

Results presented here provide sound evidence that the regional water balance of the eastern Mediterranean Sea has oscillated in the past as a result of large variations in the sources of fresh-water input and changes in seasonality. Additionally, the data provide supporting evi-

dence that evaporation remained dominant in the hydrologic balance at S1 [Rohling and DeRijk, 1999]. Compound-specific hydrogen isotopic measurements on sedimentary marine biomarkers, namely long-chain alkenones and *n*-alkanes, prove to be an important new tool for paleoceanographic interpretation. Furthermore, the δD of long-chain *n*-alkanes (*n*-C₂₇, *n*-C₂₉, and *n*-C₃₁) indicate that they are dominantly from a marine algal source and not terrestrially derived, suggesting that compound-specific hydrogen isotopes can be a valuable means for deciphering the biologic origins of molecules.

Footnote 1. - Culture Experiments

Batch cultures of the coccolithophorid *Emiliana huxleyi* were isolated from a strain collected in the North Atlantic (41°43.5N, 9°06.5W from 40 m water depth at 13.0°C) and grown in a controlled laboratory environment. Conditions included: a temperature of 18-19°C, salinity of 35 psu, and light intensity of 40-45 $\mu E m^{-2} s^{-1}$. The seawater medium was deuterated with D₂O to produce source waters with a range of varying hydrogen isotopic compositions from 0 (undeuterated) to 400‰. Results of this calibration show that C_{37:2} and C_{37:3} alkenones are approximately 232 to 242‰ depleted in δD relative to the water in which they were grown.

Footnote 2. - Stable Hydrogen Isotopes

The δD values of individual organic compounds were obtained by isotope-ratio monitoring gas chromatography-mass spectrometry using a high-dispersion Geo 20-20 (PDZ Europa) mass spectrometer [Scrimgeour *et al.*, 1999]. Compounds were separated on a high-capacity, megabore GC column (50m, 0.53mm i.d., 1 μ m film) using He as the carrier gas. H₂ gas was produced via pyrolysis at 1300°C and the possible minor by-product, methane, was separated with a mega-bore molesieve (5Å) and water was trapped by a nafion tube. A series of several *n*-alkanes was used as the standard for external calibration, using only standards with similar retention times as the sample compounds for correction. All values for δD are calculated relative to Vienna Standard Mean Ocean Water (VSMOW).

ACKNOWLEDGEMENTS

We thank the European Commission's Marine Science and Technology Program (MAST) and the Mass Transfer and Ecosystem Response (MATER) project for providing the water and sediment samples.

PART III

OXYGEN ISOTOPIC COMPOSITION OF THE MEDITERRANEAN SEA SINCE THE LAST GLACIAL MAXIMUM: CONSTRAINTS FROM PORE-WATER ANALYSES

H.A. Paul, S.M. Bernasconi, D.W. Schmid, and J.A. McKenzie
published in: *Earth and Planetary Science Letters*, 192: 1-14, 2001.

ABSTRACT

Interstitial waters recovered from Ocean Drilling Program, Leg 161, Site 976 in the western Mediterranean Sea are used in conjunction with a numerical model to constrain the $\delta^{18}\text{O}$ of seawater in the basin since the Last Glacial Maximum, including Sapropel Event 1. To resolve the oxygen isotopic composition of the deep Mediterranean, we use a model that couples fluid diffusion with advective transport, thus producing a profile of seawater $\delta^{18}\text{O}$ variability that is unaffected by glacial-interglacial variations in marine temperature. Comparing our reconstructed seawater $\delta^{18}\text{O}$ to recent determinations of 1.0‰ for the mean ocean change in glacial-interglacial $\delta^{18}\text{O}$ due to the expansion of global ice volume, we calculate an additional 0.2‰ increase in Mediterranean $\delta^{18}\text{O}$ caused by local evaporative enrichment. This estimate of $\delta^{18}\text{O}$ change, due to salinity variability, is smaller than previous studies have proposed and demonstrates that Mediterranean records of foraminiferal calcite $\delta^{18}\text{O}$ from the last glacial period include a strong temperature component. Paleotemperatures determined in combination with a stacked record of foraminiferal calcite depict almost 9°C of regional cooling for the Last Glacial Maximum. Model results suggest a decrease of ~1.1‰ in seawater $\delta^{18}\text{O}$ relative to the modern value caused by increased freshwater input and reduced salinity accompanying the formation of the most recent sapropel. The results additionally indicate the existence of isotopically light water circulating down to bottom water depths, at least in the western Mediterranean, supporting the existence of an “anti-estuarine” thermohaline circulation pattern during Sapropel Event 1.

1. INTRODUCTION

Recent studies using the $\delta^{18}\text{O}$ of interstitial waters in deep-sea sediments have shown that the global average change in seawater $\delta^{18}\text{O}$ due to polar glaciation at the Last Glacial Maximum (LGM) was approximately 1.0‰ [Schrug and DePaolo, 1993; Schrug *et al.*, 1996; Burns and Maslin, 1999; Adkins and Schrug, 2001]. Accurately constraining the glacial-interglacial variability in marine $\delta^{18}\text{O}$ attributable to global ice volume at the LGM ($\Delta\delta_{\text{LGM}}$) is extremely important for paleoceanographic reconstructions of hydrography (i.e., sea surface salinity and water mass density) and climate (i.e., sea surface temperature (SST)). Pore fluids in deep-sea sediments allow for measurement of the most recent glacial-interglacial variations in $\delta^{18}\text{O}$, in

essence providing a profile of seawater $\delta^{18}\text{O}$ variability that is unaffected by glacial-interglacial fluctuations in marine temperatures. This signal is incorporated into interstitial waters during sediment burial and compaction and is subsequently modified by transport processes acting on the pore fluids. The significance of diffusive and advective transport is a function of the diffusion coefficient and the fluid-flow rate, both controlling the movement of fluid (seawater) relative to the solid framework (sediment particles) and hence, the age-depth relationship of the fluid. Due to these processes, the oxygen isotopic composition of sediment pore fluids provides a dampened $\delta^{18}\text{O}$ record of the overlying bottom water on an attenuated time scale that can be restored by simulating the influence of diffusion and advection with a numerical model. This method of investigating paleoceanic deepwater provides an alternative to reconstructions of oxygen isotopic composition based on benthic foraminiferal calcite. Alternative methods are essential because the $\delta^{18}\text{O}$ of foraminiferal shells reflects the sum of global variations in seawater $\delta^{18}\text{O}$ due to ice volume changes, local sea surface $\delta^{18}\text{O}$ variations caused by changes in water mass advection and the freshwater budget, and the isotopic fractionation between CaCO_3 and water, which is dependent on the temperature at which foraminifera precipitate their shells.

Isotopic records from marginal marine basins exhibit the global $\delta^{18}\text{O}$ signal but are additionally complicated by a strong overprint from local climatic conditions. The Mediterranean Sea is one example of such a semi-enclosed basin, having only restricted exchange with the rest of the world's oceans, that is particularly sensitive to local environmental and climatic fluctuations. Despite its oceanographic seclusion, the Mediterranean is the source of an important intermediate water mass to the Atlantic Ocean [Zahn *et al.*, 1987; Bigg, 1994] and is considered to be a significant component in driving global thermohaline circulation [Reid, 1979]. In addition, the Mediterranean is noted for the occurrence of episodic, organic-rich sedimentary deposits called sapropels. The observation that sapropels are associated with distinct negative $\delta^{18}\text{O}$ anomalies in planktonic foraminifera [Cita *et al.*, 1977; Williams *et al.*, 1978] has led to the conclusion that significant changes in the fresh-water balance, and consequently salinity, of the Mediterranean occurred in the past and are responsible for their formation.

Currently, the Mediterranean has anomalously high salinity as the hydrologic budget is dominated by evaporative water loss that exceeds freshwater inputs via precipitation and continental runoff. Circulation is characterized by an "anti-estuarine" pattern with surface inflow from the Atlantic and subsurface outflow through the Strait of Gibraltar maintaining the basin's marine connection and water balance. Excessive evaporation and limited freshwater input cause amplification of glacial-interglacial $\delta^{18}\text{O}$ isotopic signals in foraminifera from Mediterranean surface waters of almost two times that observed in open ocean samples (e.g., compared to the North Atlantic [Thunell and Williams, 1989]). Records of deepwater $\delta^{18}\text{O}$ in the Mediterranean are limited as only sparse benthic foraminiferal data exist [Vergnaud-Grazzini *et al.*, 1989]. Thus, researchers have often resorted to examination of Atlantic benthic foraminiferal samples col-

lected outside the Strait of Gibraltar for reconstructing Mediterranean bottom-water isotopic composition [Zahn *et al.*, 1987; Vergnaud-Grazzini *et al.*, 1989; Schönfeld and Zahn, 2000].

The main objective of this study is to reconstruct the oxygen isotopic composition of Mediterranean bottom water since the Last Glacial Maximum (~20,000 years ago) and to compare the glacial-interglacial change in $\delta^{18}\text{O}$ with the results of previous studies that suggest a mean global ocean change of 0.95-1.0‰ [Schrug and DePaolo, 1993; Adkins and Schrag, 2001], a local change in Atlantic deepwater of ~0.7-0.8‰ [Schrug *et al.*, 1996; Burns and Maslin, 1999; Adkins and Schrag, 2001], and with the previously accepted value for the change in the seawater ratio of 1.3‰ [Fairbanks and Matthews, 1978; Fairbanks, 1989]. In addition, we constrain the magnitude of the negative peak in seawater $\delta^{18}\text{O}$ that occurred during Sapropel Event 1 (S1; ~10-6,000 years ago) to evaluate the extent of fresh-water input and to investigate possible circulation changes in the western Mediterranean during periods of sapropel formation. To achieve these goals, we use an approach similar to that of Schrag and DePaolo [1993] applying a mathematical model of the advective/diffusive transport in sediment pore fluids to assess changes in seawater $\delta^{18}\text{O}$. As these changes in seawater $\delta^{18}\text{O}$ are resolved independently of other geochemical proxies, we additionally use the model results to constrain the amount of $\delta^{18}\text{O}$ change due to paleo-sea surface salinity and to reconstruct Mediterranean SST by comparing our record with that of planktonic foraminiferal $\delta^{18}\text{O}$.

2. METHODS

2.1. SITE LOCATION AND HYDROGRAPHY

Site 976, drilled during ODP Leg 161, is located in the western Alboran Basin (36°12'N; 04°18'W) and is situated 60 km off the coast of Spain and 110 km east of the Strait of Gibraltar (Figure 1). Currently, the site lies within Mediterranean Intermediate Water (MIW) at a depth of 1108 m characterized by a salinity of 38.4-38.5 psu and average temperatures around 12-13°C (Figure 2). Hole 976D was dedicated to high-resolution pore water sampling, approximately every 3 m in the upper 30 meters below sea floor (mbsf), to reconstruct the oxygen isotope geochemistry of paleo-deepwater in the basin. Water samples from two other holes at Site 976 (976B and 976C) were also used to establish a more complete profile down to 200 m. At the time of drilling, a sea floor temperature of 12.67°C and a geothermal gradient in the sediments of 83.92°C/km [Revil *et al.*, 1999] existed at Hole 976B. Porosity at this site varies from approximately 0.72 at the sediment-water interface to 0.53 at 200 mbsf. Additionally, increasing concentrations of salinity, chloride, sodium, and bromide exist in interstitial waters deep in the core (approximately 2 times seawater concentration at 600 mbsf) [Comas *et al.*, 1996; Bernasconi, 1999] suggesting that these saline pore waters represent relics of ancient evaporated seawater, possibly from a Messinian-age paleo-fluid. We assume that this brine, also characterized by

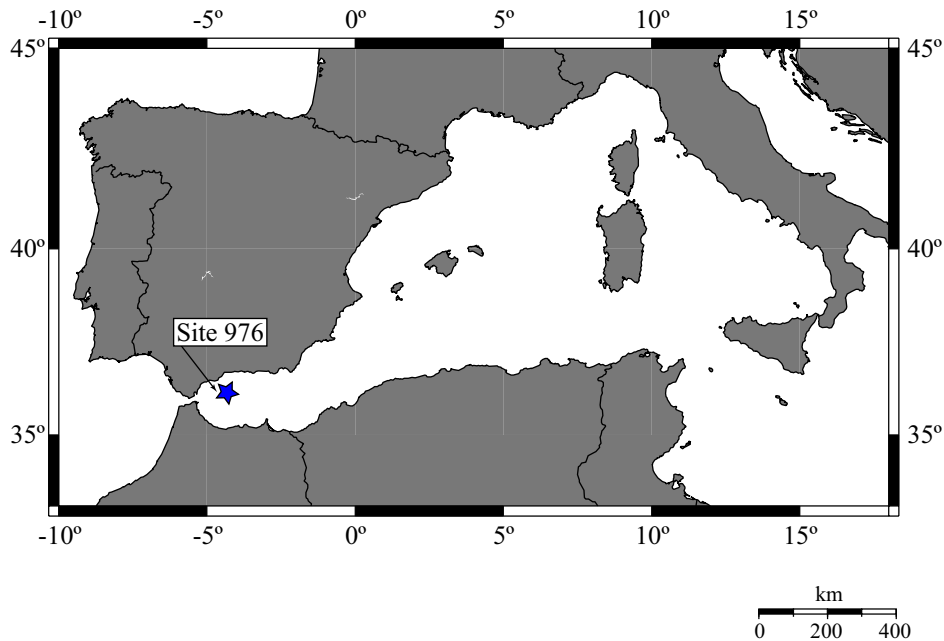


Figure 1.

Map of the western Mediterranean Sea and location of ODP Leg 161, Site 976 in the Alboran Sea. Star denotes Site 976.

enriched $\delta^{18}\text{O}$ values, has not influenced the upper 200 m of pore fluids as the $\delta^{18}\text{O}$ composition decreases with depth until below 350 mbsf [Bernasconi, 1999].

The Alboran Sea is the westernmost basin of the Mediterranean Sea into which surface waters originating in the North Atlantic flow through the Strait of Gibraltar and into the basin. These surface waters flow eastward crossing the Alboran Sea before extending throughout the entire Mediterranean at a typical depth range of 25-75 m. Thermohaline circulation in the Mediterranean is driven by seasonal variations of salinity and temperature at the sea surface, causing the formation of intermediate and deepwater masses. Levantine Intermediate Water (LIW) forms in the easternmost region of the Mediterranean, with a temperature of about 15°C and salinity of 39.1 psu. It then flows westward and can be traced down to 600-700 m in the western Mediterranean (Figure 2). This water mass is the predominant source of the saline Gibraltar outflow that is fed back into the Atlantic Ocean [Robinson *et al.*, 1992]. Deepwater in the western Mediterranean is formed in the Gulf of Lions, typically around 12.6°C and 38.4 psu. At present, the Mediterranean has an annual average SST of 19°C and a residence time of approximately 100 years [Robinson *et al.*, 1992], thus it is well-mixed relative to open-ocean, surface and deep water masses.

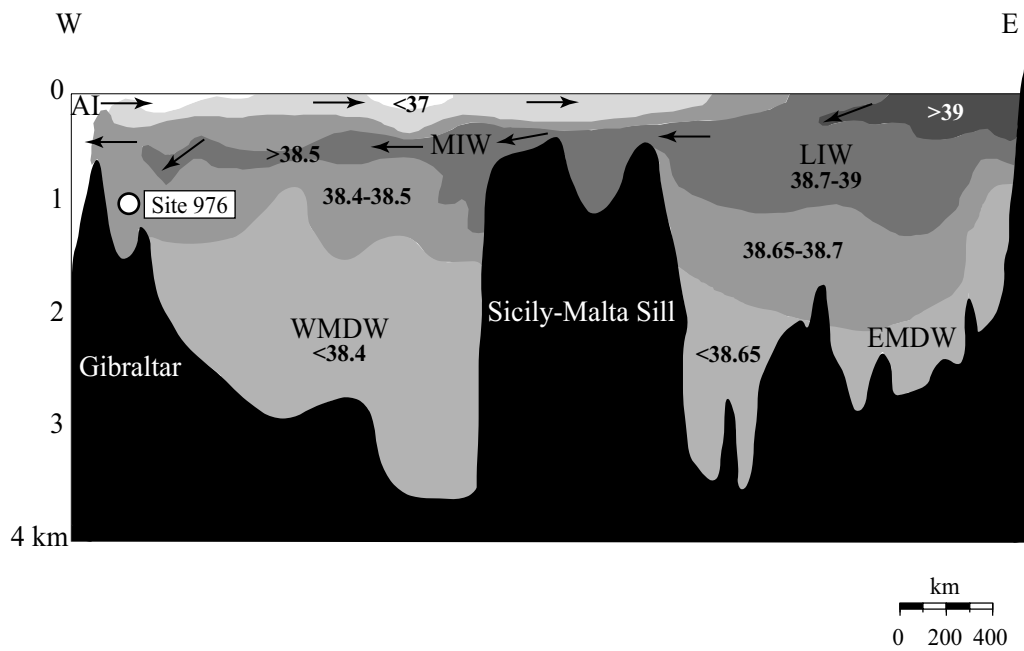


Figure 2. Cross-section displaying the bathymetry of the Mediterranean Sea (modified from *Emeis and Sakamoto* [1998]). Approximate location of Site 976 is highlighted in addition to the various water masses with their respective average salinities. AI = Atlantic Inflow, MIW = Mediterranean Intermediate Water, LIW = Levantine Intermediate Water, EMDW = Eastern Mediterranean Deep Water, and WMDW = Western Mediterranean Deep Water. Arrows depict the schematic flow pattern of modern surface-water circulation.

2.2. STABLE ISOTOPIC ANALYSES

Interstitial water samples were obtained immediately after core recovery using the standard ODP titanium/stainless-steel squeezer and teflon disks. The stable oxygen isotopic composition of the interstitial waters was determined by equilibration with CO_2 using an automated Isoprep-18 equilibration device coupled to a Micromass Optima mass spectrometer. Analytical reproducibility based on repeat analysis of internal standards is $\pm 0.05\%$. All oxygen isotope data (Table 1) are reported in the standard delta notation with respect to Vienna Standard Mean Ocean Water (VSMOW) and have been corrected for salt effects according to *Sofer and Gat* [1972].

2.3. MODEL DESCRIPTION

To constrain the record of oxygen isotopic composition of deep Mediterranean water, we have developed a numerical model that couples fluid diffusion with advective transport [*Boudreau*, 1996]. This one-dimensional model uses an implicit, unconditionally stable, conservative finite-difference scheme for calculating the isotopic evolution through time. The concentration C_f of a tracer in the fluid varies with distance z and time t based on the standard advection-diffusion equation, derived from the conservation of mass and the assumption of an incompressible fluid,

and taking into account that these processes only act in the porous volume of the sediment column:

$$\phi \frac{\partial C_f}{\partial t} = \frac{\partial}{\partial z} \left(\phi D_f \frac{\partial C_f}{\partial z} \right) - v \phi \frac{\partial C_f}{\partial z} \quad (\text{Eq. 1})$$

where the terms on the right hand side represent the expressions for diffusion and advection as a function of depth, respectively, ϕ is the sediment porosity, D_f is the effective diffusivity of the fluid ($D_f = 7.63 \cdot 10^{-10} \text{ m}^2/\text{sec}$ at the surface and varies with depth as a function of temperature, porosity, and tortuosity in the sediment [Boudreau, 1996]), and v is the upward fluid velocity relative to the subsiding sediments. Porosity is calculated as a function of depth based on a smooth fit of the measured data from Site 976 [Comas *et al.*, 1996] according to the following equation:

$$\phi_{(z)} = \phi_0 e^{(-z/\zeta)} \quad (\text{Eq. 2})$$

where z is sub-bottom depth (in mbsf), ϕ_0 is the initial porosity at the sediment-water interface, and ζ is the e-fold length of the porosity.

As Site 976 has a relatively high sedimentation rate through the Pleistocene and Holocene (approximately 20-25 cm/ky) [de Kaenel *et al.*, 1999], sedimentation is simulated by successively adding layers to the existing sediment pile. The sediment itself is treated as a fluid-saturated, porous medium and the contribution of ^{18}O to the pore fluid due to recrystallization is assumed to be insignificant on the time scale investigated [Schrug *et al.*, 1992]. Compaction of the sediments due to decreasing porosity with depth is also simulated by the model according to equation 2.

Using a method similar to that of Schrug and DePaolo [1993], theoretical profiles of fluid oxygen isotopic composition are calculated using a forward modeling approach and then compared to the observed pore-water vs. depth profile from Site 976. The lower boundary condition of C_f is constant and is appointed using the measured isotopic value of the pore waters at the base of the modeled sediment column (250 mbsf = 0.58‰). The upper boundary condition, i.e., the $\delta^{18}\text{O}$ value at the sediment-water interface (and thus the target seawater value), varies as described below. For the first 500 ky of the simulation, this value is fixed to the modern seawater value at the sediment-water interface (1.46‰). Assuming that the past $\delta^{18}\text{O}$ seawater record is identical in timing and trend (but not in magnitude) to the record of $\delta^{18}\text{O}$ from benthic foraminiferal calcite, isotopic input derived from benthic foraminifera from ODP Site 659 (eastern tropical Atlantic) [Tiedemann *et al.*, 1994] is used to simulate seawater $\delta^{18}\text{O}$ at the sediment-water interface and drive the model from 500 ka to 20 ka. This record of Atlantic $\delta^{18}\text{O}$ variability is used as no time series of adequate length or resolution derived from Mediterranean benthic foraminifera exists. From 20 ka to 0 ka (present), isotopic input is based on the model of eustatic sea level change [Fairbanks, 1989]. The amplitude of isotopic variation is then prescribed to the entire record by fixing the per mil change in $\Delta\delta_{\text{LGM}}$ relative to $\Delta\text{sea level}$ at 20 ka for each run

(i.e., $\Delta\delta_{\text{LGM}} = 0.7, 1.0, 1.3\text{‰}$, etc.) and assuming a sea level change of 120 m (illustrated in Figure 3).

Our model simulates a total of one million years at a resolution of 2000 years (i.e., deposition of ~ 0.5 m of sediment per time step) for the first 980 ky. The final 20 ky are of particular interest and are run at a higher resolution of 500 years (i.e., deposition of ~ 0.12 m). Calculations using higher temporal resolution were performed to check the influence of the time step on model results and it was found that increasing the resolution prior to 20 ka does not affect the modeled profile. A time step of 500 years after 20 ka is sufficient for obtaining numerically accurate results in a reasonable calculation time. It is important to note that the age of the sediments and the age of the contained fluids are not the same, as the fluids are altered by the advection and diffusion processes.

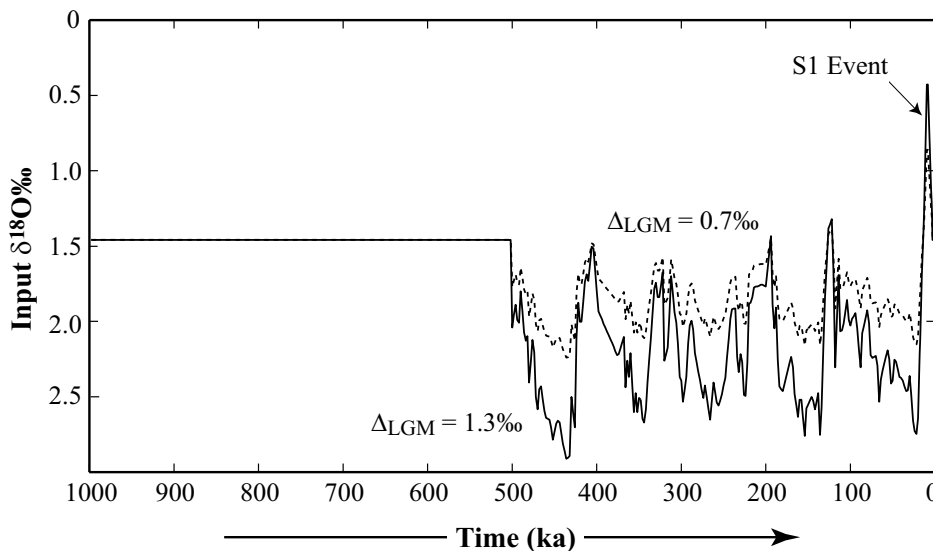


Figure 3. Sample model-input $\delta^{18}\text{O}$ (‰VSMOW) with time running from -1000 ka to present (0 ka). The solid line represents a $\Delta\delta^{18}\text{O}_{\text{LGM}}$ change of 1.3‰ and the dashed line, a change of 0.7‰.

4. RESULTS

4.1. MEASURED PORE WATERS

The isotopic measurements of sediment pore fluids from Site 976 display a distinct negative anomaly at around 15 mbsf followed by a clear positive trend with maximum $\delta^{18}\text{O}$ values occurring between 30 and 40 mbsf (Figure 4, Table 1). These two peaks in the profile are considered to represent Sapropel Event 1 (~ 9 ka) and the Last Glacial Maximum (~ 20 ka), respectively. Unfortunately, no additional samples were measured between 30 and 40 mbsf. Thus, the exact depth of the maximum $\delta^{18}\text{O}$ value, which would represent the peak of the LGM, is assumed to occur at the midpoint of these two samples.

Table 1.

Oxygen isotopic composition of interstitial waters from ODP Leg 161, Site 976 (see *Bernasconi* [1999] for extended low-resolution records).

Hole/Section	Interval (cm)	Depth (mbsf)	Salinity (p.s.u.)	$\delta^{18}\text{O}$ ‰ (VSMOW)	Cl (mM/l)
976D-1H-1	128-133	1.28	40	1.46	619
976D-2H-2	145-150	4.45	38	1.46	614
976D-2H-4	145-150	7.45	36	1.44	610
976D-2H-6	145-150	10.45	36	1.39	610
976D-3H-2	145-150	13.95	36	1.43	614
976D-3H-4	145-150	16.95	35.5	1.43	614
976D-3H-5	145-150	18.45	36	1.39	616
976D-3H-7	45- 50	20.45	35	1.45	618
976D-4H-2	145-150	23.45	34.5	1.49	610
976D-4H-4	145-150	26.45	34.5	1.50	616
976D-4H-5	145-150	27.95	34.5	1.52	619
976D-4H-6	145-150	29.45	34	1.53	616
976C-5H-6	145-150	43.45	35	1.51	620
976C-6H-4	145-150	49.95	35	1.50	620
976C-8H-4	145-150	68.95	35	1.29	632
976B-10H-3	150-155	84.00	35	1.22	628
976B-13H-3	145-150	112.45	36	0.96	645
976B-19X-3	145-150	169.57	38.5	0.75	694
976B-25X-3	140-150	226.31	42	0.58	747

Note: Data reported here with +0.1‰ to compensate for -0.1‰ offset in measurements prior to 2nd IAEA Interlaboratory Calibration, July 1999.

Admittedly, the remaining amplitude of change (0.06‰) that represents these events in the measured isotopic values of the pore waters is very small and demonstrates the importance of both diffusive and advective processes at this site. Yet, our ability to recreate the measured profile simply by implementing the modern physical conditions as model parameters, convinces us that these small, residual peaks in the observed profile are indeed ancient remnants of climatic/hydrologic perturbations. In addition, comparison of the measured $\delta^{18}\text{O}$ profile vs. depth with the profile of dissolved chloride vs. depth (Figure 4) shows a decrease from values around 620 milli-moles per liter (mM/l) near the sediment-water interface to ~610 mM/l around 11 mbsf, thus indicating a salinity decrease coincident with the negative peak in $\delta^{18}\text{O}$ representative of S1.

4.2. MODELED PORE WATERS

Initial model runs were carried out simply by varying the input $\delta^{18}\text{O}$ at the sediment-water interface based on raising sea level (i.e., without the inclusion of a negative excursion in $\delta^{18}\text{O}$ to represent S1 in the early Holocene). This produced results with a poor fit to the observed data and suggested that the glacial to interglacial change in oxygen isotopic composition of Med-

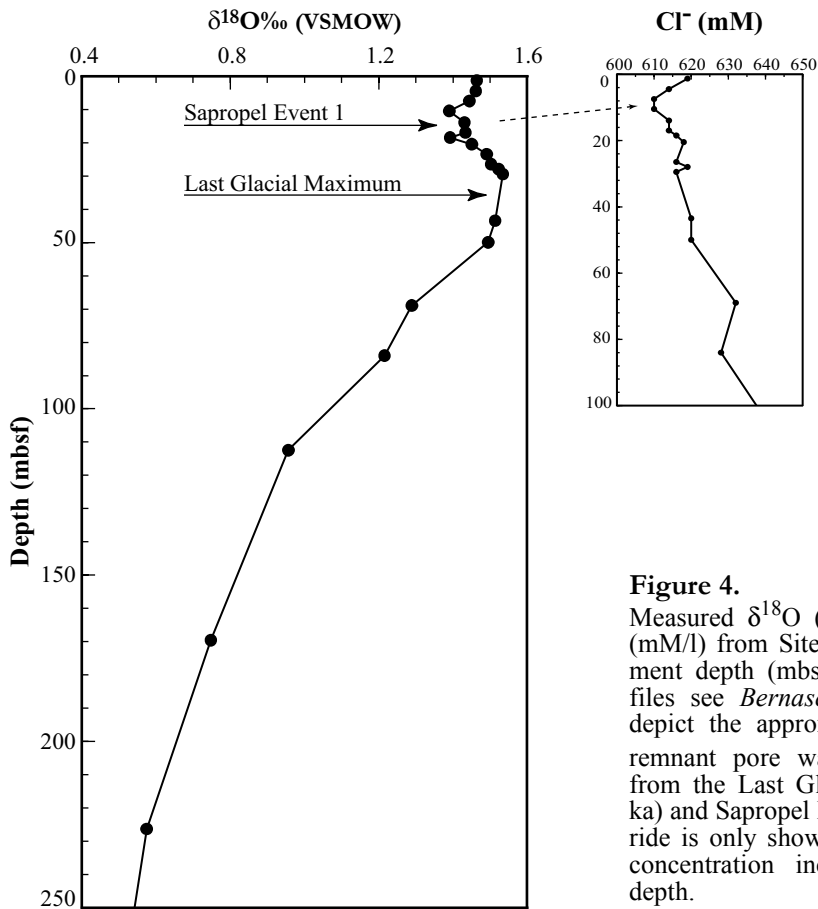


Figure 4.

Measured $\delta^{18}\text{O}$ (‰VSMOW) and Cl^- (mM/l) from Site 976 plotted vs. sediment depth (mbsf) (for extended profiles see *Bernasconi* [1999]). Arrows depict the approximate depths of the remnant pore water $\delta^{18}\text{O}$ excursions from the Last Glacial Maximum (~20 ka) and Sapropel Event 1 (~9 ka). Chloride is only shown to 100 mbsf as the concentration increases rapidly with depth.

iterranean bottom waters was less than 0.7‰. This value is even less than the ~0.8‰ glacial-interglacial change determined for the deep Atlantic [*Schrag et al.*, 1996; *Burns and Maslin*, 1999; *Adkins and Schrag*, 2001], and considerably less than the previously accepted change in the seawater ratio of 1.3‰ [*Fairbanks and Matthews*, 1978]. In later runs, we discovered that including a pulse of isotopically light $\delta^{18}\text{O}$ in the input values between 9.5-7.5 ka produced results that more closely fit the observed profile from Site 976 (Figure 5a). These runs clearly exhibit the strong influence that the most recent seawater values have on the resulting pore-fluid profile and show that a negative excursion in $\delta^{18}\text{O}$ is necessary to fit the observed data.

Preliminary runs were also done assuming that the total advective flux is caused by sediment burial and compaction, thus excluding any externally imposed hydrologic flow due to local pressure and temperature gradients in the sediment column. Using this base value for v , the best fit of the pore-water isotopic data is produced with a 0.8‰ negative excursion in $\delta^{18}\text{O}$ at 9 ka, and suggests a glacial-interglacial change in seawater $\delta^{18}\text{O}$ of 1.0 ± 0.1 ‰ (Figure 5a). We subsequently examined the effect of additional fluid flow on the pore water profile and found that increasing advection by 0.08 mm/year, an addition of ~20% to the compaction velocity, slightly

improves the fit of the modeled profile to the measured data. These results provide a best-fit solution indicating a 1.1‰ negative excursion at S1 and a glacial-interglacial change of 1.2 ± 0.1 ‰ (Figure 5b). Fluid over-pressure [Revil *et al.*, 1999] and high heat flow around the basement [Comas *et al.*, 1996] were detected at this site and could have altered the upward hydraulic flow, supporting the potential for a higher than expected advective velocity. Thus, we choose these latter results as the best reconstruction for Mediterranean seawater $\delta^{18}\text{O}$ since the LGM.

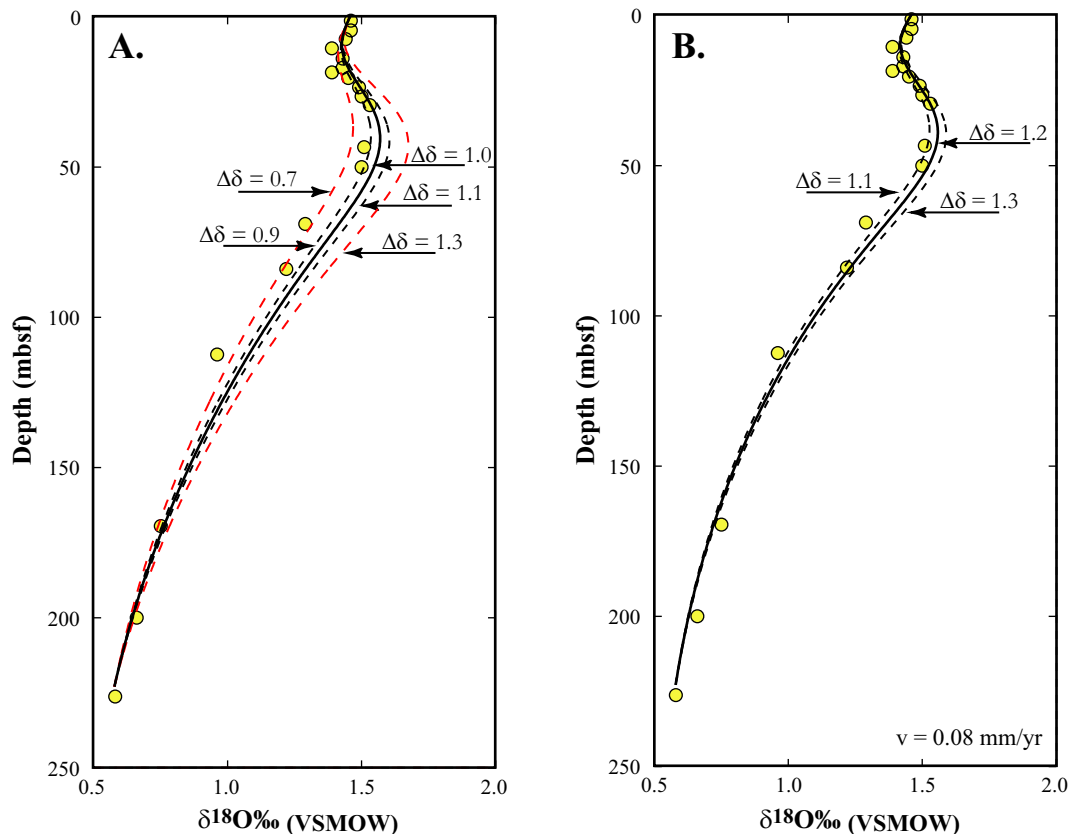


Figure 5.

Model calculations of pore fluid $\delta^{18}\text{O}$ (‰VSMOW) including a negative excursion to simulate Sapropel Event 1. (A.) Advection velocity only due to compaction, and (B.) an 0.8 mm/yr increase in advection is added due to hydraulic flow. Filled circles represent the measured, interstitial water $\delta^{18}\text{O}$ values.

4.3. ERROR ANALYSIS OF $\Delta\delta^{18}\text{O}$ DETERMINATIONS

The fact that the interstitial-water $\delta^{18}\text{O}$ profile from Site 976 contains two peaks, one from the Last Glacial Maximum and one from Sapropel Event 1, complicates the modeling procedure slightly. The two peaks strongly influence each other and hence, if the input values for one event are changed, the resultant magnitude and timing of both peaks are respectively affected. Due to this interdependence, we have to assume fixed times at which the events occur.

For the results presented here, we assume that the LGM peaked at 20 ka and that the most negative values of S1 occurred from 9.5-7.5 ka. To examine the precision with which the magnitude and timing of the sapropel event are correctly quantified by the model, a series of sensitivity tests were carried out.

In the first test, we varied the timing of the occurrence of S1. For instance, in one case we made the event older, lasting from 12-10 ka. With this modification, the $\delta^{18}\text{O}$ negative excursion must become larger to fit the observed profile and, using the same solution for the LGM, the S1 negative excursion must be increased by approximately 0.05‰. A comparable test was also carried out placing S1 at 8-6 ka, producing a similar change, though this time requiring a decrease in magnitude of $\sim 0.06\text{‰}$. Based on these results, we conclude that the simulated magnitude fluctuation of $\pm 0.05\text{‰}$ per 2 ky adequately constrains the S1 excursion and a total error of $\pm 0.1\text{‰}$ is sufficient for moving it within this 4-ky time window. Alternatively, changing the duration of the sapropel event (for instance by 1000 years) has very little influence on the determined magnitude of the $\delta^{18}\text{O}$ excursion.

One factor having a large impact on model results is the length of time chosen for the sea to recover from sapropel conditions, thus denoting the establishment of modern conditions in the basin. We varied the length of this transition such that modern conditions were initiated at either 5, 4, or 3 ka and found a range of best-fit solutions for the difference between present seawater $\delta^{18}\text{O}$ and S1 $\delta^{18}\text{O}$ values ($\Delta\delta_{\text{SAP}}$), suggesting a $\Delta\delta_{\text{SAP}}$ of -1.2, -1.1, and -1.0‰, respectively. Studies using benthic foraminiferal $\delta^{18}\text{O}$ to determine the timing of re-oxygenation and return to vigorous deepwater circulation in the Mediterranean following S1 suggest that foraminifera reached modern values between 3-4 ka [Fontugne *et al.*, 1989; Schönfeld and Zahn, 2000]. Investigations of hydrological fluctuations during the Holocene Climate Optimum suggest that reduced flooding in northern Africa and precipitation patterns similar to present were established around 4 ka [Bar-Matthews *et al.*, 1999; Gasse, 2000] and that monsoon response similar to modern was established between 5-4 ka [deMenocal *et al.*, 2000]. Based on the uncertainty concerning the actual initiation of modern conditions in the Mediterranean basin, we choose the 4-ka scenario, suggesting $\sim 1.1 \pm 0.1\text{‰}$ decrease in $\delta^{18}\text{O}$, to provide an average estimate of change. In summary, these sensitivity tests indicate that $\pm 0.10\text{‰}$ is a fair assessment of the error on the magnitude of this determination.

5. DISCUSSION

The solution for seawater $\delta^{18}\text{O}$ derived by our numerical model has been generated without reliance upon any other commonly used geochemical proxies. Thus, we are able to independently determine the effect of regional water balance (e.g., salinity (S)) on the total seawater $\delta^{18}\text{O}$ signal and subsequently, the temperature component recorded in the $\delta^{18}\text{O}$ of foraminiferal calcite. In contrast to other established methods of deriving past salinity, which in addition must

independently solve for temperature (i.e., via transfer functions or alkenone unsaturation ratios), we need only consider the glacial effect to determine salinity, thus reducing the number of assumptions that must be made. Previously, methods for resolving paleo-sea surface temperature and paleo-salinity frequently assumed a glacial-interglacial $\Delta\delta^{18}\text{O}$ of 1.3-1.4‰ that is attributable to global ice volume, which based on studies of interstitial water $\delta^{18}\text{O}$ appears to be too large [Schrag and DePaolo, 1993; Schrag et al., 1996; Burns and Maslin, 1999; Adkins and Schrag, 2001]. Furthermore, attempts at constraining paleo-salinity must assume that the modern S: $\delta^{18}\text{O}$ relationship is applicable to periods in the geologic past, thus excluding any possible temporal and spatial variance in this relationship; an assumption that is probably not true for the Mediterranean [Rohling, 1999; Rohling and DeRijk, 1999].

5.1. LAST GLACIAL MAXIMUM

Recent studies using the oxygen isotopic composition of interstitial waters from marine sediments to estimate the total glacial-interglacial $\delta^{18}\text{O}$ change of seawater produce a range of values from approximately $1.0\pm 0.25\text{‰}$ change in the Western Pacific [Schrag and DePaolo, 1993], reflecting the mean global seawater change, to a change of 0.7-0.8‰ in the deep, tropical Atlantic [Schrag et al., 1996; Burns and Maslin, 1999; Adkins and Schrag, 2001]. The value of $1.2\pm 0.1\text{‰}$ calculated for the $\Delta\delta_{\text{LGM}}$ of Mediterranean seawater in this study is larger than these estimates and suggests that a fraction of the total change is due to local salinity effects. As the interstitial water profile of $\delta^{18}\text{O}$ is impervious to changes in marine temperature fluctuations, it provides a pure reconstruction of seawater $\delta^{18}\text{O}$ composition since the last glacial period. This enables us to use our record of total $\delta^{18}\text{O}$ change to quantify the local effect of salinity and the relative temperature change over the past 20,000 years.

Close correlation between climate records derived from Mediterranean marine sediments and the Greenland ice cores [Cacho et al., 1999] indicate that surface water conditions in the Alboran Sea remained closely linked to water advection from the Atlantic Ocean during the last glaciation. Yet, since the $\delta^{18}\text{O}$ of North Atlantic surface waters may have also been susceptible to local salinity changes at this time, we take the global average value of 1.0‰ as the $\Delta\delta_{\text{LGM}}$ attributable to ice volume [Schrag et al., 1996; Burns and Maslin, 1999; Adkins and Schrag, 2001]; keeping in mind that this will provide a minimum estimate of regional salinity change. After comparison, a residual seawater $\delta^{18}\text{O}$ of approximately 0.2‰ remains that can be attributed to local salinity increase in the Mediterranean Sea during the LGM. This increase is in agreement with other studies indicating that colder, drier conditions dominated during the last glacial period, which would have decreased the freshwater influx [Cheddadi et al., 1991] and raised salinity. Intensification of the Northern Hemisphere wind system may have been responsible for increased wind speeds and cold winds that could have enhanced evaporation [Rohling et al., 1998]. In addition, restriction of Atlantic-Mediterranean exchange across the Gibraltar Sill

(today approximately 300 m deep) due to sea level fall would have greatly reduced the inflow of less-saline Atlantic surface water into the basin at the LGM.

Our study indicates that the magnitude of the salinity increase in the Mediterranean during the LGM, approximately 0.2‰, is smaller than previously estimated. For instance, *Thunell and Williams* [1989] suggest that 0.5-1.1‰ of the foraminiferal $\delta^{18}\text{O}$ signal is attributable to salinity increase in the western and eastern Mediterranean, respectively. Our estimates of salinity change, which do not rely on the isotopic composition of foraminifera, show that the $\delta^{18}\text{O}$ of foraminiferal calcite in the Mediterranean Sea includes a strong temperature component and that the variability of salinity at the LGM was slightly less than former estimates propose. Another plausible reason for the smaller than expected change in the $\delta^{18}\text{O}$ of Mediterranean seawater between the LGM and the present is that there was a temporary switch in the dominant region of deepwater formation. Studies using general circulation models [*Bigg*, 1994; *Myers et al.*, 1998] have shown evidence for a transition in the main region of deepwater production, which today occurs in the strongly evaporative Levantine and Adriatic basins of the eastern Mediterranean, to the Gulf of Lions in the western basin during the last glaciation. If such a switch were to occur, surface waters less enriched in $\delta^{18}\text{O}$ would be the source from which deep and intermediate waters would form, thus damping the total $\Delta\delta_{\text{LGM}}$ signal.

To reconstruct Mediterranean sea surface temperatures since the LGM, we use our modeled seawater $\delta^{18}\text{O}$ and a stacked planktonic foraminiferal $\delta^{18}\text{O}$ record [*Rohling*, 1999] to solve the paleotemperature equation [*Shackleton*, 1974]. Results show a maximum glacial-interglacial temperature change of approximately 9°C. This result is quite similar to other Mediterranean paleo-SST estimates that have been derived using alkenone unsaturation ratios. For example, the Alboran Sea record generated by *Cacho et al.* [1999] displays approximately the same glacial-interglacial SST range as our reconstruction. Recent records from the Ionian and the Levantine Seas by *Emeis et al.* [2000] indicate an excess of 8°C cooling at the Last Glacial Maximum compared to the present. Simulations from a coupled ocean-atmosphere model also suggest 8°C cooling at the LGM in the Mediterranean zone [*Ganopolski et al.*, 1998]. Additionally, *Guiot et al.* [1993] suggest 6-11°C cooling determined from pollen records in southern France. Glacial SSTs derived using foraminiferal transfer functions and modern analogue techniques predict approximately 6°C of cooling in the western basin [*Thiede*, 1978] and around 5-6°C of cooling in the Tyrrhenian Sea [*Kallel et al.*, 1997b], thus signifying slightly less temperature variance than our method.

5.2. SAPROPEL EVENT 1

Hypotheses explaining the origin of deep-sea sapropels tend to agree that deposition of these sediments coincides with intervals of increased seasonality caused by minima in the Earth's orbital precession cycle [*Rosignol-Strick*, 1985; *Hilgen*, 1991] and that their occurrence is

related to freshening of Mediterranean surface waters [Rossignol-Strick, 1985; Rohling and Hilgen, 1991; Kallel *et al.*, 1997b]. Intense rainfall during periods of sapropel formation has been confirmed by studies of the isotopic composition of speleothems from Soreq cave [Bar-Matthews *et al.*, 1999], pollen assemblages [Cheddadi and Rossignol-Strick, 1995], reconstructions of lake levels [Street and Grove, 1979], and by comparisons of the $\delta^{18}\text{O}$ of carbonate microfossils from sapropel and intervening, non-sapropel layers [Thunell and Williams, 1989; Tang and Stott, 1993; Rohling and DeRijk, 1999; Bernasconi and Pika-Biolzi, 2000]. To constrain the magnitude of the negative $\delta^{18}\text{O}$ excursion at S1 due to surface water freshening, we assume that the addition of freshwater depleted in ^{18}O to global seawater from deglaciation was minimal after 8 ka [Berger *et al.*, 1985; Fleming *et al.*, 1998], and that the entire magnitude of the pore water $\delta^{18}\text{O}$ excursion at 9 ka is representative of the hydrologic change within the Mediterranean basin.

Our model results indicate that at S1, a decrease in seawater $\delta^{18}\text{O}$ of around $1.1 \pm 0.1\text{‰}$ with respect to the modern value occurred. Comparison of this value to the $\Delta\delta_{\text{SAP}}$ predicted by foraminiferal $\delta^{18}\text{O}$ records shows good agreement. For instance, compilations of planktonic foraminiferal data by Thunell and Williams [1989] and Kallel *et al.* [1997a] both predict $\Delta\delta_{\text{SAP}}$ changes of -1.0‰ on average for the entire basin. Previous studies have attempted to reconstruct the salinity of Mediterranean seawater based on $\Delta\delta_{\text{SAP}}$ values using the modern Mediterranean $\delta^{18}\text{O}$:S relationship of 0.27‰/psu and the modern $\delta^{18}\text{O}$:S relationship in the Atlantic region of 0.41‰/psu [Thunell and Williams, 1989; Kallel *et al.*, 1997a; Emeis *et al.*, 2000]. More recent studies have shown, however, that due to a likely change in the source region of incoming freshwater to the Mediterranean during S1, present-day spatial relationships of $\delta^{18}\text{O}$:S are not applicable for reconstructing salinity over this period [Rohling, 1999; Rohling and DeRijk, 1999]. Accurate conversion of $\delta^{18}\text{O}$ change into salinity change for quantifying paleo-salinity will require more precise estimates of paleo-flux rates and paleo-isotopic compositions of the freshwater inputs during sapropel events.

One long-standing theory of sapropel formation proposes a reversal of the modern Mediterranean circulation pattern leading to stratification of the water masses with stagnant deepwater layers and anoxia (see comprehensive review by Rohling [1994]). Thermohaline gradients between surface and deep waters are the main cause of water-mass mixing, thus allowing changes in the temperature and salinity (and $\delta^{18}\text{O}$) of surface waters to be directly transferred to the deeper waters. We expect our model estimate of $\delta^{18}\text{O}$ to provide an average Mediterranean seawater value since deep and intermediate waters in the basin reflect their surface water source and have a fairly rapid regeneration time. Our model results indicate the existence of isotopically light seawater circulating down to bottom water depths, at least to 1000 m in the western Mediterranean, coincident with the formation of the most recent sapropel. This implies that thermohaline circulation did not cease during the formation of S1 and that deepwater, or at least intermediate water, continued to be produced and transported throughout the basin. Thus, if any

stagnation of the water column occurred, it was below 1000 m. This conclusion provides direct geochemical evidence, in agreement with studies using benthic foraminifera to study Mediterranean outflow [Zahn *et al.*, 1987; Vergnaud-Grazzini *et al.*, 1989; Emeis *et al.*, 2000] and with numerical simulations [Myers *et al.*, 1998], to show that the modern, “anti-estuarine” thermohaline circulation was maintained throughout the period of sapropel formation at S1.

6. CONCLUSIONS

Using high-resolution measurements of pore-fluid $\delta^{18}\text{O}$ recovered from ODP Leg 161, Site 976 in the western Mediterranean in conjunction with a numerical model of diffusive and advective transport, we constrain the glacial-interglacial change in the $\delta^{18}\text{O}$ of Mediterranean deepwater to be $1.2 \pm 0.1\%$. Of the total $\delta^{18}\text{O}$ shift, $\sim 0.2\%$ is attributable to local salinity increase in the Mediterranean basin. As this estimate of seawater isotopic change is unaffected by glacial-interglacial variations in marine temperature, the record of seawater $\delta^{18}\text{O}$ can be used to calculate sea surface temperatures by coupling the data with records of planktonic foraminiferal $\delta^{18}\text{O}$. The paleo-SST calculations suggest around 9°C of cooling during the last glacial period. At S1, a decrease of $\sim 1.1 \pm 0.1\%$ in seawater $\delta^{18}\text{O}$ is determined, caused by freshening of the Mediterranean basin. Our model results thus indicate the existence of less saline water circulating to bottom water depths, at least down to 1000 m in the western Mediterranean, supporting the continuance of an “anti-estuarine” circulation pattern during S1 deposition.

We recommend using interstitial water isotopic composition as an independent constraint on regional $\Delta\delta^{18}\text{O}$ back to the Last Glacial Maximum in regions where sedimentary sequences have poor calcite preservation and/or lack microfossils. As demonstrated, this technique can be used to reconstruct the paleo-isotopic and chemical composition of seawater and can be used to better constrain the relative contributions of temperature and local salinity to the foraminiferal calcite $\delta^{18}\text{O}$ signal. Additionally, this approach will help to provide a more detailed spatial view of deepwater $\delta^{18}\text{O}$ values at the LGM and to assess variance in the global $\Delta\delta_{\text{LGM}}$ value.

ACKNOWLEDGEMENTS

We would like to thank Y. Podladchikov, S. Schmalholz, and J. Connolly for useful discussions. This manuscript benefited from constructive reviews by D.P. Schrag and E.J. Rohling. Funding for this work was provided by ETH Research Project No. 02197.

PART IV REFERENCES

- Adkins, J.F., and D.P. Schrag, Pore fluid constraints on deep ocean temperature and salinity during the last glacial maximum, *Geophysical Research Letters*, 28, 771-774, 2001.
- Andersen, N., H.A. Paul, S.M. Bernasconi, J.A. McKenzie, A. Behrens, P. Schaeffer, and P. Albrecht, Large and rapid climate variability during the Messinian salinity crisis: Evidence from deuterium concentrations of individual biomarkers, *Geology*, 29, 799-802, 2001.
- Bar-Matthews, M., A. Ayalon, A. Kaufman, and G.J. Wasserburg, The Eastern Mediterranean paleoclimate as a reflection of regional events: Soreq cave, Israel, *Earth and Planetary Science Letters*, 166, 85-95, 1999.
- Bar-Matthews, M., A. Ayalon, and A. Kaufman, Timing and hydrological conditions of Sapropel events in the Eastern Mediterranean, as evident from speleothems, Soreq cave, Israel, *Chemical Geology*, 169, 145-156, 2000.
- Berger, W.H., J.S. Killingley, and E. Vincent, Timing of deglaciation from an oxygen isotope curve for Atlantic deep-sea sediments, *Nature (London)*, 314 (6007), 156-158, 1985.
- Bernasconi, S.M., Interstitial water chemistry in the western Mediterranean: Results from Leg 161, in *Proceedings of the Ocean Drilling Program, Scientific Results*, edited by R. Zahn, M.C. Comas, and A. Klaus, pp. 423-432, (Ocean Drilling Program), College Station, TX, 1999.
- Bernasconi, S.M., and M. Pika-Biolzi, A stable isotope study of multiple species of planktonic foraminifera across sapropels of the Tyrrhenian Sea, ODP site 974, *Palaeoclimatology, Palaeoclimatology, Palaeoecology*, 158, 281-292, 2000.
- Béthoux, J.P., Budgets of the Mediterranean Sea: Their dependence on the local climate and the characteristics of the Atlantic waters, *Oceanol. Acta*, 2, 157-163, 1979.
- Béthoux, J.P., Mean water fluxes across sections in the Mediterranean Sea, evaluated on the basis of water and salt budgets and observed salinities, *Oceanol. Acta*, 3, 79-88, 1980.
- Béthoux, J.P., Paléo-hydrologie de la Méditerranée au cours des derniers 20 000 ans, *Oceanol. Acta.*, 7, 43-48, 1984.
- Béthoux, J.P., B. Gentili, J. Raunet, and D. Tailliez, Warming trend in the western Mediterranean deep water, *Nature*, 347, 660-662, 1990.
- Bigg, G.R., An ocean general circulation model view of the glacial Mediterranean thermohaline circulation, *Paleoceanography*, 9, 705-722, 1994.
- Boudreau, B.P., *Diagenetic Models and Their Implementation: Modelling Transport and Reactions in Aquatic Sediments*, Springer, 1996.
- Bouloubassi, I., J. Rullkötter, and P.A. Meyers, Origin and transformation of organic matter in Pliocene-Pleistocene Mediterranean sapropels: Organic geochemical evidence reviewed, *Marine Geology*, 153, 177-197, 1999.
- Bryden, H.L., and T.H. Kinder, Steady two-layer exchange through the Strait of Gibraltar, *Deep-Sea Research*, 38, S445-S463, 1991.
- Bryden, H.L., and H.M. Stommel, Limiting processes that determine the basic features of the circulation in the Mediterranean Sea, *Oceanol. Acta*, 7, 289-296, 1984.
- Burns, S.J., and M.A. Maslin, Composition and circulation of bottom water in the western Atlantic Ocean during the last glacial, based on pore-water analyses from the Amazon Fan, *Geology*, 27, 1011-1014, 1999.

- Cacho, I., J.O. Grimalt, M. Canals, L. Sbaiffi, N.J. Shackleton, J. Schoenfeld, and R. Zahn, Variability of the western Mediterranean Sea surface temperature during the last 25,000 years and its connection with the Northern Hemisphere climatic changes, *Paleoceanography*, *16*, 40-52, 2001.
- Cacho, I., O. Grimalt Joan, C. Pelejero, M. Canals, J. Sierro Francisco, A. Flores Jose, and N. Shackleton, Dansgaard-Oeschger and Heinrich Event imprints in Alboran Sea paleotemperatures, *Paleoceanography*, *14* (6), 698-705, 1999.
- Calvert, S.E., Geochemistry of Pleistocene sapropels and associated sediments from the eastern Mediterranean, *Oceanologica Acta*, *6*, 255-267, 1983.
- Calvert, S.E., B. Nielsen, and M.R. Fontugne, Evidence from nitrogen isotope ratios for enhanced productivity during formation of eastern Mediterranean sapropels, *Nature*, *359*, 223-225, 1992.
- Cheddadi, R., and M. Rossignol-Strick, Eastern Mediterranean Quaternary paleoclimates from pollen and isotope records of marine cores in the Nile cone area, *Paleoceanography*, *10*, 291-300, 1995.
- Cheddadi, R., M. Rossignol-Strick, and M. Fontugne, Eastern Mediterranean paleoclimates from 26 to 5 ka BP documented by pollen and isotopic analysis of a core in the anoxic Bannock Basin, *Marine Geology*, *100*, 53-66, 1991.
- Chikaraishi, Y., and H. Naraoka, Hydrogen and carbon isotopic compositions of individual long-chain *n*-alkanes in a lake system with relevance to their sources, in *20th International Meeting on Organic Geochemistry*, pp. 121-122, Nancy, France, 2001.
- Cita, M.B., C. Vergnaud Grazzini, C. Robert, H. Chamley, N. Ciaranfi, and S. Donofrio, Paleoclimatic record of a long deep-sea core from the eastern Mediterranean, *Quaternary Research*, *8* (2), 205-235, 1977.
- Comas, M.C., R. Zahn, A. Klaus, and e. al., *Proc. ODP, Init. Repts.*, *161*, Ocean Drilling Program, College Station, TX, 1996.
- Craig, H., and L.I. Gordon, Deuterium and oxygen-18 variation in the ocean and the marine atmosphere, in *Stable Isotopes in Oceanographic Studies and Paleotemperatures*, edited by E. Tongiorgi, pp. 9-130, Spoleto, Cons. Naz. delle Ric., Pisa, Italy, 1965.
- Dansgaard, W., Stable isotopes in precipitation, *Tellus*, *16*, 436-467, 1964.
- de Kaenel, E., W.G. Siesser, and A. Murat, Pleistocene calcareous nannofossil biostratigraphy and the western Mediterranean sapropels, sites 974 to 977 and 979, in *Proceedings of the Ocean Drilling Program, Scientific Results*, *161*, edited by R. Zahn, M.C. Comas, and A. Klaus, pp. 159-183, College Station, TX, 1999.
- deMenocal, P., J. Ortiz, T. Guilderson, J. Adkins, M. Sarnthein, L. Baker, and M. Yarusinsky, Abrupt onset and termination of the African Humid Period: Rapid climate responses to gradual insolation forcing, *Quaternary Science Reviews*, *19*, 347-361, 2000.
- Edmunds, W.M., and E.P. Wright, Groundwater recharge and paleoclimate in the Sirte and Kufra basins, Libya, *Journal of Hydrology*, *40*, 215-241, 1979.
- Eglinton, G., R.J. Hamilton, R.A. Raphael, and A.G. Gonzales, Hydrocarbon constituents of the wax coatings of plant leaves: A taxonomic survey, *Nature*, *193*, 739-742, 1962.
- Emeis, K.C., A. Camerlenghi, J.A. McKenzie, D. Rio, and R. Sprovieri, The occurrence and significance of Pleistocene and Upper Pliocene sapropels in the Tyrrhenian Sea, *Marine Geology*, *100*, 155-182, 1991a.
- Emeis, K.C., J.W. Morse, and L.L. Mays, Organic carbon, reduced sulfur, and iron in Miocene to Holocene upwelling sediments from the Oman and Benguela upwelling systems, in *Proc. ODP, Sci. Res.*, pp. 517-527, Ocean Drilling Program, College Station, TX, 1991b.
- Emeis, K.-C., U. Struck, H.-M. Schulz, R. Rosenberg, S. Bernasconi, H. Erlenkeuser, T. Sakamoto, and F. Martinez-Ruiz, Temperature and salinity variations of Mediterranean Sea surface waters over the

- last 16,000 years from records of planktonic stable oxygen isotopes and alkenone unsaturation ratios, *Palaeogeography, Palaeoclimatology, Palaeoecology*, 158, 259-280, 2000.
- Epstein, S., P. Thompson, and C.J. Yapp, Oxygen and Hydrogen Isotopic Ratios in Plant Cellulose, *Science*, 198, 1209-1215, 1977.
- Estep, M.F., and T.C. Hoering, Biogeochemistry of the stable hydrogen isotopes, *Geochimica, Cosmochimica, Acta*, 44, 1197-1206, 1980.
- Fairbanks, R.G., A 17,000-year glacio-eustatic sea level record: Influence of glacial melting rates on the Younger Dryas event and deep ocean circulation, *Nature*, 342, 637-642, 1989.
- Fairbanks, R.G., and R.K. Matthews, The marine oxygen isotope record in Pleistocene coral, Barbados, West Indies, *Quaternary Research*, 10, 181-196, 1978.
- Fleming, K., P. Johnston, D. Zwartz, Y. Yokoyama, K. Lambeck, and J. Chappell, Refining the eustatic sea-level curve since the Last Glacial Maximum using far- and intermediate-field sites, *Earth and Planetary Science Letters*, 163, 327-342, 1998.
- Fontugne, M.R., Les isotopes stables du carbone organique dans l'océan. Application à la palaeoclimatologie, PhD thesis, University of Paris, Paris, 1983.
- Fontugne, M.R., and S.E. Calvert, Late Pleistocene variability of the carbon isotopic composition of organic matter in the eastern Mediterranean: Monitor of changes in carbon sources and atmospheric CO₂ concentrations, *Paleoceanography*, 7, 1-20, 1992.
- Fontugne, M.R., M. Paterne, S.E. Calvert, A. Murat, F. Guichard, and M. Arnold, Adriatic deep water formation during the Holocene: Implication for the reoxygenation of the deep eastern Mediterranean Sea, *Paleoceanography*, 4 (2), 199-206, 1989.
- Freeman, K.H., S.G. Wakeham, and J.M. Hayes, Predictive isotopic biogeochemistry: Hydrocarbons from anoxic marine basins, *Organic Geochemistry*, 21, 629-644, 1994.
- Friedman, I., Deuterium content of natural waters and other substances, *Geochimica et Cosmochimica Acta*, 4, 89-103, 1953.
- Ganopolski, A., S. Rahmstorf, V. Petoukhov, and M. Claussen, Simulation of modern and glacial climates with a coupled global model of intermediate complexity, *Nature*, 391 (6665), 351-356, 1998.
- Gasse, F., Hydrological changes in the African tropics since the Last Glacial Maximum, *Quaternary Science Reviews*, 19, 189-211, 2000.
- Gat, J.R., A. Shemesh, E. Tziperman, A. Hecht, D. Georgopoulos, and O. Basturk, The stable isotope composition of waters of the eastern Mediterranean Sea, *Journal of Geophysical Research*, 101, 6441-6451, 1996.
- Guiot, J., J.L. de Beaulieu, R. Cheddadi, F. David, P. Ponel, and M. Reille, The climate in western Europe during the last glacial/interglacial cycle derived from pollen and insect remains, *Palaeogeography, Palaeoclimatology, Palaeoecology*, 103, 73-93, 1993.
- Hayes, J.M., R. Takigiku, R. Ocampo, H.F. Callot, and P. Albrecht, Isotopic compositions and probable origins of organic molecules of the Eocene Messel shale, *Nature*, 329, 48-51, 1987.
- Hedges, J.I., W.A. Clark, P.D. Quay, J.E. Richey, A.H. Devol, and U.d.M. Santos, Compositions and fluxes of particulate material in the Amazon River, *Limnology and Oceanography*, 31, 717-738, 1986.
- Hilgen, F.J., Astronomical calibration of Gauss to Matuyama sapropels in the Mediterranean and implication for the geomagnetic polarity time scale, *Earth and Planetary Science Letters*, 104 (2-4), 226-244, 1991.
- IAEA/WMO, Global Network for Isotopes in Precipitation. The GNIP Database. Release 3, October 1999, URL: <http://www.iaea.org/programs/ri/gnip/gnipmain.htm>, 1998.
- Jorissen, F.J., A. Asioli, A.M. Borsetti, L. Capotondi, et al., Late Quaternary central Mediterranean biochronology, *Marine Micropaleontology*, 21, 169-189, 1993.

- Jung, M., J. Ilmberger, A. Mangini, and K.C. Emeis, Why some Mediterranean sapropels survived burn-down (and others did not), *Marine Geology*, 141, 51-60, 1997.
- Kallel, N., M. Paterne, J.-C. Duplessy, C. Vergnaud-Grazzini, C. Pujol, L. Labeyrie, M. Arnold, M. Fontugne, and C. Pierre, Enhanced rainfall in the Mediterranean region during the last sapropel event, *Oceanologica Acta*, 20, 697-712, 1997a.
- Kallel, N., M. Paterne, L. Labeyrie, J.-C. Duplessy, and M. Arnold, Temperature and salinity records of the Tyrrhenian Sea during the last 18,000 years, *Palaeogeography, Palaeoclimatology, Palaeoecology*, 135, 97-108, 1997b.
- Kidd, R.B., M.B. Cita, and W.B.F. Ryan, Stratigraphy of eastern Mediterranean sapropel sequences recovered during DSDP Leg 42A and their paleoenvironmental significance, *Initial Reports of the Deep Sea Drilling Project*, 42A, 421-443, 1978.
- Krishnamurthy, R.V., P.A. Meyers, and N.A. Lovan, Isotopic evidence of sea-surface freshening, enhanced productivity, and improved organic matter preservation during sapropel deposition in the Tyrrhenian Sea, *Geology*, 28, 263-266, 2000.
- Kroopnick, P.M., The distribution of C^{13} of ΣCO_2 in the world oceans, *Deep-Sea Research Part A*, 32 (1), 57-84, 1985.
- Kullenberg, B., On the salinity of the water contained in marine sediments, *Goteborgs Kungl. Vetenskaps. Vitt-Samhal. Handlingar*, 6, 3-37, 1952.
- Kutzbach John, E., and F.A. Street Perrott, Milankovitch forcing of fluctuations in the level of tropical lakes from 18 to 0 kyr BP, *Nature (London)*, 317 (6033), 130-134, 1985.
- Lane-Serff, G.F., E.J. Rohling, H.L. Bryden, and H. Charnock, Postglacial connection of the Black Sea to the Mediterranean and its relation to the timing of sapropel formation, *Paleoceanography*, 12, 169-174, 1997.
- Marlowe, I.T., S.C. Brassell, G. Eglinton, and J.C. Green, Long chain unsaturated ketones and esters in living algae and marine sediments, *Organic Geochemistry*, 6, 135-141, 1984.
- McKenzie, J.A., Pluvial conditions in the eastern Sahara following the penultimate deglaciation: Implications for changes in atmospheric circulation patterns with global warming, *Palaeogeography, Palaeoclimatology, Palaeoecology*, 103, 95-105, 1993.
- Meyers, P.A., and R. Ishiwatari, Lacustrine organic geochemistry: An overview of indicators of organic matter sources and diagenesis in lake sediments, *Organic Geochemistry*, 20, 867-900, 1993.
- Myers, P., K. Haines, and E. Rohling, Modeling the paleocirculation of the Mediterranean: The last glacial maximum and the Holocene with emphasis on the formation of Sapropel S1, *Paleoceanography*, 13, 586-606, 1998.
- O'Leary, M.H., Carbon isotopes in photosynthesis, *Bioscience*, 38, 328-336, 1988.
- Pierre, C., The oxygen and carbon isotope distribution in the Mediterranean water masses, *Marine Geology*, 153, 41-55, 1999.
- Prahl, F.G., J.M. Hayes, and T.-M. Xie, Diploptene: an indicator of terrigenous organic carbon in Washington coastal sediments, *Limnol. Oceanol.*, 37, 1290-1300, 1992.
- Prentice, I.C., J. Guiot, and S.P. Harrison, Mediterranean vegetation, lake levels and paleoclimate at the Last Glacial Maximum, *Nature*, 360, 658-660, 1992.
- Redfield, A.C., B.H. Ketchum, and F.A. Richards, The influence of organisms on the composition of sea water, in *The Sea*, edited by M.N. Hill, pp. 26-77, John Wiley, New York, 1963.
- Reid, J.L., On the contribution of the Mediterranean Sea outflow to the Norwegian-Greenland Sea, *Deep-Sea Res.*, 44, 1199-1223, 1979.

- Revil, A., P.A. Pezard, and F.D. Larouzière, Fluid overpressures in western Mediterranean sediments, sites 974-979, in *Proceedings of the Ocean Drilling Program, Scientific Results*, edited by R. Zahn, M.C. Comas, and A. Klaus, pp. 117-128, 1999.
- Robinson, A.R., P. Malanotte Rizzoli, A. Hecht, A. Michelato, et al., General circulation of the eastern Mediterranean, *Earth-Science Reviews*, 32 (4), 285-309, 1992.
- Robinson, N., G. Eglinton, S.C. Brassell, and P.A. Cranwell, Dinoflagellate origin for sedimentary 4a-methylsteroids and 5a-stanols, *Nature*, 308, 439-442, 1984.
- Rohling, E.J., Review and new aspects concerning the formation of eastern Mediterranean sapropels, *Marine Geology*, 122, 1-28, 1994.
- Rohling, E.J., Environmental control on Mediterranean salinity and $\delta^{18}\text{O}$, *Paleoceanography*, 14, 706-715, 1999.
- Rohling, E.J., and G.R. Bigg, Paleosalinity and $\delta^{18}\text{O}$: A critical assessment, *Journal of Geophysical Research*, 103, 1307-1318, 1998.
- Rohling, E.J., and H.L. Bryden, Estimating past changes in the eastern Mediterranean freshwater budget using reconstructions of sea level and hydrography, *Proc. Kon. Ned. Akad. v wetensch.*, 97, 201-217, 1994.
- Rohling, E.J., and S. DeRijk, Holocene Climate Optimum and the Last Glacial Maximum in the Mediterranean: The marine oxygen isotope record, *Marine Geology*, 153, 57-75, 1999.
- Rohling, E.J., A. Hayes, S. DeRijk, D. Kroon, W.J. Zachariasse, and D. Eisma, Abrupt cold spells in the northwest Mediterranean, *Paleoceanography*, 13, 316-322, 1998.
- Rohling, E.J., and F.J. Hilgen, The Eastern Mediterranean climate at times of sapropel formation: A review, *Geologie en Mijnbouw*, 70, 253-264, 1991.
- Rosignol-Strick, M., Mediterranean Quaternary sapropels, an immediate response of the African monsoon to variation of insolation, *Palaeogeography, Palaeoclimatology, Palaeoecology*, 49, 237-263, 1985.
- Rosignol-Strick, M., W. Nesteroff, P. Olive, and C. Vergnaud-Grazzini, After the deluge: Mediterranean stagnation and sapropel formation, *Nature*, 295, 105-110, 1982.
- Schimmelmann, A., M.D. Lewan, and R.P. Wintsch, D/H isotope ratios of kerogen, bitumen, oil and water in hydrous pyrolysis of source rocks containing kerogen types I, II, IIS, and III, *Geochimica et Cosmochimica Acta*, 63, 3751-3766, 1999.
- Schlitzer, R., W. Roether, H. Oster, H.-G. Junghans, M. Hausmann, H. Hohannsen, and A. Michelato, Chlorofluoromethane and oxygen in the eastern Mediterranean, *Deep-Sea Research*, 38, 1531-1551, 1991.
- Schönfeld, J., and R. Zahn, Late glacial to Holocene history of the Mediterranean outflow. Evidence from benthic foraminiferal assemblages and stable isotopes at the Portuguese margin, *Palaeogeography, Palaeoclimatology, Palaeoecology*, 159, 85-111, 2000.
- Schrag, D.P., and D.J. DePaolo, Determination of $\delta^{18}\text{O}$ of seawater in the deep ocean during the Last Glacial Maximum, *Paleoceanography*, 8, 1, 1993.
- Schrag, D.P., D.J. DePaolo, and F.M. Richter, Oxygen isotope exchange in a two-layer model of oceanic crust, *Earth and Planetary Science Letters*, 111, 305-317, 1992.
- Schrag, D.P., G. Hampt, and D.W. Murray, Pore fluid constraints on the temperature and oxygen isotope composition of the glacial ocean, *Science*, 272, 1930-1932, 1996.
- Scrimgeour, C.M., I.S. Begley, and M.L. Thomason, Measurements of deuterium incorporation into fatty acids by gas chromatography/isotope ratio mass spectrometry, *Rapid Communications in Mass Spectrometry*, 13, 271-274, 1999.

- Sessions, A.L., T.W. Burgoyne, A. Schimmelmann, and J.M. Hayes, Fractionation of hydrogen isotopes in lipid biosynthesis, *Organic Geochemistry*, 30, 1193-1200, 1999.
- Shackleton, N.J., Attainment of isotopic equilibrium between ocean water and the benthonic foraminifera genus *Uvigerina*: Isotopic changes in the ocean during the last glacial, *Centre National de la Recherche Scientifique Colloquium International*, 219, 203-209, 1974.
- Smith, B.N., and S. Epstein, Two categories of $^{13}\text{C}/^{12}\text{C}$ ratios for higher plants, *Plant. Physiol.*, 47, 380-384, 1971.
- Sofer, Z., and J.R. Gat, Activities and concentrations of oxygen-18 in concentrated aqueous salt solutions: analytical and geophysical implications, *Earth Planet Sci. Lett.*, 15, 232-238, 1972.
- Sternberg, L., D/H ratios of environmental water recorded by D/H ratios of plant lipids, *Nature*, 333, 59-61, 1988.
- Street, F.A., and A.T. Grove, Global maps of lake-level fluctuations since 30,000 years B.P., *Quaternary Research*, 12, 83-118, 1979.
- Suess, E., and P.J. Müller, Productivity, sedimentation rate and sedimentary organic matter in the oceans II: Elemental fractionation, in *Biogéochimie de la Matière Organique à l'Interface Eau-Sédiment Marin*, edited by R. Daumas, pp. 18-26, Coll. Int. C.N.R.S., 1980.
- Tang, C.M., and L.D. Stott, Seasonal salinity changes during Mediterranean sapropel deposition 9000 years B.P.: Evidence from isotopic analyses of individual planktonic foraminifera, *Paleoceanography*, 8 (4), 473-493, 1993.
- ten Haven, H.L., M. Baas, M. Kroot, J.W. de Leeuw, P.A. Schenck, and J. Ebbing, Late Quaternary Mediterranean sapropels, III. Assessment of source of input and paleotemperature as derived from biological markers, *Geochimica et Cosmochimica Acta*, 51, 803-810, 1987.
- Terwilliger, V.J., and M.J. DeNiro, Hydrogen isotope fractionation in wood-producing avocado seedlings: Biological constraints to paleoclimatic interpretations of dD values in tree ring cellulose nitrate, *Geochim. Cosmochim. Acta*, 59, 5199-5207, 1995.
- Thiede, J., A glacial Mediterranean, *Nature*, 276 (5689), 680-683, 1978.
- Thorweihe, U., P.J. Brinkmann, M. Heintz, and C. Sonntag, Hydrological and hydrogeological investigations in the Darfur area, Western Sudan, *Berliner Geowissenschaftliche Abhandlungen*, 120 (A), 279-326, 1990.
- Thunell, R.C., Eastern Mediterranean Sea during the last glacial maximum: An 18,000-years B.P. reconstruction, *Quaternary Research*, 11 (3), 353-372, 1979.
- Thunell, R.C., and D.F. Williams, Glacial-Holocene changes in the Mediterranean Sea: Hydrographic and depositional effects, *Nature*, 338, 493-496, 1989.
- Thunell, R.C., D.F. Williams, and P.R. Belyea, Anoxic events in the Mediterranean Sea in relation to the evolution of late Neogene climates, *Marine Geology*, 59, 105-134, 1984.
- Thunell, R.C., D.F. Williams, and M. Howell, Atlantic-Mediterranean water exchange during the late Neogene, *Paleoceanography*, 2, 661-678, 1987.
- Tiedemann, R., M. Sarnthein, and N.J. Shackleton, Astronomic timescale for the Pliocene Atlantic $\delta^{18}\text{O}$ and dust flux records of Ocean Drilling Program site 659, *Paleoceanography*, 9 (4), 619-638, 1994.
- Tissot, B.P., and D.H. Welte, *Petroleum Formation and Occurrence*, 699 pp., Springer-Verlag, New York, 1984.
- Vergnaud-Grazzini, C., M. Caralp, J.-C. Faugères, É. Gonthier, F. Grousset, C. Pujol, and J.-F. Saliège, Mediterranean outflow through the Strait of Gibraltar since 18,000 years BP, *Oceanologica Acta*, 12, 305-324, 1989.

- Vergnaud-Grazzini, C., W.B.F. Ryan, and M.B. Cita, Stable isotope fractionation, climatic change and episodic stagnation in the eastern Mediterranean during the Late Quaternary, *Marine Micropaleontology*, 2, 353-370, 1977.
- Volkman, J.K., G. Eglinton, E.D.S. Corner, and J.R. Sargent, Novel unsaturated straight-chain C₃₇-C₃₉ methyl and ethyl ketones in marine sediments and a coccolithophore *Emiliana huxleyi*, in *Advances in Organic Geochemistry 1979*, edited by A.G. Douglas, and J.R. Maxwell, pp. 219-227, Pergamon Press, Oxford, 1979.
- Williams, D.F., R.C. Thunell, and J.P. Kennett, Periodic freshwater flooding and stagnation of the eastern Mediterranean Sea during the late Quaternary, *Science*, 201, 252-254, 1978.
- Wüst, G., On the vertical circulation of the Mediterranean Sea, *Journal of Geophysical Research*, 66, 3261-3271, 1961.
- Zahn, R., M. Sarnthein, and H. Erlenkeuser, Benthic isotope evidence for changes of the Mediterranean outflow during the late Quaternary, *Paleoceanography*, 2, 543-559, 1987.

TROPICAL SEA SURFACE TEMPERATURE AND SALINITY CHANGE IN THE CARIACO BASIN AT THE LAST GLACIAL MAXIMUM: QUANTIFICATION FROM PORE-WATER $\delta^{18}\text{O}$

H.A. Paul, P.K. Swart, S.M. Bernasconi, L.C. Peterson, and J.A. McKenzie
submitted to: *Paleoceanography*, 2002.

ABSTRACT

As an alternative method for determining the magnitude of glacial tropical sea surface temperature variability, interstitial waters recovered from Ocean Drilling Program, Site 1002 in the Cariaco Basin are used in a numerical model to constrain the $\delta^{18}\text{O}$ of seawater since the Last Glacial Maximum (LGM). During the LGM, the basin became largely isolated due to sea-level fall, leaving only a shallow sill across which surface-water exchange with the Caribbean occurred. Amplified trade-wind strength and isolation of the basin initiated intensified vertical mixing, causing surface waters enriched in ^{18}O to be transferred to the basin's deep waters. Model runs indicate that glacial-interglacial change in the $\delta^{18}\text{O}$ value of Cariaco Basin bottom waters was about $2.4 \pm 0.2\text{‰}$. Since the modern surface-water $\delta^{18}\text{O}$ value in the Cariaco is heavier than the bottom water at 900 m, we infer that the glacial-interglacial surface water $\delta^{18}\text{O}$ change is on the order of 1.4‰ , of which 0.4‰ can be attributed to increased salinity. Subsequent comparison with the oxygen isotopic record of the planktonic foraminifer *Globigerinoides ruber* (white) indicates approximately $3\text{--}4^\circ\text{C}$ of glacial cooling in surface waters of the basin.

1. INTRODUCTION

An accurate reconstruction of past tropical temperatures is essential for assessing the influence of tropical climate variability on global climate change, as well as for understanding the sensitivity of the climate system to increased greenhouse gas levels and perturbations in radiative balance. Yet, discrepancies still exist concerning the amplitude of regional glacial cooling in the tropics derived by various proxy parameters. Original findings of the CLIMAP group suggest only moderate glacial cooling in the equatorial oceans at the Last Glacial Maximum (LGM) of $\sim 1\text{--}2^\circ\text{C}$ based on planktonic foraminiferal ecology [*CLIMAP*, 1976; *CLIMAP*, 1981]. Alkenone temperature reconstructions from tropical regions also indicate less than 2°C of cooling [*Lyle et al.*, 1992; *Sikes and Keigwin*, 1994], as do records of foraminiferal $\delta^{18}\text{O}$ from sediments depos-

ited in the open ocean [Mix, 1986; Mix *et al.*, 1986]. However, studies based on other paleoenvironmental proxies have indicated a larger temperature drop in the tropics during this period. For instance, continental proxy records based on snowline [Broecker and Denton, 1989] and vegetation changes [Rind and Peteet, 1985; Colinvaux, 1989; Bush and Colinvaux, 1990; Bush *et al.*, 1990; Clapperton, 1990; Colinvaux *et al.*, 1996] indicate a cooling of air temperature in the equatorial zone of approximately 5-6°C at the LGM. Temperature estimates from noble gases in Brazilian groundwater suggest a comparable glacial cooling [Stute *et al.*, 1995]. Additional temperature reconstructions from $\delta^{18}\text{O}$ and Sr/Ca thermometry in Barbados corals record 4.5-5°C cooler sea surface temperatures (SSTs) than at present [Guilderson *et al.*, 1994; Guilderson *et al.*, 2001]. This clear contradiction of results concerning reconstructions of tropical SSTs and between temperatures over continents and oceans presents an obstacle to climate modelers who look to the past in attempt to predict future climate change and use paleodata as a test for calibrating numerical simulations [Rind and Peteet, 1985; Webb *et al.*, 1997; Ganopolski *et al.*, 1998].

In addition to this broader controversy regarding glacial-interglacial SST change, within the Cariaco Basin there is a direct disparity among SST proxies derived from the same sediment cores. At ODP Site 1002, the alkenone unsaturation index indicates very little change in surface water temperature from the LGM to present [Herbert and Schuffert, 2000], while planktonic foraminiferal $\delta^{18}\text{O}$ records display more than 2‰ change in isotopic composition [Lin *et al.*, 1997; Peterson *et al.*, 2000a], most certainly representing some SST variability. Hence, new methods of reconstructing paleotemperature are necessary so that a consensus of tropical LGM cooling can be derived, as well as to verify proposed ocean-climate linkages.

Here we implement an alternative method for determining the magnitude of past temperature variability in the Cariaco Basin. First, the glacial-interglacial change in the isotopic composition of seawater is constrained using sedimentary interstitial waters. The isotopic composition of sedimentary pore waters provides a proxy for the actual isotopic composition of glacial bottom waters [e.g., Schrag and DePaolo, 1993], hence providing a combined record of global ice volume and local salinity (S) change. This is then coupled with published high-resolution records of planktonic foraminiferal $\delta^{18}\text{O}$ to quantify the change in tropical SST during the last glaciation. This approach has a distinct advantage over other paleothermometry techniques using the carbonate isotope record since the ability with which the magnitude of glacial-interglacial SST change can be quantified hinges on the accuracy with which fluctuations in seawater $\delta^{18}\text{O}$ can be constrained. Paleoclimatic inferences are strongly affected by assumptions regarding the co-variations of temperature, salinity, and $\delta^{18}\text{O}$ since the reconstruction of absolute SST relies on knowledge of the local isotopic composition of seawater. The use of pore water $\delta^{18}\text{O}$ allows us to forgo the usual assumptions about the isotopic composition of the whole-ocean reservoir and ambient seawater and permits direct calculation of the residual $\delta^{18}\text{O}$ fraction due to temperature

variability in the carbonate isotopic record.

This study focuses on samples collected during Ocean Drilling Program (ODP) Leg 165 in the Cariaco Basin, the world's second largest anoxic marine basin. The sediments found in this restricted oceanographic setting have a high-deposition rate and annual laminations, which provide a late Quaternary record of tropical ocean variability on sub-Milankovitch time scales [Peterson *et al.*, 1991; Hughen *et al.*, 1996; Black *et al.*, 1999]. Complementary to the basin's ideal depositional environment is the basin's location in a climatically sensitive, tropical region, well situated for recording surface-ocean changes that result from variability in Atlantic thermohaline circulation [Black *et al.*, 1999] and changes in the position of the Intertropical Convergence Zone (ITCZ) [Hughen *et al.*, 1996; Haug *et al.*, 2001]. Anoxia and lack of bioturbation allow for preservation of varved sediments with abundant microfossils, ideal for high-resolution geochemical studies with relatively little alteration of the original signal [Lin *et al.*, 1997; Peterson *et al.*, 2000a; Haug *et al.*, 2001].

1.1. SITE LOCATION AND LOCAL HYDROGRAPHY

ODP Leg 165, Site 1002 (10°42.37'N, 65°10.18'W; 893 m water depth) is situated on the western edge of a central high in the Cariaco Basin on the northern continental shelf of Venezuela (Figure 1a). The basin has restricted horizontal connection between its deeper waters and those from the open Caribbean Sea since inflow is limited by the surrounding shallow shelf with an average depth of 100 m. Two channels bisecting the shelf exist, one to the northeast that is ~135 m deep and one to the northwest at ~146 m depth [Richards and Vaccaro, 1956]. At present, the basin is anoxic below ~300 m due to limited exchange with the open Caribbean and because of the excessive demand for oxygen created by the degradation of the high flux of organic matter settling through the water column. Above the sill depth, seawater in the Cariaco Basin has water column characteristics similar to the open Caribbean [Okuda *et al.*, 1969] with a mean annual SST around 25°C (seasonal range of 22.5-28.5°C) and a mean annual salinity around 36.75 psu (seasonal range of 36.5-37.0 psu) [Herbert and Schuffert, 2000; Muller-Karger *et al.*, 2001]. Measured $\delta^{18}\text{O}$ values of the surface water have a seasonal range of 0.91-1.19‰ (R.C. Thunell, University of South Carolina, personal communication, 2001). In contrast, seawater below the controlling sill depth of ~150 m in the basin differs markedly from open Caribbean water, with temperatures below sill depth of around 17°C inside the basin as compared to 5°C outside in the Caribbean [Okuda *et al.*, 1969]. Below ~200 m, water is stratified due to the temperature gradient rather than the gradient in salinity [Scranton *et al.*, 2001]. Surface water circulation patterns are in general controlled by the North Equatorial Current flowing into the Caribbean [Ogden and Gladfelter, 1986] (Figure 1), causing the surface waters from the open Caribbean and Cariaco Basin to be well mixed.

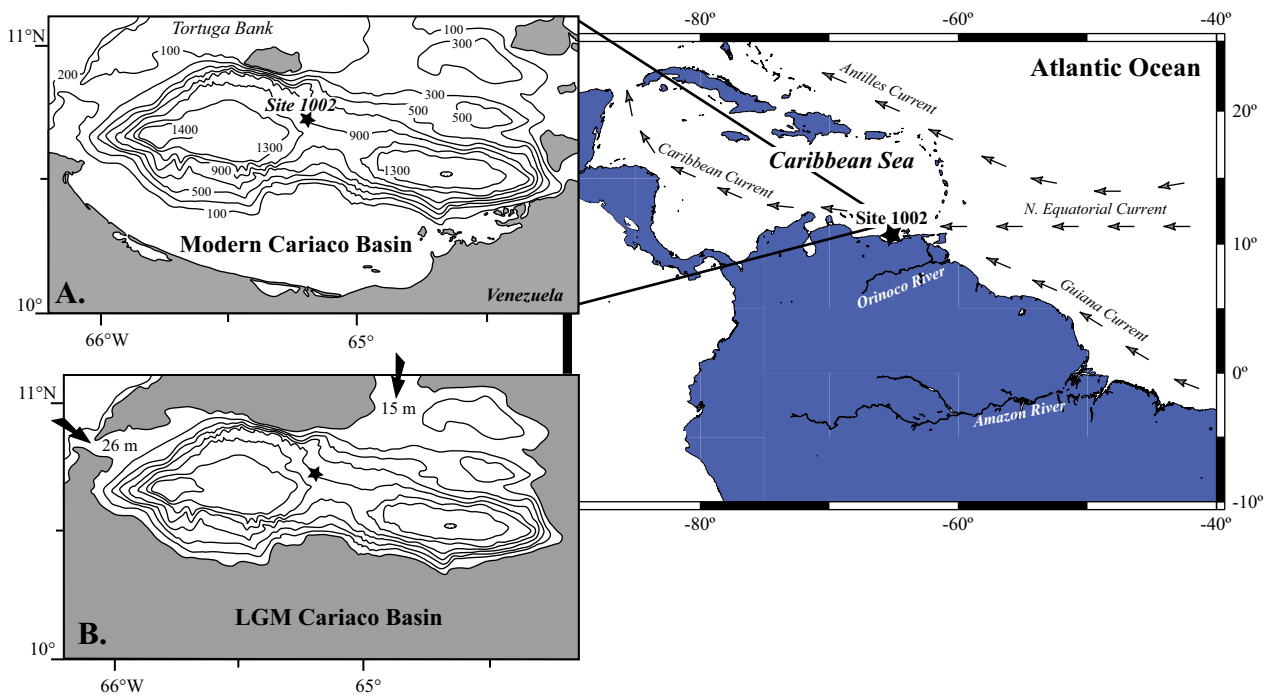


Figure 1.

Location of ODP Leg 165, Site 1002 with simplified schematic of surface ocean currents (after *Ogden and Gladfelter* [1986]) and (A.) bathymetric map (200 m contour intervals) of the modern Cariaco Basin (modified from *Peterson et al.* [2000a]). Inflow and outflow are limited to two shallow sills, approximately 135 and 146 m deep. (B.) Map showing situation in the Cariaco Basin at the Last Glacial Maximum after 100 m of sea level lowering. Clearly displayed is the increased isolation of the basin from the open Caribbean. Approximate sill depths during the glaciation would be 15 and 26 m based on 120 m of sea level fall.

The Cariaco Basin is strongly influenced by seasonal changes in trade-wind driven upwelling in waters shallower than 120 m [*Peterson et al.*, 1991; *Scranton et al.*, 2001]. Today, upwelling of cold, nutrient-rich waters occurs along the northern Venezuelan coast in response to movement of the ITCZ, which causes the prevailing trade-winds to vary in frequency and intensity. Seasonal movements of the ITCZ also control precipitation in northern South America, strongly influencing the discharge of rivers that affect the western North Atlantic and southern Caribbean. Presently, the typical annual cycle alternates between a dry, upwelling season when the NE trade winds are at maximum strength (winter-spring when the ITCZ is furthest south), and a wet, non-upwelling season (summer-fall when the ITCZ moves north and is situated almost directly above the Venezuelan coast). During the upwelling season, the introduction of cool, nutrient-rich water leads to very high surface productivity. During periods of diminished upwelling, surface waters warm to $\sim 28^{\circ}\text{C}$ and productivity across the basin is low. Runoff from local rivers during the wet season is carried directly into the basin, though this has minor impact on Cariaco Basin salinity today [*Ljoen and Herrera*, 1965]. The largest factor controlling the salinity of the basin at present is upwelling along the coast that brings up relatively saline water into the surface layer [*Richards*, 1975]. Estimates of the modern residence time of deep water in

the Cariaco Basin are on the order of 100 years [Deuser, 1973; Holman and Rooth, 1990]. In addition, lateral intrusion of oxygenated water seems to occur periodically at the sills, presumably originating from deeper waters outside, and subsequently sinks to mid-depths in the basin [Holman and Rooth, 1990; Scranton *et al.*, 2001]. This external water is a possible source for the more depleted $\delta^{18}\text{O}$ values (+0.2 to 0.0‰) of the basin's bottom waters.

Due to the strong seasonal cycle and the fact that the basin is anoxic, sedimentation patterns tracking the annual climate signal are preserved as continuously laminated sedimentary layers back to 12.6 ^{14}C ka BP [Peterson *et al.*, 1991; Hughen *et al.*, 1996; Lin *et al.*, 1997]. The varved nature of the sediments and the high accumulation rates at ODP Site 1002, averaging 30–35 cm/kyr [Peterson *et al.*, 2000b; Peterson *et al.*, 2000a], provide sections with the potential to reveal information about past changes in the tropical atmosphere and ocean, and for the study of the regional hydrologic balance over northern South America.

1.2. LAST GLACIAL MAXIMUM HYDROGRAPHY

The absence of laminated sediments between approximately 26.8 and 12.6 ^{14}C ka BP [Lin *et al.*, 1997] indicates that sediments have been bioturbated and were deposited under oxic bottom conditions during the last glacial period. The existence of benthic foraminifera (and other biota) in sediments of glacial age also attest to oxic bottom water conditions and provide additional evidence for low productivity and nutrient supply in surface waters of the Cariaco Basin at this time [Peterson *et al.*, 1991]. Numerous studies have suggested that easterly trade winds were more vigorous [Rea, 1994] and that a generally more arid climate prevailed over northern South America at the LGM. In the Cariaco Basin, a combination of arid local conditions and intensified winds, coupled with lowered sea level and more restricted exchange of waters with the Caribbean, could have resulted in higher glacial salinities and mixing that initiated local, seasonal downwelling and helped maintain the deep basin in an oxic state [Lin *et al.*, 1997].

The glacio-eustatic drawdown of sea level at the Last Glacial Maximum is estimated to have been approximately 120 to 135 m [Clark and Mix, 2002]. A lowering of sea level by 100 m would largely isolate the Cariaco Basin due to the surrounding shallow banks (Figure 1b) and the main connection with the open Caribbean Sea would be limited to very shallow sills, only 15–30 m deep, causing a much altered hydrography compared to today. Assemblages of planktonic foraminifera from glacial age sediments in the basin contain abundant *Globigerinoides ruber*, generally restricted to the non-upwelling season today [Lin *et al.*, 1997], and minor abundances of *Globigerina bulloides*, today abundant during the upwelling season [Peterson *et al.*, 1991; Black *et al.*, 1999; Poore and Dowsett, 2001]. These biologic indicators suggest an absence of strong upwelling in the basin during glacial times, a result of the low sea level stand that restricted the supply of nutrient-rich subsurface water.

2. METHODS

Approximately 170 m of sediment were recovered at ODP Site 1002 from which interstitial waters were sampled at a resolution of 1.5 to 2 m from Hole 1002E and subsequently measured for their stable oxygen isotopic composition. The $\delta^{18}\text{O}$ value of interstitial waters (Table 1) was determined using an automated water equilibration device in which CO_2 is injected into a serum bottle at atmospheric pressure and allowed to equilibrate with the sample (0.5 cm^3) for a period of 10 hours at 30°C . The CO_2 was then expanded from the bottles into a Europa, GEO mass spectrometer and measured at the Stable Isotope Laboratory of the University of Miami. Samples were processed in batches of 59 including 10 internal standards calibrated to the VSMOW scale. Analytical reproducibility based on repeat analysis of internal standards is approximately $\pm 0.08\text{‰}$ for $\delta^{18}\text{O}$. All isotope data are reported in the standard delta notation with respect to Vienna Standard Mean Ocean Water (VSMOW).

A one-dimensional, finite-difference model coupling fluid diffusion with advective transport [Paul *et al.*, 2001] has been used to calculate the isotopic evolution of the pore water through time. The isotopic composition of the fluid varies with distance z and time t based on the standard advection-diffusion equation, treating the sediment as a fluid-saturated, porous medium. Compaction of the sediments is simulated based on the profile of decreasing porosity with depth (porosity data from Site 1002 Hole C; Table 2; *L. Peterson, unpublished data*). Using a method similar to that of Schrag and DePaolo [1993], theoretical profiles of fluid isotopic composition are calculated using a forward modeling approach to monitor the top 170 m of sediment and then comparing these with the observed pore-water vs. depth profile from Site 1002. To simulate changes in the $\delta^{18}\text{O}$ of seawater due to ice volume fluctuations from 500 to 20 ka, the isotopic value at the sediment-water interface varies in accordance with the $\delta^{18}\text{O}$ of bottom-water in the tropical Atlantic based on a record of $\delta^{18}\text{O}$ from benthic foraminiferal calcite derived from ODP Site 659, eastern tropical Atlantic [Tiedemann *et al.*, 1994]. From 20 ka to 0 ka (present), isotopic input is based on the model of eustatic sea level change ($\Delta_{\text{sea level}}$) [Fairbanks, 1989]. The amplitude of isotopic variation is prescribed for the entire record by fixing the glacial-interglacial, seawater $\delta^{18}\text{O}$ change ($\Delta\delta_{\text{sw}}$) relative to $\Delta_{\text{sea level}}$ at 20 ka for each run and assuming a sea level change of 120 m. The model simulates a total of one million years, updating every 1000 years, and monitors the pore-water isotopic composition at a resolution of 0.5 meters. The lower boundary condition is constant and is appointed using the measured isotopic value of the pore waters at the base of the modeled sediment column (at 162 m, $\delta^{18}\text{O} = -0.68\text{‰}$).

3. RESULTS

The oxygen isotopic measurements of sediment pore fluids from Site 1002 (Table 1) display a clear positive trend below the sediment-water interface. Maximum isotopic values occur between 40 and 50 meters below sea floor (mbsf) representing remnant seawater from the Last

Glacial Maximum ($\sim 21,000$ years ago). The amplitude of change existing in the pore-water $\delta^{18}\text{O}$ record that denotes the glacial event ($\sim 0.90\text{‰}$) is much larger here than observed in previous studies (e.g., 0.34‰ [Adkins and Schrag, 2001], 0.3‰ [Burns and Maslin, 1999], 0.2‰ [Schrag *et al.*, 1996], and 0.35‰ [Schrag and DePaolo, 1993]) and reveals the significance of glacial-interglacial seawater $\delta^{18}\text{O}$ change at this site, even prior to modeling. Comparison of the measured isotopic profiles vs. depth with the profile of dissolved chloride [Sigurdsson *et al.*, 1997] shows an increase from values around 580 milli-moles per liter (mM/l) near the sediment-water interface to ~ 585 mM/l around 30 mbsf indicating a salinity increase coincident with the enrichment in seawater isotopic values. Unfortunately, this property was not measured at high enough resolution to reconstruct the total salinity change in the basin.

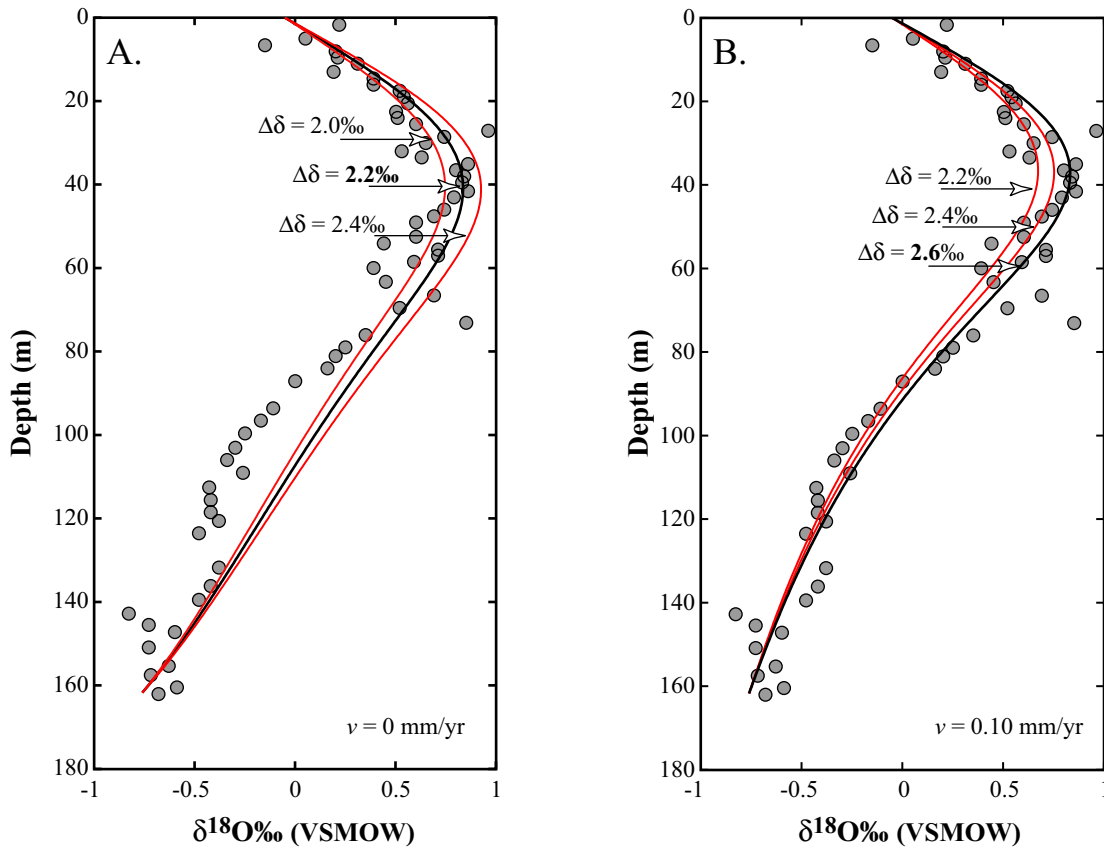


Figure 2.

Model calculations of pore fluid $\delta^{18}\text{O}$ (‰ VSMOW). (A.) Runs including advection velocity only due to compaction; a best fit is obtained using a $\Delta\delta_{\text{sw}}$ of $2.2 \pm 0.2\text{‰}$. (B.) Runs including an additional advection velocity of 0.1 mm/yr; a best fit is obtained using a $\Delta\delta_{\text{sw}}$ of $2.6 \pm 0.2\text{‰}$. Filled circles represent the measured, interstitial-water $\delta^{18}\text{O}$ values from Site 1002.

Using the model to reconstruct the isotopic composition of seawater at the LGM produces a best fit to the pore-water isotopic data indicating a glacial-interglacial change of 2.2‰ in $\delta^{18}\text{O}$ (Figure 2a). Due to the high amount of scatter in the observed isotopic data between 30-70 mbsf, the $\Delta\delta_{\text{sw}}$ estimation can only be constrained to within $\pm 0.2\text{‰}$. The $\delta^{18}\text{O}$ measurements

from the top 6 m of the sediment column also show an unexpectedly large range of values (i.e., -0.15 to +0.22). To best fit the $\delta^{18}\text{O}$ profile beneath the top 6 m, we use the average of the top 3 measured values ($\sim 0.0\%$) as the final upper boundary condition instead of the actual modern surface value (0.2%). This inconsistency in the surface sediment provides an obstacle for our determination of $\Delta\delta_{\text{sw}}$ as the amplitude of change is based on the model surface value. However, it is important to consider here that our goal is to determine the difference between the average isotopic composition of glacial vs. interglacial seawater. Since we are limited to the measurements at hand, we define the surface $\delta^{18}\text{O}$ value as the average of the top 6 m.

The $\delta^{18}\text{O}$ pore-water profile also seems to have an anomalous, negative “hump” centered around 100 m that is not matched by the model curves. Attempts to fit these measured data by amplifying the upward advection velocity requires an additional 0.05 to 0.1 mm/yr of flow. Yet, as advection velocity is increased, the $\delta^{18}\text{O}$ anomaly in the modeled curve is diminished and a larger $\Delta\delta_{\text{sw}}$ is needed to match the sediment pore-water values. Optimizing the model fit requires an increase in advection of around 0.1 mm/yr and a $\Delta\delta_{\text{sw}}$ of $\sim 2.6\%$ (Figure 2b) to match the LGM increase in seawater $\delta^{18}\text{O}$. This increase in advection velocity may be due to some horizontal fluid flow or continental contamination at approximately 90-130 m. This theory is supported by the fact that the chloride concentration decreases with depth to values below that of normal seawater salinity (i.e., ~ 520 mM/L at 160 m). The Cariaco Basin is a tectonically active region with major earthquakes occurring as recently as 1900 and 1929 [Zhang and Millero, 1993] and many faults existing in the region [Edgar *et al.*, 1973], thus, fluid may also have been transported during previous seismic events.

In light of this possible contamination, the question arises as to how accurately we can constrain the magnitude of glacial-interglacial isotopic change if a source of isotopically lighter water is present deeper in the sediment column. To evaluate the influence of a potential fresh-water flux (i.e., around 100 m depth) and possible impact on the $\Delta\delta_{\text{sw}}$ determination, sensitivity tests were carried out to examine the effect of the lower boundary condition on model output. In one instance, the lower boundary condition was raised to 80 m to avoid any contamination that may be present deeper in the sediment column. Comparing the result from this test, using a $\Delta\delta_{\text{sw}}$ of 2.2%, and the original best-fit shows that the two model curves are not identical, yet well within the $\pm 0.2\%$ error (Figure 3a). A second test was done to examine the effect of varying the lower boundary condition, here between -0.5 and -1.0% (Figure 3b). These results demonstrate the significance of the lower boundary condition in determining the model profile, and hence the final $\Delta\delta_{\text{sw}}$, though they also indicate that a 0.5% range in the lower boundary value still allows for $\Delta\delta_{\text{sw}}$ estimates within the total $\pm 0.2\%$ error. Finally, concerning the possible intrusion, and subsequent diffusion, of isotopically depleted waters upward in the sediment column; this occurrence would reduce the remnant LGM signal, hence, indicating that the existing profile of interstitial-water $\delta^{18}\text{O}$ provides a minimum estimate of glacial-interglacial isotopic variability in the

Cariaco Basin.

Based on the model results shown in Figure 2 and due to the various sources of uncertainty (i.e., the modern sediment-water interface $\delta^{18}\text{O}$ value, the scatter in the data, the possible intrusion of foreign waters, etc.), we chose a best fit based on the average of the no-advection and the 0.1 mm/yr advection model runs. This combination of parameters indicates a total glacial-interglacial $\Delta\delta_{\text{sw}}$ of $2.4\pm 0.2\text{‰}$.

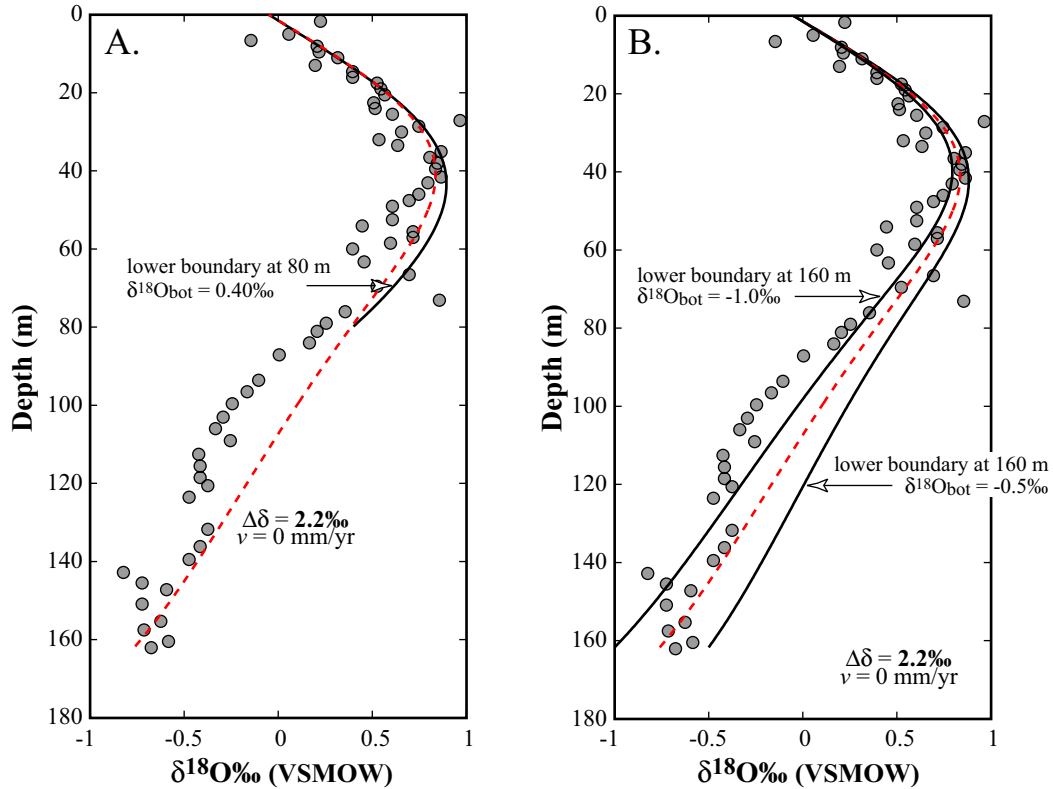


Figure 3.

Model sensitivity tests for calculations of pore fluid $\Delta\delta^{18}\text{O}$ (%VSMOW). To test the influence of the lower boundary condition on modeled curves, (A.) the lower boundary condition was moved to 80 m depth (vs. the usual 160 m) and (B.) the $\delta^{18}\text{O}$ value of the lower boundary was varied between -1.0 and -0.5‰. Dashed line in all plots is the original fit shown in Figure 2a.

4. DISCUSSION

Sill depth surrounding the Cariaco Basin controls the patterns of inflow and outflow of seawater between the basin and the Caribbean, and consequently, the nutrient and oxygen concentrations of the basin water. Inflow at current sill depth (~ 146 m) brings in nutrient-rich, oxygen-poor seawater (Figure 4a). At the LGM, global changes in sea level would have dictated the sill depth linking the Cariaco Basin with the open ocean. In addition, general circulation model results [Overpeck *et al.*, 1989] and correlation between *G. bulloides* abundance in the Cariaco Basin and SSTs in the northern North Atlantic region [Black *et al.*, 1999] have shown that trade

wind strength in this region is amplified in response to a reduction in North Atlantic SSTs. Thus, it is likely that seasonal trade-wind driven vertical mixing was increased in the Cariaco Basin during glacial times and the lack of a renewable supply of nutrient-rich, subsurface waters prevented high surface productivity. If we assume that deep water in the Cariaco Basin had a shallow water source at the LGM, i.e., from intensified vertical mixing and hindered flow out of the basin (Figure 4b), then we can use the total change in deep-water $\delta^{18}\text{O}$, as recorded in pore waters, to examine salinity and temperature changes in the basin's surface water.

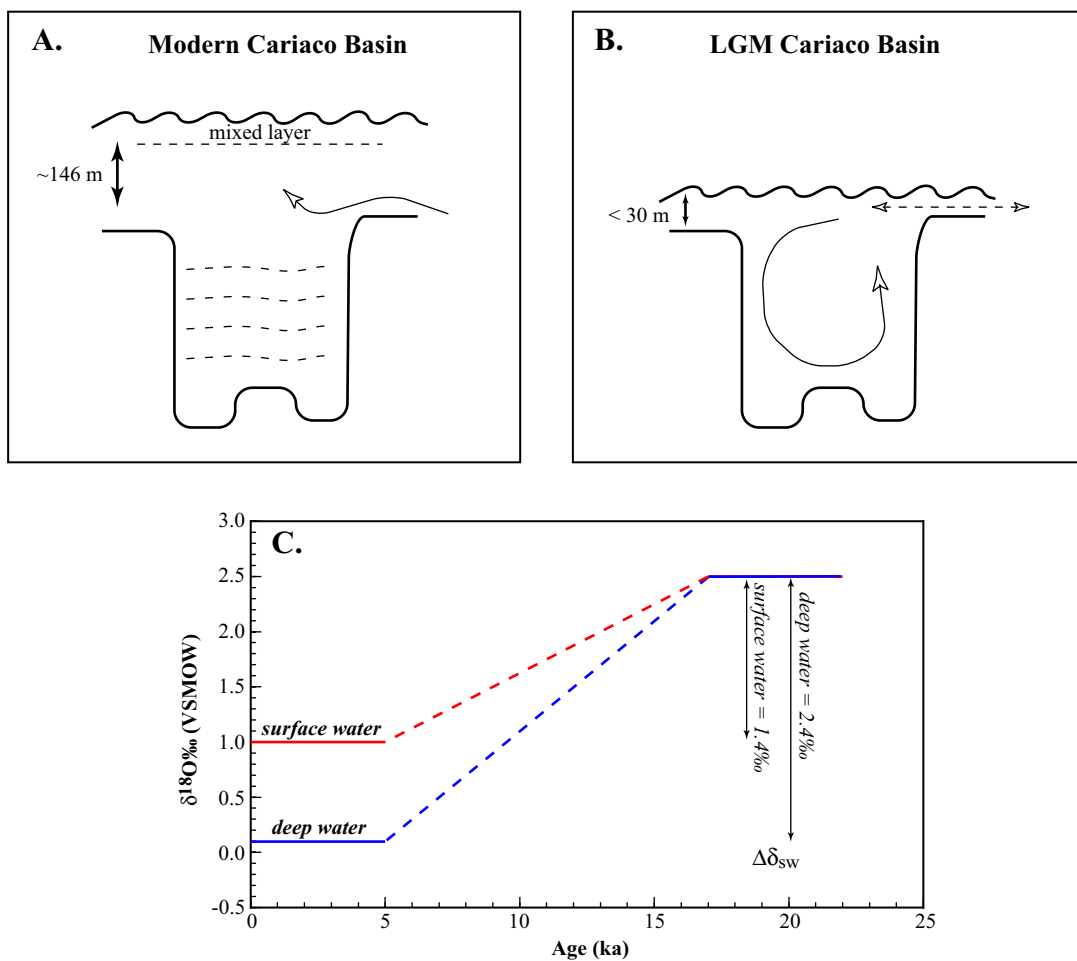


Figure 4. Comparison of glacial-interglacial change in the hydrography of the Cariaco Basin. Schematic representation of (A.) modern, stratified basin with anoxic waters below 300 m and upwelling in the surface layer; and (B.) hypothetical LGM circulation pattern with turbulent mixing between surface and deep water reservoirs. (C.) Glacial-interglacial change in oxygen isotopic composition ($\Delta\delta_{\text{sw}}$) for deep and surface water masses, based on the assumption of a well-mixed basin during the glacial period.

4.1. GLACIAL SEA SURFACE SALINITY

The modern surface-water $\delta^{18}\text{O}$ value in the Caribbean is approximately 1.0‰ heavier than bottom waters at 900 m deep in the Cariaco Basin (based on pore-water measurements from

the sediment-water interface at Site 1002). Using the average $\Delta\delta_{\text{sw}}$ of $2.4\pm 0.2\text{‰}$ for deep water in the basin as determined by the advection-diffusion model, we can infer that the $\Delta\delta_{\text{sw}}$ for surface water is on the order of 1.4‰ (Figure 4c). Subsequent subtraction of 1.0‰ for the average global change in seawater $\delta^{18}\text{O}$ due to ice volume growth at the LGM, as estimated by other studies of pore-water $\delta^{18}\text{O}$ [Schrag *et al.*, 1996], leaves a residual 0.4‰ change in the local isotopic composition of seawater due to salinity. The magnitude of this isotopic shift is in good agreement with a paleosalinity reconstruction for the western Caribbean by Schmidt *et al.* [2001], indicating a 0.5‰ increase at the LGM, and likely corresponds to an increase in evaporation, as a result of wind intensification and decrease in freshwater input that accompanied arid, glacial conditions. Using the $\delta^{18}\text{O}:\text{S}$ relationship of $0.22\text{‰}/\text{psu}$ defined by Craig [1965] for Atlantic surface waters in the trade-wind belt, this translates to an approximately 2 psu increase in the salinity concentration during the glacial period. This estimate is slightly higher than the 1.5 psu increase derived by Dürkoop *et al.* [1997] for the western tropical Atlantic at the LGM, though it is not surprising considering the relative isolation of the basin from the open ocean during the glacial period.

Our $\Delta\delta_{\text{sw}}$ value of 1.4‰ is the same as the average isotopic change recorded by the planktonic foraminifer *Neogloboquadrina dutertrei* in the Cariaco Basin [Lin *et al.*, 1997; Lin *et al.*, 2001]. This species is believed to calcify within a narrow temperature range in the water column [Fairbanks *et al.*, 1982; Curry *et al.*, 1983; Dunbar, 1983], and hence, theoretically records only changes in the isotopic composition of ambient seawater. These independent measurements from foraminiferal calcite agree well with the model-determined LGM-to-present change in the $\delta^{18}\text{O}$ of seawater, with the glacial-interglacial $\delta^{18}\text{O}$ change in *N. dutertrei* also showing a local salinity signal superimposed on the global $\Delta\delta_{\text{sw}}$ signal that dominates the record. This similarity supports the theory of stronger wind intensity and isolation of the basin at the LGM (Figure 4) causing enhanced vertical mixing and enabling the more saline surface water, enriched in $\delta^{18}\text{O}$, to be transferred to deeper depths in the basin.

4.2. GLACIAL SEA SURFACE TEMPERATURES

The $\delta^{18}\text{O}$ of foraminiferal calcite reflects a complex sum of fractionation processes including the local temperature of shell precipitation, the local freshwater budget (S), and the global isotopic composition of seawater. Sedimentary interstitial waters provide an alternative method for reconstructing the magnitude of glacial-interglacial $\delta^{18}\text{O}$ change, unique in that the $\Delta\delta_{\text{sw}}$ resolved is independent of temperature effects. Hence, we can use the pore-water model results in conjunction with a record of planktonic foraminiferal $\delta^{18}\text{O}$ to constrain the $\delta^{18}\text{O}$ change caused by fluctuations in paleo-SST. Implementing the calcite $\delta^{18}\text{O}$ record of *G. ruber* (white) that displays an approximately 2.25‰ $\Delta\delta_{\text{calcite}}$ [Lin *et al.*, 1997; Peterson *et al.*, 2000a; Lin *et al.*, 2001] (and assuming for simplicity that $\Delta\delta_{\text{sw}} = \Delta\delta_{\text{calcite}}$), we find a residual 0.8‰ due

to cooling of SSTs during the LGM. Applying the 0.21‰ per 1°C relationship [Craig, 1965; Shackleton, 1973], we determine approximately 3-4°C of cooling in glacial surface waters of the Cariaco Basin.

Cooling of the surface waters inhabited by *G. ruber* during the glacial period explains the larger $\delta^{18}\text{O}$ change recorded in the tests of this species relative to *N. dutertrei* [Lin *et al.*, 1997]. It is likely that *N. dutertrei* moved to a shallower position in the water column during the LGM to maintain its preference for cooler temperatures. In addition, the $\delta^{18}\text{O}$ time series of the foraminifera measured by Lin *et al.* [1997] show that the $\delta^{18}\text{O}$ gradient between these two species was reduced at the LGM, suggesting growth in waters of more similar isotopic composition than at present.

The estimation of ~3-4°C of cooling in the surface waters of the Caribbean Sea at the LGM based on pore-water $\delta^{18}\text{O}$ values directly conflicts with a SST reconstruction using the alkenone unsaturation index, also on sediments from Site 1002 in the Cariaco Basin. Measurements using this technique suggest very little temperature difference between the LGM and Holocene [Herbert and Schuffert, 2000], or at most 1°C. This contradiction of results may be due to a calibration bias; for instance, cultures of both *Emiliania huxleyi* and *Gephyrocapsa oceanica* show nonlinear and often sharply reduced slopes at temperature extremes [Conte *et al.*, 1998], including those greater than 22°C. This suggests that the magnitude of SST change may be underestimated in tropical waters by linear calibrations, such as that of Prahl *et al.* [1988] which was used by Herbert and Schuffert [2000] for their reconstruction. Alternatively, a number of ecological and biochemical responses exist that may be responsible for this inconsistency. For example, slight changes in depth habitat during the glacial period in response to temperature, nutrient or salt concentration, and/or oxygen availability could potentially have a large impact on the temperature that the organisms are recording, especially considering the large variations in hydrography of the basin between the present and the LGM (Figure 4). Similarly, a change in production season such that alkenones are more representative of summer growth conditions during glacial periods [Weaver *et al.*, 1999] could also mask a decrease in mean annual SSTs. This hypothesis is supported by recent work by J. Bollmann (Swiss Federal Institute of Technology, personal communication, 2001) who used recently developed coccolith transfer functions [Bollmann *et al.*, 2002] to reconstruct the glacial-interglacial temperature gradient in the Cariaco Basin. His results also indicate very little temperature change (<1°C), suggesting a variation in the growth season of these organisms at the LGM.

Despite this discrepancy, the determined Holocene-LGM SST change of 3-4°C agrees well with another SST reconstruction using alkenones from just outside the Caribbean Sea in the western tropical Atlantic, which indicates 3.5°C of cooling for the glacial ocean [Rühlemann *et al.*, 1999]. Additionally, recent examination of accumulated data from surface dwelling planktonic foraminifera *Globigerinoides sacculifer* and *G. ruber* from the tropical Atlantic suggests a

spatial range of glacial-interglacial $\Delta\delta_{\text{calcite}}$ of 1.0 to 2.3‰ [Billups and Schrag, 2000; Guilderson *et al.*, 2001], though Guilderson *et al.* [2001] suggest that this large variability is mostly a consequence of site-dependent sedimentation rates, bioturbation, and sample resolution and that the records with the highest sedimentation rates show $\Delta\delta_{\text{calcite}}$ values closer to 2.0‰. Assuming that the isolated Cariaco Basin may have been more susceptible to surface evaporation than the open ocean, the average $\Delta\delta_{\text{calcite}}$ of 2.0‰ suggests up to 4°C of cooling for the tropical Atlantic and fits well with our SST estimation. Measurements of coralline aragonite $\delta^{18}\text{O}$ in Barbados corals also show a $\Delta\delta_{\text{calcite}}$ of 2.3‰ [Guilderson *et al.*, 1994; Guilderson *et al.*, 2001], which is interpreted as representing 5°C of temperature change (though the entire change is attributed to ΔT and none to ΔS).

Our calculation of glacial-interglacial SST change is also in good agreement with recent reconstructions using the Mg/Ca ratio in foraminiferal calcite as a proxy for SST, most notably with [Lea *et al.*, 2001] who resolve approximately 4°C of cooling in Cariaco Basin surface-water temperatures and with Schmidt *et al.* [2001] who find 3°C cooler SSTs in the western Caribbean. Slightly less cooling is suggested by studies using Mg/Ca ratios in the open equatorial Atlantic indicating 2-3°C cooler temperatures at the LGM [Hastings *et al.*, 1998]. A coupled ocean-atmosphere climate model calculated 3.3°C cooling for tropical Atlantic SSTs versus 4.6° over tropical land masses [Ganopolski *et al.*, 1998] revealing that LGM cooling seems to have been more pronounced on land (and at high altitudes) than in the sea [Pinot *et al.*, 1999]. The Cariaco Basin's location directly adjacent to a continental land mass, where upwelling occurs, may have made it more susceptible to cooling than other tropical, open-ocean settings. The glacial-interglacial SST determination estimated here using pore-water $\delta^{18}\text{O}$ in conjunction with foraminiferal $\delta^{18}\text{O}$ supports recent coupled ocean-atmosphere modeling studies proposing that more moderate SST variability in the tropical oceans is compatible with more severe continental cooling of 5-6°C [Ganopolski *et al.*, 1998; Pinot *et al.*, 1999; Crowley, 2000].

5. CONCLUSIONS

Using high-resolution measurements of pore-fluid $\delta^{18}\text{O}$ recovered from ODP Leg 165, Site 1002 in the Cariaco Basin in conjunction with a numerical model of diffusive and advective transport, we constrain the glacial-interglacial change in the $\delta^{18}\text{O}$ of deepwater in the basin to be 2.4 ± 0.2 ‰. Due to increased wind strength and isolation of the basin during the glacial period, vertical mixing in the basin was intensified causing thorough mixing of surface and bottom water reservoirs. Based on this relationship, it can be inferred that the isotopic composition of tropical surface waters increased by 1.4‰. Of the total $\delta^{18}\text{O}_{\text{sw}}$ shift, 0.4‰ is attributable to a local salinity increase of 2 psu in the surface water of the basin. As this estimate of seawater isotopic change is unaffected by glacial-interglacial variations in marine temperature, the record of seawater $\delta^{18}\text{O}$ can be used to calculate sea surface temperatures by coupling the data with records of

planktonic foraminiferal $\delta^{18}\text{O}$. The paleo-SST reconstructions suggest approximately 3-4°C of cooling during the last glacial period. As demonstrated, this technique can be used to determine the paleo-isotopic and chemical composition of seawater and can be used to better constrain the relative contributions of temperature and local salinity to the foraminiferal calcite $\delta^{18}\text{O}$ signal.

Our results indicate that the Cariaco Basin experienced both salinity and temperature changes during the last glaciation. These variations can be interpreted to reflect the changing glacial surface-water hydrography in the Caribbean Sea and the western tropical Atlantic Ocean since these are the major surface-water suppliers to the basin, supporting the theory that the tropics play a dynamic role in the global climate system. Our estimate of 3-4°C for glacial-interglacial SST change is in general agreement with that determined in GCM runs by *Crowley* [2000], and indicates that the tropics are, indeed, an active participant in determining climatic behavior and not just a passive component.

ACKNOWLEDGEMENTS

Thanks to G.H. Haug, J. Bollmann, D. Schrag, and 2 anonymous reviewers for useful comments. Funding for this work was provided by ETH Research Project No. 02197.

Table 1.
ODP Site 1002 interstitial-water oxygen isotopic composition.

Depth (mbsf)	$\delta^{18}\text{O}\text{‰}$ (VSMOW)	s.d.	Depth (mbsf)	$\delta^{18}\text{O}\text{‰}$ (VSMOW)	s.d.
1.47	0.22	0.34	66.27	0.69	0.11
4.77	0.05	0.04	69.27	0.52	0.11
6.27	-0.15		72.77	0.85	0.04
7.77	0.20	0.08	75.77	0.35	0.17
9.27	0.21	0.06	78.77	0.25	
10.77	0.31	0.01	80.77	0.20	0.21
12.77	0.19	0.02	83.77	0.16	0.17
14.27	0.39	0.13	86.77	0.00	0.12
15.77	0.39	0.04	93.27	-0.11	0.17
17.27	0.52	0.20	96.27	-0.17	0.10
18.77	0.54		99.27	-0.25	0.11
20.27	0.56		102.8	-0.30	0.09
22.27	0.50	0.13	105.77	-0.34	0.12
23.77	0.51	0.06	108.77	-0.26	0.19
25.27	0.60	0.03	112.27	-0.43	0.05
26.77	0.96	0.04	115.3	-0.42	0.10
28.27	0.74	0.08	118.3	-0.42	0.07
29.77	0.65	0.04	120.27	-0.38	0.05
31.77	0.53	0.03	123.27	-0.48	0.09
33.27	0.63	0.02	131.55	-0.38	0.12
34.77	0.86	0.08	135.9	-0.42	0.09
36.27	0.80	0.13	139.18	-0.48	0.17
37.77	0.84	0.01	142.47	-0.83	
39.27	0.83	0.02	145.24	-0.73	0.34
41.27	0.86	0.01	146.97	-0.60	0.14
42.77	0.79	0.01	150.57	-0.73	0.11
45.77	0.74	0.01	155.07	-0.63	0.05
47.27	0.69	0.09	157.27	-0.72	0.06
48.77	0.60	0.07	160.27	-0.59	0.15
52.27	0.60	0.09	161.77	-0.68	0.14
53.77	0.44				
55.27	0.71				
56.77	0.71	0.06			
58.27	0.59	0.07			
59.77	0.39	0.00			
63.09	0.45	0.03			

Table 2.

ODP Site 1002 porosity measurements (*L. Peterson, unpublished data, 2002*). Corrected depth takes into account gas expansion that occurs during coring.

Depth (mbsf)	Corrected Depth (mbsf)	Porosity	Depth (mbsf)	Corrected Depth (mbsf)	Porosity	Depth (mbsf)	Corrected Depth (mbsf)	Porosity
0.75	0.75	84.9	63.64	62.49	48.6	120.73	119.74	46.2
2.25	2.25	78.6	65.24	63.86	47.9	122.23	121.05	50.9
3.75	3.75	79.3	66.73	65.13	48.7	122.75	122.71	47.1
5.25	5.25	73.7	65.87	65.81	52.7	123.71	123.56	41.3
6.75	6.75	60.7	66.69	66.52	54.1	125.22	124.89	43.7
7.84	7.84	55.2	68.17	67.81	51.9	126.73	126.23	40.4
9.14	9.12	71	69.69	69.14	52.5	128.3	127.61	36.8
10.64	10.59	65.1	71.19	70.44	54.2	129.89	129.02	40.2
12.14	12.05	62.7	72.72	71.77	46.5	132.37	132.31	47.9
13.64	13.52	64	74.24	73.1	44.2	133.31	133.13	37.1
15.14	14.98	66.4	75.72	74.39	51.1	134.84	134.46	38.2
16.64	16.45	62.5	75.67	75.64	56.9	136.31	135.73	41.3
17.62	17.4	65.6	76.85	76.78	59.1	137.81	137.04	43.2
18.66	18.63	62.9	78.35	78.23	59.9	139.34	138.37	35.2
20.14	20.05	65.2	79.91	79.74	50.1	140.72	139.57	40.3
21.64	21.49	65.1	81.35	81.13	53.8	142.22	140.87	43.9
23.17	22.96	70.4	82.85	82.58	53.8	141.8	141.75	50
24.67	24.4	64.1	84.28	83.96	43	142.36	142.24	42.3
26.2	25.87	61.8	85.15	85.05	51.5	143.93	143.62	45.3
27.18	26.81	61.4	85.92	85.72	48.3	145.69	145.16	45.4
28.14	28.12	59.1	87.43	87.04	51.1	147.21	146.5	46.1
29.64	29.58	59.9	88.96	88.37	49.6	148.71	147.81	43.2
31.17	31.07	59.9	90.5	89.71	44.3	150.26	149.17	44.5
32.74	32.6	59	92.06	91.07	48.1	151.71	150.44	47
34.32	34.14	63.5	93.5	92.32	41.6	151.63	151.61	41.1
35.88	35.65	56.9	95.07	93.69	49.2	153.21	153.13	34.2
36.82	36.57	58.3	94.92	94.86	49.8	154.77	154.64	31.8
37.65	37.6	60.7	96.41	96.26	50.1	156.35	156.17	36.2
39.15	39.01	58.8	97.97	97.72	44.7	157.9	157.67	42.3
40.65	40.42	56.7	99.67	99.32	37.2	159.4	159.12	41.1
42.22	41.89	59.5	101.27	100.83	37.9	160.38	160.07	43.3
43.72	43.3	59.3	102.8	102.26	48.9	161.13	161.1	38.5
45.22	44.71	59.4	104.25	103.63	46.5	162.63	162.54	40.6
46.72	46.12	62.9	104.2	104.08	42.7	164.13	163.97	37.2
47.41	47.31	55	105.4	105.1	41.1	166.11	165.87	38.2
48.9	48.66	57.5	106.95	106.42	35.9	167.56	167.26	36.5
50.39	50.01	56	108.45	107.7	43.1	169.11	168.74	38.2
51.9	51.37	58.7	109.95	108.98	42.2			
53.45	52.77	53.9	111.51	110.31	43.7			
55.05	54.22	46.8	113.01	111.59	46.5			
56.55	55.57	49	114.49	112.85	43			
56.64	56.53	53	113.64	113.55	45.8			
57.52	57.28	47	114.73	114.5	49.5			
59.07	58.6	48.5	116.43	115.99	46.9			
60.52	59.84	50.3	117.73	117.12	50.9			
62.09	61.17	46.7	119.23	118.43	40.8			

6. REFERENCES

- Adkins, J.F., and D.P. Schrag, Pore fluid constraints on deep ocean temperature and salinity during the last glacial maximum, *Geophysical Research Letters*, 28, 771-774, 2001.
- Billups, K., and D.P. Schrag, Surface ocean density gradients during the Last Glacial Maximum, *Paleoceanography*, 15, 110-123, 2000.
- Black, D.E., L.C. Peterson, J.T. Overpeck, A. Kaplan, M.N. Evans, and M. Kashgarian, Eight centuries of North Atlantic Ocean atmosphere variability, *Science*, 286 (5445), 1709-1713, 1999.
- Bollmann, J., J. Henderiks, and B. Brabec, Global calibration of *Gephyrocapsa* coccolith abundance in Holocene sediments for paleotemperature assessment, *Paleoceanography*, in press, 2002.
- Broecker, W.S., and G.H. Denton, The role of ocean-atmosphere reorganizations in glacial cycles, *Geochimica et Cosmochimica Acta*, 53 (10), 2465-2501, 1989.
- Burns, S.J., and M.A. Maslin, Composition and circulation of bottom water in the western Atlantic Ocean during the last glacial, based on pore-water analyses from the Amazon Fan, *Geology*, 27, 1011-1014, 1999.
- Bush, M.A., and P.A. Colinvaux, A pollen record of a complete glacial cycle from lowland Panama, *J. Vegetation Sci.*, 1, 105-118, 1990.
- Bush, M.B., P.A. Colinvaux, M.C. Wiemann, D.R. Piperno, and K.-b. Liu, Late Pleistocene temperature depression and vegetation change in Ecuadorian Amazonia, *Quaternary Research*, 34 (3), 330-345, 1990.
- Clapperton, C.M., Quaternary glaciations in the Southern Hemisphere: An overview, *Quaternary Science Reviews*, 9 (2-3), 299-304, 1990.
- Clark, P.U., and A.C. Mix, Ice sheets and sea level of the Last Glacial Maximum, *Quaternary Science Reviews*, 21, 1-7, 2002.
- CLIMAP Project Members, The surface of ice-age Earth, *Science*, 191, 1131-1137, 1976.
- CLIMAP Project Members, Geol. Soc. Am. Map and Chart Series, GSA, Boulder, CO, 1981.
- Colinvaux, P.A., Forest palaeoecology, ice-age Amazon revisited, *Nature*, 340 (6230), 188-189, 1989.
- Colinvaux, P.A., P.E. De Oliveira, J.E. Moreno, M.C. Miller, and M.B. Bush, A long pollen record from lowland Amazonia: Forest and cooling in glacial times, *Science*, 274, 85-88, 1996.
- Conte, M.H., A. Thompson, D. Lesley, and R.P. Harris, Genetic and physiological influences on the alkenone/alkenoate versus growth temperature relationship in *Emiliania huxleyi* and *Gephyrocapsa oceanica*, *Geochimica et Cosmochimica Acta*, 62, 51-68, 1998.
- Craig, H., *Proceedings of the Spoleto Conference*, 3-24 pp., Consiglio Nazionale Delle Ricerche, V. Lischio e Figli, Spoleto, Italy, 1965.
- Crowley, T.J., CLIMAP SSTs re-revisited, *Climate Dynamics*, 16, 241-255, 2000.
- Curry, W.B., R.C. Thunell, and S. Honjo, Seasonal changes in the isotopic composition of planktonic foraminifera collected in Panama Basin sediment traps, *Earth and Planetary Science Letters*, 64, 33-43, 1983.
- Deuser, W.G., Cariaco Trench: Oxidation of organic matter and residence time of anoxic water, *Nature*, 242 (5400), 601-603, 1973.
- Dunbar, R.B., Stable isotope record of upwelling and climate from Santa Barbara Basin, California, in *Coastal Upwelling, Its Sedimentary Record, Part A: Sedimentary Records of Ancient Coastal Upwelling*, edited by E. Suess, and J. Thiede, pp. 217-246, Plenum, New York, 1983.

- Dürkoop, A., W. Hale, S. Mulitza, J. Paetzold, and G. Wefer, Late Quaternary variations of sea surface salinity and temperature in the western tropical Atlantic: Evidence from $\delta^{18}\text{O}$ of *Globigerinoides sacculifer*, *Paleoceanography*, 12 (6), 764-772, 1997.
- Edgar, N.T., J.B. Saunders, et al., *Initial Reports of the Deep Sea Drilling Project*, U.S. Government Printing Office, Washington, 1973.
- Fairbanks, R.G., M. Sverdrlove, R. Free, P.H. Wiebe, and A.W.H. Bé, Vertical distribution and isotopic fractionation of living planktonic foraminifera from the Panama Basin, *Nature*, 298, 841-844, 1982.
- Fairbanks, R.G., A 17,000-year glacio-eustatic sea level record: Influence of glacial melting rates on the Younger Dryas event and deep ocean circulation, *Nature*, 342, 637-642, 1989.
- Ganopolski, A., S. Rahmstorf, V. Petoukhov, and M. Claussen, Simulation of modern and glacial climates with a coupled global model of intermediate complexity, *Nature*, 391 (6665), 351-356, 1998.
- Guilderson, T.P., R.G. Fairbanks, and J.L. Rubenstone, Tropical temperature variations since 20,000 years ago: Modulating interhemispheric climate change, *Science*, 263 (5147), 663-665, 1994.
- Guilderson, T.P., R.G. Fairbanks, and J.L. Rubenstone, Tropical Atlantic coral oxygen isotopes: Glacial-interglacial sea surface temperatures and climate change, *Marine Geology*, 172 (1-2), 75-89, 2001.
- Hastings, D.W., A.D. Russell, and S.R. Emerson, Foraminiferal magnesium in *Globigerinoides sacculifer* as a paleotemperature proxy, *Paleoceanography*, 13 (2), 161-169, 1998.
- Haug, G.H., K.A. Hughen, D.M. Sigman, L.C. Peterson, and U. Röhl, Southward migration of the inter-tropical convergence zone through the Holocene, *Science*, 293, 1304-1308, 2001.
- Herbert, T.D., and J.D. Schuffert, Alkenone unsaturation estimates of sea-surface temperatures at site 1002 over a full glacial cycle, in *Proceedings of the Ocean Drilling Program, Scientific Results*, edited by R.M. Leckie, H. Sigurdsson, D. Acton Gary, and G. Draper, pp. 239-247, Texas A&M University, Ocean Drilling Program, College Station, TX, United States, 2000.
- Holman, K.J., and C.G.H. Rooth, Ventilation of the Cariaco Trench, a case of multiple source competition?, *Deep-Sea Research*, 37, 203-225, 1990.
- Hughen, K.A., J.T. Overpeck, L.C. Peterson, and S. Trumbore, Rapid climate changes in the tropical Atlantic region during the last deglaciation, *Nature*, 380 (6569), 51-54, 1996.
- Lea, D.W., D.K. Pak, L.C. Peterson, and K.A. Hughen, Mg/Ca-based temperature record from Cariaco Basin reveals SST changes in phase with Greenland ice core records, in *EOS Trans. AGU*, AGU, San Francisco, CA, 2001.
- Lin, H.-L., L.C. Peterson, J.T. Overpeck, S. Trumbore, and D.W. Murray, Late Quaternary climate change from $\delta^{18}\text{O}$ records of multiple species of planktonic foraminifera: High-resolution records from the anoxic Cariaco Basin, Venezuela, *Paleoceanography*, 12 (3), 415-427, 1997.
- Lin, H.-L., et al., Cariaco Basin stable isotope data, IGBP PAGES/World Data Center for Paleoclimatology Data Contribution Series #2001-075. NOAA/NGDC Paleoclimatology Program, Boulder, CO, 2001.
- Ljoen, R., and L.E. Herrera, *Some oceanographic conditions of the coastal waters of eastern Venezuela: Oceanographie*, 7-50 pp., Universitate Orientale, 1965.
- Lyle, M.W., F.G. Prahl, and M.A. Sparrow, Upwelling and productivity changes inferred from a temperature record in the central equatorial Pacific, *Nature*, 355, 812-815, 1992.
- Mix, A.C., Late Quaternary paleoceanography of the tropical Atlantic: 1, Spatial variability of annual mean sea-surface temperatures, 9-20,000 years B.P., *Paleoceanography*, 1 (1), 43-66, 1986.

- Mix, A.C., W.F. Ruddiman, and A. McIntyre, Late Quaternary paleoceanography of the tropical Atlantic: 2, The seasonal cycle of sea surface temperatures, 0-20,000 years B.P., *Paleoceanography*, 1 (3), 339-353, 1986.
- Muller-Karger, F., R. Varela, R. Thunell, M. Scranton, et al., Annual cycle of primary production in the Cariaco Basin: Response to upwelling and implications for vertical export, *Journal of Geophysical Research-Oceans*, 106 (C3), 4527-4542, 2001.
- Ogden, J.C., and E. Gladfelter, Caribbean coastal marine productivity, in *UNESCO Reports in Marine Science*, pp. 59, 1986.
- Okuda, T., B.R. Gamboa, and A.J. García, *Bol. Inst. Oceanogr. Univ. Oriente*, 8, 21-27, 1969.
- Overpeck, J.T., L.C. Peterson, N. Kipp, J. Imbrie, and D. Rind, Climate change in the circum-North Atlantic region during the last deglaciation, *Nature*, 338 (6216), 553-557, 1989.
- Paul, H.A., S.M. Bernasconi, D.W. Schmid, and J.A. McKenzie, Oxygen isotopic composition of the Mediterranean Sea since the Last Glacial Maximum: Constraints from pore water analyses, *Earth and Planetary Science Letters*, 192, 1-14, 2001.
- Peterson, L.C., J.T. Overpeck, N.G. Kipp, and J. Imbrie, A high-resolution late Quaternary upwelling record from the anoxic Cariaco Basin, Venezuela, *Paleoceanography*, 6, 99-119, 1991.
- Peterson, L.C., G.H. Haug, R.W. Murray, K.M. Yarincik, J.W. King, T.J. Bralower, K. Kameo, S.D. Rutherford, and R.B. Pearce, Late Quaternary stratigraphy and sedimentation at Site 1002, Cariaco Basin (Venezuela), in *Proceedings of the Ocean Drilling Program, Scientific Results*, edited by R.M. Leckie, H. Sigurdsson, D. Acton Gary, and G. Draper, pp. 85-99, Texas A & M University, Ocean Drilling Program, College Station, TX, United States, 2000a.
- Peterson, L.C., G.H. Haug, K.A. Hughen, and U. Rohl, Rapid changes in the hydrologic cycle of the tropical Atlantic during the last glacial, *Science*, 290 (5498), 1947-1951, 2000b.
- Pinot, S., G. Ramstein, S.P. Harrison, I.C. Prentice, J. Guiot, M. Stute, and S. Jousaume, Tropical paleoclimates at the last glacial maximum: Comparison of Paleoclimate Modeling Intercomparison Project (PMIP) simulations and paleodata, *Climate Dynamics*, 15 (11), 857-874, 1999.
- Poore, R.Z., and H.J. Dowsett, Pleistocene reduction of polar ice caps: Evidence from Cariaco Basin marine sediments, *Geology*, 29 (1), 71-74, 2001.
- Prahl, F.G., L.A. Muehlhausen, and D.L. Zahnle, Further evaluation of long-chain alkenones as indicators of paleoceanographic conditions, *Geochimica et Cosmochimica Acta*, 52, 2303-2310, 1988.
- Rea, D.K., The paleoclimatic record provided by eolian deposition in the deep sea: The geologic history of wind, *Reviews in Geophysics*, 32, 159-195, 1994.
- Richards, F.A., and R.F. Vaccaro, The Cariaco Trench, an anaerobic basin in the Caribbean Sea, *Deep-Sea Research*, 3 (3), 214-228, 1956.
- Richards, F.A., The Cariaco Basin (Trench), in *Oceanography and Marine Biology*, edited by H. Barnes, pp. 11-67, Aberdeen University Press, Aberdeen, 1975.
- Rind, D., and D.M. Peteet, Terrestrial conditions at the last glacial maximum and CLIMAP sea-surface temperature estimates: Are they consistent?, *Quaternary Research*, 24 (1), 1-22, 1985.
- Rühlemann, C., S. Mulitza, P.J. Müller, G. Wefer, and R. Zahn, Warming of the tropical Atlantic Ocean and slowdown of thermohaline circulation during the last deglaciation, *Nature*, 402, 511-514, 1999.
- Schmidt, M.W., H.J. Spero, and D.W. Lea, Temperature and hydrological changes in the Western Caribbean during the Last Glacial cycle, in *EOS Trans. AGU*, AGU, San Francisco, 2001.

- Schrag, D.P., and D.J. DePaolo, Determination of $\delta^{18}\text{O}$ of seawater in the deep ocean during the Last Glacial Maximum, *Paleoceanography*, 8, 1, 1993.
- Schrag, D.P., G. Hampt, and D.W. Murray, Pore fluid constraints on the temperature and oxygen isotope composition of the glacial ocean, *Science*, 272, 1930-1932, 1996.
- Scranton, M.I., Y. Astor, R. Bohrer, T.Y. Ho, and F. Muller-Karger, Controls on temporal variability of the geochemistry of the deep Cariaco Basin, *Deep-Sea Research Part I-Oceanographic Research Papers*, 48 (7), 1605-1625, 2001.
- Shackleton, N.J., Les Methodes Quantitatives d'Etude des Variations du Climat au Cours du Pleistocene, in *Colloques Internationaux, CNRS, Verrières-le-Buisson, France*, 1973.
- Sigurdsson, H., R.M. Leckie, G.D. Acton, et al., *Proc. ODP, Init. Repts.*, (Ocean Drilling Program), College Station, TX, 1997.
- Sikes, E.L., and L.D. Keigwin, Equatorial Atlantic sea-surface temperature for the last 30-kyr: A comparison of UK'37, $\delta\text{-O}18$ and foraminiferal assemblage temperature estimates, *Paleoceanography*, 9 (1), 31-45, 1994.
- Stute, M., M. Forster, H. Frischkorn, A. Serejo, J.F. Clark, P. Schlosser, W.S. Broecker, and G. Bonani, Cooling of tropic Brasil during the last glacial maximum, *Science*, 269, 379-383, 1995.
- Tiedemann, R., M. Sarnthein, and N.J. Shackleton, Astronomic timescale for the Pliocene Atlantic $\delta^{18}\text{O}$ and dust flux records of Ocean Drilling Program site 659, *Paleoceanography*, 9 (4), 619-638, 1994.
- Weaver, P.P.E., M.R. Chapman, G. Eglinton, M. Zhao, D. Rutledge, and G. Read, Combined coccolith, foraminiferal, and biomarker reconstruction of paleoceanographic conditions over the past 120 kyr in the northern North Atlantic (59°N, 23°W), *Paleoceanography*, 14, 336-349, 1999.
- Webb, R.S., D.H. Rind, S.J. Lehman, R.J. Healy, and D. Sigman, Influence of ocean heat transport on the climate of the Last Glacial Maximum, *Nature*, 385, 695-699, 1997.
- Zhang, J.Z., and F.J. Millero, The chemistry of the anoxic waters in the Cariaco Trench, *Deep-Sea Research Part I-Oceanographic Research Papers*, 40 (5), 1023-1041, 1993.

PROXY ASSESSMENT AND FUTURE WORK

1. PROXY ASSESSMENT

The selected studies described in this thesis demonstrate the many advantages to using a multi-proxy approach for investigating past climatic variability. When used together, geochemical proxies can be powerful tools and are able to provide more precise reconstructions of environmental change than any single proxy alone. Yet, as discussed at the beginning of this work, no proxy is without its own set of problems and or list of assumptions. To further address this issue, a summary of the respective pros and cons of the two new paleoceanographic proxies applied in the previous chapters is provided in the following section.

1.1. PORE-WATER $\delta^{18}\text{O}$

PROS:

The interstitial-water $\delta^{18}\text{O}$ signal has been shown to be very effective in determining the total change in the glacial-interglacial oxygen isotopic composition of seawater. This proxy “eliminates” the influence of temperature and interference from biological vital effects (i.e., no habitat, seasonal, productivity, or nutrient considerations), leaving a pure record of $\Delta\delta_{\text{sw}}$. This has been the goal of paleoceanographers for a number of decades, allowing researchers to separate out the influence of salinity and ice volume variations over a glacial cycle. In addition, the measurement of the $\delta^{18}\text{O}$ of water is a standard laboratory technique that is fast and not labor intensive. Additionally, once the advection-diffusion model has been constructed, it can be used for analyzing data from different sites with only moderate alterations.

CONS:

The biggest drawback to this proxy is that it cannot be used for high-resolution studies due to smoothing of the record with time. The signal is also limited to the recent geologic past, and can only be traced back to the Last Glacial Maximum. Records of earlier changes in the isotopic composition of seawater are erased by the ongoing processes of diffusion and advection in the sediment column. Another limiting factor is the need for high-resolution pore-water samples. Such samples do not exist at high enough resolution from older ODP and DSDP legs, thus the number of sites where such studies can be carried out are limited and sampling for these studies will need to be considered on future cruises with paleoceanographic goals. High measurement precision is also an important prerequisite for applying this proxy, as too much scatter in the data limits the model’s ability to determine the $\Delta\delta_{\text{sw}}$ value. Interpretation of pore-water data may also

be impaired due to external influences such as a lateral flux or pressure-derived advective flow. The possibility of changing circulation or water masses on the pore water signal is an additional source of uncertainty that must be thoroughly considered.

1.2. COMPOUND-SPECIFIC δD

PROS:

The measurement of compound-specific δD on biomolecules is very effective for tracking environmental and/or physiological phenomena and will be important for examining sediment records which lack the carbonate proxies. Additionally, since the specificity of biomarkers varies (i.e., some are highly specific while others derive from many organisms) there is also the potential to gain information about regional productivity vs. individual species dynamics by comparing these signals. This proxy will also prove to be useful for determining the organic matter source of certain compounds as demonstrated in Chapter 4, Part II and in conjunction with $\delta^{13}C$ as suggested by *Chikaraishi and Naraoka* [2001]. In general, there is great potential for using this proxy in process-oriented studies and, since so little has been done up until now, the possibilities for future studies are endless!

CONS:

The largest hindrance to this method is the necessity for very high concentrations of sedimentary organic material and/or of individual organic compounds. Due to the small weight percent of hydrogen present in any sediment sample, relatively large sample sizes are needed to be able to measure the δD value. This is not a very practical prerequisite for conducting paleoceanographic work, where sedimentary material typically contains less than 1% TOC. It will also be a limiting factor for studies aimed at achieving high-resolution records. Examination of paleoenvironment may thus be better focused on lake sediments, which commonly contain higher percentages of organic material. Research utilizing cultures are also realistic targets for this proxy.

2. FUTURE STUDIES

The following sections contain a few ideas and suggestions concerning future research directions making use of these proxies. Together or separately, these studies represent the subject of potential, future doctoral theses!

2.1. PORE-WATER $\delta^{18}O$

Investigations applying the $\delta^{18}O$ from interstitial waters are well underway (see summary in *Schrag et al.* [2002]) and have been successful at constraining the glacial-interglacial change in the oxygen isotopic composition of seawater in the deep Atlantic. Future work could focus on cores in the Pacific and Indian Oceans to validate the theories concerning the global

change in $\delta^{18}\text{O}$ and in salinity. Depth transects should be investigated to resolve the glacial-interglacial $\delta^{18}\text{O}_{\text{sw}}$ change in some of the important intermediate water bodies (e.g., Atlantic Intermediate Water), though, in order to avoid a mixed signal, care must be taken to prove that the source remained the same. Another marginal or enclosed basin that may be interesting to examine using the method applied here (i.e., to examine the surface-water $\delta^{18}\text{O}$ signal) may be the Santa Barbara Basin. In addition, this approach may also eventually be applied to other chemical species (already attempted for strontium [Richter and DePaolo, 1987], though with only a few pore-water measurements), however, this will entail the high-resolution analysis of these elements.

2.2. COMPOUND-SPECIFIC δD

A modern calibration between source-water δD and compound-specific δD from biomarkers in a “trans-Alpine” series of Swiss lakes, including Lake Zürich, Lake Lugano, and Lake Lucerne, was started as part of this thesis (but not completed due to technical difficulties and time constraints). The lakes were chosen to span a climatic gradient and represent varying ecological conditions (i.e., depth, nutrient availability, productivity, etc.). This calibration should be completed and then applied to sediments from Baldeggersee to reconstruct the local paleohydrologic change in this area over the past ~60 years. Finally, these results could be used in conjunction with previous measurements of $\delta^{18}\text{O}$ and $\delta^{13}\text{C}$ [Teranes, 1998] to examine the paleoenvironmental changes on a broader, regional (northern European) scale.

Concerning future work in the Mediterranean Sea and constraining the organic matter source of individual *n*-alkanes, it would be interesting to examine the δD of *n*-alkanes extracted from wind-blown material (which should be predominantly supplied from the continents). This would allow for an assessment of the terrestrial δD signal derived from plant material and its influence on the bulk *n*-alkane signal in the sediments in the Mediterranean. Such a study would also enable the molecular and isotopic signatures from the various end-member atmospheric source regions to be defined and facilitate the making of a budget for the region.

It would be very interesting to apply the use of compound-specific δD measurements for future coccolith culture experiments to examine the effect of salinity and temperature changes and verify that the δD tracer can be used in waters with varying environmental conditions. It will be necessary to carry out a similar experiment, as described in Chapter 3, at different S and T conditions, holding these parameters constant while again varying δD to see what effect these physical properties have (if any) on the fractionation factor, ϵ . Then questions, such as does ϵ stay the same, is the slope the same, etc., can be evaluated. The effect of growth rate should also be constrained by growing cultures over a broader range of growth rates. In addition, culture studies and investigations of modern algal material from a range of organisms should be carried out to establish the fractionation factors for a variety of species (i.e., test *Gephyrocapsa spp.* to make certain that it produces the same ϵ as *Emiliania huxleyi*; studies of dinoflagellate and dia-

tom species). Experiments designed to examine biosynthetic and photosynthetic pathways and other biologic processes would also be interesting. Comparisons between the δD of various biomolecules and the δD of the bulk cell material would be beneficial to see how the various compounds fractionate the initial isotopic signal.

Investigations of the selective degradation of algal biomarkers, and especially of the influence of diagenesis on the breakdown of *n*-alkanes and related compounds, would be interesting and may offer some information concerning the stability of individual molecules and how they react to thermal maturation.

3. REFERENCES

- Chikaraishi, Y., and H. Naraoka, Hydrogen and carbon isotopic compositions of individual long-chain *n*-alkanes in a lake system with relevance to their sources, in *20th International Meeting on Organic Geochemistry*, pp. 121-122, Nancy, France, 2001.
- Richter, F.M., and D.J. DePaolo, Numerical models for diagenesis and the Neogene Sr isotopic evolution of seawater from DSDP Site 590B, *Earth and Planetary Science Letters*, *83*, 27-39, 1987.
- Schrag, D.P., J.F. Adkins, K. McIntyre, J.L. Alexander, D.A. Hodell, C.D. Charles, and J.F. McManus, The oxygen isotopic composition of seawater during the Last Glacial Maximum, *Quaternary Science Reviews*, *21*, 331-342, 2002.
- Teranes, J.L., Climatic significance and biochemical controls on stable isotopes in a lacustrine sequence from Baldeggersee, Switzerland, PhD thesis, Swiss Federal Institute of Technology, Zürich, 1998.

APPENDIX I

GEOCHEMICAL DATA

1. MEDITERRANEAN SEDIMENT CORE GEOCHEMISTRY

1.1. Sample TMC-3 Analyses (Core Collected June 15, 1999)

Sample Depth (cm)	$\delta^{18}\text{O}$ CaCO ₃	$\delta^{13}\text{C}$ CaCO ₃
7-9	1.43	1.61
9-11	1.39	1.57
10-12	1.44	1.59
11-13	1.44	1.54
12-13.5	1.39	1.61
13-15	1.58	1.58
13.5-15	1.61	1.68
15-17	1.65	1.68
17-18.5	1.41	1.35
18.5-20	1.27	1.08
20-22	1.13	0.68
22-24	0.55	0.05
26-28	0.87	0.30
28-30	0.71	0.68

All isotopic values are given in ‰ with respect to PDB.

1.2. Sample TMC-4 Analyses (Core Collected June 16, 1999)

Sample Depth (cm)	% C total	% C inorganic	% CaCO ₃	% TOC	δ ¹⁸ O CaCO ₃	δ ¹³ C CaCO ₃	δ ¹³ C organic	δ ¹⁵ N organic	C/N ratio
0-1	6.40	5.45	45.43	0.95	1.36	1.29	-21.32	2.42	7.82
1-2	6.30	5.66	47.13	0.64	1.48	1.59	-21.17	2.11	7.78
2-4	6.56	6.10	50.87	0.46	1.77	1.84	-20.96	2.21	6.00
4-6	6.59	6.19	51.61	0.39	1.73	1.76			
6-8	6.60	6.21	51.76	0.39	1.60	1.73			
6-9					1.65	1.71			
8-10	6.06	5.87	48.94	0.19	1.63	1.74			
10-11	7.03	6.61	55.07	0.42	1.65	1.73			
11-12	7.11	6.62	55.14	0.49	1.62	1.75	-21.59	1.67	7.71
12-13	7.14	6.73	56.07	0.41	1.64	1.62			
13-14	7.38	6.97	58.08	0.41	1.63	1.69			
14-15	7.34	6.92	57.65	0.42	1.69	1.71			
15-16	7.14	6.81	56.78	0.33	1.58	1.55			
16-17	6.95	6.57	54.75	0.38	1.40	1.21			
17-18	7.17	6.67	55.61	0.50	1.19	1.02	-21.86	1.72	6.09
18-19	7.17	6.77	56.45	0.40	1.08	0.73			
19-20	6.79	6.49	54.09	0.30	0.88	0.36			
20-21	6.35	5.84	48.66	0.51	0.56	0.22	-21.45	1.53	7.20
21-22	5.72	5.01	41.74	0.71	0.44	0.18	-21.98	1.86	9.37
22-23	7.64	4.98	41.49	2.66	0.46	0.09	-21.89	0.31	11.12
23-24	7.50	4.70	39.16	2.80	0.75	0.45	-22.33	-0.82	13.01
24-25	8.08	5.05	42.06	3.04	0.84	0.42	-22.36	0.03	12.70
25-26	6.32	4.91	40.89	1.41	1.18	0.96	-21.93	0.29	13.15
26-27		5.45	45.40		1.65	1.14	-21.78	2.05	8.89

All isotopic values are given in ‰; δ¹⁵N with respect to Air, all others with respect to PDB.

continued...

WaterSample Site-Info.	Depth (m)	Temperature (°C)	Salinity (p.s.u.)	$\delta^{18}\text{O}$ (SMOW)	δD (SMOW)	Std. Dev.	$\delta^{13}\text{C}$ (PDB)	$\delta^{15}\text{N}$ (Air)	POC (uMol)	PN (uMol)	POC/ PN	Chl.A (ng/l)	NO_3^- (mMol)
79	10	14.38	37.77	1.22	6.47	3.71	-26.09	5.40	4.94	0.76	6.51	106.70	0.04
3411 m	20	14.39	37.79	1.23			-25.48	6.26	4.74	0.82	5.78	110.10	0.16
40°21.4 N	50	14.53	37.87	1.22			-26.98	6.59	2.98	0.46	6.45	128.00	8.01
12°06.4 E	100	14.09	38.23	1.29			-27.67	8.49	2.63	0.38	6.93	17.30	5.70
	200			3.37			-27.14	9.00	3.33	0.46	7.26		8.09
	400						-27.89	8.89	2.60	0.27	9.57		5.46
81	10	13.62	37.94				-27.32	7.85	16.54	1.11	14.90	77.30	1.16
1230 m	20	13.60	37.97	1.32	6.57	0.02	-24.54	6.63	8.22	1.18	6.95	74.70	1.49
42°18.2 N	50	13.78	38.12	1.31			-24.97	13.72	5.75	0.68	8.45	14.50	3.31
3°54.98 E	100	13.14	38.14	1.35			-25.20	2.64	6.52	0.67	9.75	13.60	2.87
	200			1.36			-25.22	7.59	6.93	0.86	8.10		4.92
	400			1.46			-25.61	6.13	4.81	0.50	9.60		5.94
87	10	14.98	37.25	1.11	3.22	1.15	-25.65	4.96	8.05	1.14	7.06	132.00	0.47
1896 m	20	14.98	37.24	1.08			-24.50	5.84	8.37	1.46	5.73	130.70	
38°59.2 N	50	15.15	37.64	1.14			-25.90	8.02	3.27	0.54	6.03	85.40	2.13
4°01.44 E	100	13.93	38.05	1.35			-26.84	9.15	1.65	0.28	5.88	21.70	4.89
	200			1.30			-27.64	9.23	1.23	0.13	9.59		7.61
	400			1.30			-27.43	9.96	0.63	0.15	4.07		6.01

All isotopic values are given in ‰ with respect to listed reference.

Values in italics are questionable measurements and may not be reliable.

Oxygen and hydrogen isotopic data were measured at the Geological Institute, ETH Zürich; other parameters provided by K.C. Emeis, Institut für Ostseeforschung, Warnemünde, Germany, 2000.

2.2. MATER Cruise Analyses (Samples Collected June, 1999)

Water Sample Site-Info.	Depth (m)	Fluorescence	Temperature (°C)	Salinity (p.s.u.)	$\delta^{18}\text{O}$ (VSMOW)	Std. Dev.	$\delta^2\text{H}$ (VSMOW)	Std. Dev.
TMC-1 35.78° N 28.74° E 7-6-1999	3	0.0075	22.72	39.01	1.57	0.01	16.44	0.26
	11	0.0137	22.54	39.01				
	20	0.0117	20.62	39.10				
	50	0.0246	16.73	39.03				
	75	0.101	16.16	39.05				
	100	0.089	15.82	39.06				
	122	0.0934	15.63	39.05				
	151	0.0565	15.00	39.00				
	200	0.0128	14.55	38.93				
	350	0.0029	14.03	38.83				
	500	0.0022	13.88	38.80				
	751	0.002	13.78	38.76				
	1001	0.0002	13.74	38.75				
	1500	0.0034	13.78	38.74				
	2001	0.0011	13.98	38.79				
	2500	0.0047	14.15	38.83				
	3000	0.0001	14.26	38.84				
3500	0.0003	14.36	38.85					
3799	-0.0003	14.41	38.85					
TMC-2 34.15° N 32.68° E 10-6-1999	3	0.0118	24.17	38.94	1.54	0.02	10.47	2.19
	10	0.0104	23.67	39.06				
	20	0.0129	22.20	38.99				
	49	0.0164	18.41	38.87				
	75	0.0315	18.03	38.94				
	101	0.0527	17.53	38.93				
	120	0.0831	17.37	38.94				
	149	0.0707	17.12	38.92				
	202	0.004	16.93	39.02				
	350	0.0063	15.05	38.99				
	501	0.0029	14.12	38.85				
	752	0.0042	13.79	38.77				
	1001	0.0013	13.73	38.74				
	1501	0.0046	13.73	38.73				
	2002	0.003	13.95	38.78				
2500	0.005	14.12	38.82					
2670	0.0075	14.15	38.82					
TMC-3 33.39° N 28.32° E 14-6-1999	3	0.0063	22.82	38.76	1.55	0.04	11.35	3.84
	11	0.0065	22.82	38.76				
	19	0.0091	22.54	38.74				
	51	0.0204	18.23	38.78				
	76	0.0351	17.71	38.86				
	100	0.0595	17.57	38.91				
	121	0.1128	16.96	38.77				
	129	0.1185	16.80	38.75				
	150	0.0584	16.53	38.74				
	201	0.0098	15.99	38.87				
	350	-0.0016	14.58	38.93				
	501	-0.0009	14.01	38.82				
	751	0.0047	13.78	38.76				
	1001	0.005	13.70	38.73				
	1502	0.0023	13.74	38.73				
1999	0.0043	13.94	38.78					
2500	0.0036	14.13	38.82					
2998	0.0032	14.24	38.83					

continued...

Water Sample Site-Info.	Depth (m)	Fluorescence	Temperature (°C)	Salinity (p.s.u.)	$\delta^{18}\text{O}$ (VSMOW)	Std. Dev.	$\delta^2\text{H}$ (VSMOW)	Std. Dev.
TMC-4	3	0.0112	24.03	38.60	1.51	0.07	5.87 <i>GFF (9.36)</i>	0.84
34.89° N	10	0.0132	23.96	38.59	1.45	0.05	10.10	0.13
22.53° E	20	0.0212	21.76	38.53	1.39	0.08	8.91	3.09
17-6-1999	50	0.0361	16.14	38.62	1.53	0.02	10.81	0.10
	75	0.1034	15.28	38.74	1.38	0.16	9.41	0.72
	100	0.3179	15.12	38.84	1.55	0.02	12.80	2.58
	120	0.0878	15.06	38.93	1.53	--	11.40	0.87
	150	0.0433	14.77	38.93	1.46	0.13	12.46	0.46
	200	0.0013	14.49	38.91	1.52	0.07	10.46	0.23
	350	-0.0003	14.18	38.87	1.49	0.05	11.59	0.92
	500	0.0018	13.91	38.80	1.36	0.16	10.12	--
	749	0.0034	13.82	38.78	1.50	0.03	4.64	--
	1000	0.0012	13.83	38.78	1.43	0.06	13.53	
	1500	0.0017	13.94	38.80	1.47	0.01	11.37	--
	2000	0.0005	14.03	38.81	1.43	0.05	10.28	--
	2500	0.0022	14.02	38.79	1.43	--	9.59	--
	2970	0.0016	14.11	38.81	1.45	0.02	6.90	--
TMC-5	3	0.0146	24.88	38.60	1.55	0.11	16.10	--
35.72° N	10	0.0166	24.83	38.58	1.73	--	9.92	1.35
20.13° E	20	0.0193	20.12	38.27	1.42	0.04	9.03	1.43
18-6-1999	50	0.0547	15.84	38.29	1.56	--	7.84	0.39
	70	0.1065	15.63	38.57	1.44	0.09	8.87	2.18
	100	0.1126	15.11	38.65	1.38	0.03	9.00	0.07
	120	0.0877	14.94	38.69	1.53	--	8.63	5.41
	151	0.0282	15.06	38.86	1.56	--	10.91	0.35
	201	0.0116	14.95	38.94	1.58	0.03	11.13	2.04
	351	0.0034	14.63	38.96	1.62	--	11.95	1.98
	501	0.0005	14.19	38.87	1.55	--	12.45	--
	751	-0.0005	13.88	38.79	1.49	0.07	6.88	--
	1001	0.0006	13.84	38.78	1.47	0.11		
	1500	0.0009	13.87	38.77	1.63	0.05	8.75	--
	2000	-0.0009	13.96	38.79	1.54	0.03	15.57	
	2500	0.0008	13.98	38.78	1.61	--	11.14	--
	3099	0.0066	13.88	38.72	1.59	--	4.49	--
TMC-6	3	0.0185	24.53	38.54	1.51	0.00	5.46	0.17
35.62° N	10	0.0179	24.27	38.53	1.44	0.02	12.82	0.33
17.39° E	20	0.022	18.19	38.46	1.45	0.03	13.97	--
20-6-1999	50	0.0572	15.68	38.46	1.45	0.03	15.16	
	75	0.092	14.88	38.50	1.52	0.08	9.90	2.44
	100	0.0999	14.57	38.53	1.48	0.09	9.26	
	120	0.0603	14.33	38.52	1.52	0.04	8.08	0.01
	150	0.0281	14.37	38.60				
	200	0.0179	14.13	38.63				
	350	0.0017	14.27	38.86	1.67	--	1.96	1.99
	500	0.0049	13.92	38.79	1.69	0.01	1.70	--
	750	0.0057	13.72	38.74	1.62	--	10.91	--
	1000	0.0006	13.69	38.73	1.63	0.05		
	1500	0.0062	13.66	38.71	1.62	--	6.32	3.40
	1999	0.0072	13.71	38.71	1.54	--	5.90	--
	2500	0.0018	13.77	38.71	1.58	--	11.25	
	2999	0.0026	13.83	38.70	1.48	0.04	10.24	--
	3500	0.0018	13.88	38.69	1.51	--	10.04	--
	4000	-0.0009	13.93	38.68	1.53	0.05	4.94	--

continued...

Water Sample Site-Info.	Depth (m)	Fluorescence	Temperature (°C)	Salinity (p.s.u.)	$\delta^{18}\text{O}$ (VSMOW)	Std. Dev.	$\delta^2\text{H}$ (VSMOW)	Std. Dev.
TMC-7	3	0.0134	21.28	37.28	1.51	0.04	-1.97	0.16
36.61° N	10	0.0167	21.24	37.28	1.55	0.04	2.15	0.61
12.25° E	20	0.0191	21.21	37.28	1.58	0.06	3.23	0.83
23-6-1999	50	0.0389	16.19	37.45	1.69	0.03	2.99	0.46
	76	0.0779	15.33	37.61	1.58	0.17	10.73	0.30
	90	0.1335	15.16	37.74	1.68	0.07	3.07	1.75
	100	0.1065	14.94	37.77				
	120	0.051	14.63	37.81	1.67	0.03	6.10	--
	150	0.0372	14.65	38.08	1.79	0.01	5.04	1.77
	200	0.0099	14.36	38.47	1.81	0.04	1.50	--
	352	0.0066	13.92	38.77	1.54	0.10	1.38	0.11
	500	0.006	13.80	38.75	1.51	0.07	2.56	--
	750	0.0033	13.76	38.74	1.53	0.06	<i>10.92</i>	
	1000	0.0023	13.77	38.74	1.48	0.07	<i>11.30</i>	
	1302	0.0025	13.81	38.74	1.57	0.02	6.97	--
TMC-8	3	0.029	22.42	37.44				
38.4° N	10	0.0229	22.43	37.43				
6.89° E	20	0.035	18.96	37.43				
27-6-1999	50	0.0702	15.05	37.71				
	75	0.2792	14.13	37.83				
	100	0.0953	13.67	38.03				
	121	0.0371	13.55	38.13				
	150	0.011	13.39	38.25				
	200	0.0099	13.38	38.36				
	350	0.0103	13.43	38.53				
	500	0.0052	13.33	38.53				
	750	0.0055	13.17	38.50				
	1000	0.0018	13.12	38.48				
	1500	0.0061	13.05	38.44				
	2000	0.0061	13.10	38.44				
	2499	0.002	13.18	38.44				
	2800	0.0046	13.24	38.44				
TMC-10	5	0.0217	22.72	37.46				
40.58° N	11	0.0229	22.74	37.47				
4.92° E	30	0.0357	17.59	37.75				
1-7-1999	60	0.5934	13.84	38.00				
	76	0.2972	13.66	38.03				
	101	0.0755	13.53	38.15				
	121	0.0263	13.30	38.16				
	151	0.0084	12.95	38.21				
	199	0.0079	12.86	38.23				
	350	0.0106	12.88	38.31				
	501	0.0063	13.18	38.44				
	751	0.0056	13.30	38.53				
	998	0.0058	13.16	38.49				
	1502	0.0043	13.10	38.45				
	2001	0.0037	13.15	38.45				
	2500	0.0038	13.20	38.44				
	2740	0.0066	13.29	38.46				

All isotopic values are given in ‰ with respect to listed reference.

Values in italics are questionable measurements and may not be reliable.

Oxygen and hydrogen isotopic data were measured at the Geological Institute, ETH Zürich; other parameters provided by V. Lykousis, National Centre for Marine Research, Athens, Greece, 2000.

3. BALDEGGERSEE SEDIMENT CORE GEOCHEMISTRY

Core BALD-3 taken by W.T. Anderson, 1996; 62 meters water depth.

3.1. Stable Isotopic Composition of Bulk Carbonate

Depth (cm)	$\delta^{13}\text{C}$ CaCO ₃	$\delta^{18}\text{O}$ CaCO ₃
1.0	-6.00	-9.33
3.0	-4.94	-9.77
5.0	-4.83	-10.18
7.0	-5.95	-10.45
9.0	-4.87	-9.61
11.0	-4.75	-10.12
13.0	-5.08	-10.14
15.0	-4.78	-9.82
17.0	-5.38	-9.14
19.0	-5.11	-8.93
21.0	-5.96	-9.27
23.0	-6.04	-9.15
25.0	-5.70	-9.01
27.0	-5.76	-8.82
29.0	-5.94	-8.89
30.7	-5.79	-8.91
33.0	-6.11	-8.84
36.2	-5.99	-8.86
38.5	-6.45	-8.79
41.2	-5.88	-8.78
44.0	-5.83	-9.10
48.5	-6.10	-8.92

All isotopic values are given in ‰ with respect to PDB.

3.2. Multi-Sensor Track Analyses

Depth (cm)	Wet Bulk Density (gm/cc)	Magnetic Susceptibility (SI Units)	Depth (cm)	Wet Bulk Density (gm/cc)	Magnetic Susceptibility (SI Units)
0.5	1.0988	1	26.5	1.2141	2
1.0	1.2158	1	27.0	1.1664	2
1.5	1.2442	2	27.5	1.1494	1
2.0	1.1353	2	28.0	1.1416	2
2.5	1.0954	2	28.5	1.1359	2
3.0	1.1502	2	29.0	1.1191	2
3.5	1.1566	2	29.5	1.1472	3
4.0	1.1431	1	30.0	1.1661	4
4.5	1.1221	1	30.5	1.1661	4
5.0	1.1351	1	31.0	1.1624	5
5.5	1.165	2	31.5	1.1557	5
6.0	1.1754	1	32.0	1.0932	5
6.5	1.1863	2	32.5	1.1252	6
7.0	1.1617	2	33.0	1.2311	6
7.5	1.1412	1	33.5	1.2518	6
8.0	1.1431	1	34.0	1.2742	7
8.5	1.1366	2	34.5	1.2267	7
9.0	1.1672	2	35.0	1.2504	7
9.5	1.2543	1	35.5	1.2549	8
10.0	1.3155	2	36.0	1.2432	7
10.5	1.2111	1	36.5	1.259	7
11.0	1.0537	1	37.0	1.2619	7
11.5	1.0604	2	37.5	1.2572	7
12.0	1.1029	1	38.0	1.2701	7
12.5	1.1783	0	38.5	1.2994	7
13.0	1.2029	0	39.0	1.3171	7
13.5	1.2014	0	39.5	1.3447	7
14.0	1.1575	0	40.0	1.3319	7
14.5	1.1629	0	40.5	1.3674	8
15.0	1.1602	0	41.0	1.346	7
15.5	1.1296	1	41.5	1.3616	8
16.0	1.1255	0	42.0	1.3437	8
16.5	1.1717	1	42.5	1.32	7
17.0	1.2398	1	43.0	1.3264	7
17.5	1.2078	1	43.5	1.3143	7
18.0	1.1973	1	44.0	1.3096	7
18.5	1.2091	1	44.5	1.3086	7
19.0	1.155	1	45.0	1.2932	7
19.5	1.1975	0	45.5	1.3016	8
20.0	1.1921	0	46.0	1.3068	7
20.5	1.0825	0	46.5	1.2791	8
21.0	1.1168	1	47.0	1.2772	7
21.5	1.194	1	47.5	1.3065	7
22.0	1.1426	1	48.0	1.3113	7
22.5	1.1602	1	48.5	1.3479	7
23.0	1.1996	1	49.0	1.3488	7
23.5	1.1877	2	49.5	1.3791	7
24.0	1.176	1	50.0	1.3739	6
24.5	1.0812	2	50.5	1.385	7
25.0	1.0822	1	51.0	1.3696	5
25.5	1.1922	1	51.5	1.3485	5
26.0	1.1905	1			

4. SWISS LAKES WATER-COLUMN CHEMISTRY

Sample Location	Depth (m)	Sampling Date	δD	Std. Dev.	$\delta^{18}O$	Std. Dev.
Lake Zürich	surface	April 18, 2000	-78.63	0.91	-11.24	
Baldeggersee*	0	annual Avg. 1995-96	-63.56		-8.6	
	0-7.5	annual Avg. 1995-97	-64.65		-8.6	
Lake Lucerne	0-20	June 14, 2000	-87.17	0.25	-12.17	0.03
Lake Lugano	surface	May 4, 2000	-49.38	0.23	-7.61	0.02
stn. Figino	5	2-1999			-7.75	
stn. Figino	0.4	4-1999			-6.83	
stn. Figino	0.4	2-2000			-6.95	
stn. Figino	3	2-2000			-6.84	
stn. Figino	5	2-2000			-6.08	
stn. Figino	10	2-2000			-7.16	

All isotopic values are given in ‰ with respect to VSMOW.

*Oxygen and hydrogen isotopic data from Baldeggersee taken from *Teranes* [1998].

5. REFERENCES

Teranes, J.L., Climatic significance and biochemical controls on stable isotopes in a lacustrine sequence from Baldeggersee, Switzerland, PhD thesis, Swiss Federal Institute of Technology, Zürich, 1998.

NOTES ON ADVECTION-DIFFUSION MODELING

1. FINITE DIFFERENCE METHOD

This method is useful for solving systems of differential equations that cannot be solved analytically. To construct a finite-difference model, the infinitesimal derivatives from differential equations are replaced by finite differences. For instance,

$$\frac{\partial C}{\partial t} = k \frac{\partial^2 C}{\partial z^2} \quad \text{becomes:} \quad \frac{\Delta C}{\Delta t} = k \frac{\Delta^2 C}{\Delta z^2}$$

where Δ refers to the discrete finite difference between two points. This equation can then be solved by algebraic means. When Δt and Δz approach zero, the finite difference form reduces to the original differential equation.

2. IMPLICIT VS. EXPLICIT SOLUTIONS (see *Peacock* [1989])

2.1. *Explicit finite difference method*

The solution to a variable at time $n+1$ depends explicitly on the variable values at time n (i.e., the next time level depends on the current time level). For instance, the equation:

$$\frac{\partial C}{\partial t} = k \frac{\partial^2 C}{\partial z^2} \quad \text{can be written as:} \quad \frac{C_i^{n+1} - C_i^n}{\Delta t} = k \left[\frac{C_{i+1}^n - 2C_i^n + C_{i-1}^n}{(\Delta z)^2} \right]$$

(where subscripts represent depth and superscripts denote time). This method is the most straight forward since C_i^{n+1} can simply be isolated on the left-hand side and solved. The major drawback of this method is that it requires relatively small time steps to be stable.

2.2. *Implicit finite difference method*

The solution to a (concentration) variable at the next time level depends implicitly on the variables at the next time level and explicitly on the variable at the current time level. With this method, a set of equations must be solved simultaneously using matrices, thus it is slightly more complex than the explicit method, but does not suffer the time-step constraints (i.e., it is unconditionally stable for any time step). For instance, (the case with constant-concentration boundary conditions):

$$\frac{\partial C}{\partial t} = k \frac{\partial^2 C}{\partial z^2} \quad \text{can be written as:} \quad \frac{C_i^{n+1} - C_i^n}{\Delta t} = k \left[\frac{C_{i+1}^{n+1} - 2C_i^{n+1} + C_{i-1}^{n+1}}{(\Delta z)^2} \right]$$

then letting $s = k\Delta t / (\Delta z)^2$ and rearranging, the equation that must be solved is:

$$C_i^n = -sC_{i+1}^{n+1} + (1 + 2s)C_i^{n+1} - sC_{i-1}^{n+1}$$

then representing the system in matrix form, where all coefficients from the above equation are placed in A , a tridiagonal matrix:

$$C^n = A C^{n+1} \quad \text{and further, to: } C^{n+1} = A^{-1} C^n$$

3. EQUATIONS (see *Bear and Verruijt* [1987], Chapter 12)

The flux of a variable (e.g., pollutant) due to advection and diffusion in a saturated system (one dimensional case):

$$q_c = \phi \left(CV - D \frac{\partial C}{\partial x} \right) \quad (\text{Eq. 1})$$

where q_c = flux; ϕ = porosity; C = concentration of the pollutant; V = average velocity; and D = coefficient of diffusion. Excluding chemical reactions and adsorption, the mass balance equation of the pollutant is:

$$\frac{\partial(\phi C)}{\partial t} = - \frac{\partial q_c}{\partial x} \quad (\text{Eq. 2})$$

(If the soil is assumed to be incompressible, then the porosity ϕ is constant, $\partial\phi/\partial t = 0$, and V and D are also constant, and the equation would be: $\frac{\partial C}{\partial t} = -V \frac{\partial C}{\partial x} + D \frac{\partial^2 C}{\partial x^2}$). BUT, in this case the sediment *is* compressible! Thus, substituting eq. 1 into eq. 2, the resulting equation is:

$$\frac{\partial C}{\partial t} = - \frac{\partial(\phi CV)}{\phi \partial x} + \frac{\partial(\phi D \frac{\partial C}{\partial x})}{\phi \partial x} \quad (\text{Eq. 3})$$

Concentration is the dependent variable here and is a function of *two* independent variables, time and depth (this is the time-dependent linear diffusion-advection equation composed of partial differential equations). Thus, the concentration solution domain has two dimensions: time and space.

4. BOUNDARY CONDITIONS (see *Boudreau* [1996])

The above time-dependent, linear advection-diffusion equation is a second-order partial differential equation (PDE), and hence requires two boundary conditions (for the depth variable) and one initial condition (for the time variable) to be solved.

The initial condition is satisfied by (arbitrarily) setting the concentration profile to the modern (or bottom) $\delta^{18}\text{O}$ value of the site being studied. The upper boundary condition (i.e., concentration at the sediment-water interface) is assigned for each time step based on the benthic foraminiferal record from Site 659 for the past 500,000 years [Tiedemann *et al.*, 1994] (first making a correction to adjust for the modern seawater isotopic composition at the studied site). After 20,000 years, the upper boundary condition is based on the eustatic sea level record [Fairbanks, 1989] and using the following rates of sea level rise from Fleming *et al.* [1998]:

22-20 ka	maximum ice volume
19-15 ka	7 m/ky
14-7 ka	10 m/ky
6-2 ka	1 m/ky
2 ka-present	constant at modern level.

The lower boundary condition (i.e., at the base of the sediment column) is assigned as a constant based on the measured pore-water values at that depth.

5. REFERENCES

- Bear, J., and A. Verruijt, *Modeling Groundwater Flow and Pollution*, 414 pp., D. Reidel Publishing Company, Dordrecht, Holland, 1987.
- Boudreau, B.P., *Diagenetic Models and Their Implementation: Modelling Transport and Reactions in Aquatic Sediments*, Springer, 1996.
- Fairbanks, R.G., A 17,000-year glacio-eustatic sea level record: Influence of glacial melting rates on the Younger Dryas event and deep ocean circulation, *Nature*, 342, 637-642, 1989.
- Fleming, K., P. Johnston, D. Zwart, Y. Yokoyama, K. Lambeck, and J. Chappell, Refining the eustatic sea-level curve since the Last Glacial Maximum using far- and intermediate-field sites, *Earth and Planetary Science Letters*, 163, 327-342, 1998.
- Peacock, S.M., Thermal modeling of metamorphic pressure-temperature-time paths: A forward approach, in *Metamorphic Pressure-Temperature-Time Paths*, edited by F.S. Spear, and S.M. Peacock, pp. 57-68, American Geophysical Union, Washington, D.C., 1989.
- Tiedemann, R., M. Sarnthein, and N.J. Shackleton, Astronomic timescale for the Pliocene Atlantic $\delta^{18}\text{O}$ and dust flux records of Ocean Drilling Program site 659, *Paleoceanography*, 9 (4), 619-638, 1994.

ADVECTION-DIFFUSION MODEL SENSITIVITY STUDIES

In the course of writing the model code and developing the proper set of equations appropriate for applying advection and diffusion in a marine sediment column, many tests were carried out to check the influence of certain parameters on model outcome. Presented here is a summary of some of the more important tests demonstrating the model's sensitivity to various input values and/or to show how specific parameters and boundary conditions were chosen.

1. DIFFUSION AND ADVECTION PROCESSES

Diffusion is the process that acts to eliminate concentration gradients and is caused by the random molecular motions of water and solute molecules in solution. Advection is the flow of a medium, in this case pore water, moving through a unit area per unit time. This flux can be due to burial and compaction, an external hydrologic flow, and/or temperature gradients in the sediment column.

Figure 1 demonstrates the influence of the diffusion (A.) and advection (B.) processes on a sharp $\delta^{18}\text{O}$ gradient, implemented in the model as a simple step function (C.). In addition, the influence of time-step size (dt in years) is displayed in the advection results.

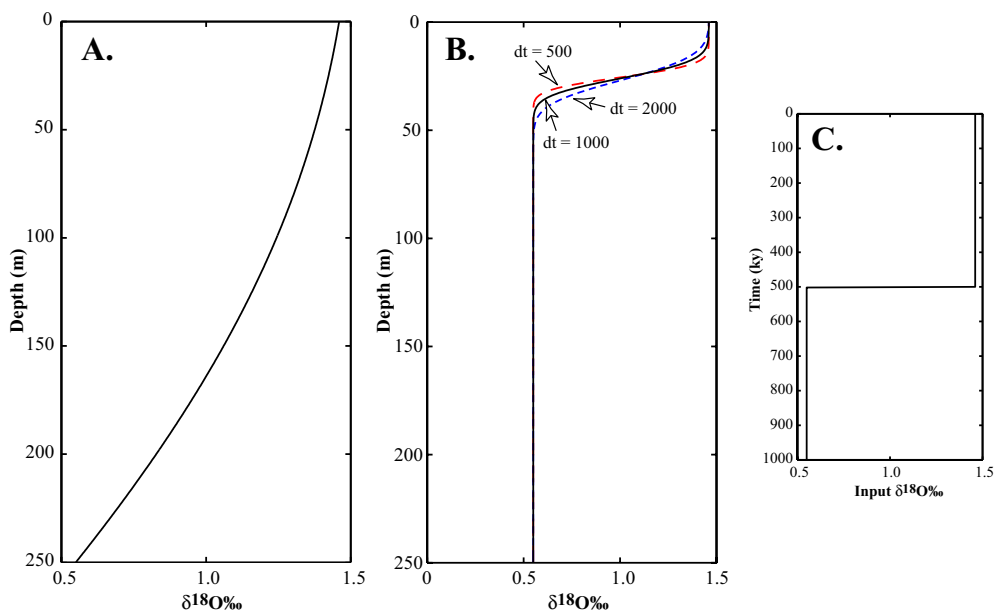


Figure 1.

2. GENERAL TESTS

2.1. Initial Value

Comparison between different initial $\delta^{18}\text{O}$ values assigned to the sediment-water interface (i.e., upper boundary condition) as constant for the first 500,000 years of the model run (constant to make sure model is stable). Here the values tested are the modern $\delta^{18}\text{O}$ value at the sediment-water interface (1.36‰ at Site 976) and the $\delta^{18}\text{O}$ value of the deepest measured pore-water sample (0.58‰ at Site 976). As seen in Figure 2, the choice of this value has little impact on the final $\Delta\delta^{18}\text{O}$ determinations.

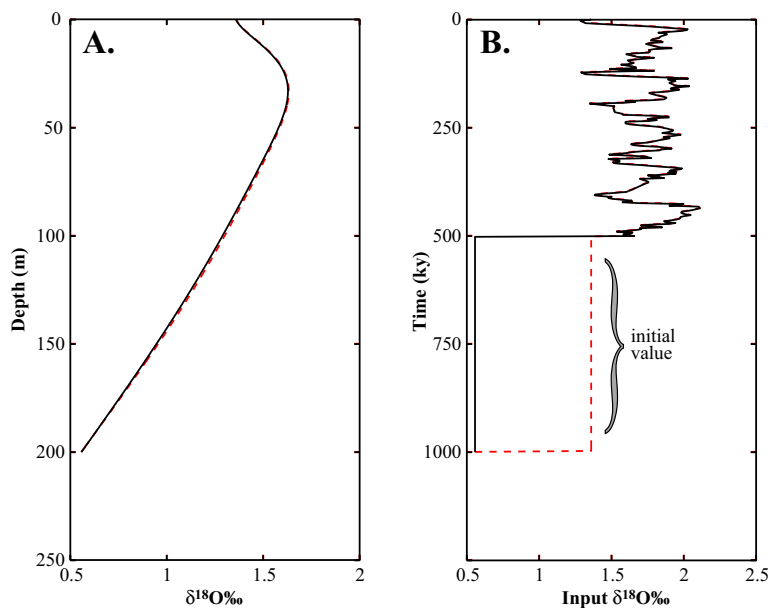


Figure 2. (A.) Model runs using different initial values as displayed in (B.) with the assigned input functions. Solid line uses 0.56‰ (modern 200 m value) and dashed line uses 1.36‰ (modern surface sediment value) prior to 500 ka.

2.2. Time step

To determine the frequency with which model iterations must be made to obtain stable and accurate numerical results, model runs were carried out using various time steps (dt in years) until a suitable resolution was found. This procedure is demonstrated in Figure 3 for both (A.) the “fixed depth” (i.e., Cariaco Basin) and (B.) the “sediment flux” (i.e., Mediterranean Sea) model cases. (Final model calculations utilize a $dt = 1000$ -500 years).

2.3. Depth step

In the “sediment flux” model case, the depth step (dz in meters) is a function of the sedimentation rate and the assigned time step. For the case of diffusion and advection in a sediment column of fixed depth, the depth interval at which the model must solve for concentration is prescribed. Similar to dt , dz is determined by identifying a resolution that will provide sufficient numerical stability and accuracy, as demonstrated in Figure 4. (Final model calculations utilize a $dz = 0.5$ m).

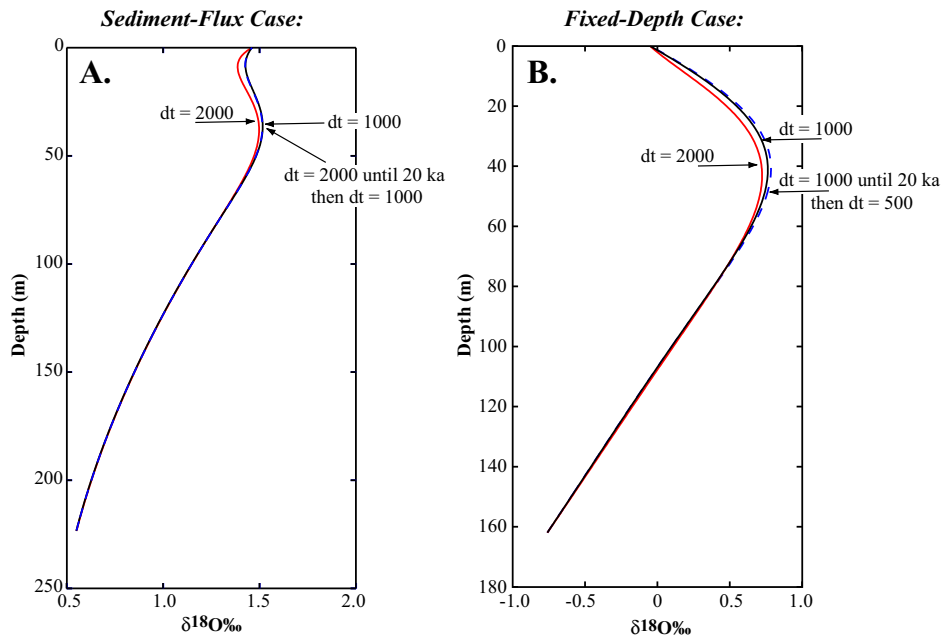


Figure 3.

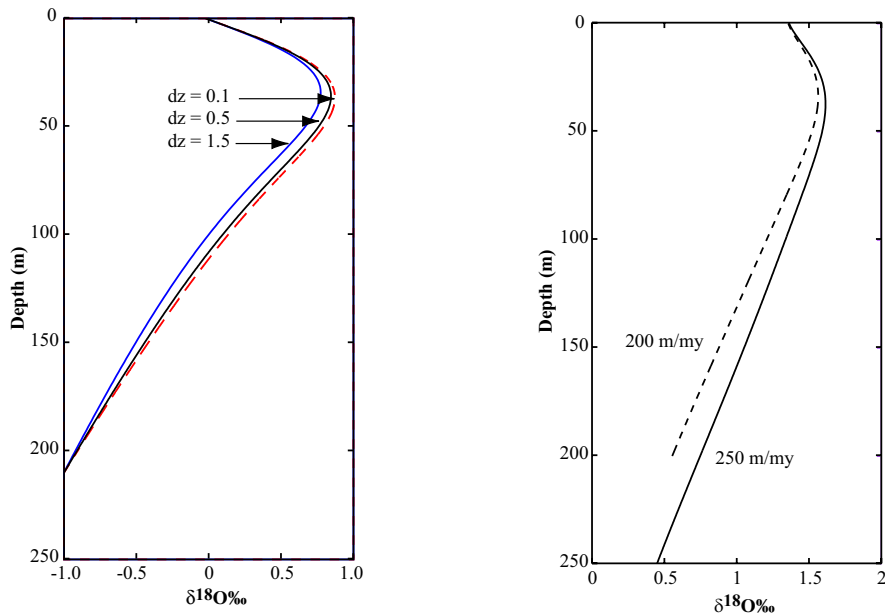


Figure 4.

Figure 5.

2.4. Sedimentation Rate

To examine the influence of sedimentation rate on model results (sedimentation is held constant throughout model runs), a comparison was made for two different sediment fluxes as shown in Figure 5. This test demonstrates that, for the “sediment flux” model simulating sediment deposition, the faster the sedimentation rate, the slower the dilution of the $\delta^{18}\text{O}$ signal.

2.5. Effective Diffusivity

The effective diffusivity can be calculated based on the temperature, porosity, and tortuosity of the sediment [Boudreau, 1996], though this value must often be slightly modified to more accurately fit the pore-water $\delta^{18}\text{O}$ profile, and hence a coefficient k is introduced for calculating this term [Schrage and DePaolo, 1993]. The value of k is influential in determining the depth at which the maximum of the modeled peak in $\delta^{18}\text{O}$ appears as shown in Figure 6.

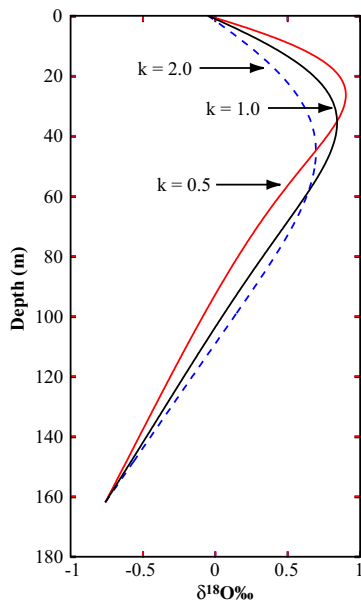


Figure 6.

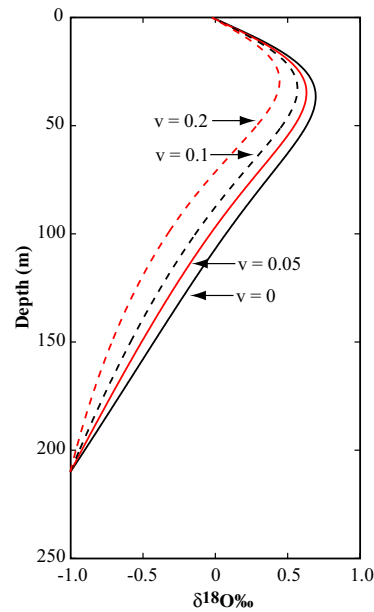


Figure 7.

2.6. Advection Velocity

The term, v (in mm/year), is influential in determining both the magnitude and depth of the modeled $\delta^{18}\text{O}$ peak. In initial model runs, it is always assumed that the entire advective velocity results from sediment compaction. If this produces a poor fit to measured pore water data, additional flow can be added as necessary. The effect of changing the fluid advection can be seen in Figure 7.

2.7. Lower Boundary Condition

For model simulations, the lowest point in the sediment column is assigned a $\delta^{18}\text{O}$ value (normally the measured isotopic composition of the pore water at that depth) that remains constant throughout the calculation. To examine the effect of this fixed lower-boundary condition on model output a couple of sensitivity tests were carried out (as discussed in Chapter 5). First, the depth of the lower boundary condition was changed (A.) and second, the $\delta^{18}\text{O}$ value was varied (B.; here between -0.5 and -1.0‰). These results (Figure 8) clearly show that the lower boundary

condition is significant in determining the model profile and hence, the final $\Delta\delta_{sw}$ and should be selected appropriately.

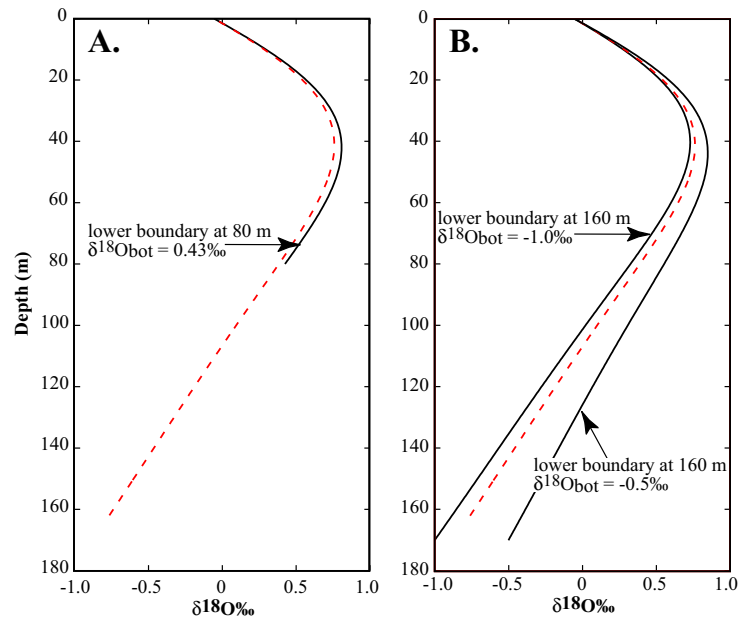


Figure 8.

2.8. Temperature

The temperature of seawater at the sediment-water interface is used in the model for determining the effective diffusivity. It is usually possible to find this value in the literature or to ascertain a close estimate. Figure 9 illustrates the effect of varying the temperature value (using the Cariaco Basin as an example) and suggests that it is important to try to constrain this parameter as accurately as possible.

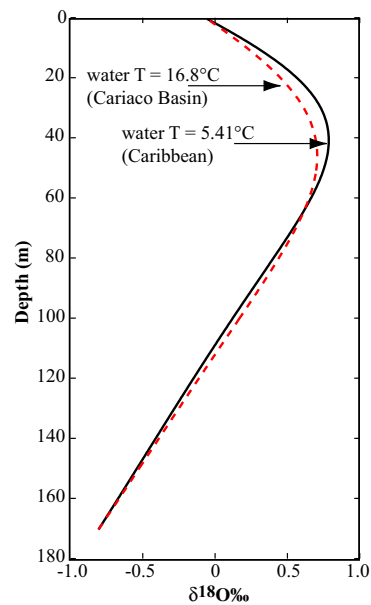


Figure 9.

3. SPECIFIC TO SAPROPEL STUDY

3.1. Duration of S1 Event

Changing the duration of the negative $\delta^{18}\text{O}$ pulse at S1 by 1,000 years (i.e., lasting from 12-10 ka and from 12-9 ka) makes very little difference in the resulting model curve (Figure 10).

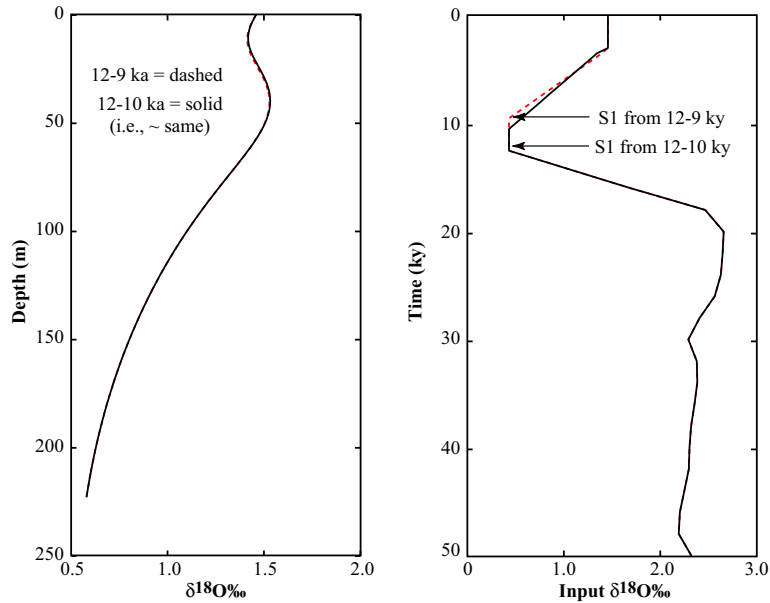


Figure 10.

3.2. Timing of S1 Event

Changing the time at which the model simulates the S1 event, i.e., when the minimum $\delta^{18}\text{O}$ value is assigned, does have a slight influence on the size of the calculated $\Delta\delta$ value, thus all possible scenarios must be considered to depict the potential range of $\Delta\delta$ (Figure 11).

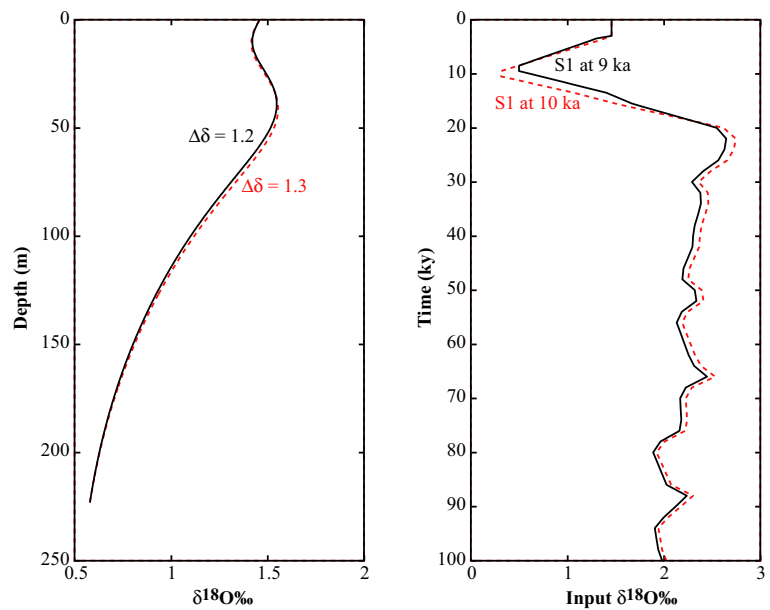


Figure 11.

4. REFERENCES

- Boudreau, B.P., *Diagenetic Models and Their Implementation: Modelling Transport and Reactions in Aquatic Sediments*, Springer, 1996.
- Schrag, D.P., and D.J. DePaolo, Determination of delta ^{18}O of seawater in the deep ocean during the Last Glacial Maximum, *Paleoceanography*, 8, 1, 1993.

LARGE AND RAPID CLIMATE VARIABILITY DURING THE MESSINIAN SALINITY CRISIS: EVIDENCE FROM DEUTERIUM CONCENTRATIONS OF INDIVIDUAL BIOMARKERS

N. Andersen, H.A. Paul, S.M. Bernasconi, J.A. McKenzie, A. Behrens, P. Schaeffer, and P. Albrecht
published in: *Geology*, 29: 799-802, 2001.

ABSTRACT

During the Messinian, ~6 m.y. ago, massive sea-level fall and widespread deposition of evaporites occurred in the Mediterranean Sea when it became isolated from the world oceans. Here we present the first hydrogen isotope data from individual sedimentary biomarkers, *n*-alkanes and isoprenoids, that tracked climatically driven hydrographic changes in response to extreme evaporation during the Messinian salinity crisis. The stable hydrogen and carbon isotope compositions of these biomarkers show a range of 160‰ in δD values and 14‰ in $\delta^{13}C$ values, and roughly covary. This indicates that the source waters of the biomarkers were therefore in some cases extremely enriched in deuterium, having average δD as great as 166‰ VSMOW (Vienna standard mean ocean water). Such values are only known from desert climates today. Because the offset between the δD values of *n*-alkanes and isoprenoids preserved in the Miocene sedimentary rocks is similar to the offset found in modern biological samples, we conclude that diagenesis did not significantly affect the primary deuterium concentrations.

1. INTRODUCTION

Hydrogen has the largest relative mass difference between its stable isotopes (1H and 2H or D) and, consequently, the largest natural variations in stable isotope ratios. The hydrogen isotope composition of environmental waters and ice (e.g., *Waelbroeck et al.* [1995]), bulk organic matter (e.g., *Krishnamurthy et al.* [2000]), and individual organic compounds ([*Sauer et al.*, 2001; *Sessions et al.*, 1999; *Xie et al.*, 2000]) has been widely used as a natural tracer in reconstructions of environmental and climatic change and in biological pathway studies. The recent development of compound-specific analysis of hydrogen isotopes ([*Scrimgeour et al.*, 1999; *Sessions et al.*, 1999]) has launched a new field for geochemical research.

To elucidate the potential of this technique for paleoenvironmental studies, we measured the hydrogen isotope composition of long-chain *n*-alkanes and isoprenoids from the sulfur-bound fraction of Messinian sedimentary rocks from Sicily (Italy) [*Schaeffer et al.*, 1995]. The sediments were deposited during the Messinian salinity crisis (late Miocene, 5–7 Ma), a period of

drastic environmental change that yielded evaporitic sediments throughout the Mediterranean basin [Krijgsman *et al.*, 1999]. The large variability in the carbon isotope composition of individual sulfur-bound biomarkers, previously found by Behrens [1999], is still enigmatic: rather than being a productivity-driven signature, salinity fluctuations in the upper oxic water column influencing the solubility of CO₂ have been suggested as the main driving process [Behrens, 1999]. In this study we analyze the same samples, to determine if the hydrogen isotope composition of these biomarkers displays similar variability and could provide more information on environmental change.

2. MATERIALS

Basin-wide evaporite deposition occurred in the Mediterranean Sea in two major phases during the Messinian and formed the Lower and Upper Evaporites (e.g., Krijgsman *et al.* [1999]). We analyzed seven samples (G5–G11; ~12 m apart in the profile) of marls with intercalated gypsum conglomerates that are of allochthonous, turbiditic origin [Schreiber *et al.*, 1976]. Our samples were collected from the Lower Evaporites (torbiditi gessose [Bommarito, 1984]) from an outcrop near the town of Gibellina in western Sicily. These organic-rich marls (0.9%–4% total organic carbon) were deposited in the small, ~30-km wide Gibellina basin located northwest of the main Sicilian evaporitic basin. To obtain samples with the best preservation of the primary isotopic composition, we chose organic-rich marls that accumulated under anoxic bottom-water conditions [Schaeffer *et al.*, 1995] and analyzed sulfur-bound biomarkers that are incorporated into macromolecular matter, and are therefore thought to be more resistant to biotic or abiotic degradation than the labile-free lipids [Behrens, 1999].

On the basis of the geological map of Bommarito [1984], we estimate the thickness of the Lower Evaporites from the Gibellina basin to be ~300 m. From this thickness and the duration of the Lower Evaporites (~370 k.y. [Krijgsman *et al.*, 1999]), we calculated a mean sedimentation rate of ~80 cm/k.y. Consequently, the entire sediment section studied (40 m from G2 to G17) is equivalent to ~50 k.y.

3. METHODS

The techniques for extraction, fractionation, and Raney-nickel desulfurization of the samples were described by Schaeffer *et al.* [1995]. Compound-specific $\delta^{13}\text{C}$ values were determined with a Finnigan MAT 252 mass spectrometer coupled to a gas chromatograph (GC) equipped with a DB 5-MS column (60 m, 0.25 mm i.d., 0.1 μm film). The samples were combusted at 1000°C on a homemade Ni-Pt catalyst. The δD values of individual organic compounds were obtained by isotope-ratio-monitoring gas chromatography–mass spectrometry using a high-dispersion Geo 20-20 (PDZ Europa) mass spectrometer [Scrimgeour *et al.*, 1999]. The organic compounds were separated on a high-capacity GC column (50 m, 0.53 mm i.d., 1 μm film) with

He as the carrier gas. H₂ gas was produced via pyrolysis at 1195°C (conversion efficiency of 99.8%–99.9%; *Ian Begley, personal communication, 1999*). The minor by-product methane was separated with a megabore molesieve (5Å), and water was trapped by a Nafion tube. A series of several *n*-alkanes was used as the standard for external calibration and H₃⁺ correction. To compensate for the effect of changing column bleed, only standards with retention times similar to those of the sample compounds were used for correction. Standard errors of the means (SEM) depend mainly on peak intensity and vary between 0.5‰ and 11.1‰; mean values are 5.3‰ and 4.1‰ for *n*-C₂₂ and 5α-cholestane, respectively. Each extract was measured between two and six times on the same day. Duplicate measurements of sample G10 on different days produced the following results: *n*-C₂₂: -136‰, ±2.7‰ SEM, *n* = 3, and -135‰, ±1.0‰ SEM, *n* = 3; 5α-cholestane: -218‰, ±3.2‰ SEM, *n* = 4, and -207‰, ±6.9‰ SEM, *n* = 3. All results are given with reference to VSMOW (Vienna standard mean ocean water).

4. RECONSTRUCTION OF MIOCENE SURFACE WATER COMPOSITION

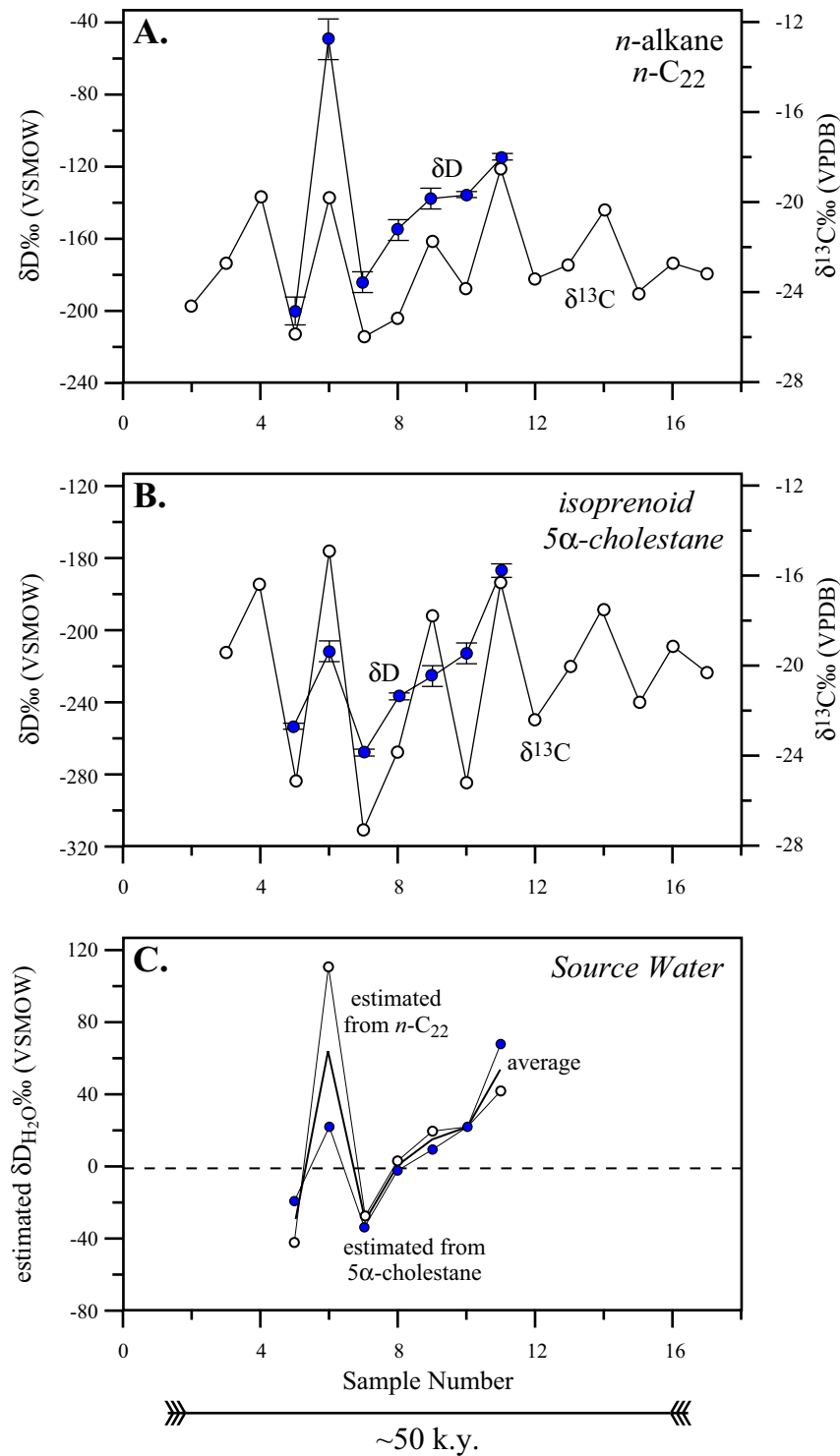
The results of two biomarkers from different compound classes, the *n*-alkane *n*-C₂₂ and the isoprenoid 5α-cholestane, are presented in Figure 1. The stable hydrogen and carbon isotopes of these biomarkers show large variability that is roughly covariant. Data display a range of 160‰ in δD values and 14‰ in δ¹³C values.

Because photosynthetic organisms utilize water as the main hydrogen source (photosynthesis: CO₂ + H₂O → CH₂O + O₂), the deuterium concentration in the source water is reflected by the deuterium composition of the organism [*Estep and Hoering, 1980; Sessions et al., 1999*]. To estimate the δD of the original source water (Figure 1c), we assume a constant fractionation between water and lipids of 158‰ and 235‰ for the *n*-alkane and the isoprenoid, respectively [*Estep and Hoering, 1980; Sessions et al., 1999*]. These averaged values are based on analyses of individual compounds [*Sessions et al., 1999*] and total fractions of alkanes and sterols [*Estep and Hoering, 1980*] from modern samples in comparison with the source water. These fractionations agree well with the values 156‰ and 232‰ for saponifiable and nonsaponifiable lipids, respectively, that have been documented in a broader data set [*Estep and Hoering, 1980*].

With the exception of sample G6, the estimated source-water δD values are similar for both biomarkers (Figure 1), suggesting a common origin. This first biomarker-based δD record from the Messinian indicates large variability of the source water; -31‰ to +66‰ based on the average of both biomarkers.

5. PRIMARY SIGNATURE OR DIAGENETIC ALTERATION?

Compared to bulk organic matter, individual lipid biomarkers are much less prone to diagenetic alteration of their deuterium concentrations because there is no effect due to the preferential degradation of less stable compounds and because hydrogen in lipids is mainly bound to

**Figure 1.**

Stable carbon and hydrogen isotope compositions of sulfur-bound hydrocarbons from Miocene evaporites: (A.) *n*-alkane *n*-C₂₂, (B.) isoprenoid 5 α -cholestane, (C.) estimated δD values of source water. Carbon isotope data are from Behrens [1999]. Error bars of δD values are equal to standard errors of the means. Source-water estimates were derived from measured δD of organic compounds by correcting for constant fractionation of 158‰ and 235‰ (*n*-alkanes and isoprenoids, respectively) [Estep and Hoering, 1980; Sessions et al., 1999]. VPDB is Vienna Pee Dee belemnite; VSMOW is Vienna standard mean ocean water.

carbon. In contrast to heteroatomic (N, S, O) bound hydrogen, which readily exchanges with the surrounding water during diagenesis [Schimmelmann *et al.*, 1999], carbon-bound hydrogen is very stable. Because of the stability of the carbon-bound hydrogen in aliphatic hydrocarbons, the δD values of *n*-alkanes are preserved at temperatures well above 150°C [Schimmelmann *et al.*, 1999]. Both the large variability and the preserved offset between the δD values of the *n*-alkane and the isoprenoid, which is similar to the offset seen in modern biological samples, indicate that diagenesis affected the primary values of our samples only slightly, if at all. If diagenesis had caused significant alterations, a much more homogeneous distribution of the hydrogen isotope content would be expected [Hoering, 1977].

Additional alterations due to diagenesis and the extraction methodology have to be considered in the case of sulfur-bound lipids. Because sulfur-bound biomarkers are derived from formerly functionalized (notably unsaturated) compounds [Schaeffer *et al.*, 1995], the original double bonds are reduced with additional hydrogen atoms during diagenesis. Furthermore, during desulfurization, each of the desulfurized C-S bonds are replaced by C-H bonds, with the addition of hydrogen atoms from the catalyst. In addition, S-bound compounds still bearing double bonds will be reduced with adsorbed hydrogen from the Raney-nickel catalyst. Experiments to evaluate the influence of the catalytic hydrogenation of double bonds on the primary δD signature are in progress. However, we consider these problems to be of minor importance because of the well-preserved offset between the δD values of *n*-alkanes and isoprenoids. The large discrepancy for sample G6 might suggest diagenetic alteration of this sample. To minimize this potential bias, we discuss our results in terms of average source water composition. On the basis of these lines of evidence, we conclude that the δD values reflect mainly primary signatures. Other recent results of compound-specific hydrogen isotope analyses from the Eocene Green River Formation indicate that paleoenvironmental information is preserved, even in the fraction of free sedimentary lipids [Andersen *et al.*, 2000].

6. PALEOENVIRONMENTAL IMPLICATIONS

On the basis of averaged samples, we estimate the δD values of the source waters to have varied by $\sim 100\%$ over the period of deposition. The D-rich isotope composition of the waters, up to $+66\%$, indicates intense evaporation at low relative humidity. In general, residual water becomes progressively enriched in deuterium during evaporation (Figure 2a). Because deuterium enrichment increases with decreasing humidity, extremely D-enriched isotope values as great as $+129\%$ have only been reported from environments with low relative humidity, such as deserts, and have been found in small desiccating ponds that existed temporarily after flooding events [Fontes and Gonfiantini, 1967].

Only the initial stages of the desiccating pond model [Gonfiantini, 1986] can be applied to the Gibellina basin because (1) the biomarker data indicate a marine to mesosaline deposi-

tional environment [Schaeffer *et al.*, 1995], (2) these marls do not contain autochthonous gypsum, indicating that the salinity probably stayed below 120 psu [Schaeffer *et al.*, 1995], and (3) the continuous sedimentation of these marls indicates that this part of the basin was not subject to periods of total desiccation. However, under conditions of low relative humidity, the initial stages of the desiccating pond model are sufficient to describe our data, because large deuterium enrichments are already attained after a small decrease in the amount of remaining water (Figure 2a).

As an alternative model, we can also consider a terminal lake where the inflow is in hydrological balance with the evaporation. The inflow of water over a range of δD values and how this influx affects the isotopic composition of the lake is illustrated for a short time period (1 yr) in Figure 2b. Large deviation from the initial δD value of the lake water is caused by short residence times. During water-column stratification, the effect caused by the influx will be amplified because the volume of the lake, which is in exchange with the atmosphere, will be drastically reduced. Even an inflow of moderately deuterium-enriched water into a stratified lake can strongly increase the δD values of the lake. From biomarker data, Schaeffer *et al.* [1995] inferred that during the deposition of these marls the water column was strongly stratified, with an oxygenated upper layer characterized by high primary productivity and anoxic bottom waters. For samples G7 and G10, the presence of biomarkers originating from green-sulfur photosynthetic bacteria indicates that the oxic-anoxic boundary was located within the photic zone [Behrens, 1999; Schaeffer *et al.*, 1995].

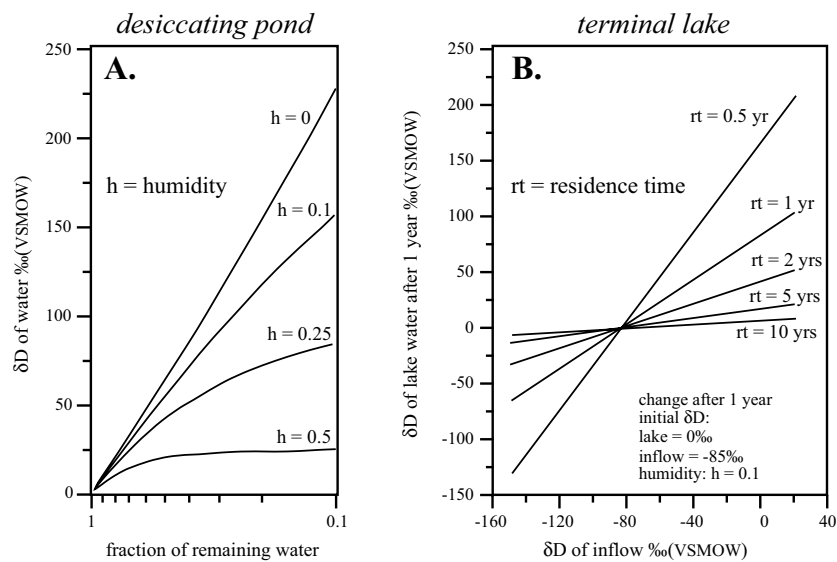


Figure 2.

(A.) Progressive increase of δD values of water in a desiccating pond. Deuterium enrichment increases with decreasing humidity (h). (B.) Short-time change of δD values of lake water (after 1 yr) caused by different δD values of inflow. Model is for a terminal lake where inflow is in hydrological balance with evaporation. Large deviation from initial δD values of lake water is caused by small residence time (volume of lake/annual in-flow). Displayed graphs are calculated as described in detail by Gonfiantini [1986].

We used the terminal lake model to illustrate how stratification can amplify the short-term change in the isotopic composition of a lake caused by the inflow. A persistent shift to deuterium-enriched inflow will always be connected with a transition to drier climatic conditions. According to both models, the initial stage of the desiccating pond and the terminal lake, extreme deuterium enrichment is a clear indication of strong evaporation in a dry environment. The extremely D-enriched isotope values of G6 and G11 are coupled with ^{13}C -enriched isotope values, well known to be characteristic of hypersaline environments [Grice *et al.*, 1998; Schidlowski *et al.*, 1994], and can be explained by a salinity increase corresponding to the very dry climate. In such environments, the ^{13}C enrichment can be caused by high productivity [Schidlowski *et al.*, 1994] or by the decrease in solubility of CO_2 with high salinity [Behrens, 1999]. The lowest $\delta^{13}\text{C}$ values are displayed under conditions where the oxic-anoxic boundary was probably located within the photic zone (samples G7 and G10). In general, during periods when the oxic part of the photic zone is compressed, a more efficient usage of ambient CO_2 is likely and causes the remains of aerobic organisms, like *n*- C_{22} and 5α -cholestane, to show ^{13}C -enriched isotope values. However, the opposite is observed and therefore, increased concentrations of dissolved CO_2 at low salinity can be inferred.

The D-depleted source waters indicated by samples G5 and G7, values from -40‰ to -20‰ and more typical of fresh water, are unexpected in the marine to mesosaline environment of the Gibellina basin [Schaeffer *et al.*, 1995], but are consistent with the findings of mother waters from Messinian gypsum (-17‰ to +34‰ [Bellanca and Neri, 1986; Pierre and Catalano, 1976; Pierre and Fontes, 1978]). The low δD values may indicate the inflow of meteoric waters that underwent only moderate evaporation.

Similar short-term changes in hydrogen isotope composition, but less drastic in magnitude compared to our findings, were found in fluid inclusions from laminar gypsum of the Messinian section in the main Sicilian evaporitic basin (δD values of -7‰ to +23‰ [Bellanca and Neri, 1986]). This highly saline basin containing autochthonous gypsum was subject to cyclic desiccation [Lugli *et al.*, 1999] and flooding events characterized by open-marine conditions with normal surface salinity [Bertini *et al.*, 1998]. Under conditions in which salinity is high enough to precipitate autochthonous gypsum or even salt, the isotopic composition of an evaporating water body is additionally affected by the amount of dissolved salts. Consequently, the variations observed in the gypsum are less drastic because (1) under identical climatic conditions, evaporation of fresh water will result in stronger deuterium enrichment than that of marine waters or brines [Gat, 1995; Gonfiantini, 1986]; (2) a continuous decrease in the thermodynamic activity of water can reverse the trend of deuterium enrichment [Gonfiantini, 1986]; and (3) the deuterium enrichment of water with similarly high salinity is probably much smaller in permanent water bodies (e.g., the Dead Sea, a large and deep salt lake, has a δD value of +9‰ [Horita and Gat, 1989]) than in desiccating ponds that exist temporarily (δD values as great as +100‰

[*Fontes and Gonfiantini, 1967*]). A coastal sabkha (δD values $<+30\text{‰}$ [*Gat and Levy, 1978; Robinson and Gunatilaka, 1991*]) might serve as a model for the precipitation conditions of the Messinian gypsum because their δD values agree well.

Debate still exists concerning the significance of climatic change in association with the Messinian salinity crisis [*Bertini et al., 1998; Krijgsman et al., 1999*]. Our results showing large variability in δD values suggest large climatic variations with changes in evaporation and relative humidity.

7. CONCLUSIONS

Analysis of the hydrogen isotope composition of individual biomarkers from ancient sedimentary deposits offers great potential for elucidating environmental conditions, for example, paleohumidity. Our results, which are the first compound-specific analyses from ancient sedimentary rocks, indicate that the large variability in δD values of biomarkers was caused by climate change during the Messinian. At certain periods, the source water was extremely D enriched and indicates intense evaporation at low relative humidity. This D enrichment can be explained by the initial stages of a desiccating pond model, maybe amplified by stratification, as demonstrated by the terminal lake model. Our results show that paleoenvironmental information from organic material as old as Miocene age can be preserved and that diagenesis had a negligible effect on the primary deuterium concentrations of the sedimentary lipids.

Further studies on the biogeochemistry of stable hydrogen isotopes in individual biomarkers will improve this tool. A wide range of further research in Earth and natural sciences is possible (e.g., bioremediation and food-chain studies), with potential applications as diverse as those for the extensively utilized, compound-specific carbon isotope measurements.

ACKNOWLEDGEMENTS

We thank Rolf Warthmann for useful comments on the manuscript, and Michael Bird and Paul A. Wilson for helpful and constructive reviews.

8. REFERENCES

- Andersen, N., S.M. Bernasconi, R.M. Carlson, and M. Schoell, Early diagenetic incorporation of strongly deuterium-depleted hydrogen in poly-unsaturated bio-molecules, in *AGU Fall Meeting*, AGU, San Francisco, 2000.
- Behrens, A., Lipides de milieux anoxiques riches en soufre: Identification et évolution diagénétique, Ph.D. thesis, Université Louis Pasteur, Strasbourg, 1999.
- Bellanca, A., and R. Neri, Evaporite carbonate cycles of the Messinian, Sicily: Stable isotopes, mineralogy, textural features, and environmental implications, *Journal of Sedimentary Petrology*, *56*, 614-621, 1986.
- Bertini, A., L. Londeix, R. Maniscalco, A. Di Stefano, J.-P. Suc, G. Clauzon, F. Gautier, and M. Grasso, Paleobiological evidence of depositional conditions in the Salt Member, Gesso-Solfifera Formation (Messinian, Upper Miocene) of Sicily, *Micropal.*, *44*, 413-433, 1998.
- Bommarito, S., La successione Miocene Superiore-Pliocene nella zona di Gibellina (Trapani), *Il Naturalista Siciliano*, *7*, 49-62, 1984.
- Estep, M.F., and T.C. Hoering, Biogeochemistry of the stable hydrogen isotopes, *Geochimica, Cosmochimica, Acta*, *44*, 1197-1206, 1980.
- Fontes, J.-C., and R. Gonfiantini, Comportement isotopique au cours de l'évaporation de deux bassins sahariens, *Earth and Planetary Science Letters*, *3*, 258-266, 386, 1967.
- Gat, J.R., Stable isotopes of fresh and saline lakes, in *Physics and Chemistry of Lakes*, edited by A. Lerman, D. Imboden, and J. Gat, pp. 139-165, Springer-Verlag, 1995.
- Gat, J.R., and Y. Levy, Isotope hydrology of inland sabkhas in the Bardawil area, Sinai, *Limnology and Oceanography*, *23*, 841-850, 1978.
- Gonfiantini, R., Environmental isotopes in lake studies, in *Handbook of Environmental Isotope Geochemistry, Vol.2, The Terrestrial Environment, B*, edited by P. Fritz, and J.-C. Fontes, pp. 113-168, Elsevier, Amsterdam, 1986.
- Grice, K., S. Schouten, A. Nissenbaum, J. Charrach, and J.S. Sinninghe Damsté, Isotopically heavy carbon in the C₂₁ to C₂₅ regular isoprenoids in halite-rich deposits from the Sdom Formation, Dead Sea Basin, Israel, *Organic Geochemistry*, *28*, 349-359, 1998.
- Hoering, T.C., The stable isotopes of hydrogen in Precambrian organic matter, in *Chemical Evolution of the Early Precambrian*, edited by C. Ponnampertuma, pp. 81-86, Academic Press, New York, 1977.
- Horita, J., and J.R. Gat, Deuterium in the Dead Sea: Remeasurement and implications for the isotopic activity correction in brines, *Geochimica, Cosmochimica, Acta*, *53*, 131-133, 1989.
- Krijgsman, W., F.J. Hilgen, I. Raffi, F.J. Sierro, and D.S. Wilson, Chronology, caused and progression of the Messinian salinity crisis, *Nature*, *400*, 652-655, 1999.
- Krishnamurthy, R.V., P.A. Meyers, and N.A. Lovan, Isotopic evidence of sea-surface freshening, enhanced productivity, and improved organic matter preservation during sapropel deposition in the Tyrrhenian Sea, *Geology*, *28*, 263-266, 2000.
- Lugli, S., B.C. Schreiber, and B. Triberti, Giant polygons in the Realmonte mine (Agrigento, Sicily): Evidence for the desiccation of a Messinian halite basin, *Journal of Sedimentary Research*, *69*, 764-771, 1999.
- Pierre, C., and R. Catalano, Stable isotopes (¹⁸O, ¹³C, ²H) in the evaporitic sequence of the Cimmina Basin (Sicily), *Memorie della Società Geologica Italiana*, *16*, 55-62, 1976.
- Pierre, C., and J.C. Fontes, Isotope composition of Messinian sediments from the Mediterranean Sea as indicators of paleoenvironments and diagenesis, in *Initial reports of the Deep Sea Drilling Project*, edited by K.J.e.a. Hsu, pp. 635-650, U.S. Government Printing Office, Washington D.C., 1978.

- Robinson, B.W., and A. Gunatilaka, Stable isotope studies and the hydrological regime of sabkhas in southern Kuwait, Arabian Gulf, *Sedimentary Geology*, 73, 141-159, 1991.
- Sauer, P.E., T.I. Eglinton, J.M. Hayes, A. Schimmelmann, and A.L. Sessions, Compound-specific D/H ratios of lipid biomarkers from sediments as a proxy for environmental and climatic conditions, *Geochimica et Cosmochimica Acta*, 65, 213-222, 2001.
- Schaeffer, P., C. Reiss, and P. Albrecht, Geochemical study of macromolecular organic matter from sulphur-rich sediments of evaporitic origin (Messinian of Sicily) by chemical degradations, *Organic Geochemistry*, 23, 567-581, 1995.
- Schidlowski, M., H. Gorzawski, and I. Dor, Carbon isotope variations in a solar pond microbial mat: Role of environmental gradients as steering variables, *Geochimica, Cosmochimica, Acta*, 58, 2289-2298, 1994.
- Schimmelmann, A., M.D. Lewan, and R.P. Wintsch, D/H isotope ratios of kerogen, bitumen, oil and water in hydrous pyrolysis of source rocks containing kerogen types I, II, IIS, and III, *Geochim., Cosmochim, Acta*, 63, 3751-3766, 1999.
- Schreiber, B.C., G.M. Friedman, A. Decima, and E. Schreiber, Depositional environments of Upper Miocene (Messinian) evaporite deposits of the Sicilian Basin, *Sedimentology*, 23, 729-760, 1976.
- Scrimgeour, C.M., I.S. Begley, and M.L. Thomason, Measurements of deuterium incorporation into fatty acids by gas chromatography/isotope ratio mass spectrometry, *Rapid Communications in Mass Spectrometry*, 13, 271-274, 1999.
- Sessions, A.L., T.W. Burgoyne, A. Schimmelmann, and J.M. Hayes, Fractionation of hydrogen isotopes in lipid biosynthesis, *Organic Geochemistry*, 30, 1193-1200, 1999.
- Waelbroeck, C., J. Jouzel, L. Labeyrie, C. Lorius, M. Labracherie, M. Stiévenard, and N.I. Barkov, A comparison of the Vostok ice deuterium record and series from Southern Ocean core MD 88-770 over the last two glacial-interglacial cycles, *Climate Dynamics*, 12, 113-123, 1995.
- Xie, S., C.J. Nott, L.A. Avsejs, F. Volders, D. Maddy, F.M. Chambers, A. Gledhill, J.F. Carter, and R.P. Evershed, Palaeoclimate records in compound-specific δD values of a lipid biomarker in ombrotrophic peat, *Organic Geochemistry*, 31, 1053-1057, 2000.

CURRICULUM VITAE

HILARY A. PAUL

DATE OF BIRTH: October 23, 1970

PLACE OF BIRTH: Bangor, Maine, USA

CITIZENSHIP: United States of America

EDUCATION:

- 1984-1988 High School Diploma
Portland High School, Portland, ME
- 1988-1989 University of Southern Maine, Portland/Gorham, ME
- 1990-1993 Honors, Bachelor of Arts
Occidental College, Los Angeles, CA
Major: Geology Minor: Art History
Thesis Title: Paleointensity of the Earth's Magnetic
Field Across a Magnetic Polarity Reversal
- 1994-1997 Master of Science
Department of Earth Sciences
University of California, Santa Cruz, CA
Thesis Title: A High-Resolution Stable Isotope Chronology
of Climate and Ocean Chemistry Variability Across
the Oligocene/Miocene Boundary
- 1998-2002 Doctor of Natural Science
Geological Institute
Swiss Federal Institute of Technology, ETH-Zürich
Thesis Title: Alternative Methods with Stable Isotopes for
Paleoenvironmental Reconstructions: Compound-
Specific Hydrogen Isotopes and Pore-water Oxygen
Isotopes